Identification of host proteins that interact with non-structural proteins -1α and -1β of porcine reproductive and respiratory syndrome virus-1

Thesis submitted in accordance with the requirements of the University of Liverpool for the degree of Doctor in Philosophy

by

Sofia Riccio

March 2022

Institute of Infection, Veterinary and Ecological Sciences,

University of Liverpool

The Pirbright Institute

Declaration of Originality

I certify that the work presented in this thesis is my own and that to the best of my knowledge all work and contributions by others, published or unpublished, are fully acknowledged in the text and figure or table legends.

Acknowledgements

Firstly, I want to thank my supervisors, **Dr Julian Seago** and **Professor Simon Graham** from the Pirbright Institute, and **Professor Julian Hiscox** from the University of Liverpool, for their endless help and supervision and for providing me with this opportunity. **Julian**, your knowledge, expertise, and day to day guidance in the lab were invaluable and **Simon** your advice, especially with writing and presenting, was most appreciated.

I would like to thank all past and present members of the **Molecular Virology Group** and **Viral Immunology Group** at the Pirbright Institute for welcoming me into the group, as well as for all their advice, patience, company, cake and dumplings throughout my studies. In particular **Dr Ben Jackson**, for the constant technical advice and football chats, and **Dr Kay Childs** for all your insight and help with troubleshooting, I've learnt so much from you. Thank you to the **Bioimaging Department** for their assistance with the confocal immunofluorescence microscopy, especially **Joanna Wells** for her time, expertise and for teaching me how to use photoshop. **Jemma Wadsworth** and **Hayley Hicks**, thank you for accommodating all my sequencing requests and providing troubleshooting advice. Thanks also to **Dr Jean-Pierre Frossard**, Animal and Plant Health Agency, for the PRRSV-1 NSP1 sequences. **Yvonne Walsh**, thank you for being kind and supportive all the way through my PhD, especially when things were difficult, and **Lynda Moore** for help throughout.

I am thankful for the multiple people who've supported me and made the last 4 and half years so memorable. Of note, my boyfriend **Luke Sefton**, for always having my back, cooking me endless pasta and herby bread, cheering me up whenever I was stressed and putting up with me at my worst during lockdown and thesis writing. I am so grateful to have had you all the way through this. My amazing family, especially my **Mum** and **Dad** for always believing in me and giving me a push when I needed it, as well as my lovely niece **Martha** for making me laugh when I needed it most. My best friends **Demi Brant**, **Helen Murphy**, **Laura Springer**, and **Leah Woodward**, for always being there, listening to me rant about failed experiments and for making time for much needed Liverpool reunions. **London crew**, thanks for the countless dinners,

drinks, and nights out which got me through this. **Elle Campbell** and **Kelly Roper**, thank you for the constant support and girls' weekends when I needed a break, and **Lucy Gordon** for being there from beginning to end both in the lab and out. Finally, thanks to the **Sefton family** for looking after me in Surrey and for help with last minute proofreading.

Lastly, I would like to thank the **Pirbright Institute**, the **University of Liverpool**, and the **BBSRC** for funding this PhD project. Although challenging at times, I have thoroughly enjoyed and learned a lot from my PhD.

Abstract: Identification of host proteins that interact with non-structural proteins -1α and -1β of porcine reproductive and respiratory syndrome virus-1

Sofia Riccio

Porcine reproductive and respiratory syndrome viruses (PRRSV) are the causative agent of one of the most important infectious diseases affecting the global pig industry. PRRSV is endemic in most major pig producing countries where it is responsible for major economic losses, estimated in the USA and Europe to exceed US$600 million and €1.5 billion per annum, respectively. Both species of PRRSV, PRRSV-1 and 2, are rapidly evolving and existing vaccines are failing to control the PRRS panzootic. PRRSV produces 16 non-structural proteins (NSPs) that are involved in viral replication and/or modulating the host immune response. Previous studies have shown that PRRSV NSP1α and NSP1β modulate host cell responses; however, the underlying molecular mechanisms remain to be fully elucidated and most studies have focussed on PRRSV-2 due to its prominence in North America and Asia. Therefore, this project aimed to identify and characterise novel PRRSV-1 NSP1-host protein interactions to improve our knowledge of NSP1-mediated immunomodulation. NSP1α and NSP1β from a representative Western European PRRSV-1 subtype 1 field strain (215-06) were screened for interactions using a cDNA library generated from porcine alveolar macrophages (PAMs), the primary target cell of PRRSV-1, and the yeast-2-hybrid (y-2-h) system, a method for detecting protein-protein interactions. The NSP1α y-2-h screen, using the bait plasmid pGBKT7-NSP1α/β, identified 63 putative binding partners for NSP1α; the NSP1β y-2-h screen, using pGBKT7-NSP1β, identified 126 putative binding partners for NSP1β. Subsequent y-2-h screens using pGBKT7-NSP1α and pGBKT7-NSP1β as bait and with additional controls to check for PAM protein self-activation of the system, confirmed three interactions with NSP1α and 28 with NSP1β. These proteins were involved in the immune response (type I IFN signalling, the NF-κB pathway), ubiquitination, nuclear transport or transcription and translation. Use of y-2-h with 3-AT, an inhibitor of an enzyme involved in histidine production, revealed NSP1α interacts very strongly with PIAS1 and strongly with PIAS2, which both negatively regulate IFN signalling. NSP1β interacts weakly with TAB3, an NF-κB pathway and autophagy regulator, and CPSF4, which functions in mRNA processing. Confocal immunofluorescence microscopy was used to analyse subcellular localisation of selected PAM proteins with NSP1α or NSP1β. Minimal co-localisation was observed between NSP1β and TAB3 in the cytoplasm of transfected cells. NSP1β also altered the cytoplasmic distribution of beclin-1 in the cytoplasm. No other co-localisation was observed between NSP1α and NSP1β with their interacting partners. This project identified a large list of putative interacting proteins for NSP1α and NSP1β and confirmed a selection of these. This list, in combination with the future work described, could help to reveal novel functions of the respective PRRSV proteins, as well as provide mechanistic detail to previously published immunomodulatory functions. Identifying and characterising these novel interactions will increase further our understanding of how PRRSV-1 NSP1α and NSP1β modulate the host cellular immune response, which could subsequently be exploited to rationally attenuate PRRSV-1 as a basis for improved vaccines.

Table of Contents

List of Abbreviations

µg	Micrograms
µL	Microlitres
µm	Micrometres
µM	Micromolar
215-06	PRRSV-1 subtype 1 strain 215-06
3-AT	3-amino-1,2,4-triazole
ABS	Adult bovine serum
AC	Accession number
AD	Activation domain
Ade	Adenine
ANAPC10	Anaphase-promoting complex subunit 10
APC	Antigen presenting cell
ASB8	E3 ubiquitin ligase ankyrin repeat and SOCS box-containing 8
Asp	Aspartate
ATP	Adenosine triphosphate
Bad	Bcl 2 associated agonist of cell death
Bcl (Bcl-2, Bcl-6)	B-cell lymphoma
Bcl-xL	Bcl-extra large
BCR	B cell receptor
BHK-21	Baby hamster kidney 21 cells
BLAST	Basic local alignment search tool
bp	Base pairs
BSR-T7	BHK-21 cells expressing bacteriophage T7 RNA polymerase
CBP	cAMP response element-binding protein (CREB) binding protein
CD (CD4, CD8, CD151, CD163, CD209)	Cluster of differentiation
cDNA	Complementary DNA
CO_2	Carbon dioxide
CPSF4	Cleavage and polyadenylation specificity factor subunit 4
CRM-1	Chromosomal region maintenance 1
CTE	C terminal extension
CTL	Cytotoxic T cell
DAPI	4’,6-diamidino-2-phenylindole
DBD	DNA binding domain
DDX (DDX1, DDX5, DDX18)	DEAD-box helicase
dH_2O	Distilled water
DMEM	Dulbecco's modified eagle medium
DMV	Double membrane vesicle

DNA	Deoxyribonucleic acid
DNAJA3	DNAJ homolog subfamily A member 3
DNAJC10	DNAJ homolog subfamily C member 10
DNase	Deoxyribonuclease
dsRNA	Double stranded RNA
E	PRRSV envelope protein
E. coli	*Escherichia coli*
EAV	Equine arteritis virus
EDTA	Ethylenediaminetetraacetic acid
EGR2	E3 SUMO-protein ligase early growth response 2
eIF (eIF2α, eIF-3, eIF-3 subunit K)	Eukaryotic translation initiation factor
EndoU	Endoribonuclease
EPAS-1	Endothelial PAS domain-containing protein 1
ER	Endoplasmic reticulum
FMDV	Foot-and-mouth disease virus
g	Grams
GAL4	Galactose-responsive transcription factor 4
GLE1	Nucleoporin GLE1
GP	Glycoprotein
gRNA	Genomic RNA
GTP	Guanosine-5'-triphosphate
HEK	Human embryonic kidney
HIF (HIF2α)	Hypoxia-Inducible Factor
His	Histidine
HIV (HIV-1, HIV-2)	Human immunodeficiency virus
hpt	Hours post transfection
hr	Hours
HSC70	Heat shock cognate 71 kDa protein
HSP (HSP10, HSP27, HSP40, HSP70)	Heat shock protein
HTRA2	High temperature requirement protein A2
IAV	Influenza A virus
IFI35	IFN induced protein 35
IFN (IFN-α, IFN-β, IFN-γ)	Interferon
Ig (IgA, IgD, IgE, IgG, IgG2a, IgM)	Immunoglobulin
IKK	IκB kinase
IL	Interleukin

(IL-1α, IL-1β, IL-6, IL-7, IL-8, IL-10, IL-12, IL-15, IL-21)	
IRES	Internal ribosome entry site
IRF3	IFN regulatory transcription factor 3
ISG (ISG15,ISG56)	IFN-stimulated gene
IκBα	Inhibitor of NF-κB
JAK	Janus kinase
kb	Kilobases
kDa	Kilodaltons
KIV	Killed/inactivated virus
KPNA (KPNA1, KPNA6)	Karyopherin subunit α
L	Litres
LB	Luria lysogeny broth
LB agar	LB containing agar
LBS	Lactate buffered saline
Leu	Leucine
LPS	Lipopolysaccharide
M	PRRSV unglycosylated membrane protein
MAX	SV40 immortalised, NIH minipig kidney cells expressing a d/d MHC class I haplotype
MDA5	Melanoma differentiation-associated protein 5
MDFIC	Myoblast determination protein 1 (MyoD) family inhibitor domain-containing protein
MED4	Mediator of RNA polymerase II transcription subunit 4
mg	Milligrams
MHC	Major histocompatibility complex
MIF	Macrophage migration inhibitory factor
min	Minutes
miRNA	MicroRNA
mL	Millilitres
MLV	Modified live virus
mRNA	Messenger RNA
mTOR	Mechanistic target of rapamycin
MVA-T7	Modified vaccinia Ankara expressing bacteriophage T7 RNA polymerase
MVP	Major vault protein
MW	Molecular weight
N	PRRSV nucleocapsid protein
NADPH	Nicotinamide adenine dinucleotide phosphate
NEMO	NF-κB essential modulator
NES	Nuclear export signal
NF-κB	Nuclear factor κ-light-chain-enhancer of activated B cells
NHLRC2	NHL repeat-containing protein 2

NK	Natural killer
NLRP3	Nucleotide-binding domain (NOD)-like receptor family pyrin domain-containing 3
NLS	Nuclear localisation signal/sequence
nm	Nanometres
NPC	Nuclear pore complex
NSP	Non-structural protein
NTD	N terminal domain
NUP (NUP42, NUP62, NUP93, NUP98, NUP153, NUP155, NUP210)	Nucleoporin
NXF1	Nuclear RNA export factor 1
NXT1	Nuclear transport factor 2 like export factor 1
Oligo	Oligonucleotide
ORF	Open reading frame
OTU	Ovarian tumour domain
PAK1	p21 (RAC1) activated kinase 1
PAK2	p21 (RAC1) activated kinase 2
PAM	Porcine alveolar macrophage
PAMP	Pathogen associated molecular pattern
PBS	Phosphate-buffered saline
PBS-M-T	PBS containing milk and tween
PBS-T	PBS containing tween
PCBP (PCBP1, PCBP2)	Poly r(C)-binding protein
PCP	Papain-like cysteine protease
PCR	Polymerase chain reaction
PEI	Polymer linear-polyethylenimine
pH	Potential hydrogen
PIAS (PIAS1, PIAS2, PIASx)	Protein inhibitor of activated STAT
POMP	Proteasome maturation protein
pp (pp1a, pp1ab)	Polyprotein
PRF	Programmed ribosomal frameshifting
PRR	Pattern recognition receptor
PRRS	Porcine reproductive and respiratory syndrome
PRRSV (PRRSV-1, PRRSV-2)	Porcine reproductive and respiratory syndrome virus
PSMA1	Proteasome subunit α type-1
PSMB	Proteasome subunit β type

(PSMB4, PSMB5i, PSMB8, PSMB9, PSMB10)	
RdRp	RNA-dependent RNA polymerase
RFS	Ribosomal frame shift
RIG-I	Retinoic acid-inducible gene I
RNA	Ribonucleic acid
RNase (RNase L)	Ribonuclease
RNF122	Ring finger protein 122
rpm	Revolutions per minute
rSAP	Recombinant shrimp alkaline phosphatase
RT	Room temperature
RTC	Replication and transcription complex
RVN	Reticulovesicular network
SAP	SAF-A/B, acinus and PIAS
SARS-CoV (SARS-CoV-2)	Severe acute respiratory syndrome coronavirus
SD	Synthetic defined / drop-out
SDS-PAGE	Sodium dodecyl sulphate-polyacrylamide gel electrophoresis
sec	Seconds
Ser	Serine
SF	Serum-free
sgRNA	Subgenomic mRNA
SHFV	Simian haemorrhagic fever virus
SIGLEC (SIGLEC-1, SIGLEC-10)	Sialic acid-binding immunoglobulin-type lectin
SLA	Swine leukocyte antigen
SP (SP-A, SP-D)	Surfactant protein
STAT (STAT1, STAT2, STAT3, STAT4)	Signal transducer and activator of transcription
SU1-Bel	PRRSV-1 subtype 3 strain SU1-Bel
SUMO	Small ubiquitin-like modifier
SV40	Simian vacuolating virus 40
TAB3	TAK1 binding protein 3
TAK1	Transforming growth factor-β (TGF-β) activated kinase 1
TCR	T cell receptor
Tfh	T follicular helper
Th	T helper
TID-1	Tumorous imaginal disc 1
TIM (TIM1, TIM4)	Translocase of the inner membrane
TLR	Toll-like receptor

(TLR3, TLR4, TLR7, TLR8)	
T_M	Melting temperature
TNF (TNFα)	Tumour necrosis factor
TPR	Translocated promoter region
tRNA	Transfer RNA
Trp	Tryptophan
TRS	Transcriptional regulatory sequence
U	Units
UPS	Ubiquitin-proteasome system
UTR	Untranslated region
VP	Virus protein
VSIG4	V-set and immunoglobulin domain-containing protein 4
VSV	Vesicular stomatitis virus
X-α-Gal	5-Bromo-4-chloro-3-indolyl-α-D-galactopyranoside
Y-2-h	Yeast-2-hybrid
YPDA	Yeast peptone dextrose adenine
ZF	Zinc finger
ZMIZ1	Zinc finger MIZ-type containing 1

List of Figures

List of Tables

Chapter 1: Introduction

1.1 Porcine reproductive and respiratory syndrome

The porcine reproductive and respiratory syndrome virus (PRRSV) is the causative agent of porcine reproductive and respiratory syndrome (PRRS), one of the most important infectious diseases affecting the global pig industry (Lunney *et al.*, 2016). PRRSV is endemic in most major pig-producing countries where it is responsible for major economic losses, estimated in the USA and Europe to exceed US$600 million and €1.5 billion per annum, respectively (Holtkamp *et al.*, 2013; Paz, 2015).

PRRSV infects both pigs and wild boar, and is a myelotropic virus, with the porcine alveolar macrophage (PAM) considered the primary target cell (Albina, Carrat and Charley, 1998; Morgan *et al.*, 2016). PRRSV disseminates from the lungs and infects macrophages in both lymphoid and non-lymphoid tissues, resulting in a prolonged infection in lymphoid organs (Rowland *et al.*, 2003). PRRSV is spread via direct contact or indirect contact through objects, such as clothes and tools (Pileri and Mateu, 2016). Infection with PRRSV occurs by either the respiratory route, oral route, through the mucosae or percutaneously (e.g., cuts, bites, scrapes). Methods of exposure include aerosol transmission, coitus or insemination, direct contact, accidental inoculation during medical examination, and vertical transmission during the final trimester of pregnancy (Pileri and Mateu, 2016).

PRRSV causes mild to severe respiratory disease in new-born piglets and growing pigs and reproductive failure in sows, with clinical signs including fever, pneumonia, lethargy, anorexia, stillbirth, mummified foetuses, and abortion; consequently impacting both growing and breeding sectors (Rossow, 1998; Zimmerman *et al.*, 2012).

Infection with PRRSV can also lead to more complicated diseases, since PRRSV induced-suppression of the immune system makes pigs more susceptible to secondary infections, making PRRSV a major contributor to the porcine respiratory disease complex (Opriessnig, Giménez-Lirola and Halbur, 2011; Lunney *et al.*, 2016).

New strains are constantly evolving, including more virulent strains, allowing the virus to continue to evade the host immune response and re-infect pigs. Both live

attenuated and inactivated PRRSV vaccines are available and are widely used; however, they are evidently failing to control the PRRS panzootic (Nan *et al.*, 2017).

The huge economic costs demonstrate the global importance of PRRS and the need to increase our understanding of the PRRSV to improve vaccines and other control strategies.

1.2 Porcine reproductive and respiratory syndrome virus

1.2.1 Species and subtypes

PRRSV is a member of the *Arteriviridae* family, order Nidovirales (Cavanagh, 1997), together with simian haemorrhagic fever virus (SHFV) and equine arteritis virus (EAV). There are two PRRSV species within the *Betaarterivirus* genus: *Betaarterivirus suid 1* (PRRSV-1) and *Betaarterivirus suid 2* (PRRSV-2) (Siddell *et al.*, 2019). PRRSV-1 and PRRSV-2 were formerly known as the European type and the North American type, respectively (Meng *et al.*, 1995; Huang, Zhang and Feng, 2015). PRRSV-1 emerged in the early 1990s in Western Europe (Wensvoort *et al.*, 1991), whereas PRRSV-2 appeared in the late 1980s in North America (Keffaber, 1989; Benfield and Nelson, 1992); both have since spread to almost all major pig-producing countries around the world (Nan *et al.*, 2017). PRRSV-1 strains circulate predominately in Europe (Stadejek *et al.*, 2013) and PRRSV-2 strains in North America (Shi *et al.*, 2010); both species are currently circulating in most Asian countries (Choi *et al.*, 2015; Jiang *et al.*, 2020). Additionally, for both species there are multiple subtypes; there are 4 PRRSV-1 subtypes, and multiple lineages within each subtype (Stadejek *et al.*, 2013; Balka *et al.*, 2018). Homology is approximately 55-70% between species at the nucleotide level, and approximately 85% within species (depending on gene or protein compared) (Shi *et al.*, 2010; Kappes and Faaberg, 2015; Lunney *et al.*, 2016).

Both PRRSV species are rapidly evolving (Nan *et al.*, 2017), as PRRSV has the highest evolutionary rate of all known ribonucleic acid (RNA) viruses, with a rate of 10^{-2} /site/year (Hanada *et al.*, 2005). As a result, highly pathogenic strains have sporadically emerged; in 2006, the Chinese swine industry was devastated following the emergence of a highly pathogenic PRRSV-2 strain, which killed pigs of all ages (Li *et al.*, 2007; Tian *et al.*, 2007) Highly pathogenic PRRSV-1 strains have also been identified, such as the PRRSV-1 subtype 3 strain Lena (Karniychuk *et al.*, 2010).

PRRSV-1 and PRRSV-2 both cause respiratory and reproductive disease, but PRRSV-2 is generally more virulent than PRRSV-1 (Han *et al.*, 2013; Choi *et al.*, 2015), with co-infections causing more severe disease than infections with PRRSV-1 alone (Choi *et al.*, 2015; Yang *et al*., 2020). Significant differences in virulence are also observed between strains of the same species: PRRSV-1 high pathogenic strain SU1-Bel is more virulent than PRRSV-1 strains 215-06 and Lelystad, causing more pulmonary and lymphoid lesions and a higher number of infected cells (Morgan *et al.*, 2016).

Possible reasons for differences in virulence include genetic determinants, expanded cell tropism, use of alternative entry receptors and variation in immune responses (Ruedas-Torres *et al.*, 2021). The presence of a large deletion in the NSP2 coding region of approximately 30 amino acids correlates to highly virulent strains (Tian *et al.*, 2007), although this has been observed in some low virulent strains (Li *et al.*, 2010). NSP9 and NSP10 have been suggested to be determinants of virulence (Y.Li, Zhou, *et al.*, 2014), with amino acids NSP9 586 and 592 having a role in the pathogenicity of PRRSV-2 strain HuN4 (Xu *et al.*, 2018). With more virulent strains, there is a higher number of infected cells in various tissues compared to low virulence strains (Morgan *et al.*, 2016), with an expanded tissue tropism also observed (Li *et al.*, 2012). It postulated than more virulent strains may use alternative entry receptors, as PRRSV-1 Lena is able to infect cells lacking 2 of the main PRRSV entry receptors (sialoadhesin and cluster of differentiation (CD) 163 (CD163) (van Breedam *et al.*, 2010; Frydas *et al.*, 2013). Additionally, a PRRSV strain can use both the traditional and alternative entry receptors, but the rate of infection differs between the two (Xie *et al.*, 2018).

More virulent strains trigger stronger inflammatory cytokine responses (tumour necrosis factor (TNF) α (TNFα), interleukin (IL) -6 and IL-1α) resulting in more clinical signs and more severe lung tissue damage (X.Li *et al.*, 2017). The relationship between the type I interferon (IFN) pathway and PRRSV is more complex: both low and high virulence strains inhibit it (Albina, Carrat and Charley, 1998; Baumann *et al.*, 2013), but in some studies IFN-α levels increase with viral load (X.Li *et al.*, 2017). Multiple virulent PRRSV-2 strains additionally have been shown to promote an anti-inflammatory response, causing increases in IL-10 (Sánchez-Carvajal *et al.*, 2020), and

infection with PRRSV-1 Lena increases the level of Fox3p positive cells (Sánchez-Carvajal *et al.*, 2020).

1.2.2 Virus structure

PRRSV is a small enveloped spherical or oval virus (diameter ~55 nanometres (nm)) with a single stranded, positive sense, RNA genome (Dokland, 2010; Snijder, Kikkert and Fang, 2013). The PRRSV genome is approximately 15.4 kilobases (kb) in length, 5' capped and 3' polyadenylated (Snijder, Kikkert and Fang, 2013). It is polycistronic and has 11 open reading frames (ORFs), which code for at least 16 non-structural proteins (NSPs) and 8 structural proteins (**Figure 1.1**). ORF1a and ORF1b encode NSP1α, NSP1β, NSP2-6, NSP2N, NSP2TF, NSP7α, NSP7β and NSP8-12. ORF2-7 code for the structural proteins: envelope (E) protein; glycosylated membrane proteins (glycoproteins (GP)) GP2a, GP3, GP4, GP5 and GP5a; non-glycosylated membrane protein (M); and nucleocapsid (N) protein (Rascón-Castelo *et al.*, 2015).

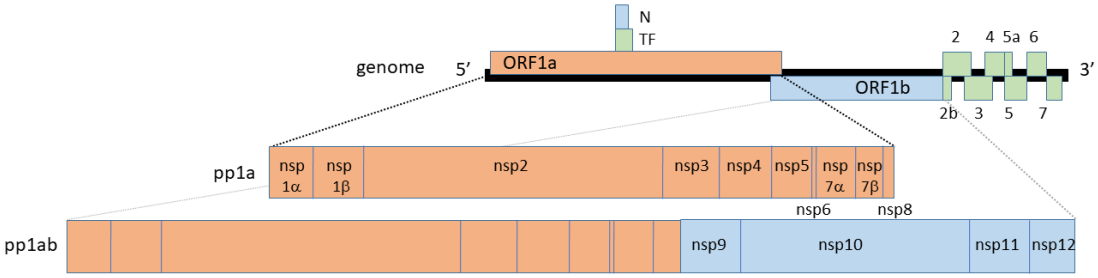

Figure 1.1: Schematic representation of the PRRSV genome. NSP1-8 are translated from ORF1a to yield polyprotein 1a (pp1a), and NSP9-12 are translated from ORF1b to yield pp1ab (a C-terminal extension of pp1a produced through a -1 frameshift); both are subsequently proteolytically cleaved to release the individual NSPs. NSP2N and NSP2TF are produced by -1 and -2 frameshifts, respectively. Structural proteins are translated individually from subgenomic mRNAs carrying ORF2-7.

The viral genome is packaged by N proteins, which in turn is encased in a lipid bilayer envelope containing surface GPs and membrane proteins (**Figure 1.2**) (Lunney *et al.*, 2016). GP5 and M are the major envelope proteins, forming di-sulphide linked heterodimers, and GP2a, GP3 and GP4 are the minor envelope proteins present as

heterotrimers and heterodimers; E and GP5a are also minor envelope proteins, with E associating with the heterotrimer (Snijder, Kikkert and Fang, 2013).

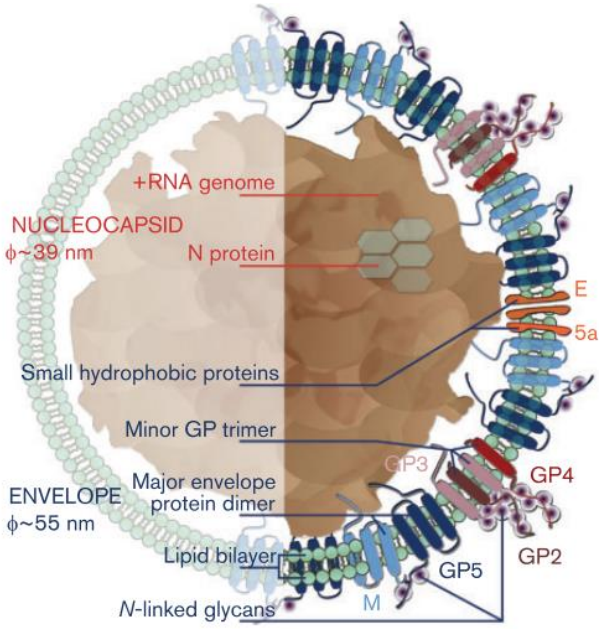

Figure 1.2: Arterivirus structure. Structure of an arterivirus particle, such as PRRSV. *Figure 7e used with permission from Journal of General Virology,* (Snijder, Kikkert and Fang, 2013).

1.2.3 Viral life cycle and replication

1.2.3.1 Entry

PRRSV primarily infects PAMs but can infect other members of the monocyte-macrophage lineage, such as macrophages in lymphoid tissues and the placenta (van Breedam *et al.*, 2010). The virus uses a range of membrane-associated entry mediators for either attachment, internalisation, or endocytosis into the cell (**Table 1.1**). The most important receptors are heparin sulphate, sialoadhesins and CD163 (van Breedam *et al.*, 2010).

Table 1.1: List of cellular receptors of PRRSV and their functions during PRRSV infection.

Receptor name	Function during virus infection	Interacting counterpart on PRRSV virion	References
Heparan sulphate	Initial PRRSV attachment	Disulphide linked M/GP5 complex	(Delputte *et al.*, 2002; Delputte, Costers and Nauwynck, 2005)
Vimentin	Opsonise and endocytosis of PRRSV virion	N protein	(Zheng *et al.*, 2021)
CD151	Unknown	3' UTR RNA of PRRSV	(Shanmukhappa, Kim and Kapil, 2007)
CD163	PRRSV entry	GP2a and GP4	(Calvert *et al.*, 2007; Das *et al.*, 2010)
Sialic acid-binding immunoglobulin-type lectins 1 (SIGLEC-1) (*CD169*, *sialoadhesin*)	Virion attachment and endocytosis	Sialic acids on the surface of PRRSV GP5 protein	(Vanderheijden *et al.*, 2003; Delputte, Costers and Nauwynck, 2005)
SIGLEC-10	Virion attachment and endocytosis	Sialic acids on the surface of PRRSV GP5 protein	(Xie *et al.*, 2017)
CD209 (*DC-SIGN*)	Unknown	Unknown	(Huang *et al.*, 2009)
Non-muscle myosin heavy chain 9	Endocytosis of PRRSV virion	GP5	(Gao *et al.*, 2016)
Translocase of the inner membrane 1 (TIM1) and TIM4	Macropinocytosis of PRRSV virion	Phosphatidylserine (PS) in PRRSV envelope	(Wei *et al.*, 2020)
Heat shock cognate 71 kDa protein (HSC70) (*HSPA8, HSP73*)	Attachment and internalisation	GP4	(Wang *et al.*, 2022)

Alternative protein names are shown italicised in brackets. *Table 1, used with permission from Frontiers in Microbiology,* (Nan *et al.*, 2017). Additional information and references have been added.

The following is the current accepted model of PRRSV entry (van Breedam *et al.*, 2010). The virus initially attaches to the cell using its GP5/M complex to bind heparan sulphate. This interaction concentrates virus on the cell surface (Delputte, Costers and Nauwynck, 2005), helping the virus to subsequently bind to the sialic acid-binding

immunoglobulin-type lectin (SIGLEC) 1 (SIGLEC-1) N terminal immunoglobulin domain via sialic acids on GP5 (Delputte and Nauwynck, 2004; van Breedam *et al.*, 2010). However, recent studies have shown the knockout of SIGLEC-1 had no effect on viraemia in PRRSV-infected pigs, suggesting other sialoadhesins may be involved in entry (Prather *et al.*, 2013). Another member of the sialoadhesin family, SIGLEC-10, is an alternative entry receptor to SIGLEC-1 (Xie *et al.*, 2017), and different species and strains of PRRSV have different preferences for which receptor combination they use during entry (Xie *et al.*, 2018). The virus-receptor complex is then internalised by clathrin-mediated endocytosis (Nauwynck *et al.*, 1999). Uncoating and genome release occurs in the early endosome and is dependent on acidification of the endosome and CD163 (van Gorp *et al.*, 2008). CD163 interacts with GP2 and GP4 (Das *et al.*, 2010) using its scavenger receptor cysteine-rich 5 domain (van Gorp *et al.*, 2010), but the exact mechanism for uncoating is unknown. Deletion of CD163 scavenger receptor cysteine-rich 5 domain protects PAM and pigs from infection (Burkard *et al.*, 2017). Non-muscle myosin heavy chain 9 interacts with CD163, as well as PRRSV GP5, and is essential for efficient PRRSV infection (Gao *et al.*, 2016). A new study has shown heat shock cognate protein 71 kilodalton (kDa) (HSC70) to be essential for PRRSV attachment and internalisation, as HSC70 binds to GP4 and is involved in clathrin-mediated endocytosis of the PRRSV virion (Wang *et al.*, 2022).

Vimentin binds to PRRSV N (Kim *et al.*, 2006), but only in the presence of annexin A2 (Chang *et al.*, 2018), and expression of vimentin on the surface non-susceptible cell lines renders them susceptible to infection (Kim *et al.*, 2006). The role of vimentin in entry is not fully understood, but post-entry PRRSV induces vimentin phosphorylation and reorganisation to enhance viral replication (Zheng *et al.*, 2021). The exact roles of CD151 and CD209 in PRRSV entry have not yet been identified. CD151 binds to the 3’ untranslated region (UTR) of PRRSV RNA, and cells transfected to express CD151 became susceptible to PRRSV infection, whereas knockdown of CD151 in susceptible cells reduced infection (Shanmukhappa, Kim and Kapil, 2007). Cells stably expressing porcine CD209 enhanced PRRSV transmission (Huang *et al.*, 2009). Additionally, unidentified serine proteases and the aspartic protease cathepsin E have also been

implicated in uncoating, although their specific roles are unknown (Misinzo, Delputte and Nauwynck, 2008).

Recently, an alternative method of cell entry for PRRSV was discovered – macropinocytosis. PRRSV uses viral apoptotic mimicry by incorporating phosphatidylserine into the viral envelope, making the viral particle appear to be apoptotic debris. The exposed phosphatidylserine is recognised by T-cell immunoglobulin and mucin domain (TIM) 1 (TIM1) and TIM4, inducing CD163 dependent micropinocytosis (Wei *et al.*, 2020).

1.2.3.2 Genome replication, sgRNA synthesis and protein expression

In the cell, PRRSV replication has three key steps: rearrangement of host membranes, synthesis and expression of genomic RNA (gRNA), and synthesis and expression of subgenomic mRNA (sgRNA) (Kappes and Faaberg, 2015). Expression of gRNA yields the NSPs, and expression of sgRNA the structural proteins. PRRSV uses different strategies to express NSPs and structural proteins to control the timing and levels of protein expression. An overview of PRRSV gRNA and sgRNA replication and protein synthesis is provided in **Figure 1.3**.

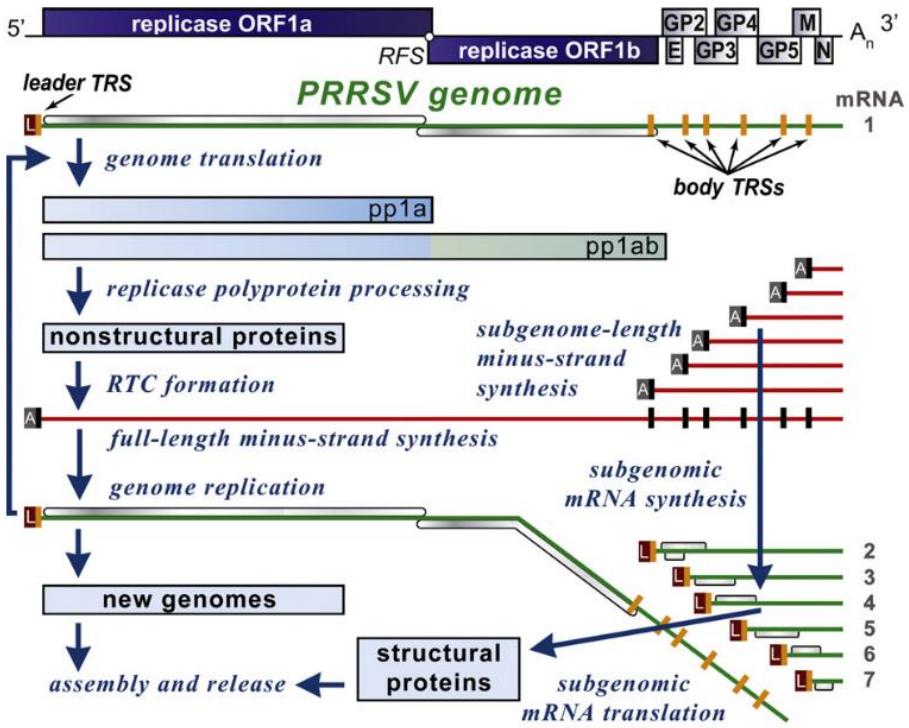

Figure 1.3: Overview of the PRRSV replicative cycle, highlighting the key steps in viral RNA and protein synthesis. Translation of the PRRSV genome produces the two polyproteins, pp1a and pp1b, which are subsequently cleaved to produce the NSPs. These form the replication and transcription complex (RTC) that synthesises gRNA and sgRNA. The RTC binds to the 3' end of the genome and begins -RNA synthesis until a body transcription-regulating sequence (TRS), shown in orange, is reached. Continuation of transcription and full read through of all TRSs results in -gRNA, which is then transcribed into +gRNA. In sgRNA synthesis, transcription is halted and instead the body TRS interacts with the 5' leader TRS sequence (L), translocating the RTC to the leader and RNA synthesis continues. The -sgRNA produced depends on the TRS at which transcription was halted; these then act as templates for +sgRNA synthesis. *Figure 3 reprinted from* (Fang and Snijder, 2010) *with permission from Elsevier.*

The PRRSV gRNA is translated immediately upon uncoating as it is a capped, positive sense RNA with a poly A tail like host messenger RNA (mRNA); this produces polyprotein1a (pp1a), and after a frame shift, pp1ab. pp1a and pp1ab are cleaved to produce the NSPs (**Section 1.3.1**).

Arterivirus double membrane vesicles (DMVs) are derived from the endoplasmic reticulum (ER) and are the site of viral genome replication (Pedersen *et al.*, 1999; W. Zhang *et al.*, 2018). The outer membranes of arterivirus DMVs are connected to both

each other and the ER, forming a reticulovesicular network (RVN) (Knoops *et al.*, 2012); however, it has been suggested that the DMV connection to the ER is an intermediate step in the formation of fully isolated DMVs (W. Zhang *et al.*, 2018). NSP2 and NSP3 are required to induce perinuclear DMVs (Snijder *et al.*, 2001), but the exact mechanism of their formation is unknown. NSP5, though not essential, regulates membrane curvature and DMV size (van der Hoeven *et al.*, 2016). NSP2, NSP3 and NSP5 have been predicted to have hydrophobic membrane spanning domains (Fang and Snijder, 2010; van der Hoeven et al., 2016), and are thought to form a scaffold that recruits the replication transcription complex (RTC) to the DMVs (**Figure 1.4**) (van der Meer *et al.*, 1998; Nan *et al.*, 2018). Within the scaffold, NSP2 and NSP5 both interact with NSP3 (Nan *et al.*, 2018). Use of DMVs by viruses carries multiple benefits: it creates an optimal microenvironment for RNA synthesis; compartmentalises and therefore separates different life cycle stages; and can prevent or delay detection of pathogen associated molecular patterns (PAMPs) generated during replication, such as double-stranded RNA (dsRNA) (van der Hoeven *et al.*, 2016). Additionally, PRRSV dsRNA and N protein has also been found in autophagosomes, suggesting they also may be a site of viral replication (W. Zhang *et al.*, 2018).

ORF1b encodes the core replicative machinery of PRRSV - NSP9, NSP10 and NSP11 - which are the RNA-dependent RNA polymerase (RdRp), RNA helicase and nidovirus uridylate specific endoribonuclease (EndoU), respectively (Ulferts and Ziebuhr, 2011). NSP9 N terminal domain (NTD) is a nidovirus RdRp-associated nucleotidyltransferase (Lehmann *et al.*, 2015), and RdRp activity is found in its C terminal domain (Fang and Snijder, 2010). The RdRp active site contains a nidovirus specific Serine-Aspartate-Aspartate (Ser-Asp-Asp or SDD) motif; mutations in this region do not impair PRRSV gRNA replication, but affect sgRNA synthesis (Zhou *et al.*, 2011). Additionally, NSP9 RdRp does not have 3' proofreading activity, which contributes to a high mutation rate (Lauber *et al.*, 2013). NSP10, as well as helicase activity, has an N terminal zinc-binding domain and ATPase activity (Bautista *et al.*, 2002). Although not directly involved in replication, the zinc-binding domain is crucial for both ATPase and helicase activities (Seybert *et al.*, 2000). NSP11 is important for

PRRSV replication, as mutations in its conserved residues reduce both gRNA and sgRNA synthesis, with a stronger effect on sgRNA; however, its exact role in RNA synthesis is unknown (Posthuma *et al.*, 2006). NSP11 structure and immunomodulatory functions are discussed in **Section 1.3.2.** The exact function of NSP12 is unknown, but it is essential for sgRNA synthesis, as deletion of NSP12 or mutation of NSP12 cysteines 35 and 79 abolishes sgRNA production (T. Y. Wang *et al.*, 2019). Additionally, it prevents ubiquitin-proteasomal degradation of karyopherin α (KPNA) 6 (KPNA6), a cellular transport receptor that enhances viral replication and is essential for nuclear translocation of NSP1β (Yang *et al.*, 2018).

NSP9 and NSP10 are the core components of the PRRSV RTC, a complex of viral proteins, viral RNA and host cell proteins which mediate both gRNA and sgRNA synthesis (Nan *et al.*, 2018). The exact PRRSV RTC composition and interactions involved are unknown, but NSP9 and NSP12 have been identified as interaction hubs that between them interact with NSP1α, NSP1β, NSP3, NSP5, NSP7α, NSP7β, NSP8, NSP10 and NSP11 (**Figure 1.4**) (Nan *et al.*, 2018). The PRRSV NSP interactome is discussed further in **Section 1.3.5**. Related arterivirus EAV NSPs NSP9, NSP10, NSP1, NSP2, NSP3 and NSP5 co-sediment with the RTC, suggesting they are part of the RTC; additionally, membranes and an unidentified conserved host factor have been shown to be essential for EAV RTC function (Van Hemert *et al.*, 2008). EAV N protein has also been shown to co-localise with the RTC, but it, along with all the other structural proteins, are not essential for RNA synthesis (Molenkamp *et al.*, 2000). It is not known how PRRSV RTC initiates replication and transcription (Kappes and Faaberg, 2015). NSP10 uses energy from ATP hydrolysis to unwind dsRNA in a 5’ to 3’ direction (Bautista *et al.*, 2002), allowing NSP9 to synthesis new RNA in a 3’ to 5’ direction; how they coordinate whilst functioning in opposite directions is unclear (Fang and Snijder, 2010).

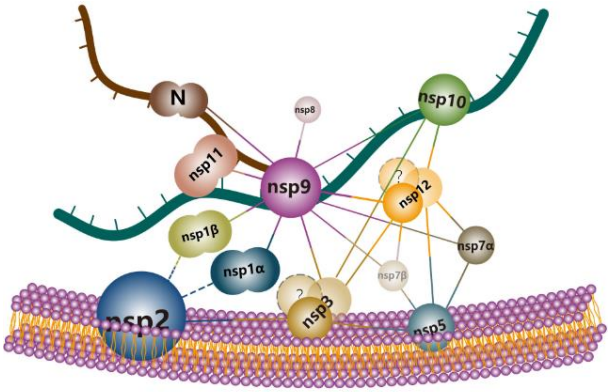

Figure 1.4: A model of PRRSV replication and transcription complex in DMVs. PRRSV NSP2, NSP3, and NSP5 interact to form a membrane-bound scaffold for the RTC, with NSP9 and NSP12 acting as interaction hubs. Figure shows interactions identified in (Nan *et al.*, 2018) (solid lines) and identified by others (dashed lines). *Figure 5, used with permission from Frontiers in Microbiology,* (Nan *et al.*, 2018).

PRRSV synthesises gRNA continuously and sgRNA discontinuously (Fang and Snijder, 2010; Kappes and Faaberg, 2015) (**Figure 1.5**). gRNA synthesis generates genome copies to be packaged into new virus particles. sgRNAs are required to produce PRRSV structural proteins; they contain both the 5' and 3' untranslated regions, have a poly A tail and encode one or more ORF from ORF2-7. Starting at the 3' end, the RTC uses +gRNA as a template to produce -gRNA and -sgRNA. Synthesis continues until the RTC reaches a body transcription-regulating sequence (TRS) near the 5' end of each ORF 2-7. Body TRSs are conserved heptanucleotides that form stem loops which halt transcription. At each TRS, RTC either continues transcription until the next TRS/end of the gRNA, or translocates and binds the conserved leader TRS (UUAACC) hairpin at the 3' end of the 5'UTR (**Figure 1.5**) (Meulenberg, de Meijer and Moormann, 1993; Snijder, Kikkert and Fang, 2013). Continuation of transcription and full read through of all TRSs results in -gRNA, which is then transcribed into +gRNA. In sgRNA synthesis, the body TRS instead forms a kissing-loop interaction with the leader TRS sequence through complementary base pairing. This allows the RTC to translocate to the 5' end of gRNA and transcription resumes from the leader TRS, producing -sgRNA. The RTC then synthesises +sgRNA using the -sgRNAs as templates, which are then translated by host cell machinery to produce structural proteins. The structural protein translated depends on the sgRNA produced and therefore on the TRS at which transcription was halted.

It is suspected that PRRSV NSP1α regulates the switch between continuous and discontinuous RNA synthesis (Fang and Snijder, 2010), as it has been shown to be essential for sgRNA synthesis (Kroese *et al.*, 2008), and NSP1 regulates the switch for related arterivirus, EAV (Nedialkova, Gorbalenya and Snijder, 2010). There is limited sequence similarity between PRRSV and EAV (Tian *et al.*, 2012), but the NSP1 papain-like cysteine protease (PCP) α (PCPα) and PCPβ motifs, required for self-cleavage of NSP1, are relatively conserved between arteriviruses (Han *et al.*, 2014); however, unlike PRRSV NSP1, EAV NSP1 does not cleave into NSP1α and NSP1β as the PCPα in EAV NSP1 is inactive.

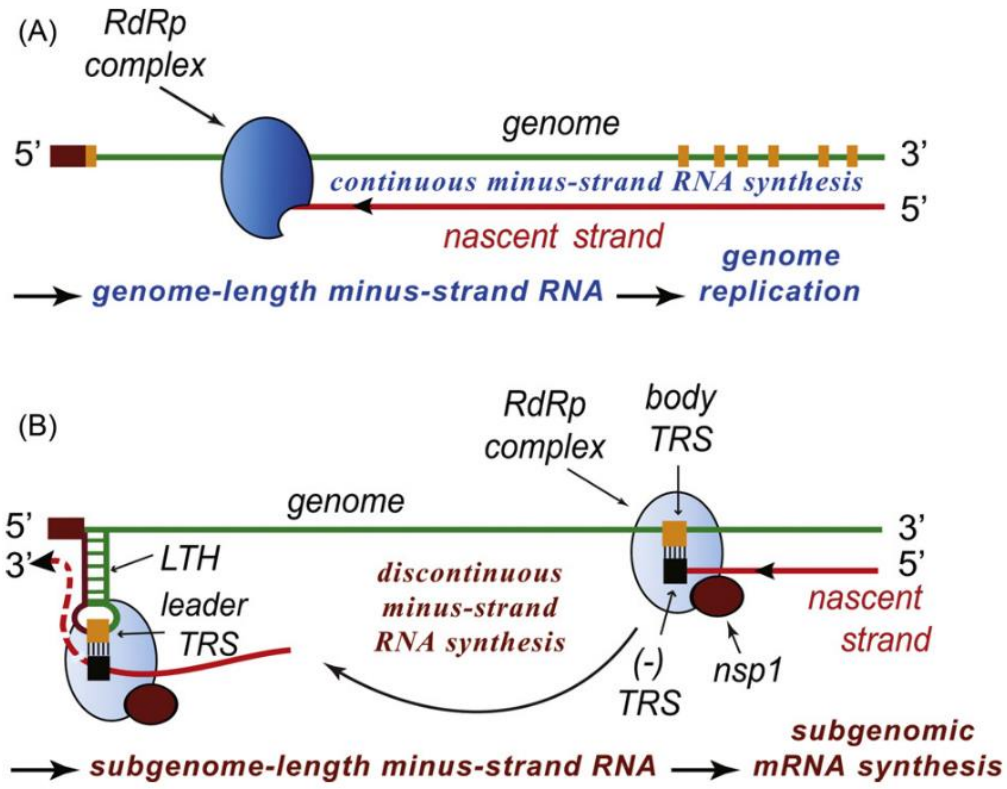

Figure 1.5: Arterivirus NSP1 modulates genome replication and transcription at the level of minus-strand RNA synthesis. The viral RTC, labelled here as RdRp complex, synthesises RNA both continuously (**A**) and discontinuously (**B**) to produce gRNA and sgRNA, respectively. NSP1 is required for sgRNA synthesis, but not for gRNA synthesis; for PRRSV NSP1α is required. In sgRNA synthesis, transcription is halted at a body TRS. The body TRS interacts with the 5' leader TRS sequence, translocating the RTC, and -sgRNA synthesis continues. *Figure 4, reprinted from* (Fang and Snijder, 2010) *with permission from Elsevier; adapted from* (Nedialkova, Gorbalenya and Snijder, 2010).

PRRSV RNA, like other arteriviruses, has a 5' cap and 3' poly A tail. However, as arteriviruses replicate in the cytoplasm and capping of host mRNA occurs in the nucleus (Ramanathan, Robb and Chan, 2016), they cannot acquire a 5' cap using the host cell nuclear machinery (Fang and Snijder, 2010). None of the arterivirus NSPs have been shown, nor predicted, to possess one of the three enzymatic activities – RNA triphosphatase, RNA guanylyltransferase and guanine-N7 methyltransferase – required for capping. The related arterivirus SHFV genome contains a type 1 5' cap structure with a methylation pattern that differs to host mRNA caps, implying it originates from outside the nucleus (Sagripanti, Zandomeni and Weinmann, 1986); therefore, PRRSV is also suspected to have a putative type 1 cap structure in the 5' UTR (Kappes and Faaberg, 2015). The exact mechanism, signals and proteins involved have yet to be fully investigated.

1.2.3.3 Assembly and Exit

PRRSV assembly and exit is not completely understood, with current knowledge based on a combination of PRRSV and EAV studies. Genome encapsidation and assembly is thought to occur at the DMVs and ER (the RVN), as PRRSV N protein and dsRNA localised to both and newly assembled viral particles are linked to or enveloped by the ER (W. Zhang *et al.*, 2018). Additionally, a network of EAV N protein tubules intertwine with the RVN (Knoops *et al.*, 2012). The EAV nucleocapsid is then wrapped by either the smooth ER or Golgi body, which contains the envelope proteins; virions are then transported via the secretory pathway to the plasma membrane and released by exocytosis (Dea *et al.*, 1995; Snijder, Kikkert and Fang, 2013). Furthermore, exosomes have been shown to contain PRRSV genomes and partial proteins and are able to transmit the virus (T. Wang *et al.*, 2017).

The current model for PRRSV life cycle is summarised below in **Figure 1.6**, but more studies are required on PRRSV specifically, rather than EAV and other arteriviruses, to confirm this (Kappes and Faaberg, 2015). To achieve successful replication, PRRSV also modulates the immune response throughout infection using both its structural and NSPs (**Section 1.3.2**).

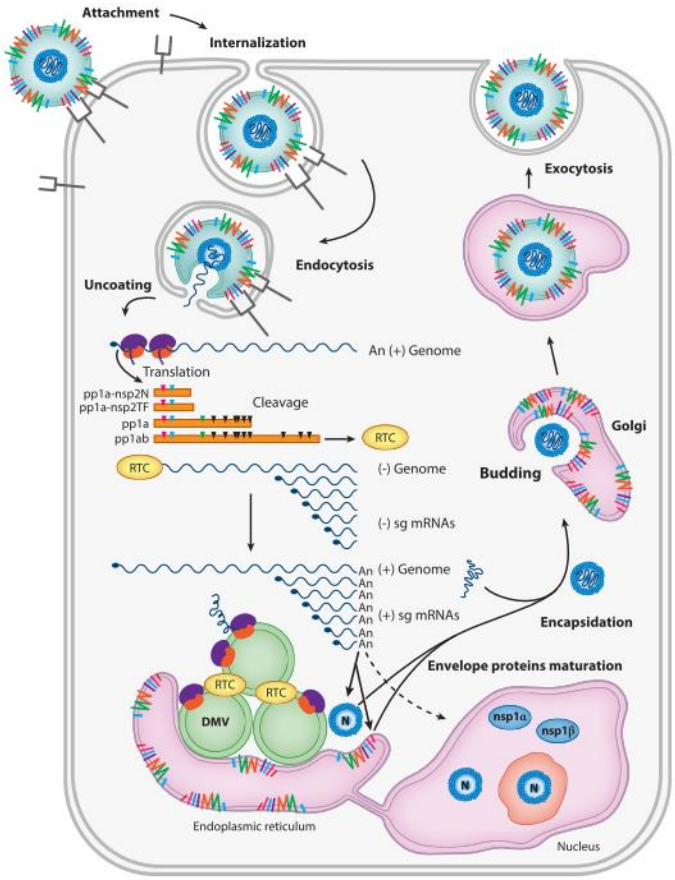

Figure 1.6: Porcine reproductive and respiratory syndrome virus (PRRSV) replication cycle. PRRSV enters cells by receptor-mediated endocytosis. After uncoating, the genome is translated by host cell machinery to produce pp1a, pp1a-NSP2TF, pp1a-NSP2N, pp1ab; these are subsequently cleaved to produce the NSPs. NSPs form the RTC, which uses the gRNA template to produce gRNA for packaging into new virions and sgRNA for structural protein synthesis. Nucleocapsids, containing gRNA, become enveloped by budding from intracellular membranes; new virus particles are then released by exocytosis. *Figure 3, republished with permission of Annual Review of Animal Biosciences, from* (Lunney *et al.*, 2016)*; permission conveyed through Copyright Clearance Center,Inc.*

1.2.4 PRRSV control and vaccines

Current measures to control PRRSV include management, biosecurity, test and removal, and vaccination (Charerntantanakul, 2012). However, given the global prevalence of PRRSV and the number of new outbreaks, these are failing to control the PRRS panzootic (Nan *et al.*, 2017).

Both modified live virus (MLV) and killed/inactivated virus (KIV) PRRSV vaccines are available and are widely used. MLV vaccines have been licensed for both PRRSV-1 and PRRSV-2, but none provide complete protection, inducing weak humoral and cell mediated responses (Nan *et al.*, 2017). They can provide effective late protection, between three-four weeks post vaccination, against closely related strains, but there is limited cross protection between more divergent strains or species (Charerntantanakul, 2012) and outbreaks have been reported in vaccinated herds (Mengeling, Lager and Vorwald, 1998).

Even if they can provide some protection, MLV vaccines have safety issues. MLV vaccinated pigs and piglets born to vaccinated sows have been shown to be viraemic for up to four weeks post-immunisation, allowing the spread of the vaccine virus to naïve pigs (Charerntantanakul, 2012). Rapid virus evolution also means that live attenuated vaccine strains are prone to revert to virulence and have also been reported to recombine with wild-type virus (Bøtner *et al.*, 1997; Wenhui *et al.*, 2012; A. Wang *et al.*, 2019). KIV vaccines are safer than MLV vaccines, but lack efficacy (Zuckermann *et al.*, 2007), as they fail to induce production of neutralising antibodies (Kim *et al.*, 2011) or cell mediated responses (Bassaganya-Riera *et al.*, 2004). Alternative vaccine types, such as subunit, deoxyribonucleic acid (DNA) and virus vectored, are also under development (Nan *et al.*, 2017).

Current vaccines lack efficacy for multiple reasons. The virus is constantly mutating and evolving, making it difficult to produce vaccines capable of protecting against the ever-expanding diversity of circulating PRRSV strains (Nan *et al.*, 2017); furthermore, it is not known what the correlates of protection are for PRRSV (Montaner-Tarbes *et al.*, 2019). Numerous studies suggest GP5 as the major neutralising antibody target, with M, GP2a, GP3 and GP4 also shown to contain virus neutralising epitopes for some strains (Nan *et al.*, 2017). PRRSV also shields GP5 neutralising epitopes by

'glycan shielding' to impair neutralising antibodies (Jiang *et al.*, 2007). Additionally, the vaccines fail to induce strong immune responses due to immunomodulation by PRRSV structural and NSPs (Kimman *et al.*, 2009). As all the interactions and mechanisms involved have yet to be fully elucidated, it is difficult to rationally attenuate PRRSV for use in vaccines.

Given the economic repercussions of PRRSV, safer and more efficacious vaccines are urgently needed. An improved understanding of virus-host interactions that lead to immunomodulation could aid in the design of improved vaccines.

1.3 Functions and interactions of PRRSV non-structural proteins

1.3.1 Non-structural proteins

PRRSV produces 16 NSPs, which are the first proteins to be expressed during infection and are involved in viral replication and/or modulating the host immune responses (Rascón-Castelo *et al.*, 2015). NSP1-8 are translated from ORF1a to yield pp1a and NSP9-12 are translated from ORF1b to yield pp1ab (a C-terminal extension of pp1a), which are both proteolytically cleaved by NSP proteases to release the individual NSPs. NSP1α, NSP1β, NSP2 and NSP4 are the non-structural proteases. NSP1α, NSP1β and NSP2 cleave themselves off pp1a; NSP4 cleaves NSP3-12 (Fang and Snijder, 2010). ORF1b is accessed through a -1 ribosomal frame shift (RFS) at a frequency of 20% (den Boon *et al.*, 1991). PRRSV also produces NSP2N and NSP2TF through -1 and -2 RFSs, respectively, with a frequency of 6-7% for -1 RFS and 16-20% for -2 RFS (Fang, Ying, Treffers, *et al.*, 2012; Li, Shang, *et al.*, 2018). For both PRRSV species, NSP2 is the most variable NSP with an identity of 24.4 – 28.0% due to its hypervariable region, which can accommodate large deletions (Zhou *et al.*, 2009); between species, NSP9 is the most conserved NSP with an identity of 73.2% (Rascón-Castelo *et al.*, 2015).

A summary of NSP known or predicted functions is listed in **Table 1.2**. Immunomodulation is discussed in **Section 1.3.2**; NSP1α and NSP1β are discussed in further detail in **Sections 1.3.3** and **1.3.4**.

Table 1.2: PRRSV NSP functions.

NSP	Known or predicted functions	References
NSP1α	Regulator of sgRNA synthesis Immunomodulation	(Kroese *et al*., 2008)
NSP1β	Transactivation of ribosomal frameshifting Immunomodulation	(Y. Li, Treffers, *et al.*, 2014)
NSP2	NSP4 co-factor Membrane modification Immunomodulation	(Wassenaar *et al.*, 1997)
NSP2N	Immunomodulation	(Li, Shang, et al., 2018)
NSP2TF	Immunomodulation	(Li, Shang, et al., 2018)
NSP3	Membrane modification Induces autophagy	(Zhang, Chen, *et al.*, 2019)
NSP4	Main protease Immunomodulation	
NSP5	Membrane modification Immunomodulation Induces autophagy	(Yang *et al.*, 2017) (Zhang, Chen, *et al.*, 2019)
NSP6	ND	
NSP7α	ND	
NSP7β	ND	
NSP8	N terminal extension of NSP9	(Y. Liu *et al.*, 2018)
NSP9	RNA-dependant RNA polymerase	
NSP10	RNA helicase Nucleoside-triphosphatase (NTPase) Inducer of apoptosis	(Yuan *et al.*, 2016)
NSP11	Endoribonuclease (EndoU) sgRNA and gRNA synthesis Immunomodulation	(Posthuma *et al.*, 2006) (An *et al.*, 2020)
NSP12	sgRNA synthesis Supports viral replication	(T. Y. Wang *et al.*, 2019) (Yang *et al.*, 2018)

Information obtained from Table 1 (Fang and Snijder, 2010) as well as the additional noted references. Key: ND – unknown function.

1.3.2 Modulation of the host immune response by PRRSV NSPs

PRRSV interferes with both the innate and adaptive immune responses by using multifunctional non-structural and structural proteins (Huang, Zhang and Feng, 2015). Previous studies have shown that NSP1α, NSP1β, NSP2, NSP2N, NSP2TF, NSP4, NSP5 and NSP11, as well as structural protein N, are capable of modulating host cell responses.

Between them, NSP1α and NSP1β have been shown to modulate both the innate and adaptive immune response. NSP1α downregulates swine leukocyte antigen (SLA) surface expression (porcine major histocompatibility complex (MHC)), and both prevent production of type I IFN and TNF, as well as inhibiting nuclear factor κ-light-chain-enhancer of activated B cells (NF-κB) signalling, as discussed in further detail in **Sections 1.3.3** and **1.3.4**.

NSP2 is a PCP with four domains: an NTD with PCP activity; a hypervariable central region; C terminal hydrophobic domain; and a C terminal tail (Rascón-Castelo *et al.*, 2015). The PCP NTD is also a member of the ovarian tumour domain (OTU) family and possesses both de-ubiquitinating and deISGylating activity (Sun *et al.*, 2010). NSP2 cleaves itself away from pp1a using its cysteine protease domain (Han, Rutherford and Faaberg, 2009). NSP2 prevents type I IFN production by interfering with toll-like receptor (TLR) and retinoic acid-inducible gene I (RIG-I) signalling pathways using its OTU domain (An *et al.*, 2020). Additionally, it inhibits IFN regulatory transcription factor 3 (IRF3) and NF-κB activation to prevent IFN-β production. NSP2 has been found to be involved in inducing host protein shutoff via attenuation of the mechanistic target of rapamycin (mTOR) signalling pathway (Li, Fang, *et al.*, 2018).

NSP2N and NSP2TF are produced by -1 and -2 frameshifts respectively and are truncations of NSP2 (Fang, Ying, Treffers, *et al.*, 2012). All three contain the NTD with PCP activity and OTU and were shown to inhibit expression of IFN-β (Fang, Ying, Treffers, *et al.*, 2012; Li, Shang, *et al.*, 2018).

NSP4 is a serine proteinase with three domains and is the main protease of PRRSV. Domains I and II form the active site containing a catalytic triad of His-Asp-Ser (Tian *et al.*, 2009), which it uses to process pp1a and pp1ab to release NSP3-12 (Snijder *et*

al., 1996). NSP4 downregulates SLA-I expression to prevent antigen presentation (Qi *et al.*, 2017), as well preventing both IFN-β production and NF-κB activation by cleaving NF-κB essential modulator (NEMO) (Huang *et al.*, 2014). NSP4 also induces apoptosis late in infection, by activating pro-apoptotic Bcl 2 interacting mediator of cell death and inducing degradation of anti-apoptotic protein Bcl-extra large (Bcl-xL) (Yuan *et al.*, 2016).

NSP5 is a hydrophobic transmembrane protein; using its C terminal domain, it causes signal transducer and activator of transcription (STAT) 3 (STAT3) degradation by the ubiquitin-proteasomal pathway (Yang *et al.*, 2017). Additionally, it can induce autophagy and subsequently autophagic cell death (Yang *et al.*, 2015; Zhang, Chen, *et al.*, 2019).

NSP7 (α/β was unspecified), NSP1α and NSP9 have been shown recently to upregulate expression of the E3 ubiquitin ligase ring finger protein 122 (RNF122) (Sun *et al.*, 2022). NSP7 and NSP1α downregulate the helicase like transcription factor, whereas NSP9 targets the transcription E2F complex, both of which negatively regulate expression of RNF122. RNF122 ubiquitinates NSP4, increasing its stability and therefore viral replication, as well as the pattern recognition receptor (PRR) melanoma differentiation-associated protein 5 (MDA5) leading to its proteasomal degradation (Sun *et al.*, 2022).

NSP11 is an EndoU, an enzyme unique to the order *Nidovirales* (Nedialkova *et al.*, 2009), and has de-ubiquitinating activity (D. Wang *et al.*, 2015). It has two subdomains and forms an asymmetric dimer (Y. Shi *et al.*, 2016). NSP11 inhibits IFN-β, IRF3 and NF-κB promoters (Beura *et al.*, 2010; X. Shi *et al.*, 2016). It modulates type I IFN and NF-κB signalling pathways by inducing STAT2 degradation to prevent IFN-stimulated gene (ISG) production (Yang *et al.*, 2019), and by de-ubiquitinating inhibitor of NF-κB (IκBα) to inhibit NF-κB activation (D. Wang *et al.*, 2015). Additionally, NSP11 inhibits the nucleotide-binding domain (NOD)-like receptor family pyrin domain-containing 3 (NLRP3) inflammasome to prevent interleukin-1β production (C. Wang *et al.*, 2015).

Although immunomodulatory functions and interactions have been identified for multiple NSPs, not all have been fully characterised. Moreover, it is likely that additional interactions and functions remain to be discovered, as illustrated by a co-immunoprecipitation and mass spectrometry study that identified 285 host proteins that potentially interact with NSP2 (L. Wang *et al.*, 2014). Since PRRSV is incredibly successful at evading the immune response, knowledge of such interactions could be crucial in improving vaccines.

1.3.3 NSP1α

NSP1α is a 19 kDa protein, that forms homodimers and has three domains: N terminal zinc finger (ZF) domain, PCP domain and a C terminal extension (CTE) domain (**Figure 1.7**) (Sun *et al.*, 2009).

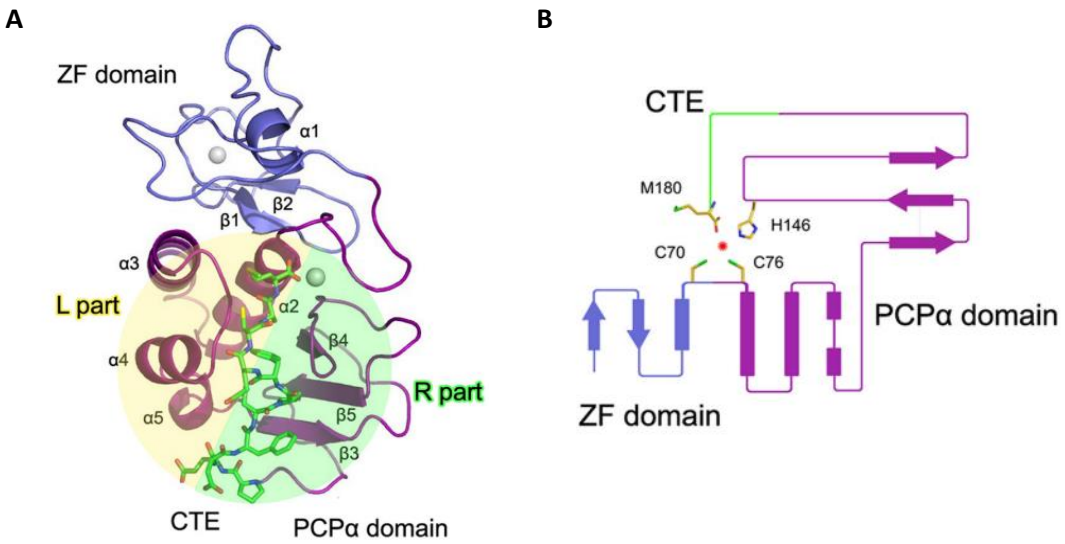

Figure 1.7: Crystal structure of PRRSV NSP1α. The PRRSV NSP1α monomer fold (**A**). The N-terminal ZF domain, C-terminal PCPα domain, and CTE are represented as slate and purple ribbons, and green sticks, respectively. Topology diagram (**B**). The colour scheme is the same as that used in panel (**A**). The α-helices and β-strands are shown as bars and arrows, respectively. The residues that correspond to PCPα activity are shown as sticks. L and R indicate the left and right parts, respectively. *Figures 1B and 1C, republished with permission of American Society for Microbiology, from* (Sun *et al.*, 2009); *permission conveyed through Copyright Clearance Center,Inc.*

NSP1α uses its PCPα activity to auto-cleave itself from pp1a at amino acid position 180/181 (den Boon *et al.*, 1995; Chen *et al.*, 2010); post-cleavage, the protease is inactive. NSP1α is required for sgRNA synthesis but not for genome replication (Kroese *et al.*, 2008), and modulates the immune response at various stages. NSP1α functions and interactions involved in immunomodulation are summarised in **Table 1.3**. It is found in both the nucleus and cytoplasm and contains a highly conserved nuclear export signal (NES), which is required for type I IFN inhibition (Chen *et al.*, 2016).

Table 1.3: PRRSV NSP1α functions and interactions with host proteins

Function	Interaction	PRRSV Species	Reference
Downregulate porcine MHC (SLA) class-I surface expression	With both SLA-I chains – β2m and heavy chain	2	(Du *et al.*, 2016)
Suppress IFN-β production by causing CREB binding protein degradation	CREB binding protein	2	(Han *et al.*, 2013) (Kim *et al.*, 2010)
Inhibit NF-κB by preventing NEMO ubiquitination	Linear ubiquitin chain assembly complex (LUBAC) components HOIP & HOIL-1L	2	(Jing *et al.*, 2016)
Suppress TNF by inhibiting NF-κB binding to CRE-κB3 of TNF promoter	Unknown	2	(Subramaniam *et al.*, 2010)
Unknown	PIAS1	NN	(Song *et al.*, 2010)
To increase NSP1α stability and boost PRRSV replication	E3 ubiquitin ligase ankyrin repeat and SOCS box–containing 8 (ASB8)	2	(Li *et al.*, 2019)
Upregulate expression of E3 ubiquitin ligase RNF122 to increase NSP4 stability, degrade MDA5 and reduce IFN-β production	Unknown	2	(Sun *et al.*, 2022)

*NN – PRRSV species used was not reported in the publication.

1.3.4 NSP1β

NSP1β is a 23 kDa protein produced following cleavage and release of NSP1α, which allows NSP1β to auto-cleave itself from the remaining pp1a using its own PCPβ (den Boon *et al.*, 1995). NSP1β also forms dimers and has four domains: NTD with ion-dependant nuclease activity; linker domain; C terminal PCP; and a CTE (**Figure 1.8**) (Xue *et al.*, 2010); additionally, it contains a SAF-A/B, Acinus, and PIAS (SAP) motif found to be essential for IFN suppression (Han *et al.*, 2017; Ke *et al.*, 2018). NSP1 is the second most variable NSP with an identity of 50.5 – 54.3% (Rascón-Castelo *et al.*, 2015), with most variation in NSP1β (Darwich *et al.*, 2011).

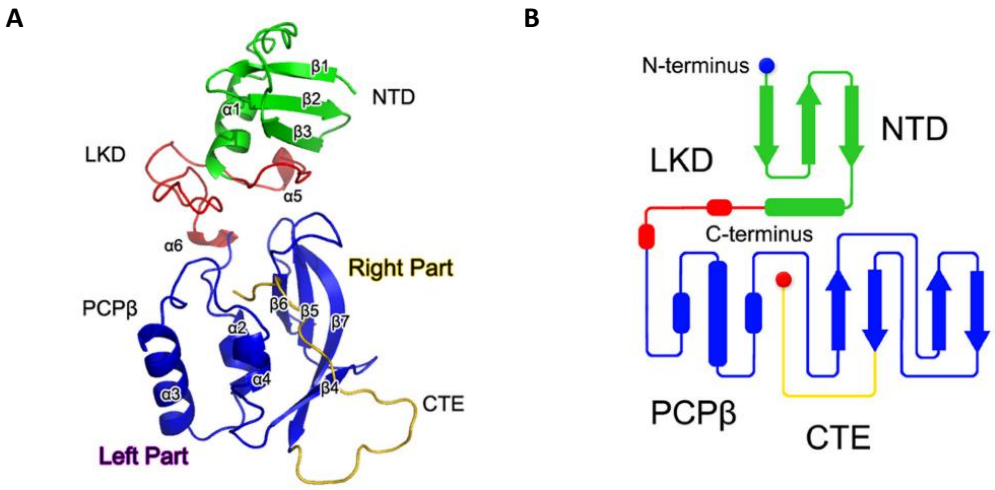

Figure 1.8: Crystal structure of PRRSV NSP1β. Overall structure of the NSP1β monomer (**A**) and topology (**B**). The monomer structure of NSP1β is shown as a coloured ribbon. The NTD, linker domain (LKD), PCP domain, and CTE are coloured green, red, blue, and gold, respectively. The topology of NSP1β is coloured using the same scheme. The α-helices and β-strands are shown as bars and arrows, respectively. *Figures 2A and 2B, republished with permission of American Society for Microbiology, from* (Xue *et al.*, 2010)*; permission conveyed through Copyright Clearance Center,Inc.*

NSP1β is found in both the nucleus and cytoplasm (Beura *et al.*, 2010) and is required for transactivation of programmed ribosomal frameshifting (PRF) used to express NSP2TF (Y. Li, Treffers, *et al.*, 2014). NSP1β functions and interactions involved in immunomodulation are summarised in **Table 1.4:**

Table 1.4: PRRSV NSP1β functions and interactions with host proteins

Function	Interaction	PRRSV Species	Reference
Imprison host cell mRNA using SAP motif	Unknown	1 and 2	(Han *et al.*, 2017)
Inhibit TNFα by targeting extracellular signal-regulated kinase (ERK) pathway	Unknown	2	(He *et al.*, 2015)
Inhibit IFN-β by preventing IRF3 phosphorylation and translocation	Unknown	2	(Beura *et al.*, 2010)
Inhibit IFN-β by inducing proteasomal degradation of CREB binding protein (CBP)	Unknown	2	(Kim *et al.*, 2010)
Suppress TNFα expression by inhibiting Sp-1	B domain of Sp-1	2	(Subramaniam *et al.*, 2010)
Support viral replication	Cellular poly r(C) binding proteins (PCBP) 1 and 2	2	(Beura *et al.*, 2011) (Wang *et al.*, 2012)
Unknown	Bind ssRNA and dsDNA	2	(Xue *et al.*, 2010)
Block interferon stimulated gene factor 3 nuclear translocation by inducing KPNA1 degradation	Unknown, Valine-19 of NSP1β essential	2	(Patel *et al.*, 2010) (Wang *et al.*, 2013)
Inhibit host mRNA nuclear export by causing nuclear pore complex disintegration	C terminal residues 328 -522 of Nucleoporin 62	2	(H. Ke, Han, *et al.*, 2019)
Unknown	SUMO E2 conjugating enzyme ubiquitin carrier protein 9 (Ubc9)	2	(C. Wang *et al.*, 2017)

1.3.5 PRRSV NSP interactions

PRRSV NSPs have been shown to interact with both other NSPs and host proteins using yeast-2-hybrid (y-2-h), co-immunoprecipitations and confocal immunofluorescence microscopy. Y-2-h is a method of identifying protein-protein interactions (**Section 2.12**) and has been used to screen multiple PRRSV proteins (both structural and non-structural). A summary of published interactions detected using y-2-h screens is provided in **Table 1.5**. This method was used in this project to identify novel PRRSV-1 NSP1-host protein interactions.

Table 1.5: Interactions between PRRSV NSPs and host proteins detected in y-2-h screens

Protein	Interactions detected	PRRSV Species	Reference
NSP1α	PIAS1	NN*	(Song *et al.*, 2010)
NSP1β	cellular PCBP2	2	(Wang *et al.*, 2012)
N	Viral NSP9 and host cellular RNA DExH-box helicase 9	1 and 2	(Liu *et al.*, 2016)
NSP9	Annexin A2	2	(J. Li *et al.*, 2014)
NSP9	DEAD-box RNA helicase 5 (DDX5)	2	(S. Zhao *et al.*, 2015)
NSP1β NSP4 NSP9, NSP10 N	SUMO E2 conjugating enzyme ubiquitin carrier protein 9 (Ubc9)	2	(C. Wang *et al.*, 2017)

*NN – PRRSV species used was not reported in the publication.

Additionally, a combination of approaches has been used to identify interactions between NSPs (Nan *et al.*, 2018; Song *et al.*, 2018); the PRRSV NSP interactome is summarised in **Figure 1.9**. These have provided insight into RTC composition, showing NSP9 and NSP12 to be interaction hubs that are thought to mediate RTC formation, and that NSP2, NSP3 and NSP5 form a scaffold to recruit the RTC.

Increasing our understanding of PRRSV NSP-host protein interactions during immunomodulation may aid vaccine design, as these interactions could be targeted and promoted or inhibited to improve vaccine efficacy.

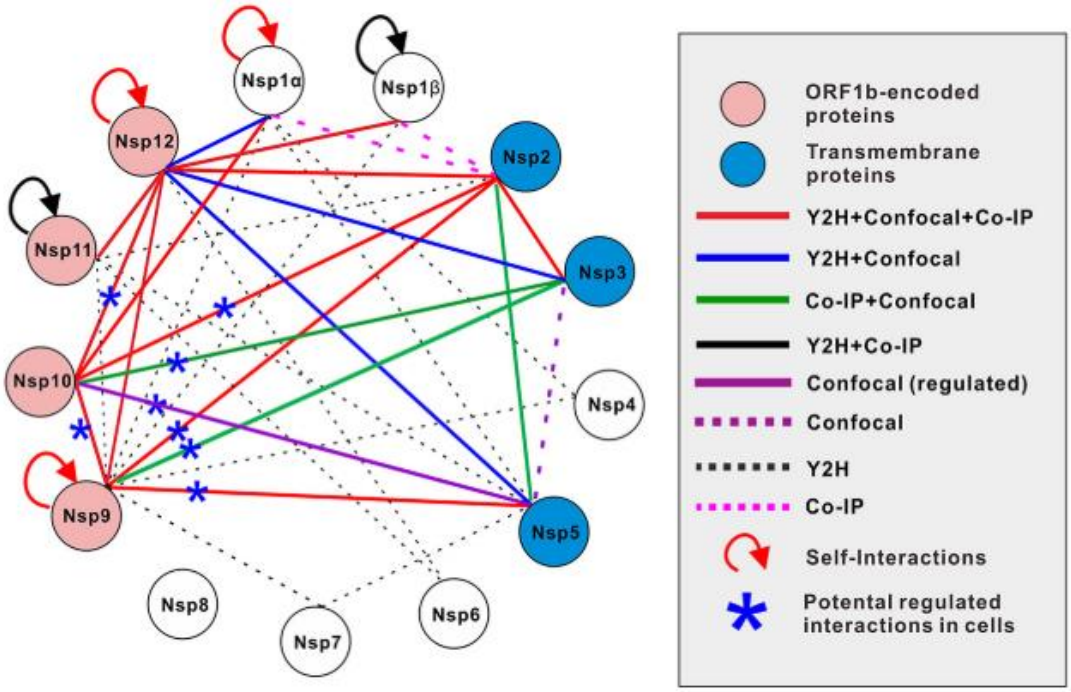

Figure 1.9: Summary of the interactome of PRRSV NSPs. Interactions between PRRSV NSPs and the method used to identify each interaction are shown. Interactions were identified by y-2-h, co-immunoprecipitations (Co-IP) and/or confocal immunofluorescence microscopy (confocal). The key in the figure shows the method used. *Figure 1D, republished with permission of American Society for Microbiology, from* (Song *et al.*, 2018)*; permission conveyed through Copyright Clearance Center,Inc.*

1.4 The innate and adaptive immune responses

The immune response is divided into 2 parts: the innate and the adaptive. The innate immune response is the first defence against pathogens and is not specific to the pathogen detected, whereas the adaptive is extremely specific and develops later during infection (Dempsey, Vaidya and Cheng, 2003).

1.4.1 The innate response

The innate immune response consists of physical barriers, immune cells, inflammation, pattern-recognition receptors, and soluble factors (cytokines, chemokines). The physical barriers, such as skin and mucous membranes, prevent pathogens encountering and infecting target cells (Gallo and Nizet, 2008). Phagocytic immune cells, such as macrophages and neutrophils, engulf pathogens into a phagosome, this then fuses with a lysosome to degrade the pathogen (Uribe-Querol and Rosales, 2020). Dendritic cells instead ingest pathogens to present their antigens for the adaptive immune response (Liu and Roche, 2015).

Immune signalling pathways begin with PRRs (Mogensen, 2009). There are different types of PRR including TLRs, NOD-like receptors and cytoplasmic receptors such as RIG-I (Takeuchi and Akira, 2010). These detect PAMPs, highly conserved molecules across a group of pathogens. Important PRRs in RNA virus infections are endosomal TLR3 (recognises dsRNA), endosomal TLR7 and TLR8 (both recognise single stranded RNA); and cytoplasmic RIG-I and MDA5 (both recognise dsRNA) (Takeuchi and Akira, 2010). Stimulation of these receptors results activation of the type I IFN and NF-κB pathways and inflammation (Takeuchi and Akira, 2010).

The NF-κB family of transcription factors are involved in the regulation of the immune response, inflammation, cell survival and proliferation (Oeckinghaus and Ghosh, 2009; Liu *et al.*, 2017). NF-κB upregulates expression of inflammatory cytokines such as IL-6, IL-12 and TNF-α (Liu *et al.*, 2017). IL-6 controls T cell differentiation (Dienz and Rincon, 2009), and IL-12 regulates the cytotoxicity of cytotoxic T cells (CTLs) (L.Li *et al.*, 2017).

IFNs are secreted inflammatory cytokines involved in inflammation and the antiviral response (Platanias, 2005). There are 3 types, type I (e.g. IFN-α, IFN-β), type II (IFN-γ)

and type III (IFN-λ). IFNs bind to IFN receptors on the same cell (autocrine) or neighbouring cells (paracrine) and activate janus kinase (JAK)-STAT signalling pathways, resulting in expression of ISGs (Platanias, 2005). ISGs, such as ISG15, myxovirus resistance protein and oligoadenylate synthase, induce an antiviral state in cells. ISG15 is a ubiquitin homologue, and ISGylation of the IFN signalling protein IRF3 prevents its degradation and enhances IFN signalling (Lu *et al.*, 2006; Perng and Lenschow, 2018). Oligoadenylate synthase produces 2'-5' oligoadenylate to activate RNase L; activated RNase L then cleaves mRNA and viral RNA to inhibit both cellular and viral protein production (Drappier and Michiels, 2015). Protein inhibitor of activated STAT (PIAS) proteins regulate JAK-STAT signalling, and therefore ISG expression, by competing with STAT proteins for the same promoter, the interferon stimulation response element, recruiting other transcriptional co-regulators, and through sumoylation (Shuai and Liu, 2005).

The acute inflammatory response during infection occurs when tissue is damaged; its purpose is to destroy the infectious agent responsible and repair tissue damage to restore homeostasis (Ahmed, 2011). It is fast activating and short lived (a few days), bringing all the immune cells required straight to the damaged site whilst also preventing further spread of the pathogen. It is localised to the area of infection and is characterised by heat, pain, swelling and redness of this area (Hannoodee and Nasuruddin, 2021). Inflammation is divided into 4 stages: inducers, sensors, mediators, and effectors (Hannoodee and Nasuruddin, 2021).

Inflammation is induced by PAMPs, exogenous microbial inducers, resulting in the release of inflammatory mediators (Ahmed, 2011). These include cytokines and chemokines, vasoactive amines, complement proteins, lipid mediators and proteolytic enzymes.

Vasoactive amines, such as histamines and serotonin, are produced by mast cells and released via granulation (Theoharides *et al.*, 2012). They bring about an increase in vascular permeability (resulting in swelling) and vasodilation (heat and redness). Complement fragments (C5a, C3a), synthesised by enzyme cascades after activation of the 3 complement pathways, increase vascular permeability (Williams, 1983) by recruiting granulocytes and monocytes and induce mast cell degranulation

(Hannoodee and Nasuruddin, 2021). Lipid mediators, derived from phospholipids, cause the production of arachidonic acid metabolites such as platelet activating factor, prostaglandins and leukotrienes (Hannoodee and Nasuruddin, 2021). Platelet activating factor recruits and activates eosinophils and neutrophils (Ashraf and Nookala, 2022), whereas prostaglandins cause vasodilation and induce fever (Ricciotti and Fitzgerald, 2011).

Cytokines are secreted by cells to affect other cell behaviour, whereas chemokines direct cell movement via chemotaxis. They are produced by most cells, mainly macrophages, although some are made as pro-forms requiring activation by the inflammasome. Inflammasomes are intracellular complexes consisting of a caspase, NOD-like receptor and adaptor protein (Guo, Callaway and Ting, 2015). Macrophage cytokines include IL-1α and IL-1β, are cleaved by caspases to become active (Galliher-Beckley, 2013; Guo, Callaway and Ting, 2015; Wiggins *et al.*, 2019); these bind to their receptors to activate pro-inflammatory molecules (e.g. NF-κB) (Pugazhenthi *et al.*, 2013; Dinarello, 2018), and interact with the hypothalamus to induce fever (El-Radhi, 2018). Chemokine IL-8 recruits neutrophils to the site of infection by chemotaxis (Harada *et al.*, 1994).

After local cell activation and IL-6 release, the liver is activated to produce acute phase proteins (Jain, Gautam and Naseem, 2011). These have a variety of roles including leukocyte recruitment (serum amyloid A) (Mullan *et al.*, 2006), clotting to prevent infection spread (C-reactive protein) (Xu *et al.*, 2015) and complement activation (mannose binding protein) (Beltrame *et al.*, 2014). The activated endothelium produces L selectin and integrin; these proteins bind to immune cells in the blood, allowing them to transmigrate using enzymes into the damaged tissue (Ala, Dhillon and Hodgson, 2003).

1.4.2 The adaptive response

The adaptive response is a specific immune response against pathogens and is mediated by two types of lymphocyte: T and B cells.

1.4.2.1 T cells

T cells are broadly grouped into 2 categories, CD4+ and CD8+, based on the presence of molecules on their cell surface. CD4+ T cells are T helper (Th) cells, involved in activation and maturation of other immune cells, whereas CD8+ cells are cytotoxic (Seder and Ahmed, 2003). Both types have T cell receptors (TCRs) on their cell surface, which like B cell receptors (BCRs) are generated by V-D-J recombination, a process where gene segments are cut and recombined to generate a highly diverse repertoire of receptors to maximise the chances of antigen recognition (Roth, 2014). T cells undergo positive and negative selection in the thymus to ensure TCRs can recognise MHC efficiently but don't recognise self-antigens (Klein *et al.*, 2014). CD8+ cells TCRs bind endogenous antigen presented on MHC class I, whereas CD4+ TCRs bind antigen bound to MHC class II (Seder and Ahmed, 2003).

In the thymus, T cells possess TCRs that bind to specific viral epitopes. Engagement of the TCR with a peptide:MHC complex on antigen presenting cells (APCs), along with co-stimulatory signals via CD28 binding CD80 on the APCs, activates the T cell which then proliferates and migrates to the site of infection (Lanzavecchia, Iezzi and Viola, 1999).

CTLs are CD8+ T cells that directly kill virus-infected cells (Groscurth and Filgueira, 1998). After infecting host cells viral proteins are processed by the proteasome and displayed on MHC class I on the cell surface. Activated CTLs eliminate virus infected cells in both lytic and non-lytic ways, as well regulating other immune cells using cytokines.

CTL cytotoxicity is antigen specific and relies on cell to cell contact (Groscurth and Filgueira, 1998). Cell death is caused either by lytic granules or mediated by Fas signalling (Hassin *et al.*, 2011). Engagement of the TCR leads to cytoskeleton rearrangement and pseudopod formation. Lytic granules, specialised secretory granules containing perforin and granzymes, move along the cytoskeleton to the

immunological synapse where they are exocytosed (Cullen and Martin, 2008). Perforin forms a pore in the target cell membrane and granzymes are then delivered through this into the infected cell to induce apoptosis. Fas ligand is found on the surface of CTLs and NK cells and engages its trimer receptor Fas on the infected cell membrane (Waring and Müllbacher, 1999; Paul and Lal, 2017) . This results in activation of caspase 3, which causes chromatin condensation and DNA fragmentation, triggering apoptosis (Meng *et al.*, 2000).

Additionally, CTLs produce the pro-inflammatory cytokines IFN-γ and TNFα. IFN-γ induces expression of nitric oxide synthetase to produce the anti-microbial and cytotoxic nitric oxide which kills infected cells (Blanchette, Jaramillo and Olivier, 2003). IFN-γ also maximises antigen presentation by increasing expression of MHC class I as well as the immunoproteasome subunits proteasome subunit β (PSMB) type-8 (PSMB8), PSMB9 and PSMB10, to process peptides more efficiently (Zhou, 2009). It also increases the levels of the transcription factor T-bet in T cells, needed to produce a Th1 cell (Szabo *et al.*, 2000). IFN-γ is also potent activator of macrophages (Schroder *et al.*, 2004), promoting phagocytosis of virions, and activates antibody class switching to produce the complement activating subset immunoglobulin (Ig) G2a (IgG2a) (Duarte, 2016). TNFα acts through the TNF receptor to kill infected cells by signalling through a complex of TNF receptor associated death domain, FAS-associated death domain and caspase 8 to activate caspase 3 and induce apoptosis (Micheau and Tschopp, 2003).

Some CTLs will be induced to form memory T cells. Their induction and maintenance relies on the cytokines IL-2, IL-7 and IL-15 (Schluns and Lefrançois, 2003).

There are multiple subsets of Th cells (Th1, Th2, Th17, T follicular helper (Tfh)) each with different roles. Cytokines secreted from APCs activate specific transcription factors in T cells which determine their subtype: T-bet is required for Th1 differentiation (Szabo *et al.*, 2000) and B-cell lymphoma (Bcl) protein 6 (Bcl-6) for Tfh cells (Hatzi *et al.*, 2015). Th1 cells are inflammatory and antiviral, releasing IFN-γ and IL-2 (Raphael *et al.*, 2015). Tfh cells present antigen on MHC class II to B cells (Crotty, 2015).

1.4.2.2 B cells and antibodies

B cells are part of the adaptive immune response and use their BCRs to recognise antigen presented on MHC class II (Yuseff *et al.*, 2013). If a BCR is engaged with a peptide:MHC class II complex, the B cell is co-stimulated by CD40L on a CD4+ Tfh cell (Crotty, 2015). B cells then undergo somatic hypermutation to increase the affinity of the BCR for the antigen. Activation induced cytidine deaminase induces random point mutations in the variable regions of both the BCR heavy and light chains by deaminating cytosine to uracil (di Noia and Neuberger, 2007). The new BCR is then screened for its affinity for antigen by testing the interaction with peptide:MHC class II complexes on the surface of follicular dendritic cells (Kranich and Krautler, 2016). Eventually, the B cell with the highest affinity differentiates into a plasma cell, which requires the cytokine IL-21 (Ettinger *et al.*, 2005), and produces antibodies – soluble BCRs – against the specific viral epitope.

Antibodies are secreted, soluble BCRs that bind to antigen via their fragment antigen-binding region and mediate effector functions using their fragment crystallizable region (Chiu *et al.*, 2019). Antibodies have different fragment crystallizable regions, allowing them to interact with different effector cells, depending on the type of pathogen they are specific against; this is achieved through class switching (Stavnezer, Guikema and Schrader, 2008). There are 5 antibody isotypes: IgA, IgM, IgG, IgD and IgE, with subtypes within these. Antibody functions include neutralization, agglutination, opsonisation, antibody dependant cell-mediated cytotoxicity and interacting with complement (Forthal, 2015).

Antibodies neutralise viruses and their proteins to reduce viral infectivity. They can inhibit entry into target cells – antibodies against CD163 scavenger receptor cysteine-rich 5–9 domain block PRRSV entry in PAMs (Xu *et al.*, 2020), or disrupt viral structure to prevent function or expose proteins – antibodies against the trimer interface of severe acute respiratory syndrome coronavirus (SARS-CoV) 2 (SARS-CoV-2) spike protein disrupt the trimer structure (Suryadevara *et al.*, 2022). Agglutination of viral particles reduces the effective viral titre as well as making it easier for phagocytes to engulf virions. Antibody dependant cell-mediated cytotoxicity focuses NK cells and macrophages onto virus particles and infected cells (Yu *et al.*, 2021). Finally,

antibodies interact with complement proteins to produce larger tertiary structures, again to achieve agglutination and opsonisation (Dunkelberger and Song, 2009).

Memory B cells are formed in germinal centres of lymphoid follicles following primary viral infection (Kurosaki, Kometani and Ise, 2015). If they encounter antigen from a secondary infection, they rapidly differentiate and proliferate into antibody producing plasma cells (Zabel *et al.*, 2014). This secondary response is much stronger and faster than when the antigen was first encountered, allowing more rapid viral clearance.

1.5 Project aims and significance

PRRS is one of the economically most important infectious diseases affecting swine. Safer and more effective PRRSV vaccines are needed to combat the PRRS panzootic. To achieve this, a deeper understanding of virus-host interactions involved in immunomodulation is required.

PRRSV NSP1α and NSP1β, between them, have been shown to modulate both the porcine innate and adaptive immune responses. However, the molecular mechanisms underlying immunomodulation remain to be fully elucidated, and most studies have focussed on PRRSV-2 due to its prominence in North America and Asia. Therefore, this project focussed on improving our understanding of the modulation of host cell responses by NSP1α and NSP1β from PRRSV-1.

The aims of this project were to:

- Identify novel PRRSV-1 NSP1α and NSP1β interactions with PAM proteins
- Functionally characterise confirmed interactions

This project aimed to increase our understanding of how PRRSV interacts with the host using its NSPs during immunomodulation. Novel identified interactions could provide insight into unknown immunomodulatory NSP functions, as well as revealing mechanisms of known functions.

As current vaccines lack efficacy, new information discovered during this project could potentially be exploited to rationally attenuate PRRSV as a basis for improved vaccines or used to design new antivirals.

Chapter 2: Materials and methods

2.1 Mammalian cell culture

2.1.1 Cells and cell maintenance

BHK-21 (baby hamster kidney 21 cells) (#85011433, ECACC, Salisbury, UK); BSR-T7 (BHK-21 cells expressing bacteriophage T7 RNA polymerase) (Buchholz, Finke and Conzelmann, 1999); Max cells (Simian vacuolating virus 40 (SV40) immortalised, NIH minipig kidney cells expressing a d/d MHC class I haplotype, Federal Research Centre for Virus Diseases of Animals, Tübingen, Germany); and HEK-293-TLR3 (human embryonic kidney 293 cells stably expressing TLR3) (#293-htlr3, Invivogen, Toulouse, France) were used as described in **Section 2.13**.

For cell culture, media was supplemented with bovine viral diarrhoea virus genome free 0.2 micrometres (µm) sterile filtered, gamma irradiated Australian adult bovine serum (ABS) (Selbourne Biological, Alton, UK), and penicillin (100 units per millilitre (U/mL))/streptomycin (100 micrograms per millilitre (µg/mL)) (#15140122, Gibco, Thermo Fisher Scientific, Basingstoke, UK). Serum-free (SF) and antibiotic-free media was used where stated.

Cells were cultured in their respective media (**Table 2.1**) and grown at 37°C, 5% carbon dioxide (CO_2) and split when confluent. Medium was aspirated, cells were washed in phosphate-buffered saline (PBS, Central Services Unit, The Pirbright Institute, Woking, UK) and then passaged using 0.05% (w/v) Trypsin-ethylenediaminetetraacetic acid (EDTA) (#25300054, Gibco) or 0.25% (w/v) Trypsin-EDTA (#25200056, Gibco).

Table 2.1: Cell types, culture media and trypsin-EDTA used in the project.

Cell	Medium	Serum percentage (v/v)	Trypsin-EDTA (w/v %)
BHK-21	Glasgow's Modified Eagle's Minimal Essential Medium (#11710035, Gibco)	10	0.25
BSR-T7	Dulbecco's Modified Eagle Medium (DMEM) (high glucose, GlutaMAX™ Supplement, HEPES) (#32430100, Gibco)	10	0.25
Max cells	DMEM (high glucose, GlutaMAX™ Supplement, HEPES) (#32430100, Gibco)	10	0.05 0.25
HEK-293-TLR3	DMEM/F-12 (Dulbecco's Modified Eagle Medium/Nutrient Mixture F-12) (#31330095, Gibco)	5	0.05

2.1.2 Generating cell stocks

After passaging, the remaining cells in suspension were pelleted by centrifugation, at 178 × *g* for 5 minutes (min) at room temperature (RT) and then re-suspended in DMEM supplemented with 20% (v/v) bovine viral diarrhoea virus genome free ABS and 10% (v/v) dimethyl sulfoxide (#D2650, Merck, Gillingham, UK). When freezing BSR-T7 cells, 40% (v/v) ABS was used instead. Cell stocks were frozen in Mr. Frosty™ Freezing Containers (#5100-0001, Thermo Fisher Scientific) containing isopropanol (#20842.312, VWR Chemicals, Lutterworth, UK) at -80^{o}C; cells were stored in long term storage at -80^{o}C.

2.2 Viruses

A modified vaccinia Ankara virus expressing the T7-polymerase (MVA-T7) (Sutter, Ohlmann and Erfle, 1995) was used where stated to enhance protein expression in transfected BSR-T7 cells; this was available within the Molecular Virology Group (The Pirbright Institute). Cells were first transfected, then infected with MVA-T7 3 hours (hr) later (**Section 2.13.2**), and lysates were collected 24 hr later.

MVA-T7 was produced by infecting a flask of BHK-21 cells and leaving for 2-3 days. The flask was then frozen at -20°C and defrosted twice. The defrosted lysate was then clarified at 1600 × *g* for 10 min at RT; the supernatant, containing MVA-T7, was collected, aliquoted and kept at -20 °C.

2.3 Plasmids

2.3.1 Plasmids constructed by others

Existing plasmids available within the Molecular Virology Group (The Pirbright Institute) were used throughout the project.

A PAM complementary DNA (cDNA) library, obtained from a Large White x Landrace hybrid sow, cloned into pACT2 (#638822, Takara Bio, Saint-Germain-en-Laye, France) (**Figure 9.2**) was previously extracted from the respective lambda library and amplified by Dr Julian Seago (The Pirbright institute). The lambda ACT2 library was originally constructed by Dr James Miskin (Miskin *et al.*, 1998).

PRRSV-1 NSP1 from the conventional low virulence PRRSV-1 subtype 1 strain (UK field isolate 215-06, sequence kindly provided by Dr Jean-Pierre Frossard (Animal and Plant Health Agency (APHA), Addlestone, UK) and the high virulence PRRSV-1 subtype 3 strain SU1-Bel (GenBank accession number (AC) KP889243) (Morgan *et al.*, 2013) were cloned into pGBKT7 (**Figure 9.3**). Their sequences are shown below in **Table 2.2**; PRRSV-1 215-06 pGBKT7-NSP1α/β was used in the NSP1α y-2-h screen.

Table 2.2: Full-length PRRSV-1 NSP1 sequences from 2 strains.

PRRSV NSP1	Gene sequence
215-06	ATGTCTGGGACGTTCTCCCGGTGCATGTGCACCCCGGCTGCCCGGGTATTTTGGAAC GCCGGCCAAGTCTTTTGCACACGGTGTCTCAGTGCGCGGTCTCTTCTTTCTCCTGAGC TTCAAGACACTGACCTTGGAGCAATTGGCTTGTTTTACAAGCCAAGGGTAAAGCTCC ACTGGAGGGTCCCTCTCGGCATCCCTCAGGTGGAATGTACCCCATCCGGGTGCTGTT GGCTCTCAGCTGTATTCCCTCTGGCGCGCATGACCTCCGGTAATCACAACTTCTCCCA ACGACTGGTGAAGGTTGCTGATGTTTTGTATCGTGATGGTTGCTTGGCACCTCGACA TCTTCATGAACTCCAAGTTTACGAGCGTGGTTGCAACTGGTACCCGATCACGGGGCC CGTGCCCGGGATTGGTTTGTTTGCGAACTCCATGCACGTGTCCGACCAACCGTTCCC TGGTGCCACCCATGTGCTGACTAACTTGCCTCTGCCTCAACAAGCTTGCCGACAGCC GTTCTGTCCATTTGAAGAGGCTCAT*TCCAGCGTGTACAGGTGGAAAAAGTTTGTGG TTTTCACGGACTCCTCCCCTAACGGCCGATCTCGCGTGATGTGGACGCCGGGGTCCG ATGATTCAGCCGCCTTGGAGGTACTGCCGCCTGAACTAGAACGCCAGGTCGAGATT CTTATTAGGAGTTTTCCTGCTCACCACCCTGTCGACCTGACCGACTGGGGGTTCACT GATTCCCCTGAGGACGGTTTTTCTTTTAACATGTCTTATTCTTGTGGTTACCTTGTCCA AAATCCTGACATGTTTAATGGTAAATGCTGGCTCTCCTGCTTTTTGGACCAATCGGTT GAAGTGCGCCGCAATGAGGAATATCTAGCCGACGCCCTCGGCTACCAAACCAAGTG GGGCGTACATGGTAAATACCTTCAGCGTAGGCTTCAAGTTCGCGGCCTTCGTGCTGT AGTCGATCCCGATGGTCCCGTTCACGTTGAGGCGCTGTCTTGCTCCCAGTCTTGGAT TAGGCACCTGACTCTGGAAGATGATGTCACCCCAGGATTCGTTCGACTGACATCCCT TCGCATTGTGCCGAACACAGAGCCTACTACTCTCCCGGTCTTTCGGTTTGGAGCGCA TAAGTGGTATTAA
SU1-Bel	ATGTCTGGGACGTTCTCCCGGTGCAAGTGCACCCCGGCAGCTCGGGTAATGTGGGA AGCCGGCCAAGTCTATTGCACACGGTGTCTCAGTGCACGGTCTCTCCTTCCTTTGGA CCTCCAGGACACTGACCTTGGTGCAGTTGGCTTGTTTTACAAGCCCAGGGAAAAGCT TCCTTGGAAAATTCCTATGGGCATCCCCCAGGCAGAGTGTACTCCGTCCGGATGTTG CTGGCTTTCGGCCATTTTTCCAATAGCACGCATGACCTCAGGCAATCACAACTTCGCC CAACGGCTTGTGAAGGTCGCTGATGTGTTGTATCGTGAGGGCTGCCTGGCCCCACG ACACCTTCGTGAACTCCAAGTTTACGAACGTGGCTGCAGCTGGTACCCGATTACGGG GCCTGTACCCGGGATAGGTTTGTACGCGAACTCCATGCATGTGTCCGACAAGCCATT TCCCGGAGCCACCCATGTATTGACGAACTCACCATTGCCTCAGCAGGCCTGTCGACA GCCGTTCTGTCCGTTTGAGGAAGCCCAC*TCTGATGTGTATAAATGGAAGGGCTTTG TGGTGTTTGTGGATAGTTCTTCTGATGGTTTGCTCCGCATGATGTGGACCCCCGGAA GTGTCGACTCAGCAAACCTGGAACCTCTACCATCCGGGTTGGAACAAAAGGCCGAA ATTCTTACGCGTAGTTTCCCGGCTCACCACCCCGTCGATTTCACCGATTGGGACTTCA CTGAGTCTCCCGAAAACGGGTTTTCTTTTAGCATGTCTCATTCTCATGGCTACCTCGT TCCGGGTGACGATAGGTATAATGGTAAGTGTTGGCTCTCGTGTTTTTTGGGCCTGTC AGCCGAAGGGCGCCTCCGCGAAGAGTTCCTAGCCGTTGCCTTTGGTTACAACACCA AATGGGGTGTGCCTGGCAAGTACCTCCAACGCAGGCTTCAAGTTAACGGCCTCCGT GCCGTAACCGACCCTAATGGCAACATCCATGTTGAGGCGTTGTCTTGCCCCCAATCT TGGGTTAGGCATCTAACTCTGAGCGATGACGTCACTCCGGGTTTTGTCCGCCTTGTG TCCATTCGCATCGAACCAAACACAGAGCCCACCGACCGCCCGTTCTTCCGGTTCGGA GCGCATAGGTGGTATTAA

*Represents cleavage point between NSP1α and NSP1β. Start codons are in green, stop codons in red.

Existing plasmids were used for cloning and subsequent confocal immunofluorescence microscopy experiments; these included pcDNA 3.1+ plasmids (#V790-20, Invitrogen, Thermo Fisher Scientific) (**Figure 9.4**) encoding PRRSV-1 Myc-tagged NSP1α and NSP1β from 215-06 and SU1-Bel strains (**Table 2.3**), and the pEF-FLAG plasmid (**Figure 9.5**) kindly provided by Professor Stephen Goodbourn (St George's, University of London, London, UK).

2.3.2 Plasmids constructed for the project

2.3.2.1 pGKBT7 constructs

The following primer combinations: 215-06 NSP1α F with 215-06 NSP1α R; 215-06 NSP1β F with 215-06 NSP1β R; SU1-Bel NSP1α F with SU1-Bel NSP1α R; and SU1-Bel NSP1β F with SU1-Bel NSP1β R (**Table 2.8**), were used with pGBKT7-NSP1α/β to polymerase chain reaction (PCR) amplify the respective NSP1α and NSP1β ORFs of 215-06 and SU1-Bel. These primers also introduced start and stop codons and restriction sites (see **Table 2.3** for sequences). These PCR products were then cloned into the pGBKT7 plasmid by digestion with *Nde*I and *Eco*RI restriction enzymes (**Section 3.2**).

Table 2.3: PRRSV-1 individual NSP1α and NSP1β sequences from 2 strains.

PRRSV NSP1	PCR product sequence
215 NSP1α	GCG**CATATG**TCTGGGACGTTCTCCCGGTGCATGTGCACCCCGGCTGCCCGGGTATTT TGGAACGCCGGCCAAGTCTTTTGCACACGGTGTCTCAGTGCGCGGTCTCTTCTTTCT CCTGAGCTTCAAGACACTGACCTTGGAGCAATTGGCTTGTTTTACAAGCCAAGGGTA AAGCTCCACTGGAGGGTCCCTCTCGGCATCCCTCAGGTGGAATGTACCCCATCCGG GTGCTGTTGGCTCTCAGCTGTATTCCCTCTGGCGCGCATGACCTCCGGTAATCACAA CTTCTCCCAACGACTGGTGAAGGTTGCTGATGTTTTGTATCGTGATGGTTGCTTGGC ACCTCGACATCTTCATGAACTCCAAGTTTACGAGCGTGGTTGCAACTGGTACCCGAT CACGGGGCCCGTGCCCGGGATTGGTTTGTTTGCGAACTCCATGCACGTGTCCGACC AACCGTTCCCTGGTGCCACCCATGTGCTGACTAACTTGCCTCTGCCTCAACAAGCTTG CCGACAGCCGTTCTGTCCATTTGAAGAGGCTCAT**TAA**GAATTCCGC
215 NSP1β	GCG**CATATG**TCCAGCGTGTACAGGTGGAAAAAGTTTGTGGTTTTCACGGACTCCTCC CCTAACGGCCGATCTCGCGTGATGTGGACGCCGGGGTCCGATGATTCAGCCGCCTT GGAGGTACTGCCGCCTGAACTAGAACGCCAGGTCGAGATTCTTATTAGGAGTTTTC CTGCTCACCACCCTGTCGACCTGACCGACTGGGGGTTCACTGATTCCCCTGAGGACG GTTTTTCTTTTAACATGTCTTATTCTTGTGGTTACCTTGTCCAAAATCCTGACATGTTT AATGGTAAATGCTGGCTCTCCTGCTTTTTGGACCAATCGGTTGAAGTGCGCCGCAAT GAGGAATATCTAGCCGACGCCCTCGGCTACCAAACCAAGTGGGGCGTACATGGTAA ATACCTTCAGCGTAGGCTTCAAGTTCGCGGCCTTCGTGCTGTAGTCGATCCCGATGG TCCCGTTCACGTTGAGGCGCTGTCTTGCTCCCAGTCTTGGATTAGGCACCTGACTCT GGAAGATGATGTCACCCCAGGATTCGTTCGACTGACATCCCTTCGCATTGTGCCGAA CACAGAGCCTACTACTCTCCCGGTCTTTCGGTTTGGAGCGCATAAGTGGTAT**TAA**GA ATTCCGC
SU1-Bel NSP1α	GCG**CATATG**TCTGGGACGTTCTCCCGGTGCAAGTGCACCCCGGCAGCTCGGGTAAT GTGGGAAGCCGGCCAAGTCTATTGCACACGGTGTCTCAGTGCACGGTCTCTCCTTCC TTTGGACCTCCAGGACACTGACCTTGGTGCAGTTGGCTTGTTTTACAAGCCCAGGGA AAAGCTTCCTTGGAAAATTCCTATGGGCATCCCCCAGGCAGAGTGTACTCCGTCCGG ATGTTGCTGGCTTTCGGCCATTTTTCCAATAGCACGCATGACCTCAGGCAATCACAA CTTCGCCCAACGGCTTGTGAAGGTCGCTGATGTGTTGTATCGTGAGGGCTGCCTGG CCCCACGACACCTTCGTGAACTCCAAGTTTACGAACGTGGCTGCAGCTGGTACCCGA TTACGGGGCCTGTACCCGGGATAGGTTTGTACGCGAACTCCATGCATGTGTCCGAC AAGCCATTTCCCGGAGCCACCCATGTATTGACGAACTCACCATTGCCTCAGCAGGCC TGTCGACAGCCGTTCTGTCCGTTTGAGGAAGCCCAC**TAA**GAATTCCGC
SU1-Bel NSP1β	GCG**CATATG**TCTGATGTGTATAAATGGAAGGGCTTTGTGGTGTTTGTGGATAGTTCT TCTGATGGTTTGCTCCGCATGATGTGGACCCCCGGAAGTGTCGACTCAGCAAACCTG GAACCTCTACCATCCGGGTTGGAACAAAAGGCCGAAATTCTTACGCGTAGTTTCCCG GCTCACCACCCCGTCGATTTCACCGATTGGGACTTCACTGAGTCTCCCGAAAACGGG TTTTCTTTTAGCATGTCTCATTCTCATGGCTACCTCGTTCCGGGTGACGATAGGTATA ATGGTAAGTGTTGGCTCTCGTGTTTTTTGGGCCTGTCAGCCGAAGGGCGCCTCCGCG AAGAGTTCCTAGCCGTTGCCTTTGGTTACAACACCAAATGGGGTGTGCCTGGCAAG TACCTCCAACGCAGGCTTCAAGTTAACGGCCTCCGTGCCGTAACCGACCCTAATGGC AACATCCATGTTGAGGCGTTGTCTTGCCCCCAATCTTGGGTTAGGCATCTAACTCTG AGCGATGACGTCACTCCGGGTTTTGTCCGCCTTGTGTCCATTCGCATCGAACCAAAC ACAGAGCCCACCGACCGCCCGTTCTTCCGGTTCGGAGCGCATAGGTGGTAT**TAA**GA ATTCCGC

Start (green text) and stop (red text) codons, and *Nde*I (underlined, in bold) and *Eco*RI (underlined) restriction sites were introduced to each sequence as indicated.

2.3.2.2 pGADT7 constructs

Three plasmids could not be amplified after the y-2-h screens - these encoded IFN-induced protein 35 (IFI35, AC XP_003358072.1), major vault protein (MVP, AC XP_020942083.1) and DEAD-box RNA helicase 18 (DDX18, AC XP_005654221.2). The gene sections matching each cDNA insert, obtained from the NCBI reference pig genome (taxid: 9823), coding for these 3 proteins were synthesised cloned into pMA-RQ (GeneArt, Thermo Fisher Scientific), with the restriction sites for *Nde*I and *Bam*HI added to the 5' and 3' ends respectively to facilitate cloning (**Table 2.4**). The sequences ordered were not full-length genes, only the sections found in the original cDNA inserts were ordered, but any mismatches between these and the reference genes were corrected; additionally, the full-length IFI35 gene was ordered. Each plasmid containing the insert, plus the target plasmid pGADT7 (**Figure 9.6**), were sequentially digested with *Nde*I and *Bam*HI, gel purified and ligated (**Section 4.2.1**).

Table 2.4: Partial and full gene sequences for PAM proteins cloned into pGADT7

Protein	Insert Sequence
IFI35 full-length (AC **XP_003358072.1**)	**CATATG**TCGGCCCTCCATGCCCTTCAGAAGAAACAGGCCCAACTAA AGATGAGGCTGTGGGAGCTGCAGCAGCTGAAAATGAAGCTCAGGG ACAGAGAAAGCTTCCCACCAGACAAGGTCCCATTCCCAATGCCTGA GGTCCCCCTGGTATTCCGAGGACACATTCAGCAGGGCAGGGAAAT GGCCAAGTCTGTGGTCTCCAACCTGCAGATCTGTTACCCTCTGCCTG GAGGCTCTGCTCTGGTCACCTTTGATGACCCCAATGTGGCCAAGCA AGTGCTGCAGCAAAAGGAGCATACGATCGATATGGAAGAGTTCCG GCTGCGGGTGCAGGTCCAGCCCTTGGAGCTGCCCATGCTGACCACC ATCCAGGTGGCCAGCCAGATGAGTGATAAGAAAGTGTTCGTCAGT GGGATTCCTGCTGGGCTCAAGCTGAGTGAAGAGGAGCTGCTGGAC AAGCTGGAGATCTTCTTTGGCAAGACCAAGAACGGGGGTGGTGAT GTGGAGACACGGGAACTGCTACAAGGGGGTGTTGTGCTGGGCTTC ACTAAGGATGAAGTGGCCCAGCAGCTGTGCCAGAAGGGTCAGTTC TCAGTGCCACTGGGTAAGCAGCAGTTCCCTCTGACAGTCTCTCCCTA CGTGAGCGGGGAGATCCAGAAGGCCGAGGTCAGGTCCCAGCCTGT GCCCCAGTCGGTGCTGGTGCTCAACATTCCTGACGTCCTGGACGGC CCGGAGCTGCAGGACGTCTTGGAGATCCACTTCCAGAAGCCTACCC GTGGGGGTGGGGAGGTGGAAGCCGTGACAGTTGTGCCCCCAGGA CAGCGGGGCCTGGCAGTCTTCACTGCCAAGTCGGTC**TAG**GGATCC
IFI35 partial (AC **XP_003358072.1**)	**CATATG***CCAATGCCTGAGGTCCCCCTGGTATTCCGAGGACACATTCA GCAGGGCAGGGAAATGGCCAAGTCTGTGGTCTCCAACCTGCAGATC TGTTACCCTCTGCCTGGAGGCTCTGCTCTGGTCACCTTTGATGACCCC AATGTGGCCAAGCAAGTGCTGCAGCAAAAGGAGCATACGATCGAT ATGGAAGAGTTCCGGCTGCGGGTGCAGGTCCAGCCCTTGGAGCTG CCCATGCTGACCACCATCCAGGTGGCCAGCCAGATGAGTGATAAGA AAGTGTTCGTCAGTGGGATTCCTGCTGGGCTCAAGCTGAGTGAAGA GGAGCTGCTGGACAAGCTGGAGATCTTCTTTGGCAAGACCAAGAAC GGGGGTGGTGATGTGGAGACACGGGAACTGCTACAAGGGGGTGT TGTGCTGGGCTTCACTAAGGATGAAGTGGCCCAGCAGCTGTGCCAG AAGGGTCAGTTCTCAGTGCCACTGGGTAAGCAGCAGTTCCCTCTGA CAGTCTCTCCCTACGTGAGCGGGGAGATCCAGAAGGCCGAGGTCA GGTCCCAGCCTGTGCCCCAGTCGGTGCTGGTGCTCAACATTCCTGAC GTCCTGGACGGCCCGGAGCTGCAGGACGTCTTGGAGATCCACTTCC AGAAGCCTACCCGTGGGGGTGGGGAGGTGGAAGCCGTGACAGTTG TGCCCCCAGGACAGCGGGGCCTGGCAGTCTTCACTGCCAAGTCGGT C**TAG**GGATCC
MVP (AC **XP_020942083.1)**	**CATATG***GCAACTGAAGAGTCCATCATCCGCATCCCACCGTACCACTA CATCCACGTGCTGGACCAGAACAGCAACGTGTCCCGCGTGGAGGTT GGACCGAAGACTTACATCCGGCAGGACAATGAGAGGATTCTGTTTG CCCCCGTGCGCATGGTGACTATCCCCCCACGCCACTACTGCACCGTG GCCAACCCGGTGTCCCGGGACGCCCAGGGCTCTGTGCAGTGTGACG TCACAGGGCAAGTACGGCTCCGCCACGCTGACCTGGAGATCCGGCT GGCCCAGGACCCTTTCCCCCTGTACCCAGGGGAGGTGCTGGAAAAG GACATCACCCCACTGCAGGTGGTTCTGCCCAACACCGCCCTCCACCT TAAGGCGCTGCTGGATTTTGAGGATAAGAACGGAGACAAGGTGGT GGCCGGAGATGAGTGGCTGTTTGAGGGACCCGGCACGTATGTTCCC CGGAAGGAGGTGGAGGTGGTGCAGATCATTCAGGCCTCCGTCATC AAGCAGAACCAGGCCCTGCGGCTG**TAG**GGATCC

DDX18 (AC **XP_005654221.2**)	**CATATG***TCTCATTTACCGATGAAACTTTTGCGCAAGAAGATCGAGA* *AGCGTAACCTCAAGTTGAGACAGCGCAACCTAAAGCTCCAAGGGAC* *CTTGGGTGTGGGCCTGTCAGAAACTCAAAATGGAGATGTGTCTGAA* *GAAACAATGGGAGATGGAAAAGTTAAAAAGTCCCTAAAACAGTCG* *GTGAATGCAGACCTGTCAGAAACCCCAAATGGAGACATATCTAAAG* *AAACAGTAGGAAGTGGGAAAGTTAAAAAATCTCTAAAACAGTCTAT* *GAATGTGGACCTATCAGAAACCCAAAGTGGAGACATATCTAAAACA* *GTGGGAGGTGGAAAAGTTAAAAAATCCCTAAAACACTCTGTGAATG* *TGGACCTGTCAGAAACCCAAAATGGAGACGTATCTAAAGAAACAGT* *GGTAAGTGGAAAAGTTAAAAAATCCCTAAAACAGTCTGTGAATGCA* *GGCTTGTCAGAAGCCCAAAATGGAGATATATCTAAAGAAACAGTGG* *GAAGTGGAAAAGTTAAAAAGTCCAGGAAAGAGTCGGTGAATGCAG* *GCTTGTCAGAAGCCCAAAATGGAGATGTATCTAAAGAAACAGGGG* *AAAATGTTAAAAAACCCTCCAAGAAATCTAGCATATTGACCAGTGAT* *GAA***TAG**GGATCC

The full or the indicated partial (italicised text) sequence was ordered. Start (green text) and stop (red text) codons, and *Nde*I (underlined, in bold) and *Bam*HI (underlined) restriction sites were introduced to each sequence as indicated.

2.3.2.3 pEF-FLAG constructs

To express PAM proteins in mammalian cells, the respective cDNA sequence of eleven interacting PAM proteins, situated between the two *Xho*I restriction sites of the pACT2 plasmid, was obtained by sequencing as described (**Section 2.10**) using the pGADT7 F and pGADT7 R primers. Primers (**Table 2.5**, **Table 2.8**) containing the appropriate combination of restriction sites, *Bam*HI, *Eco*RI, *Nco*I, *Xba*I and *Spe*I present in the multi cloning site of the pEF-FLAG plasmid, were then used to PCR amplify (**Section 2.7**) and clone each fragment (**Section 2.11**) into pEF-FLAG.

The Q5® High-Fidelity DNA Polymerase was used, due to its proof-reading ability; the annealing temperature for each individual PCR reaction was calculated using the NEB T_m calculator (**Section 2.7**). Extension time was adjusted based on insert size, 30 sec/kb. The expected PCR product size and annealing temperatures are shown below (**Table 2.5**).

Table 2.5: Cloning into pEF.

Protein	Primers used	PCR product size (bp)	Annealing Temperature (°C)	Restriction Sites
TAB3	TAB3 F BAMHI TAB3 R SPEI	861	67	*Bam*HI *Spe*I
STAT3	STAT3 F NCOI STAT3 R SPEI	834	68	*Nco*I *Spe*I
EPAS-1	EPAS-1 F BAMHI EPAS-1 R XBAI	1393	67	*Bam*HI *Xba*I
Beclin-1	BECLIN-1 F BAMHI BECLIN -1 R SPEI	1337	67	*Bam*HI *Spe*I
Cullin-9	CUL9 F BAMHI CUL9 R XBAI	489	70	*Bam*HI *Xba*I
Nucleoprotein TPR	TPR F NCOI TPR R SPEI	294	66	*Nco*I *Spe*I
Nucleoporin GLE1	GLE1 F NCOI GLE1 R SPEI	1002	69	*Nco*I *Spe*I
PSMB4	PSMB4 F ECORI PSMB4 R SPEI	794	66	*Eco*RI *Spe*I
PSMB8	PSMB8 F BAMHI PSMB8 R XBAI	519	67	*Bam*HI *Xba*I
PSMA1	PSMA1 F NCOI PSMA1 R SPEI	574	66	*Nco*I *Spe*I
PIAS2	PIAS2 F NCOI PIAS2 R XBAI	576	64	*Nco*I *Xba*I

Key: F – forward; R – reverse; TAB3 – TAK1 binding protein 3; STAT3 – signal transducer and activator of transcription 3; EPAS-1 – endothelial PAS domain-containing protein 1; TPR – translocated promoter region; PSMB – proteasome subunit β type; PSMA1 – proteasome subunit α type-1; PIAS2 – protein inhibitor of activated STAT.

2.3.3 Plasmids purchased for the project

For the y-2-h screens, control plasmids (**Table 2.6**) were previously purchased as part of a kit (Yeast-2-hybrid system 3 kit, Clontech, Takara Bio, Saint-Germain-en-Laye, France) and amplified within the group as described in **Section 2.6**.

Table 2.6: Plasmids purchased for use in y-2-h.

Plasmid Name	Protein Expressed
pGADT7	Empty vector
pGADT7-T	SV40 large T antigen
pGBKT7-53	p53
pGBKT7-LAM	Human lamin C
pGBKT7	Empty vector

2.4 Antibodies

Antibodies were used to detect proteins in western blotting (WB) (**Section 2.14**) and confocal immunofluorescence microscopy (IF) (**Section 2.15**). The primary (1°) and secondary (2°) antibodies used, along with their working dilution, are shown below in **Table 2.7**.

Table 2.7: Antibodies used in the project.

Antibody	1° or 2°	Host & Isotype	Use	Working Dilution	Supplier Catalogue Number
Anti HA, polyclonal	1°	Rabbit	WB	1/2500	H6908 Merck
Anti Myc tag, monoclonal, (clone 9E10)	1°	Mouse IgG1	WB IF	1/2000 1/200	13-2500 Invitrogen
Anti Myc tag, polyclonal	1°	Rabbit	WB IF	1/5000 1/200	PA1-981 Invitrogen
Anti-FLAG®, monoclonal, (clone M2)	1°	Mouse IgG1	WB IF	1/1000 1/200	F1804 Merck
Anti-FLAG, polyclonal	1°	Rabbit	WB	1/2000	R1180 Origene Technologies
Anti-γ-tubulin, monoclonal, (clone GTU-88)	1°	Mouse IgG1	WB	1/5000	T6557 Merck
Anti-γ-Tubulin (AK-15), polyclonal	1°	Rabbit IgG	WB	1/1000	T3320 Merck
Anti-mouse IgG, conjugate IRDye® 800CW	2°	Goat	WB	1/15000	926-32210 LI-COR
Anti-rabbit IgG, conjugate IRDye 680RD	2°	Goat	WB	1/15000	926-68071 LI-COR
Anti-Mouse IgG (H+L), conjugate HRP	2°	Goat	WB	1/5000	W4021 Promega
Anti-Rabbit IgG (H+L), conjugate HRP	2°	Goat	WB	1/5000	W4011 Promega
Anti-Mouse IgG1, conjugate Alexa Fluor 488	2°	Goat	IF	1/500	A-21121 Invitrogen
Anti-rabbit IgG (H+L), conjugate Alexa Fluor 568	2°	Goat	IF	1/500	A-11011 Invitrogen

Key: 1° – Primary antibody, 2° – Secondary antibody; WB – Western blotting, IF – confocal immunofluorescence microscopy; HRP – horseradish peroxidase enzyme.

2.5 Primers and Oligos

Table 2.8 details the primers used in PCR and sequencing. All primers were made up in deoxyribonuclease (DNase)/ ribonuclease (RNase)/ protease free distilled H_2O (dH_2O) (#W4502, Merck) to 100 micromolar (µM) and were ordered from Merck and stored frozen at -20 ^oC. For PCR, primers were diluted to a final concentration of 0.5 µM; for use in sequencing, primers were first diluted to 3.4 µM.

Table 2.8: DNA oligonucleotide primers used in the project.

Primer name	Sequence (5' to 3')
pGADT7 F	AACCACTGTCACCTGGTTG
pGADT7 R	ACAGTTGAAGTGAACTTGC
pGADT7 R2	CGATGCACAGTTGAAGTGAACTTG
T7 F	TAATACGACTCACTATAGGG
215 NSP1α F	GCGCATATGTCTGGGACGTTCTCC
215 NSP1α R	GCGGAATTCTTAATGAGCCTCTTC
215 NSP1β F	GCGCATATGTCCAGCGTGTACAGGTG
215 NSP1β R	GCGGAATTCTTAATACCACTTATG
SU1-Bel NSP1α F	GCGCATATGTCTGGGACGTTCTCC
SU1-Bel NSP1α R	GCGGAATTCTTAGTGGGCTTCCTC
SU1-Bel NSP1β F	GCGCATATGTCTGATGTGTATAAATG
SU1-Bel NSP1β R	GCGGAATTCTTAATACCACCTATG
pEF F	CTCAAGCCTCAGACAGTGGT
pEF R	GCAAGAAAGCGAGCTTAGTG
TAB3 IN F	GGTAACTTTGATCCAAAAGCC
PSMB4 IN F	GGTTACGTGGACATGCTTGGTGTAG
STAT3 IN F	GTCAAGGAGATATGCAAGACCTGAATG
GLE1 IN F	CATGTCTCTTCCCAAGCTGTCTTC
PSMA1 IN F	GGGCTACTTATTGCTGGTTATGATG
PSMB8 IN F	CTATTGTTCATGCCACTCATCGAGAC
CUL9 IN F	GTGCAGGTCTTCTGGCAGTCAAC
TPR IN F	GTGAAACCTGGCATGAAATTGACTG
KLHL20 IN F	GGCTATGGAACTACTGATAGACTTCGC
NUP210 IN F	CTTCTAAGTTCTTCCGCAATGTCAC
EPAS-1 IN F	GCATGGACATGAAGTTCACCTACTG
BECLIN-1 IN F	CAGGATGGTGTCTCTCGCAGATTC
T7 pACT2 F	TAATACGACTCACTATAGGGGCCATGGCGTACCCATACGACGTA CCAGATTACGCTGGGATCCGAATTCGAGCTC
PSMB4 F ECORI	CCGAGAATTCATGGAATCGATTTTGGAGTCGC
PSMB4 R SPEI	CTGACTACTAGTTCATTCAAAGCCACTGATCATGTG
TAB3 F BAMHI	CATGGATCCCCTTCAAGAGGGATATCCAGTCAA
TAB3 R SPEI	GATCATACTAGTTCAGTTTAGAAAGGTGCAGCTGTCACAATT
STAT3 F NCOI	GCATCCATGGCCCAATGGAATCAGCTAC

STAT3 R SPEI	GACTGCACTAGTTTAGCGGGTCTGAAGTTGAGATTCTGCTAATG
GLE1 F NCOI	GCAGCCATGGGCATGCCTTCGGAAGGTCGC
GLE1 R SPEI	GAACTGACTAGTTTACTCCTGGGCCCTGGTGAT
PSMA1 F NCOI	GCGACCATGGGAATTGCGGGACTTACTGCC
PSMA1 R SPEI	CAGCGAACTAGTTTAATGTTCCATTGGTTCATCAGCC
PSMB8 F BAMHI	GCATGGATCCAAGGTGATTGAGATTAACCCTTACCTG
PSMB8 R XBAI	GAACTGTCTAGATTACAGACTGGCCTCCCG
CUL9 F BAMHI	GACTGGATCCGAGAAAAGCCGAGGGCAGC
CUL9 R XBAI	GTGACTTCTAGACCCCCTTCTCTGCAGCTG
TPR F NCOI	GACTCCATGGCAGCAGCTGTAGCTAAGATAGTGAAACC
TPR R SPEI	TCGACTACTAGTAAGAATGTTTGTTGGCTTTATCTGTGT
EPAS-1 F BAMHI	CAGTGGATCCCAGGATGGCGACATGAT
EPAS-1 R XBAI	CTCAAGTCTAGAGATCTCTCGAGGCCACG
BECLIN-1 F BAMHI	GCATGGATCCTCTAAGACATCCAGCAGCACCA
BECLIN -1 R SPEI	GCATGTAACTAGTTCATTTGTTATAAAACTGTGAGGATACCCAAG
PIAS2 F NCOI	GATGCCATGGGTCTAATTTTAGATGGGCTTTTTATGGAAA
PIAS2 R XBAI	TACATATCTAGAGGCTGGTGGTGGTGACAGAC
PEF XBAI R	CTGACGTCTAGACGATGCACAGTTGAAGTGAACTTG
PEF SPEI R	CTGCGAACTAGTCGATGCACAGTTGAAGTGAACTTG

Key: F – FORWARD primer; R – REVERSE primer; IN – INTERNAL primer.

Table 2.9 lists the DNA oligonucleotides (oligos) used for cloning, ordered from Merck. They were designed already digested by specific restriction enzymes at their 5' end (mentioned in their oligo name).

Table 2.9: Modified DNA oligonucleotide primers used in the project.

Oligo name	**Sequence**	**Modification**
T7 BAMHI promoter F	GATCCTAATACGACTCACTATAGGGGCCGCCGCCATGGCGTACGACGTACCAGATTACGCTGG	5' Phosphate
T7 BAMHI promoter R	GATTATGCTGAGTGATATCCCCGGCGGCGGTACCGCATGCTGCATGGTCTAATGCGACCCTAG	5' Phosphate
T7 ECORI promoter F	AATTCTAATACGACTCACTATAGGGGCCGCCGCCATGGCGTACGACGTACCAGATTACGCTGG	5' Phosphate
T7 ECORI promoter R	GATTATGCTGAGTGATATCCCCGGCGGCGGTACCGCATGCTGCATGGTCTAATGCGACCTTAA	5' Phosphate
T7 BAMHI ECORI Promoter F	GATCCTAATACGACTCACTATAGGGGCCGCCGCCATGGCGTACGACGTACCAGATTACGCTGG	5' Phosphate
T7 BAMHI Promoter R	GATTATGCTGAGTGATATCCCCGGCGGCGGTACCGCATGCTGCATGGTCTAATGCGACCTTAA	5' Phosphate

Key: F – FORWARD oligo; R – REVERSE oligo.

2.6 Plasmid amplification

2.6.1 Bacteria strains

Two strains of *Escherichia coli* were used for plasmid amplification:

- *E. coli* JM109 (#L2005, Promega, Chilworth, UK).

  Genotype: *end*A1, *rec*A1, *gyr*A96, *thi*, *hsd*R17 (r_k^-, m_k^+), *rel*A1, *sup*E44, Δ(*lac-pro*AB), [F´ *tra*D36, *pro*AB, *laq*I^qZΔM15].

- New England Biolabs (NEB®) 10-beta Competent *E. coli* (High Efficiency) (#C3019H, NEB, Hitchin, UK).
  Genotype: Δ*(ara-leu) 7697 araD139 fhuA* Δ*lacX74 galK16 galE15 e14-* φ*80*d*lacZ*Δ*M15 recA1 relA1 endA1 nupG rpsL* (Str^R) *rph spoT1* Δ*(mrr-hsdRMS-mcrBC)*

2.6.2 Bacterial cell culture

Bacteria were grown in Luria lysogeny broth (LB) or plated on LB containing agar (LB agar) with or without the presence of antibiotic.

LB powder (#L3397, Merck) was added to dH_2O at 15 grams per litre (g/L) and autoclaved to sterilise. To make LB agar, agar (#A1296, Merck) was also added at 15 g/L and autoclaved to sterilise.

In both LB and LB agar, the antibiotics kanamycin (#BP861, Merck) and ampicillin (#A9518, Merck) were used at 50 µg/mL and 100 µg/mL, respectively. Antibiotics were added after autoclaving and cooling of broth/agar.

2.6.3 Generation of rubidium competent *E. coli* JM109

New stocks of *E. coli* JM109 were generated according to an in-house protocol. TFB1 and TFB2 solutions were made up as described and filter sterilised.

A -80°C preserved stock of *E. coli* JM109 was defrosted at RT and streaked onto LB agar. Once grown, a single colony was picked, added to 20 mL LB, and incubated with shaking for 18 hr at 37°C, 200 revolutions per minute (rpm). Four mL of the culture

was added to 400 mL LB in a sealed 1 L conical flask and incubated at 37°C, 200 rpm until the culture reached an optical density at 550 nm [OD_{550}] of 0.48 (0.45-0.50). The culture was divided into 50 mL volumes and centrifuged for 8 min at 1600 × *g*, 4°C to pellet the bacteria. The supernatants were discarded, and the pellets gently re-suspended in 10 mL of cold (4°C) TFB1 solution, then incubated at RT for 5 min. The cell suspension was centrifuged for 5 min at 1600 × *g*, 4°C to pellet the bacteria. The supernatants were removed, the pellets put on ice and gently re-suspended in 1 mL of cold (4°C) TFB2 solution. Cultures were pooled and then incubated on ice for 15 min. Finally, the bacterial cultures were aliquoted on ice in 0.2 mL volumes into sterile screw tubes and stored at -80°C.

TFB1 solution pH 5.8 200 mL

- 30 mM potassium acetate (#P1190, Merck)
- 100 mM rubidium chloride (#R2252, Merck)
- 10 mM calcium chloride (#100704Y, VWR Chemicals)
- 50 mM manganese chloride (#1375127, Merck)
- 15% glycerol (v/v) (#G5516, Merck)

TFB2 solution pH 6.5 20 mL

- 10 mM MOPS (#475922, Merck)
- 10 mM rubidium chloride (#R2252, Merck)
- 75 mM calcium chloride (#100704Y, VWR Chemicals)
- 15% glycerol (v/v) (#G5516, Merck)

2.6.4 Bacterial transformation and plating

Bacteria were defrosted on ice, mixed gently with the plasmid to be amplified and then incubated on ice for 10 min. The bacteria were heat shocked at 42°C for 45 seconds (sec) and then placed back on ice. 300 microlitres (µL) of LB were added and the tubes were incubated shaking at 37°C, 200 rpm for 1.5 hr. Bacteria were plated onto LB agar plates containing either kanamycin or ampicillin (depending on plasmid) and incubated overnight at 37°C. The next day, individual colonies were picked and

cultured in LB containing either kanamycin or ampicillin (depending on plasmid). Bacterial cultures were incubated overnight at 37^{o}C, 200 rpm.

2.6.5 Plasmid extraction

Plasmids were extracted using the QIAprep Spin Miniprep Kit (#12123, Qiagen, Manchester, UK) or the QIAGEN Plasmid Midi Kit (#12143, Qiagen) according to the manufacturer's protocol and eluted in DNase/RNase/protease free dH_2O (#W4502, Merck).

2.6.6 Quantification of DNA

Concentrations of plasmid preparations were calculated using a NanoDrop One Microvolume UV-Vis Spectrophotometer (#ND-ONE-W, Thermo Fisher Scientific). The machine was first blanked with 2 µL of DNase/RNase/protease free dH_2O (#W4502, Merck) before a 2 µL sample of plasmid was added and concentration and purity were read using measurements at wavelengths of 230 nm, 260 nm and 280 nm.

2.7 Polymerase chain reaction

PCR was used to amplify DNA for cloning, investigating the size and presence of plasmid inserts and to generate DNA samples for sequencing. Forward and reverse primers were diluted 1/20 (to 5 µM) in dH_2O (#W4502, Merck) before use. Different polymerases were used for different PCR purposes based on their proof-reading abilities. For analysis, sequencing, and colony PCR, 1× ReadyMix™ Taq PCR Reaction Mix (#P4600, Merck) was used. For cloning, either Long-Range PCR: GoTaq® Long PCR Master Mix (#M4021, Promega) or Q5® High-Fidelity DNA Polymerase (#M0494S, NEB) were used due to their low error rates and proof-reading ability.

PCR reactions contained varying amounts of template (5-50 ng), primers at a final concentration of 0.5 µM, the DNA polymerase and its respective buffer diluted to 1×, and nuclease-free dH_2O (#W4502, Merck) to make a final volume of either 25 µL or 50 µL.

Table 2.10 shows the standard PCR protocol used; annealing temperatures, extensions times and number of cycles were adjusted based on primer melting temperature (T_m) and PCR product length. Extension time was based on 30 sec per kb.

Table 2.10: Standard PCR Protocol

Stage	Temperature	Number of cycles
1	95-98°C for 2-3 min	1
2	95-98°C for 20 sec	25-40 cycles
3	57-72°C for 30 sec	
4	72°C for 30 sec - 2 min	
5	72°C for 3-4 min	1
6	4°C hold	∞

Typically, 2-10 µL of each PCR amplification product was analysed on a 1% (w/v) agarose gel (**Section 2.8**).

2.8 Agarose gel electrophoresis

Agarose gels were used to visualise and purify DNA. To make a 1% (w/v) gel, 500 milligrams (mg) of agarose (UK #BIO-41025, Meridian Bioscience, London) were added to 50 mL of 1× TBE buffer (#15581044, Invitrogen™, diluted in deionised water) and heated to dissolve the agarose. Once cool, 2 µL of ethidium bromide (#17898, Invitrogen) was mixed in before pouring into a sealed gel tray. The gel was left to set at RT.

Before loading, the appropriate volume of BlueJuice™ Gel Loading Buffer (10×) (#10816015, Invitrogen) was added to each sample. Gels were loaded and run at 90 V. Gels were imaged using a BioRad GelDoc Go Gel Imaging System (#12009077, BioRad, Watford, UK), or for gel purification, visualised on a UV transilluminator (#CSLUVTSDUO365L, Cleaver Scientific, Rugby, UK).

Depending on the expected size of the samples, 5 µL of either the Quick-Load® Purple 1 kb DNA Ladder (#N0552, NEB) or Quick-Load® Purple 100 bp DNA Ladder (#N0551, NEB) was used.

2.9 DNA purification

2.9.1 DNA clean-up and concentration

PCR products, plasmids and digests were purified or concentrated where stated using the DNA Clean & Concentrator-5 kit (#D4004, ZYMO, Cambridge, UK) according to manufacturer's protocol, with an additional dry spin before elution. Samples were eluted in DNase/RNase/protease free dH_2O (#W4502, Merck).

2.9.2 Gel purification

PCR products or digests were purified using agarose gel electrophoresis (**Section 2.8**) and the QIAquick Gel Extraction Kit (#28704, Qiagen). Samples were subjected to agarose gel electrophoresis before DNA was visualised using a BioRad GelDoc Go Gel Imaging System (#12009077, BioRad). The portion of gel containing the desired DNA fragment was excised using a clean scalpel blade and subsequently processed according to the manufacturer's protocol, without using isopropanol. DNA samples were eluted in DNase/RNase/protease free dH_2O (#W4502, Merck).

2.10 Sanger sequencing

2.10.1 Sample preparation

Purified PCR samples and plasmids were Sanger sequenced (**Table 2.11**) using the primers listed in **Table 2.8** and BigDye® sequencing reagents (#4337454, Applied Biosystems, Waltham, Massachusetts, USA) Reactions were set up in either individual thin walled 0.2 mL PCR tubes or 96-well plates.

Before adding sequencing reagents, plasmids were first denatured; plasmid and dH_2O (#W4502, Merck) were mixed and heated at 95°C for 2 min before placing on ice. Each sequencing reaction was set up as follows: purified PCR product or denatured plasmid (200-400 ng), 1.5 µL of primer (pre-diluted to 3.4 µM), 1.9 µL BigDye® 10x buffer, 0.3 µL of BigDye® sequencing enzyme (kept on ice) and dH_2O (#W4502, Merck) to make a final volume of 10 µL.

The reaction mixes were then subjected to the PCR below:

Table 2.11: Sequencing PCR Protocol

Stage	Temperature	Number of cycles
1	96°C for 3 min	1
2	96°C for 20 sec	25
3	50°C for 10 sec	
4	60°C for 4 min	
5	4°C hold	∞

To end the reaction, 2.5 µL of 0.1 M EDTA (#03690, Merck) was added to each tube and mixed. Next, 70 µL of 100% ethanol was added before centrifugation at maximum speed in a bench top centrifuge (or 2204 × g if using plates) to precipitate and pellet the DNA, respectively. After centrifugation, the remaining liquid was carefully removed. The pellets were then washed in 400 µL of 70% (v/v) ethanol and centrifuged at maximum speed in a bench top centrifuge. Again, the remaining liquid was carefully removed, and the DNA pellets were air dried. The DNA pellets were each resuspended in 20 µL Hi-Di™ Formamide (#4311320, Applied Biosystems) and sequenced internally using an ABI 3730 DNA analyser (Applied Biosystems).

2.10.2 Sequence analysis

Nucleotide sequences obtained were analysed using a standard nucleotide basic local alignment search tool (BLAST) https://blast.ncbi.nlm.nih.gov/Blast.cgi?PROGRAM=blastn&PAGE_TYPE=BlastSearch&LINK_LOC=blasthome. To analyse protein sequence, sequences were first translated in 3 reading frames using ExPASy translate tool software https://web.expasy.org/translate/; the correct in frame amino acid sequence was then analysed using a standard protein BLAST https://blast.ncbi.nlm.nih.gov/Blast.cgi?PROGRAM=blastp&PAGE_TYPE=BlastSearch&BLAST_SPEC=&LINK_LOC=blasttab&LAST_PAGE=blastn.

2.11 Cloning

2.11.1 Restriction Digests

Plasmids and PCR products were cleaved using the restriction enzymes and respective buffers/solutions listed in **Table 2.12**. A standard cleavage reaction contained 1-3 µg of DNA, 1× Buffer (Promega), 1x acetylated BSA (Promega), 1 µL of restriction enzyme (kept on ice) and dH_2O to make a final volume of 30 µL (#W4502, Merck). If enzymes were compatible (at least 75% cutting efficiency in a particular buffer), double digests were carried out with both enzymes present simultaneously in the reaction. If not, sequential digests were performed with a purification step in between (as described in **Section 2.9**). Reactions were incubated at 37°C for either 2 hr or overnight.

Table 2.12: Restriction enzymes and corresponding buffers

Restriction enzyme	Optimal Buffer	Promega Catalogue Number
*Xho*I	D	R6165
*Nde*I	D	R6801
*Bam*HI	E	R6021
*Eco*RI	H	R6011
*Xba*I	D	R6181
*Nco*I	D	R6513
*Spe*I	B	R6591

2.11.2 Ligation

DNA inserts were ligated into plasmids using T4 DNA ligase (#M0202S, NEB). A standard ligation reaction contained restriction digested DNA insert (0.05-3 µg) and plasmid at a respective ratio of 3:1, 1× T4 DNA Ligase Buffer (NEB), 1 µl T4 DNA ligase (kept on ice) and dH_2O to make a final volume of 20 µl (#W4502, Merck)

Ligations were incubated between 3 hr to overnight (see specific ligation for time) at RT. After incubation, ligation products were used to transform bacteria as described in **Section 2.6**.

For some cloning, it was necessary to first anneal two DNA oligos with complementary portions to produce double-stranded DNA (dsDNA). Modified oligos in **Table 2.9** containing 5’ phosphates were mixed, 1.5 µL of each at 100 µM (ratio

1:1) and then heated at 95°C for 5 min to denature. The heater block containing the tubes was removed from the heater and left to cool, allowing the oligos to slowly anneal. Once cool, ~40^{o}C, the dsDNA was ready to be used in ligations.

Additionally, where stated, linearised plasmids were pre-treated with recombinant shrimp alkaline phosphatase (rSAP) (#M0371S, NEB) prior to use in ligations. rSAP treatment removed the phosphate groups present on either end of the dsDNA, preventing self-ligation and therefore reducing background (transformants not containing an insert). After restriction digestion, 1 µL rSAP (kept on ice) was added to the reaction. The sample was incubated at 37°C for 30 min and then either ran on an agarose gel or heated at 65°C for 5 min to inactivate the rSAP. rSAP treated plasmids were purified (as described in **Section 2.9**) before being used in ligations.

2.11.3 Colony PCR

To screen colonies for successful ligation, colony PCR was used. Colonies were picked and added to a PCR mix containing: 1x ReadyMix™ Taq PCR Reaction Mix (#P4600, Merck), forward and reverse primers (both at a final concentration of 0.5 µM) and dH_2O (#W4502, Merck) to a final volume of 24 µl. PCR amplification was then performed using the reaction parameters described in **Section 2.7** prior to sample analysis by agarose gel electrophoresis (**Section 2.8**).

2.12 Yeast-2-hybrid

2.12.1 Theory

The y-2-h is a method of detecting protein-protein interactions (Fields and Song, 1989; Brückner *et al.*, 2009). PRRSV-1 NSP1α and NSP1β from a conventional low virulence PRRSV-1 subtype 1 strain (UK field isolate 215-06) (Morgan *et al.*, 2013) were screened for host protein interactions using the y-2-h system and a cDNA library generated from PAMs.

The y-2-h screen involved transforming competent yeast with a bait and a prey plasmid. The bait plasmid pGBKT7 encoded the bait protein (PRRSV-1 NSP1α or NSP1β) fused to the galactose-responsive transcription factor 4 (GAL4) DNA binding domain (DBD). Each prey plasmid of the pACT2 library encoded a PAM protein fused to the GAL4 activation domain (AD). If the bait and prey proteins expressed in a yeast cell interacted, they reconstituted the GAL4 transcription factor and activated expression of specific reporter genes (**Figure 2.1**).

The auxotrophic yeast strain AH109 (yeast-2-hybrid system 3 kit, Clontech) was used for the interaction screens.

AH109 genotype (Holtz and Zhu, 1995; James, Halladay and Craig, 1996)**:**
MATa, trp1-901, leu2-3, 112, ura3-52, his3-200, gal4Δ, gal80Δ,
LYS2 : : GAL1$_{UAS}$*-GAL1*$_{TATA}$*-HIS3,*
GAL2$_{UAS}$*-GAL2*$_{TATA}$*-ADE2,*
URA3 : : MEL1$_{UAS}$*-MEL1* $_{TATA}$*-lacZ*

AH109 has 3 reporter genes: *ADE2*, *HIS3* and *MEL1* under the control of three completely heterologous GAL4-responsive upstream activating sequences and promoter elements - GAL2, GAL1, and MEL1, respectively. *ADE2* and *HIS3* code for essential enzymes involved in the production of the nucleobase adenine (Ade) and the amino acid histidine (His), respectively. *MEL1* encodes an alpha-galactosidase, a secreted enzyme which hydrolyses 5-Bromo-4-chloro-3-indolyl-α-D-galactopyranoside (X-α-Gal) to produce a blue end product; this aids visualisation of positive colonies.

Therefore, if bait and prey interacted, Ade, His and α-galactosidase were produced, so the yeast grew on media deficient in these and appeared blue if X-α-Gal was present.

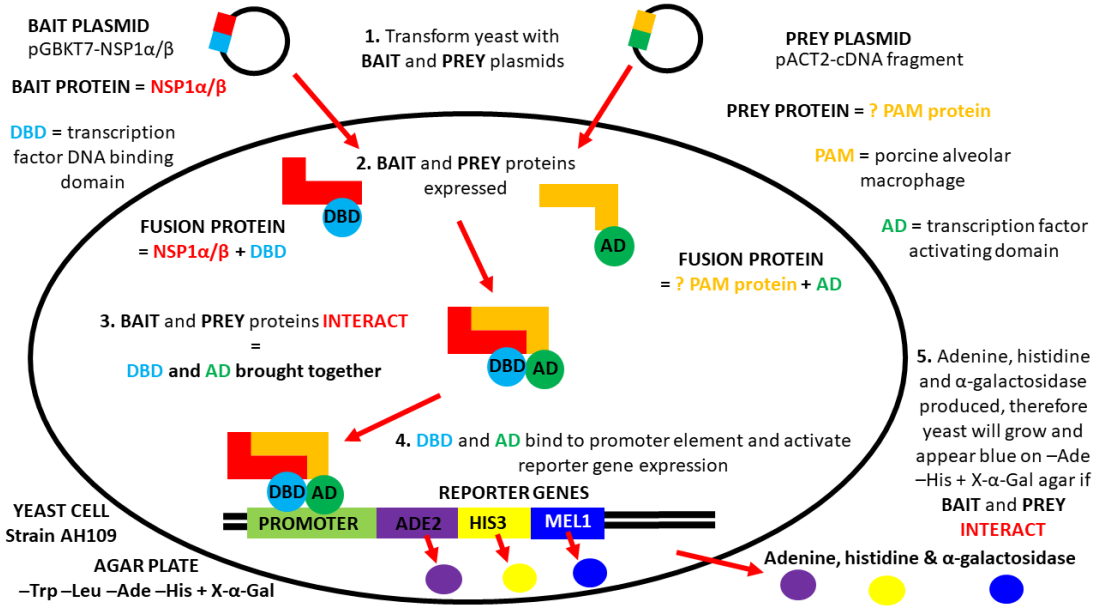

Figure 2.1: An overview of the yeast-2-hybrid system for detection of protein-protein interactions. The auxotrophic yeast strain AH109 was transformed with bait and prey plasmids that expressed a bait protein (NSP1α or NSP1β) fused to the GAL4-DBD and a prey protein (a PAM protein from the porcine protein library) fused to the GAL4-AD, respectively. Interaction of bait and prey proteins resulted in reconstitution of the GAL4 transcription factor and expression of three reporter genes (*ADE2*, *HIS3*, and *MEL1*) – expression of these reporter genes enabled the yeast to grow on media deficient in adenine (Ade) and histidine (His) and the appearance of blue colonies in the presence of the substrate X-α-Gal, respectively.

2.12.2 Yeast cell culture

Yeast were cultured using yeast extract peptone dextrose adenine (YPDA) broth or agar medium (termed YPDA broth/agar), or synthetic drop-out/synthetic defined (SD) broth or agar medium (termed SD broth/agar) deficient in various combinations of essential amino acids (tryptophan (Trp), leucine (Leu) and His) and the nucleobase Ade. SD broth/agar was made by adding the entire contents of the respective media pouch (Takara Bio) to 500 mL of dH_2O and autoclaving. Media pouches used are listed in **Table 2.13**.

Table 2.13: Yeast media pouches used in yeast cell culture

SD broth/agar	Takara Bio Catalogue Number
YPDA Broth	630306
YPDA with Agar	630307
SD/-Trp Broth	630308
SD/-Trp with Agar	630309
SD/-Leu Broth	630310
SD/-Leu/-Trp with Agar	630317
SD/-Ade/-His/-Leu/-Trp Broth	630322
SD/-Ade/-His/-Leu/-Trp with Agar	630323

Key: SD – synthetic defined premixes; -Ade – deficient in Adenine; -His – deficient in Histidine; - Leu – deficient in Leucine; -Trp – deficient in Tryptophan.

Trp or Leu deficient SD agar was used to check for successful transformation with pGBKT7 or pGADT7/pACT2 plasmids, respectively; SD agar additionally lacking Ade and His was used to check for y-2-h system activation (reporter gene expression). Additionally, where stated, X-α-gal (#630463, Takara Bio) was added to SD agar before pouring plates, according to the manufacturer's instructions (Takara Bio).

2.12.3 Yeast transformation and plating

The auxotrophic yeast strain AH109 (yeast-2-hybrid system 3 kit, Clontech) was used for the interaction screens. A -80°C stock of AH109 was streaked onto a YPDA agar plate and incubated at 30°C alongside a beaker of sterile dH_2O to maintain a favourable humid environment. Yeast were then transformed using the LiAc yeast transformation procedure according to the manufacturer's instructions (PT3247-1, Clontech). Small scale transformations were used to generate control plates (**Section 3.4**) and for y-2-h retesting (**Sections 4.2 & 4.3**), and library scale transformations were used for the y-2-h screens (**Section 3.5**).

The control plasmids used for the y-2-h system were pGADT7-T, pGBKT7-53, and pGBKT7-LAM (**Table 2.14**). pGADT7-T and pGBKT7-53 together are the positive control and pGADT7-T and pGBKT7-LAM are the negative control (Fields, 1993; Iwabuchi *et al.*, 1993). pGBKT7-53 and pGBKT7-LAM encode fusions between murine p53 and human lamin C with GAL4 DBD, respectively. pGADT7-T encodes a fusion protein of GAL4 AD and SV40 large T-antigen. SV40 large T antigen and p53 are known to interact and therefore activate expression of the y-2-h reporter genes; human

lamin C is an unreactive protein that does not interact with most proteins, including SV40 large T-antigen (Bartel *et al.*, 1993; Ye and Worman, 1995). **Table 2.14** lists the plasmid combinations that yeast were transformed with, the SD media used to culture respective transformants and the purpose of each transformation.

Table 2.14: Yeast transformation control plates: plasmid combinations and plates

Plasmid Combination	SD agar	Purpose
pGBKT7-NSP1	-Trp -Trp, -Ade, -His	Check for self-activation
pGBKT7-NSP1 & pGADT7	-Trp -Leu -Trp, -Leu, -Ade, -His	Check for self-activation
pGBKT7-NSP1 & pGADT7-T	-Trp -Leu -Trp, -Leu, -Ade, -His	Check for self-activation
pGBKT7-LAM & pGADT7-T	-Trp -Leu -Trp, -Leu, -Ade, -His	Negative control
pGBKT7-53 & pGADT7-T	-Trp -Leu -Trp, -Leu, -Ade, -His	Positive control

Key**:** Trp – tryptophan; Leu – Leucine; Ade – Adenine; His – Histidine. E.g. -Trp indicates agar was deficient in tryptophan.

For the library scale transformations, yeast were sequentially transformed with the bait plasmid, either pGBKT7-NSP1α/β or pGBKT7-NSP1β, and then the pACT2-cDNA library. pGBKT7-NSP1α/β was used for convenience, as NSP1 is cleaved into NSP1α and NSP1β, meaning only NSP1α would be fused to the GAL4 DBD; additionally, NSP1α and NSP1β do not interact (Nan *et al.*, 2018; Song *et al.*, 2018), so it is unlikely NSP1β would interfere in the NSP1α screen. The yeast, transformed with bait and prey plasmids, were numbered, and streaked (twice, sequentially) onto fresh SD agar deficient in Trp, Leu, Ade and His. Yeast were incubated at 30°C with sterile dH_2O for 1 week. Once the colonies had grown the plates were stored at 4°C**.**

To confirm interactions, initial candidates were re-tested using y-2-h (**Section 4.2**). Yeast were co-transformed with the respective bait plasmid, either pGBKT7-NSP1α or pGBKT7-NSP1β, and either the pGBKT7-53 or pGBKT7 control plasmid, or an individual prey pACT2 plasmid extracted and amplified from an individual colony during the screen. Plasmids individually expressing NSP1α were used to confirm interactions identified in the NSP1α y-2-h screen to show that NSP1β was definitely not involved in the interaction. The transformed yeast were plated onto SD agar

deficient in Trp and Leu to confirm the presence of both plasmids. Five colonies from each plate were then streaked onto fresh SD agar deficient in Trp, Leu, Ade, and His and containing X-α-Gal. Once colonies had grown the plates were imaged using a scanner. **Table 2.15** lists the plasmid combinations that yeast were transformed with for y-2-h retesting, the SD media used to culture respective transformants and the purpose of each transformation.

Table 2.15: Y-2-h retesting plasmid combinations and plates

Plasmid Combination	SD agar	Purpose
pGBKT7-53 & pGADT7-T	-Trp, -Leu -Trp, -Leu -Ade -His + X-α-gal	Positive control
pGBKT7-LAM & pGADT7-T	-Trp, -Leu -Trp, -Leu -Ade -His + X-α-gal	Negative control
pGBKT7 & pACT2-prey protein	-Trp, -Leu -Trp, -Leu -Ade -His + X-α-gal	Negative control
pGBKT7-53 & pACT2-prey protein	-Trp, -Leu -Trp, -Leu -Ade -His + X-α-gal	Positive/negative control
pGBKT7-NSP1 & pACT2-prey protein	-Trp, -Leu -Trp, -Leu -Ade -His + X-α-gal	Test for interaction

2.12.4 Plasmid extraction and purification

Positive colonies from the y-2-h screens were picked and cultured in Leu deficient SD broth, to encourage retention of the prey plasmid and loss of the bait plasmid, for 2 days at 30°C, 140 rpm. Plasmids were then extracted from the yeast cultures using the Easy Yeast Plasmid Isolation Kit (#630467, Takara Bio) following the manufacturer's protocol. Plasmids were eluted in DNase/RNase/protease free dH_2O (#W4502, Merck).

2.12.5 Identification of interacting proteins

To identify putative interacting host proteins, the cDNA insert of each extracted prey plasmid was first PCR amplified using the pGADT7 F and pGADT7 R primers (**Table 2.8**; **Section 2.7**). The PCR products were then purified and Sanger sequenced.

PCR samples were analysed by 1% (w:v) agarose gel electrophoresis (as described in **Section 2.8**) to determine the number and size of amplified inserts; multiple bands of different sizes indicated different prey plasmids had been transformed into a single yeast cell during the screening process.

For simplicity, PCR products from yeast colonies yielding only one PCR band, therefore containing only one prey protein, were selected, and purified (**Section 2.9.1**).

Purified PCR samples were then Sanger sequenced using the pGADT7 F primer and protocol described in **Section 2.10**. Sequences were translated (in all 3 forward ORFs) and analysed using BLAST with the reference pig genome taxid: 9823 to identify putatively interacting porcine proteins.

Proteins were grouped manually based on function. Sequences were also checked manually for the presence of the three ubiquitin motifs: $K^{ub}XXP$, $RXXXXLXK^{ub}$ and $K^{ub}Q$ (where K = lysine; X = any amino acid; R = arginine; P = proline, Q = glutamine; L = Leucine) as it has been shown PRRSV alters the ubiquitome of the target cell via these motifs (H. Zhang *et al.*, 2018).

2.12.6 Testing the strength of interactions using 3-AT

To test the strength of interactions, and rule out the possibility of both self-activation and the occurrence of an interaction at the same time, colonies harbouring putative interactions were retested (**Section 4.3**) by streaking onto SD agar containing 3-amino-1,2,4-triazole (3-AT; #A8056, Merck) at concentrations ranging from 2.5-60 mM. 3-AT is a competitive inhibitor of the *HIS3* gene product, an enzyme in the production pathway of His. In y-2-h, yeast will only grow in the presence of 3-AT if the level of His is sufficient to overcome the inhibitory effect of 3-AT. Therefore, the presence of 3-AT will select yeast with high levels of *HIS3* and His, which depends on the strength of the interaction between the bait and prey. The higher the 3-AT concentration, the stronger the interaction must be to overcome it. 3-AT can also be used to reduce background levels of non-specific activation (Durfee *et al.*, 1993; Fields, 1993).

2.13 Expression of Myc-NSP1α, Myc-NSP1β and FLAG-tagged host proteins

2.13.1 Transfection of mammalian cells

Cells (**Section 2.1**) were seeded in either 6-well or 24-well plates, 1-2 × 10^5 cells/well, and when 70-80% confluent, transfected with plasmid/plasmids according to one of two protocols.

The TransIT®-LT1 Transfection Reagent (#MIR2304, Mirus, Madison, WI, USA,) was used according to the manufacturer's protocol; with the exception that TransIT®-LT1 Transfection Reagent and SF, antibiotic free DMEM (#32430100, Gibco) were mixed together first before adding DNA. This method was only used to transfect cells seeded in 6-well plates; transfection mixes had a final volume of 650 µL to ensure wells were fully coated.

Alternatively, cells were transfected using acidified polymer linear-polyethylenimine (PEI; molecular weight (MW) 25 kDa, #23966-2, Polysciences, Inc, Bergstrasse, Germany). The PEI was dissolved at 5 mg/mL in 0.2 Molar hydrochloric acid that had been diluted in dH_2O (#W4502, Merck)

Plasmids to be used in transfection were first diluted to 0.02 µg/µL in sterile lactate buffered saline (LBS; 20 mM sodium lactate (#71716, Merck), 150 mM sodium chloride (#S3014, Merck) pH 4); PEI was diluted 1:50 in LBS.

Plasmids were combined as required to a total volume of 10 µL or 50 µL, according to **Table 2.16**. An equal volume of diluted PEI was added to each tube of DNA. The mix was vortexed and incubated at RT for 30 min. SF-DMEM was added, according to the table below, the entire mix was added to media in the well. Cells were incubated overnight at 37°C, 5% CO_2, and lysates collected as described in Section **2.13.3**.

Table 2.16: Volumes per well of each reagent for PEI/LBS transfection method

Reagent	24-well plate	6-well plate
DNA (0.02 µg/µL in LBS)	10 µl	50 µl
PEI (1:50 in LBS)	10 µl	50 µl
SF-DMEM	100 µl	500 µl

2.13.2 Infection with MVA-T7

To induce protein expression off plasmids containing the T7 promoter, cells were infected with MVA-T7. Three hr after transfection, 75 µL of MVA-T7 was added dropwise to each well of a 6-well plate and incubated for 1 hr at 37°C, 5% CO_2. After 1 hr, the serum percentage was adjusted to 2.5% (v/v); plates were then incubated overnight at 37°C, 5% CO_2.

2.13.3 Preparation of whole cell lysates for SDS-PAGE

Media was aspirated and cells were washed in PBS. Cells were lysed in 2× loading lysis buffer (loading lysis buffer 4× diluted in dH_20, see below) and scraped off the well using a pipette tip.

Samples were heated at 95°C for 5 min to denature proteins prior to sodium dodecyl sulphate-polyacrylamide gel electrophoresis (SDS-PAGE).

Loading lysis buffer (4×)

- 12 mL Tris-HCl pH 6.8 (#10812846001, Merck)
- 20 mL 100% glycerol (#G5516, Merck)
- 4 g sodium dodecyl sulphate (#442444H, VWR chemicals)
- 2.5 mL β-mercaptoethanol (#M6250, Merck)
- 20 mg Bromophenol Blue (#B0126, Merck)
- dH_20 up to 50 ml

2.14 SDS-PAGE and western blotting

SDS-PAGE and western blotting were used to separate and detect proteins, respectively.

The following buffers and solutions were prepared and used throughout:

10× Running buffer

- 30.3 g Tris-HCl (#10812846001, Merck)
- 144.2 g Glycine (#G8898, Merck)
- 10 g sodium dodecyl sulphate (#442444H, VWR chemicals)
- Final volume made up to 1 L with dH_2O

1× Running buffer

- 100 mL 10x Running buffer
- 900 mL dH_2O

10× Transfer buffer

- 38 g Tris-HCl (#10812846001, Merck)
- 144 g Glycine (#G8898, Merck)
- Final volume made up to 1 L with dH_2O

1× Transfer buffer

- 100 mL 10× Transfer buffer
- 200 mL isopropanol (#20842.312, VWR Chemicals)
- 700 mL dH_2O

PBS-Milk-Tween (PBS-M-T)

- 500 mL PBS
- 25 g powdered milk (5% skimmed milk (w/v) (#CH0097, Marvel, St Albans, UK)
- 250 µl Tween 20 (0.05% (v/v)) (#P1379, Merck)

PBS-Tween (PBS-T)

- 500 mL PBS
- 250 µl Tween 20 (0.05% (v/v)) (#P1379, Merck)

Cell lysates, premixed with loading lysis buffer, were first heated at 95°C for 5 min to denature proteins. Samples were loaded onto 4-20% Tris-Glycine gels (#XP04200BOX, Thermo Fisher) alongside protein ladder and gels were run at 220 V in 1x running buffer. Ladders used included: Amersham™ ECL™ Rainbow™ Marker - Full range (#GERPN800E, Merck) and Chameleon® Duo Pre-stained Protein Ladder (#928-60000, LI-COR, Cambridge, UK).

Following the separation of proteins by SDS-PAGE, the respective gel was transferred onto pre-soaked blotting paper and placed onto a transfer cassette containing transfer pads. A pre-soaked membrane was placed on top of the gel and then an additional layer of pre-soaked blotting paper placed on top (#1620118, Bio-Rad) (**Figure 2.2**). The cassette was then closed and placed into the transfer tank so that the gel faced the cathode and the membrane the anode. Proteins were transferred onto a nitrocellulose membrane (#GE10600002, Merck) at 100 V for 1 hr in pre-chilled 1× transfer buffer with an ice block in the transfer tank.

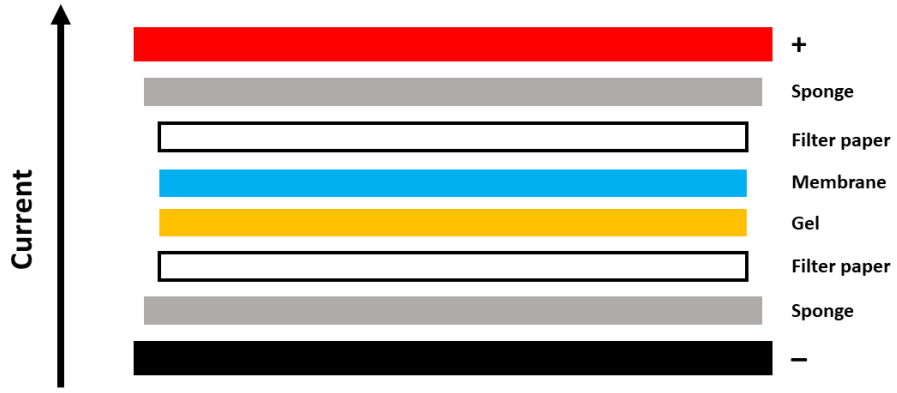

Figure 2.2: Western blotting transfer stack set up. Proteins were transferred from the gel onto a nitrocellulose membrane at 100 V in 1× transfer buffer. The stack was layered as follows: sponge pad, filter paper, gel, membrane, filter paper, sponge pad; with the gel facing the cathode and the membrane the anode. Sponge pads, filter paper and membrane were all pre-soaked in 1× transfer buffer.

Membranes were blocked in PBS-M-T for 1 hr at RT with shaking (60 rpm). After blocking, the membranes were incubated with the primary antibody diluted (see **Table 2.7** for dilutions) in 10 mL of PBS-M-T at 4°C with shaking overnight. Membranes were then washed 3 times in PBS-M-T, each for 10 min at RT with shaking (60 rpm). After washing, 10 mL of the corresponding secondary antibody diluted (**Table 2.7**) in PBS-M-T was added and the membranes were incubated at RT for 1 hr with shaking. The membranes were then washed 3 times in PBS-T and once in PBS, each for 10 min at RT with shaking (60 rpm). Membranes were stored in PBS at 4°C until imaged.

If secondary antibodies conjugated to HRP were used, blots were developed using Immobilon Western Chemiluminescent HRP substrate (#WBKLS0500, Millipore, Burlington, MA, USA) and imaged using a Syngene G:BOX and GeneSys image acquisition software. Prior to imaging, membranes were dried and coated in 2 mL of pre-mixed substrate for 5 min. Coated membranes were placed into a clear sleeve and then imaged. Exposure time varied for each antibody, ranging from less than a sec up to 10 min.

Alternatively, if LICOR IRDye secondary antibodies were used, membranes were imaged using the LI-COR Odyssey® CLx Imaging System and analysed using LI-COR Image Studio Software.

2.15 Confocal immunofluorescence microscopy

Coverslips were washed in 70% (v/v) ethanol and dried upright individually in wells of a 24-well plate. Max cells were then seeded onto the coverslips and transfected as previously described (**Section 2.13**). The next day, cells were washed in PBS and then fixed in 4% (w/v) paraformaldehyde solution in PBS (#J19943.K2, Thermo Scientific™) for 20 min. Cells were washed again and then permeabilised in 0.1% Triton™ X-100 (#T8787-100ML, Merck) for 10 min. The cells were washed twice, and then blocked for 30 min in blocking buffer (10% (w/v) goat serum (#G9023, Merck) in PBS), with shaking (60 rpm) at RT. Primary antibodies were diluted (**Table 2.7**) in blocking buffer prior to their addition to the respective well and incubated with shaking (60 rpm) for 30 min at RT. Following incubation of the primary antibody, the cells were washed 4 times before addition of the secondary antibody, also diluted in blocking buffer (**Table 2.7**). Cells were incubated, covered and with shaking (60 rpm), for 30 min at RT. The cells were washed two times in PBS, and then nuclei were stained by the addition of 4',6-diamidino-2-phenylindole (DAPI) (#40011, Biotium) diluted 1/10,000 in PBS and incubation with shaking for 20 min at RT. The cells were then washed a final two times and left covered at 4°C until mounted. To mount the coverslips, a drop of Vectashield® mounting media (#H-1000, Vector laboratories) was placed on the centre of a glass slide. The coverslip was hooked out of the well with forceps and placed top down onto the Vectashield® so the whole of the coverslip was coated. Slides were left overnight at 4°C. The next day, slides were dried using blue roll, to remove excess Vectashield®, and then sealed using clear nail varnish. Once dry, slides were stored at 4°C until imaged. Slides were imaged using a Leica TCS SP2 confocal microscope.

Chapter 3: Identification of novel interactions with PRRSV-1 NSP1α and NSP1β using yeast-2-hybrid screening

3.1 Introduction

Both PRRSV NSP1α and NSP1β have been shown to modulate the immune system in multiple ways, including inhibiting NF-κB activation, suppressing TNF expression, and inhibiting IFN-β production (Song, Krell and Yoo, 2010; Subramaniam *et al.*, 2010; He *et al.*, 2015). However, the molecular mechanisms underlying their immunomodulation remain to be fully elucidated and most studies have focussed on PRRSV-2, due to its prominence in North America and Asia. Therefore, this project aimed to improve our understanding of the modulation of host cell responses by NSP1α and NSP1β from PRRSV-1 through identifying their interactomes.

PRRSV-1 subtype 1 strain 215-06 is a low pathogenicity strain isolated at APHA from the serum of a post-weaning piglet showing signs of wasting and poor condition on a farm in Suffolk, England, in 2006. PRRSV-1 subtype 3 strain SU1-Bel (Morgan *et al.*, 2013) was also isolated at APHA from lung tissue homogenate provided by Professor Tomasz Stadejek (Warsaw University, Warsaw, Poland); this came from a 30-day-old piglet on a swine farm of overall poor health status in Belarus in 2010. PRRSV-1 SU1-Bel is more pathogenic than 215-06, as SU1-Bel infected pigs showed more clinical signs and greater lung and lymphoid organ pathology (Morgan *et al.*, 2013, 2016). NSP1α and NSP1β from these two strains were used in the project.

Novel interactions with PRRSV-1 NSP1α and NSP1β were identified using the y-2-h system and a cDNA library generated from PAMs (**Figure 3.1**). Y-2-h is a method of identifying protein-protein interactions and has been used previously to screen PRRSV NSP1α, PRRSV-1 N and PRRSV-2 NSP1β, NSP4, NSP9, NSP10 and N (**Section 1.3.5**) (Wang *et al.*, 2012; J. Li *et al.*, 2014).

In these screens, NSP1α and NSP1β served as bait proteins and the library of PAM proteins served as the prey. Yeast (AH109 strain) were co-transformed with both bait (pGBKT7) and prey (pACT2) plasmids at a concentration determined to deliver a single copy of each plasmid per cell. If bait and prey proteins interacted, yeast grew on SD agar deficient in the amino acids Trp, Leu, and His, as well as the nucleobase

Ade; and colonies were blue if X-α-gal was present in the SD agar. Plasmids were extracted from positive colonies and sequenced to identify the interacting porcine proteins.

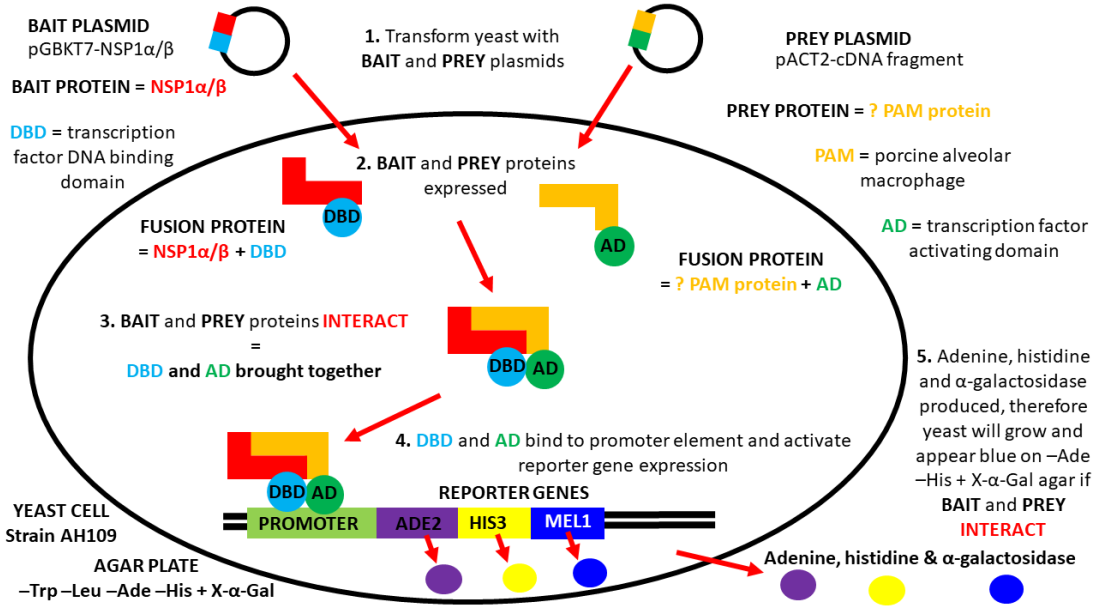

Figure 3.1: An overview of the yeast-2-hybrid system for detection of protein-protein interactions. Yeast are transformed with bait and prey plasmids that express a bait protein fused to GAL4-DNA binding domain and a prey protein fused to a GAL4-activation domain respectively. If the bait and prey interact, then the two transcription factor domains are brought together, activating reporter gene expression. In this case, proteins involved in the production of adenine (Ade) and histidine (His) and the α-galactosidase protein are produced; therefore, the yeast will grow on SD agar deficient in these and appear blue if X-α-Gal is present.

3.2 Cloning of PRRSV-1 NSP1α and NSP1β into pGBKT7

To perform the y-2-h screens, first the NSP1 genes had to be cloned into the vector pGBKT7 (Clontech), the bait plasmid used in the y-2-h system. The sequences of the respective NSP1 genes from the PRRSV-1 subtype 1 strain 215-06 and the PRRSV-1 subtype 3 strain SU1-Bel (AC# KP889243) were provided by Dr Jean-Pierre Frossard (APHA). NSP1α and NSP1β are translated from a single ORF as a pp from which they self-cleave to produce discrete proteins (den Boon *et al.*, 1995). As it was necessary to individually express NSP1α and NSP1β for the y-2-h screens, the NSP1α/β cleavage point that occurs after methionine 180 (Sun *et al.*, 2009) was used to separate their respective ORFs, and start and stop codons were introduced to each. The full-length NSP1 genes from each strain were synthesised by GeneArt (Thermo Fisher Scientific), sequences shown in **Figure 3.2,** and cloned into pGBKT7 by the Molecular Virology Group (The Pirbright Institute).

A

215-06 NSP1α/β

ATGTCTGGGACGTTCTCCCGGTGCATGTGCACCCCGGCTGCCCGGGTATTTTGGAACGCCGGCCAAGTCTTTTGCACACGGTGTCTCAGTGCGCGGT
CTCTTCTTTCTCCTGAGCTTCAAGACACTGACCTTGGAGCAATTGGCTTGTTTTACAAGCCAAGGGTAAAGCTCCACTGGAGGGTCCCTCTCGGCAT
CCCTCAGGTGGAATGTACCCCATCCGGGTGCTGTTGGCTCTCAGCTGTATTCCCTCTGGCGCGCATGACCTCCGGTAATCACAACTTCTCCCAACGA
CTGGTGAAGGTTGCTGATGTTTTGTATCGTGATGGTTGCTTGGCACCTCGACATCTTCATGAACTCCAAGTTTACGAGCGTGGTTGCAACTGGTACC
CGATCACGGGGCCCGTGCCCGGGATTGGTTTGTTTGCGAACTCCATGCACGTGTCCGACCAACCGTTCCCTGGTGCCACCCATGTGCTGACTAACTT
GCCTCTGCCTCAACAAGCTTGCCGACAGCCGTTCTGTCCATTTGAAGAGGCTCAT*TCCAGCGTGTACAGGTGGAAAAAGTTTGTGGTTTTCACGGA
CTCCTCCCCTAACGGCCGATCTCGCGTGATGTGGACGCCGGGGTCCGATGATTCAGCCGCCTTGGAGGTACTGCCGCCTGAACTAGAACGCCAGGTC
GAGATTCTTATTAGGAGTTTTCCTGCTCACCACCCTGTCGACCTGACCGACTGGGGGTTCACTGATTCCCCTGAGGACGGTTTTTCTTTTAACATGT
CTTATTCTTGTGGTTACCTTGTCCAAAATCCTGACATGTTTAATGGTAAATGCTGGCTCTCCTGCTTTTTGGACCAATCGGTTGAAGTGCGCCGCAA
TGAGGAATATCTAGCCGACGCCCTCGGCTACCAAACCAAGTGGGGCGTACATGGTAAATACCTTCAGCGTAGGCTTCAAGTTCGCGGCCTTCGTGCT
GTAGTCGATCCCGATGGTCCCGTTCACGTTGAGGCGCTGTCTTGCTCCCAGTCTTGGATTAGGCACCTGACTCTGGAAGATGATGTCACCCCAGGAT
TCGTTCGACTGACATCCCTTCGCATTGTGCCGAACACAGAGCCTACTACTCTCCCGGTCTTTCGGTTTGGAGCGCATAAGTGGTATTAA

215-06 NSP1α

ATGTCTGGGACGTTCTCCCGGTGCATGTGCACCCCGGCTGCCCGGGTATTTTGGAACGCCGGCCAAGTCTTTTGCACACGGTGTCTCAGTGCGCGGT
CTCTTCTTTCTCCTGAGCTTCAAGACACTGACCTTGGAGCAATTGGCTTGTTTTACAAGCCAAGGGTAAAGCTCCACTGGAGGGTCCCTCTCGGCAT
CCCTCAGGTGGAATGTACCCCATCCGGGTGCTGTTGGCTCTCAGCTGTATTCCCTCTGGCGCGCATGACCTCCGGTAATCACAACTTCTCCCAACGA
CTGGTGAAGGTTGCTGATGTTTTGTATCGTGATGGTTGCTTGGCACCTCGACATCTTCATGAACTCCAAGTTTACGAGCGTGGTTGCAACTGGTACC
CGATCACGGGGCCCGTGCCCGGGATTGGTTTGTTTGCGAACTCCATGCACGTGTCCGACCAACCGTTCCCTGGTGCCACCCATGTGCTGACTAACTT
GCCTCTGCCTCAACAAGCTTGCCGACAGCCGTTCTGTCCATTTGAAGAGGCTCATTAA

215-06 NSP1β

ATGTCCAGCGTGTACAGGTGGAAAAAGTTTGTGGTTTTCACGGACTCCTCCCCTAACGGCCGATCTCGCGTGATGTGGACGCCGGGGTCCGATGATT
CAGCCGCCTTGGAGGTACTGCCGCCTGAACTAGAACGCCAGGTCGAGATTCTTATTAGGAGTTTTCCTGCTCACCACCCTGTCGACCTGACCGACTG
GGGGTTCACTGATTCCCCTGAGGACGGTTTTTCTTTTAACATGTCTTATTCTTGTGGTTACCTTGTCCAAAATCCTGACATGTTTAATGGTAAATGC
TGGCTCTCCTGCTTTTTGGACCAATCGGTTGAAGTGCGCCGCAATGAGGAATATCTAGCCGACGCCCTCGGCTACCAAACCAAGTGGGGCGTACATG
GTAAATACCTTCAGCGTAGGCTTCAAGTTCGCGGCCTTCGTGCTGTAGTCGATCCCGATGGTCCCGTTCACGTTGAGGCGCTGTCTTGCTCCCAGTC
TTGGATTAGGCACCTGACTCTGGAAGATGATGTCACCCCAGGATTCGTTCGACTGACATCCCTTCGCATTGTGCCGAACACAGAGCCTACTACTCTC
CCGGTCTTTCGGTTTGGAGCGCATAAGTGGTATTAA

B

SU1-Bel NSP1α/β

ATGTCTGGGACGTTCTCCCGGTGCAAGTGCACCCCGGCAGCTCGGGTAATGTGGGAAGCCGGCCAAGTCTATTGCACACGGTGTCTCAGTGCACGGTCTCTCCTTCCT
TTGGACCTCCAGGACACTGACCTTGGTGCAGTTGGCTTGTTTTACAAGCCCAGGGAAAAGCTTCCTTGGAAAATTCCTATGGGCATCCCCCAGGCAGAGTGTACTCCG
TCCGGATGTTGCTGGCTTTCGGCCATTTTTCCAATAGCACGCATGACCTCAGGCAATCACAACTTCGCCCAACGGCTTGTGAAGGTCGCTGATGTGTTGTATCGTGAG
GGCTGCCTGGCCCCACGACACCTTCGTGAACTCCAAGTTTACGAACGTGGCTGCAGCTGGTACCCGATTACGGGGCCTGTACCCGGGATAGGTTTGTACGCGAACTCC
ATGCATGTGTCCGACAAGCCATTTCCCGGAGCCACCCATGTATTGACGAACTCACCATTGCCTCAGCAGGCCTGTCGACAGCCGTTCTGTCCGTTTGAGGAAGCCCAC
*TCTGATGTGTATAAATGGAAGGGCTTTGTGGTGTTTGTGGATAGTTCTTCTGATGGTTTGCTCCGCATGATGTGGACCCCCGGAAGTGTCGACTCAGCAAACCTGGA
ACCTCTACCATCCGGGTTGGAACAAAAGGCCGAAATTCTTACGCGTAGTTTCCCGGCTCACCACCCCGTCGATTTCACCGATTGGGACTTCACTGAGTCTCCCGAAAA
CGGGTTTTCTTTTAGCATGTCTCATTCTCATGGCTACCTCGTTCCGGGTGACGATAGGTATAATGGTAAGTGTTGGCTCTCGTGTTTTTTGGGCCTGTCAGCCGAAGG
GCGCCTCCGCGAAGAGTTCCTAGCCGTTGCCTTTGGTTACAACACCAAATGGGGTGTGCCTGGCAAGTACCTCCAACGCAGGCTTCAAGTTAACGGCCTCCGTGCCGT
AACCGACCCTAATGGCAACATCCATGTTGAGGCGTTGTCTTGCCCCCAATCTTGGGTTAGGCATCTAACTCTGAGCGATGACGTCACTCCGGGTTTTGTCCGCCTTGT
GTCCATTCGCATCGAACCAAACACAGAGCCCACCGACCGCCCGTTCTTCCGGTTCGGAGCGCATAGGTGGTATTAA

SU1-Bel NSP1α

ATGTCTGGGACGTTCTCCCGGTGCAAGTGCACCCCGGCAGCTCGGGTAATGTGGGAAGCCGGCCAAGTCTATTGCACACGGTGTCTCAGTGCACGGTCTCTCCTTCCT
TTGGACCTCCAGGACACTGACCTTGGTGCAGTTGGCTTGTTTTACAAGCCCAGGGAAAAGCTTCCTTGGAAAATTCCTATGGGCATCCCCCAGGCAGAGTGTACTCCG
TCCGGATGTTGCTGGCTTTCGGCCATTTTTCCAATAGCACGCATGACCTCAGGCAATCACAACTTCGCCCAACGGCTTGTGAAGGTCGCTGATGTGTTGTATCGTGAG
GGCTGCCTGGCCCCACGACACCTTCGTGAACTCCAAGTTTACGAACGTGGCTGCAGCTGGTACCCGATTACGGGGCCTGTACCCGGGATAGGTTTGTACGCGAACTCC
ATGCATGTGTCCGACAAGCCATTTCCCGGAGCCACCCATGTATTGACGAACTCACCATTGCCTCAGCAGGCCTGTCGACAGCCGTTCTGTCCGTTTGAGGAAGCCCAC
TAA

SU1-Bel NSP1β

ATGTCTGATGTGTATAAATGGAAGGGCTTTGTGGTGTTTGTGGATAGTTCTTCTGATGGTTTGCTCCGCATGATGTGGACCCCCGGAAGTGTCGACTCAGCAAACCTG
GAACCTCTACCATCCGGGTTGGAACAAAAGGCCGAAATTCTTACGCGTAGTTTCCCGGCTCACCACCCCGTCGATTTCACCGATTGGGACTTCACTGAGTCTCCCGAA
AACGGGTTTTCTTTTAGCATGTCTCATTCTCATGGCTACCTCGTTCCGGGTGACGATAGGTATAATGGTAAGTGTTGGCTCTCGTGTTTTTTGGGCCTGTCAGCCGAA
GGGCGCCTCCGCGAAGAGTTCCTAGCCGTTGCCTTTGGTTACAACACCAAATGGGGTGTGCCTGGCAAGTACCTCCAACGCAGGCTTCAAGTTAACGGCCTCCGTGCC
GTAACCGACCCTAATGGCAACATCCATGTTGAGGCGTTGTCTTGCCCCCAATCTTGGGTTAGGCATCTAACTCTGAGCGATGACGTCACTCCGGGTTTTGTCCGCCTT
GTGTCCATTCGCATCGAACCAAACACAGAGCCCACCGACCGCCCGTTCTTCCGGTTCGGAGC
GCATAGGTGGTATTAA

Figure 3.2: PRRSV-1 215-06 and SU1-Bel NSP1α and NSP1β gene sequences. Nucleotide sequences encoding NSP1α and NSP1β proteins from both PRRSV-1 215-06 (**A**) and SU1-Bel (**B**). The NSP1α/β cleavage site methionine 180 (shown by *) and start and stop codons (shown in green and red, respectively) are indicated.

The respective NSP1α and NSP1β genes were PCR amplified using the pGBKT7-NSP1α/β plasmids as templates with the following combinations of primers: 215-06 NSP1α F with 215-06 NSP1α R; 215-06 NSP1β F with 215-06 NSP1β R; SU1-Bel NSP1α F with SU1-Bel NSP1α R; and SU1-Bel NSP1β F with SU1-Bel NSP1β R (**Table 2.8**). These primers also introduced *Nde*I and *Eco*RI restriction sites for cloning into the y-2-h plasmid pGBKT7. The PCR products were size checked and purified by agarose gel

electrophoresis (**Sections 2.8 & 2.9.2**). Bright bands approximately 500-600 base pairs (bp) for each NSP1α and 600-700bp for each NSP1β were observed; this matched the expected sizes. (**Figure 3.3**).

Figure 3.3: Purified PRRSV-1 NSP1α and NSP1β PCR products. PCR with the respective forward and reverse NSP1 primers was used to amplify the NSP1 genes and introduce *Nde*I and *Eco*RI restriction sites for cloning into pGBKT7. The PCR products were analysed by agarose gel electrophoresis.

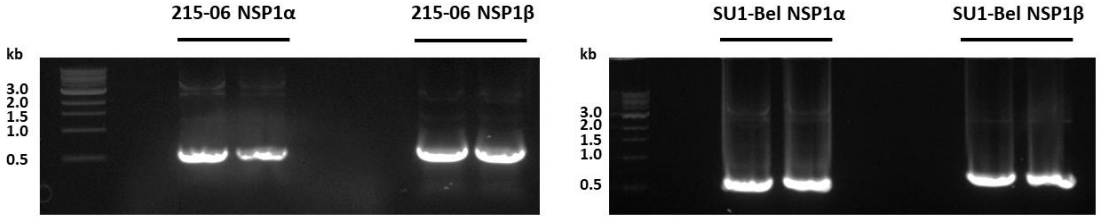

To generate 'bait' plasmids, the purified PCR products and pGBKT7 were restriction digested using *Nde*I and *Eco*RI, and ligations were performed (**Section 2.11**). The ligation products were then used to transform bacteria (**Section 2.6.4**). Colonies were screened by PCR to identify bacterial clones that contained the respective pGBKT7-NSP1 plasmid (**Section 2.11.3**); 10 colonies from each plate were analysed using the T7 forward primer and the respective NSP1 reverse primer (**Table 2.8**). PCR products were analysed by gel electrophoresis, as shown in **Figure 3.4**. The presence of a bright band of the expected size (~600bp) indicated the presence of a plasmid containing the corresponding NSP1α or NSP1β gene inserted in the correct orientation.

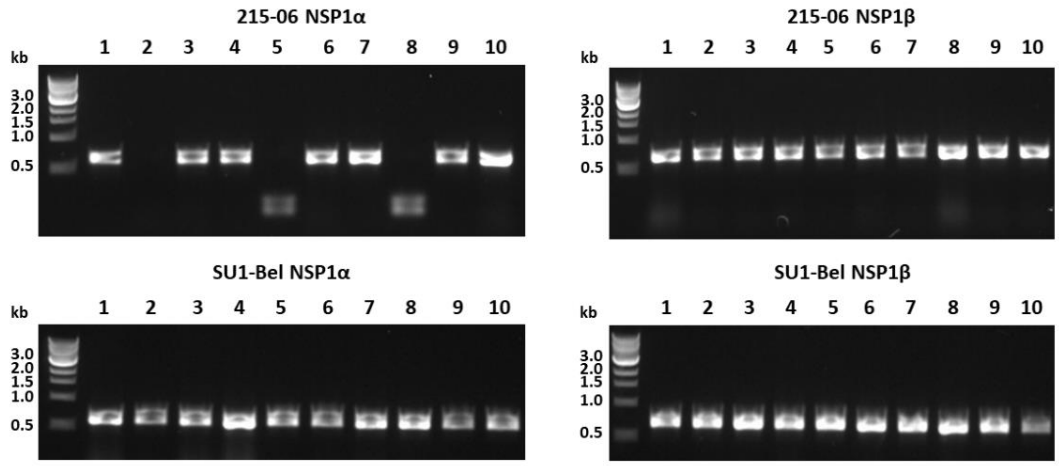

Figure 3.4: Colony PCR to identify colonies containing bait plasmids. Bacterial colonies were screened by colony PCR for either pGBKT7-NSP1α or pGBKT7-NSP1β, using the T7 forward primer and the respective NSP1 reverse primer. The PCR products were analysed by agarose gel electrophoresis.

Two positive colonies from each plate were subsequently amplified and the corresponding plasmids extracted (**Section 2.6.5**) and sequenced (**Section 2.10**), using the T7 forward primer to check the sequence and ensure the cloning was in frame. Plasmids with the correct sequence and frame were used for y-2-h analyses.

3.3 Verifying PRRSV-1 NSP1α and NSP1β protein expression

After successful cloning, expression of each NSP1α and NSP1β protein was checked in mammalian cells via transfection and western blot analysis. pGBKT7 contains the T7 promoter and an in frame Myc-tag upstream of the respective NSP1 ORF. Therefore, BSR-T7 cells expressing the T7 RNA polymerase were used for these transfection experiments in combination with MVA-T7 infection to further increase expression of the NSP1 proteins. BSR-T7 cells were seeded in 6-well plates and, when 70% confluent, were transfected (**Section 2.13.1**) with either 215-06 pGBKT7-NSP1α, 215-06 pGBKT7-NSP1β, SU1-Bel pGBKT7-NSP1α or SU1-Bel pGBKT7-NSP1β. Three hr later, the cells were infected with MVA-T7; and 24 hr later, whole cell lysates were prepared (**Section 2.13.3**) and analysed by SDS-PAGE and western blot using a mouse anti-Myc antibody (**Table 2.7**). NSP1α and NSP1β alone are predicted to be approximately 19 kDa and 23 kDa, respectively (Sun *et al.*, 2009; Xue *et al.*, 2010), but have been shown to run slightly larger (NSP1α at ~20 kDa and NSP1β at ~27 kDa) (Kroese et al., 2008). Membranes were also probed with a rabbit anti-γ-tubulin (**Table 2.7**) to confirm equal loading (**Figure 3.5**).

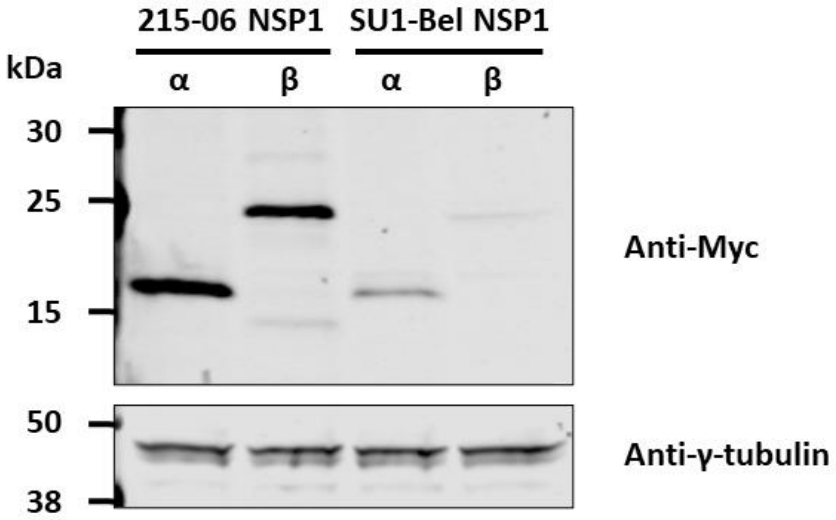

Figure 3.5: Western blot analysis of BSR-T7 cells transfected with pGBKT7-NSP1 constructs. To check for protein expression, BSR-T7 cells were transfected with either 215-06 pGBKT7-NSP1α, 215-06 pGBKT7-NSP1β, SU1-Bel pGBKT7-NSP1α or SU1-Bel pGBKT7-NSP1β. Cells were infected with MVA-T7 and lysates analysed by western blot. NSP1α and NSP1β have predicted molecular weights of approximately 19 kDa and 23 kDa, respectively. The membranes were probed with mouse anti-Myc antibody and rabbit anti-γ-tubulin, respectively.

Western blot analysis of whole cell lysates of cells transfected with 215-06 pGBKT7-NSP1α using the anti-Myc antibody revealed a strong band of ~19-20 kDa, as predicted (**Figure 3.5, lane 1**). Conversely, in cells transfected with SU1-Bel pGBKT7-NSP1α a less-intense band of comparable size was visible (**Figure 3.5, lane 3**). Similar analysis of whole cell lysates of cells transfected with 215-06 pGBKT7-NSP1β revealed a strong band at ~25 kDa (**Figure 3.5, lane 2**), which matches the predicted size for NSP1β. In comparison, a less intense band was visible for whole cell lysates of cells transfected with SU1-Bel pGBKT7-NSP1β (**Figure 3.5, lane 4**). Gamma tubulin (band at between 38-50 kDa, **Figure 3.5**) was expressed equally in all lysates, suggesting equal levels of basal protein expression and protein loading across the wells.

All proteins were expressed at the predicted sizes, supporting the sequence data that the NSP1 genes had been cloned in frame. However, there were differences in levels of expression: NSP1α and NSP1β from PRRSV-1 215-06 expressed significantly higher than PRRSV-1 SU1-Bel NSP1α and NSP1β. The reasons for these observed differences in protein expression are unknown.

3.4 Testing PRRSV-1 NSP1α and NSP1β for self-activation of yeast-2-hybrid

Before NSP1α and NSP1β could be used as bait to screen the PAM cDNA library, they were first checked for self-activation of the y-2-h system. Self-activation induces reporter gene expression and enables the yeast to grow on selective SD agar, preventing the identification of true protein interactions. To confirm that the NSP1 proteins do not self-activate the y-2-h system, the auxotrophic yeast strain AH109 was transformed with different combinations of bait and prey plasmids, using a small scale LiAc yeast transformation procedure (**Section 2.12.3**), and then grown on selective SD agar. For both PRRSV strains, the plasmid combinations and corresponding SD agar plates shown in **Table 3.1** were used.

Yeast were either transformed with the respective pGBKT7-NSP1 plasmid and plated onto medium lacking Trp (**-Trp**, **Table 3.1**), or co-transformed with the respective pGBKT7-NSP1 plasmid and either the empty pGADT7 plasmid or the pGADT7-T control plasmid and plated onto Trp and Leu deficient SD agar (**-Trp -Leu**, **Table 3.1**). Co-transformation of pGBKT7-LAM and pGADT7-T, or pGBKT7-53 and pGADT7-T plasmids served as negative and positive controls, respectively.

Table 3.1: Yeast transformation plasmid combinations and plates to test for self-activation.

Plasmid Combination	SD Agar Plate	Comment
pGBKT7-NSP1α	-Trp & -Trp, -Ade, -His	
pGBKT7-NSP1β	-Trp & -Trp, -Ade, -His	
pGBKT7-NSP1α & pGADT7	-Trp -Leu & -Trp, -Leu, -Ade, -His	
pGBKT7-NSP1β & pGADT7	-Trp -Leu & -Trp, -Leu, -Ade, -His	
pGBKT7-NSP1α & pGADT7-T	-Trp -Leu & -Trp, -Leu, -Ade, -His	
pGBKT7-NSP1β & pGADT7-T	-Trp -Leu & -Trp, -Leu, -Ade, -His	
pGADT7-T & pGBKT7-LAM	-Trp -Leu & -Trp, -Leu, -Ade, -His	Negative control
pGADT7-T & pGBKT7-53	-Trp -Leu & -Trp, -Leu, -Ade, -His	Positive control

Key**:** Trp – tryptophan; Leu – Leucine; Ade – Adenine; His – Histidine. E.g. -Trp indicates SD agar was deficient in tryptophan.

The bait plasmid pGBKT7 encodes a protein involved in the synthesis of Trp. The prey pGADT7 plasmid is similar to the library plasmid pACT2 and was used as a prey plasmid control; both pACT2 and pGADT7 encode a protein involved in Leu synthesis. Therefore, -Trp medium was initially used to plate yeast transformed with the pGBKT7 plasmid, and -Trp, -Leu medium to plate yeast co-transformed with both pGBKT7 and pGADT7 plasmids.

The positive (pGADT7-T and pGBKT7-53) and negative (pGADT7-T and pGBKT7-LAM) control plasmids (Clontech) encode proteins which are known to interact or not interact, respectively. pGADT7-T encodes the GAL4 AD fused to SV40 large T antigen whilst pGBKT7-53 encodes p53 fused to the GAL4 DBD. Large T antigen and p53 have been shown to interact and activate the y-2-h system, so together act as the positive control (Li and Fields, 1993). pGBKT7-LAM encodes the GAL4 DBD fused to human lamin C, an inert protein which does not interact or complex with most proteins; this, therefore, does not interact with large T antigen or activate the y-2-h system and so is the negative control (Ye and Worman, 1995).

Following growth of the transformed yeast on -Trp medium, four colonies were streaked onto the same medium (**Table 3.1, Figure 3.6 B**) to confirm they contained the respective plasmid, as well as higher stringency medium additionally lacking Ade and His (-Trp, -Ade, -His, **Table 3.1**) to investigate self-activation (**Figure 3.6 C**). Similarly, four yeast colonies from the -Trp, -Leu medium (pGBKT7 and pGADT7 transformants) were re-streaked onto the same medium (**Figure 3.6 E**), as well as higher stringency medium (-Trp, -Leu, -Ade, -His, **Table 3.1**) (**Figure 3.6 F**).

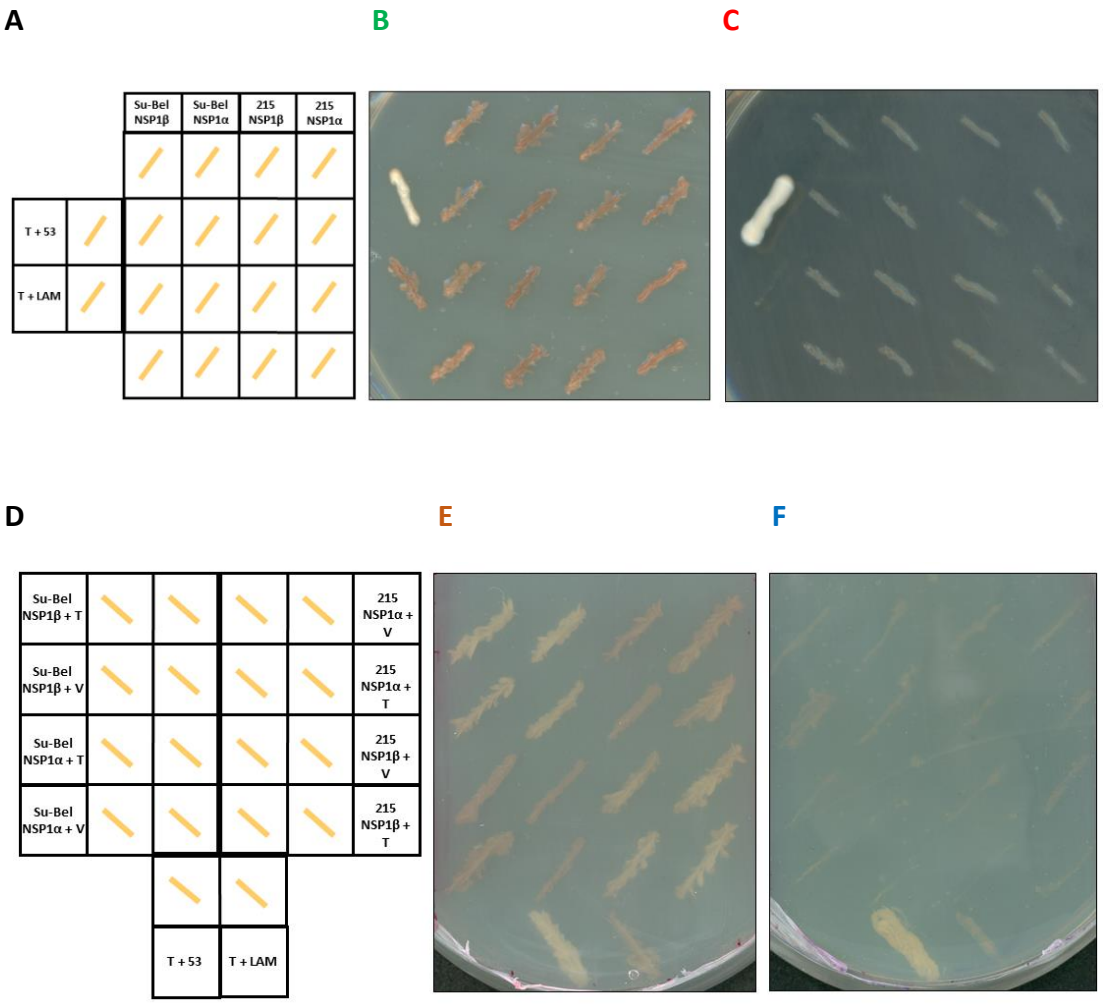

Figure 3.6: Yeast control plates to check for self-activation of the y-2-h system by NSP1α/β. Key: V – pGADT7; T – pGADT7-T; 53 – pGBKT7-53; LAM – pGBKT7-LAM. To confirm NSP1α and NSP1β did not activate the y-2-h system, yeast were transformed with combinations of plasmids and then grown on selective SD agar. Plate layout (**A**) for plates (**B**) and (**C**). Yeast were transformed with a pGBKT7 plasmid encoding NSP1α or NSP1β from 215-06 or SU1-Bel PRRSV-1 strains. Four yeast colonies were then streaked onto (**B**) -Trp medium to confirm the presence of the plasmid, and (**C**) -Trp, -Ade, -His higher stringency medium to investigate self-activation of the y-2-h system. Plate layout (**D**) for plates (**E**) and (**F**). Yeast were co-transformed with a pGBKT7 plasmid encoding NSP1α or NSP1β from 215-06 or SU1-Bel PRRSV-1 strains, together with either the empty pGADT7 or pGADT7-T control plasmid. Two yeast colonies were then streaked onto (**E**) -Trp, -Leu medium to confirm the presence of the plasmids, and (**F**) -Trp, -Leu, -Ade, -His higher stringency medium to investigate self-activation of the y-2-h system. In the y-2-h system, T+53 and T+LAM act as positive and negative controls, respectively.

All yeast streaked onto either the -Trp or -Trp, -Leu selective SD agar grew, confirming successful transformation of the respective plasmids. However, all the transformed yeast, except those expressing the T and 53 positive control proteins, were unable to grow on the higher stringency SD agar (-Trp, -Ade, -Leu or -Trp, -Leu, -Ade, -His) and appeared red as they could not synthesise Ade. As expected, co-transfection of the T+53 positive control plasmids successfully activated the y-2-h system, leading to the synthesis of Ade and growth of white colonies. These results confirmed that neither the NSP1α or NSP1β proteins of PRRSV-1 215-06 or SU1-Bel strains self-activated the y-2-h system when expressed alone or in combination with the SV40 T antigen control.

As yeast transformed with pGBKT7-NSP1α or pGBKT7-NSP1β, either alone or in combination with pGADT7 or pGADT7-T, did not activate the y-2-h system, the proteins were then able to be tested for protein interactions using y-2-h.

3.5 Yeast-2-hybrid screening of PRRSV-1 NSP1α and NSP1β

Although none of the viral proteins self-activated the system, only PRRSV 215-06 NSP1α and NSP1β were taken forward and used in the y-2-h screen. Due to time constraints, it was not possible to screen proteins from both strains, and 215-06 is more representative of PRRSV-1 strains that are predominant in Western, Central and Southern Europe, North America, and Asia.

For the NSP1α and NSP1β y-2-h screens, yeast were transformed with either pGBKT7-NSP1α/β or pGBKT7-NSP1β, respectively, and plated on -Trp SD agar. A single colony from either the pGBKT7-NSP1α/β or the pGBKT7-NSP1β transformed yeast plate was selected and grown up in Trp deficient broth to retain and amplify the bait plasmid. The yeast were then transformed with the pACT2 cDNA PAM library using a library scale LiAc yeast transformation (**Section 2.12.3**). The amount of library (200 µg in a volume of 450 µL) used for the transformation was determined from previous screens in which approximately 1.5×10^6 yeast transformants were screened using the same protocol. The yeast, now transformed with both bait and prey plasmids, were plated onto high stringency medium (-Trp, -Leu, -Ade and -His) and incubated at 30°C for 1 week. Plates were checked daily and yeast colonies that grew were numbered and streaked onto the same high stringency medium; the colonies were subsequently re-streaked a further two times onto the high stringency medium, to reduce false positives. Restreaking prevented yeast growing due to residual nutrients that were present from the transformation protocol. Once colonies had grown, the plates were stored at 4°C until plasmid extraction.

To identify the PAM proteins potentially interacting with NSP1α or NSP1β, the prey plasmids first needed to be extracted from the positive colonies and their respective cDNA inserts sequenced. A maximum of approximately 200 putative interactions for each screen were selected to be investigated. Positive colonies (those that had grown on high stringency SD agar) from both the PRRSV-1 215-06 NSP1α and NSP1β screens were selected and grown up in -Leu broth for 2 days, shaking at 30°C. This was to amplify and encourage retention of the prey plasmid and to encourage loss of the bait plasmid, as only the prey plasmid needed to be sequenced. Plasmids were then extracted from the yeast using a commercial kit (**Section 2.12.4**).

3.6 Identification of PAM proteins that interact with PRRSV-1 NSP1α and NSP1β

3.6.1 Checking presence, number, and size of inserts of prey plasmids

To identify putative interacting host proteins, the cDNA insert of each plasmid was sequenced and analysed using web-based bioinformatic software. It was noted that the yield of plasmid cDNA obtained using the kit had been problematic for other members of the group. Therefore, to amplify the respective cDNA inserts the extracted prey plasmids were used as templates in PCR with pGADT7 F and pGADT7 R primers (**Section 2.7**). PCR samples were analysed by 1% (w:v) agarose gel electrophoresis to determine the number and size of amplified inserts (**Section 2.8**); multiple bands of different sizes indicated that different prey plasmids had been transformed into a single yeast cell during the screening process. It was important to know the number of prey plasmids present in each colony, as an interaction could have been due to just one of the prey proteins, or due to all of them interacting together.

Figure 3.7 and **Figure 3.8** show the PCR products produced using plasmids encoding putative interactors of NSP1α and NSP1β, respectively; additional gels analysing NSP1β PCR products can be found in **Appendix 9.1**. The brightest band in each lane was expected to be the PCR product that encoded a putative interactor. Each colony contained a different cDNA insert; therefore, the bands were different sizes. Most colonies yielded one bright band and were therefore single transformants, but some, such as colony 39 (**Figure 3.7**), contained two bands of comparable intensity; in such cases, it was presumed that two prey plasmids had been transformed into a single yeast cell.

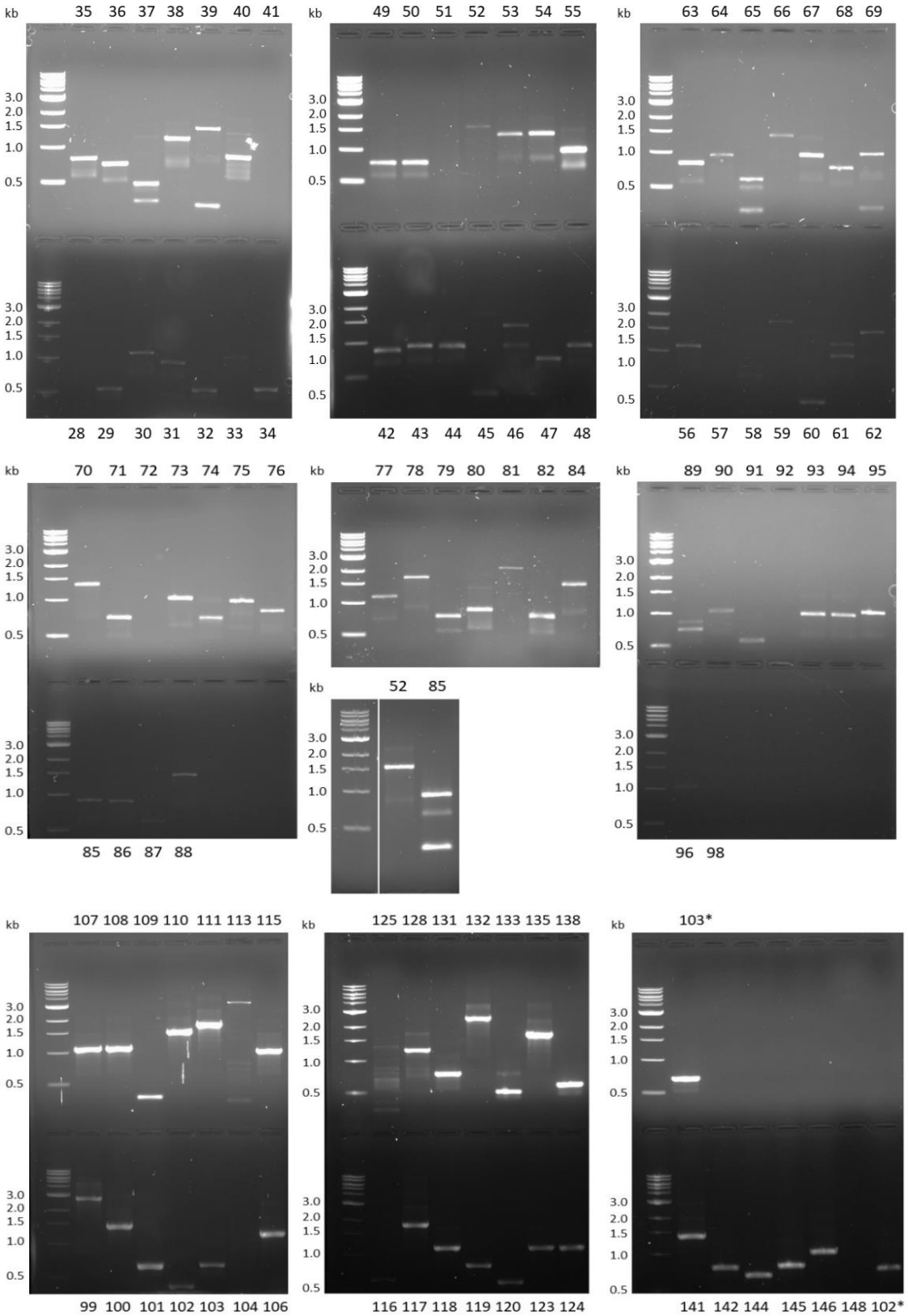

Figure 3.7: PCR of inserts of prey plasmids from PRRSV-1 NSP1α colonies. PCR was used to amplify the cDNA inserts within 120 extracted plasmids from the NSP1α screen. The PCR products were analysed by agarose gel electrophoresis. The lane number indicates the colony number; 102 and 103 were misnumbered and were different colonies to 102* and 103*.

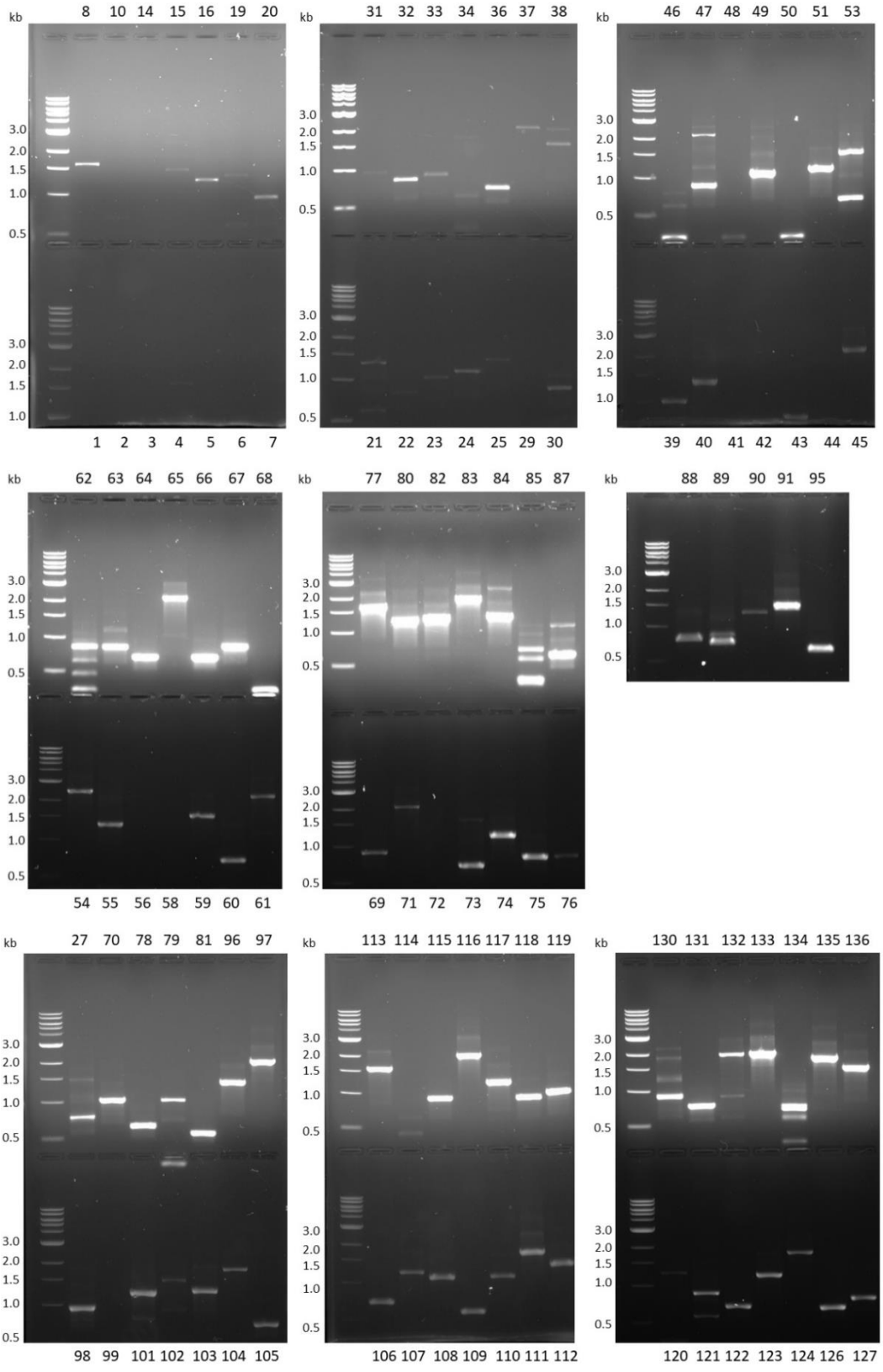

Figure 3.8: PCR of inserts of prey plasmids from PRRSV-1 NSP1β colonies. PCR was used to amplify the cDNA inserts within 308 extracted plasmids from the NSP1β screen. The PCR products were analysed by agarose gel electrophoresis. The lane number indicates the colony number. Selected samples were re-run if they had run off the gel/into the next gel.

Yeast colonies yielding only one PCR product, therefore presumably containing only one prey plasmid encoding a prey protein, were selected for subsequent purification and sequencing. From the NSP1α and NSP1β screens, 84 and 233 colonies, respectively, were selected based on the PCR gels; the NSP1β screen produced more than 350 colonies, so therefore more could be analysed. PCR products were purified using a commercial kit (**Section 2.9.1**).

3.6.2 Sequencing of cDNA inserts

Purified PCR samples were then Sanger sequenced using BigDye® reagents (**Section 2.10**) and an internal sequencing service using an ABI 3730 DNA analyser (Applied Biosystems). Sequences obtained were translated in all three forward ORFs using ExPASy translate tool software https://web.expasy.org/translate/. The sequence in frame with the HA epitope tag (YPYDVPDYA) in the vector sequence was selected and prey proteins were identified using NCBI protein BLAST software https://blast.ncbi.nlm.nih.gov/Blast.cgi?PAGE=Proteins. If an insert was not in frame but gave the best match, this was recorded. Blast comparisons were performed using the reference pig genome taxid: 9823. If there was no obvious reading frame or protein identified, NCBI nucleotide BLASTs were performed instead using https://blast.ncbi.nlm.nih.gov/Blast.cgi?PAGE_TYPE=BlastSearch. The reference sequence with the highest similarity to the query sequence was recorded.

The putative binding proteins were grouped broadly based on their primary function, their location or pathway they functioned in. There were 29 groups: ubiquitin related, MHC related, heat shock proteins (HSPs), secretion and endocytic pathways, IFN related, DNA binding/modifying, apoptosis, complement, ribosomal, receptors/cell surface molecules, extracellular matrix, structural, cell division, signalling, RNA binding/modifying, guanosine-5'-triphosphate (GTP) related, galectin, nicotinamide adenine dinucleotide phosphate (NADPH) oxidase, DNA/RNA processing, protein processing, mitochondria, protease/protease related, enzymes, transcriptional regulation, autophagy, nuclear proteins, PRRs, translation, intracellular transport, antibodies, cell migration/movement, proteasome, NF-κB and miscellaneous. Function was recorded along with name, interacting region (the portion of the protein in pACT2 that was expressed), NCBI sequence ID, E value, and which and how

many clones gave this result (**Table 3.2, Table 3.3**). The E value indicates the significance of the result, it 'describes the number of hits one can "expect" to see by chance when searching a database of a particular size'; the smaller the E value the more significant the result (https://blast.ncbi.nlm.nih.gov/Blast.cgi?CMD=Web&PAGE_TYPE=BlastDocs&DOC_TYPE=FAQ#expect). The protein sequences were also checked for the presence of the three ubiquitin motifs: $K^{ub}XXP$, RXXXXLXK^{ub} and $K^{ub}Q$ (where K = lysine; X = any amino acid; R = arginine; P = proline, Q = glutamine; L = Leucine) as it has been shown PRRSV alters the ubiquitome of the target cell via these motifs (H. Zhang *et al.*, 2018). Not all inserts matched the full-length protein, because the library contained partial and full-length cDNA, so the region of the protein identified was also recorded. Information on protein function and known interactions with PRRSV or other viruses was recorded directly from a combination of https://www.uniprot.org/, https://en.wikipedia.org/wiki/Main_Page, https://www.ncbi.nlm.nih.gov/ and selected papers (**Appendix 9.2**, **Appendix 9.3**). If sequences from different colonies gave the same protein but with alternative sequence IDs and/or different isoforms, they were recorded together in the same row.

3.6.2.1 Sequence results from PRRSV-1 NSP1α screen

From the NSP1α screen, 88 sequences were obtained and analysed as described in **Section 3.6.2**; these identified 63 potential binding partners for NSP1α. **Table 3.2** shows the results of the NSP1α screen. Proteins selected for further characterisation are highlighted in green and were selected based on the reported pathways that PRRSV is known to use or antagonise; residues highlighted in blue are ubiquitinated. A more detailed table can be found in **Appendix 9.2**.

Table 3.2: Proteins identified in the NSP1α yeast-2-hybrid screen.

Clone #	Protein and NCBI Sequence ID	Region N or AA	Ubiquitin motifs: KXXP RXXXXLXK KQ	E value
Ubiquitin related				
29 32	**Ubiquitin B** AB084843.1	23-96 23-96	KQ KQ	3e-46 4e-46

47	**E3 ubiquitin-protein ligase MARCH7 isoform X8** XP_020930440.1	313-444	KNVP RDPERLQK	1e-88
42	**anaphase-promoting complex subunit 10** NP_001171398.1	1-149	KTPP, KQ	1e-08
MHC related				
10 93 94 128	**beta-2-microglobulin precursor** NP_999143.1	 25-118 25-118 25-118	 - - -	 3e-66 2e-66 5e-65
100 108	**zinc finger protein ZXDC** NP_001231151.1	575-821 703-842	KQ KQ	3e-162 5e-84
Heat shock proteins				
35 76	**heat shock cognate 71 kDa protein** NP_001230836.1	400-485 332-498	3 KQ KQ	2e-116 3e-112
84	**DNAJ homolog subfamily A member 3, mitochondrial isoform X2** XP_003354674.1	175-453	KGIP KQ	4e-174
Secretion and Endocytic pathways/compartments				
30 142	**VPS29** XM_003483426.4 **vacuolar protein sorting-associated protein 29 isoform X2** XP_003483474.1	590-872 104-182 *In frame?*	 KKCP, KCPP, KTPP	2e-128 0
91	**vesicle-trafficking protein SEC22a isoform X4** XP_020925910.1	233-255		2e-06
102	**oxysterol binding protein like 9 (OSBPL9), transcript variant X11** XM_021096665.1	2403-2519	-	1e-52
137	**phosphatidylinositol 4-phosphate 3-kinase C2 domain-containing subunit alpha** XP_020938934.1	400-501	-	2e-67
IFN related				
6 53	**interferon induced protein 35 mRNA** XM_003358024.3 **interferon-induced 35 kDa protein (IFP35)** XP_003358072.1	 27-275	 	 4e-136
19	**E3 Sumo ligase PIAS1** XP_003121797	383-595		
62	**Zinc finger MIZ domain-containing protein 1 (ZMIZ1)** XP_013838828.2	580-832		1e-179

86	**E3 SUMO-protein ligase PIAS2 isoform 7** XP_020948317.1	352-542		9e-130
DNA binding/modifying				
36	**histone-binding protein RBBP4** XP_013854580.1	1-145	KNTP	1e-92
55	**GA-binding protein alpha chain isoform X1** XP_020927099.1	45-254		2e-150
64	**TATA box-binding protein-associated factor RNA polymerase I subunit B isoform X3** XP_020943519.1	7-175 *In frame?*	KQ	2e-122
75	**proliferating cell nuclear antigen** NP_001278854.1	149-261	2 KQ KATP	7e-77
Apoptosis				
101	**NHL repeat-containing protein 2** NP_001230490.1	626-725	-	2e-63
Complement				
110	**complement C3 precursor** NP_999174.1	22-313	-	3e-173
Ribosomal				
120	**40S ribosomal protein S20** AAS55928.1	33-105	KQ	7e-49
Receptors/Cell surface molecules/Plasma membrane				
1	**cadherin-23 isoform X3** XP_020928318.1			
11 54	**integrin beta-2 precursor** ABU86738.1	361-667	54 -	0
25	**Macrosialin-like** XP_013847091.1			
95	**sialoadhesin precursor** NP_999511.1	442-649	-	2e-128
106	**stabilin-1 isoform X2** XP_020924550.1	176-480	-	8e-167
117	**CB1 cannabinoid receptor-interacting protein 1** XP_003481247.1	1-115	KIKP	1e-71
131	**integrin beta-1 isoform X1** XP_020919724.1	351-497	KIKP	1e-83
18 103*	**Na/K transporting ATPase subunit beta** NP001001542.1 **Na+/K+ transporting ATPase beta 1 polypeptide** AAX55911.1	228-303	KQ	2e-39
56	**sodium/potassium-transporting ATPase subunit beta-3 isoform X1** XP_013837554.1	150-279	-	2e-91

Extracellular Matrix				
15 43 60 68 111	**fibronectin** XP_003133690.2 AAV88080.1	1160-1334 991-1188 1615-1766 32-305	43 - KQ, KLAP 60 -KKVP KSSP KPLT, RTCSLWK, KQ 68 – 111 - KTGP	2e-102 3e-16 2e-94 2e-156
79	**EMILIN-2 isoform X1** XP_020951794.1	946-1070		6e-81
Structural				
45 78 132 135 113 135 141	**filamin-A isoform X10** XP_020936395.1 **filamin-A isoform X11** XP_020936398.1 **filamin A (FLNA), transcript variant X9** XM_021080731.1 **filamin-A isoform X11** XP_020936390.1	1769-1896 743-1074 1685-1912 1024-1324 5107-5596 3619-4549 1024-1305	RTAKSLGK KVLP 132 - 135 - 113 – 135 - 141 -	6e-26 7e-159 1e-68 4e-134 3e-80 0 1e-172
48 73	**actin gamma 1 (ACTG1)** XM_003357928.4 **actin, cytoplasmic 2** XP_003357976.1	196-781 *In frame?* 1-210 *In frame?*	- RGILTLK	0 2e-155
58	**drebrin like (DBNL), transcript variant X2** XM_005673326.2	1546-1832	/	2e-116
Cell division				
2	**serologically defined colon cancer antigen 8 (SDCCAG8), transcript variant X14** XM_021064185.1			
Signalling				
3	**thioredoxin like 1 (TXNL1), transcript variant X2** XR_002337500.1			
34	**TYRO protein tyrosine kinase binding protein (TYROBP), transcript variant X1**	303-562		2e-129

	XM_005664506.3			
102*	**p21 (RAC1) activated kinase 2 (PAK2), transcript variant X4** XM_021070138.1	4161-4601		0
RNA binding/modifying				
33	**RNA-binding protein 39 isoform X7** XP_020933927.1	201-373	R K I - S L	1e-109
44 63 82 119	**small nuclear ribonucleoprotein G** XP_003125100.1	1-76 *In frame?* 1-76 1-76 1-76 *In frame?*	44 - KAHP 63 - KAHP 82 - KAHP 119 - KAHP	5e-49 3e-49 5e-50 9e-51
52	**heterogeneous nuclear ribonucleoprotein H isoform X4** XP_005654996.1	294-472	2 KQ	2e-118
77	**valine-tRNA ligase** NP_001182307.1	77-338	KQ	5e-127
99	**RNA-binding protein 39 isoform X7** XP_020933927.1	116-364	-	5e-105
109	**serine and arginine rich splicing factor 2 (SRSF2), transcript variant X7, misc_RNA** XR_002336827.1	649-732	-	2e-34
144	**protein virilizer homolog isoform X1** XP_020944755.1	50-173	KRNP	2e-81
GTP related				
20 71	**rho GDP-dissociation inhibitor 2** XP_ 008069400 NP_001231169.1	 1-143	 KPPP	 3e-82
81	**putative GTP-binding protein 6** XP_020937869.1	308-476 *In frame?*		1e-102
146	**A-kinase anchor protein 13 isoform X2** XP_020955571.1	122-347	KQ	1e-153
Transcriptional regulation				
90	**forkhead-associated domain-containing protein 1** XP_020953256.1	128-306	KLLP	5e-128
Galectin				
31 98 107 118 123	**Galectin 3** NP_001090970.1	29-234 5-62 *In frame?* 1-241 34-260 34-259	KGGP KGGP KPNP 118 - 123 – KIYP, KKRP	2e-141 2e-25 3e-134 6e-162 5e-129
NADPH Oxidase				

38	**neutrophil cytosol factor 2 isoform X1** XP_005667867.2	390-571		8e-128
DNA/RNA processing				
59 96	**protein archease** XP_005665243.2 **isoform X1** XP_005665243.2	1-141 1-159	KYPP KSFP – *not in matching sequence* KYPP	2e-100 6e-117
Protein processing				
124	**cytosol aminopeptidase isoform X2** XP_003356918.4	15-278	R-RPPDLLK 3 KQ	7e-116
Mitochondria				
67	**voltage-dependent anion-selective channel protein 2 isoform X1** NP_999534.1	185-294	KQ – *not in matching sequence*	1e-72
24 74 103	**cytochrome c oxidase subunit II** YP-220722.1 ABP63291.1	 130-229 77-229	 - KNPP	 2e-63 2e-65
Protease/protease related				
4 49 50 70	**cathepsin D protein** AY792822.1 **cathepsin D protein, partial** AAV90625.1	 143-584 143-584 *In frame?* 81-395 *In frame?*	 49 - 50 – KQ 70 - KSSP KQ	 0 2e-103 2e-158
57	**inter-alpha-trypsin inhibitor heavy chain 3 (ITIH3) transcript variant X7** XM_021068271.1	1878-2246		2e-149
Enzymes				
66	**ribulose-phosphate 3-epimerase isoform X3** XP_003133677.1	22-228	KQ	2e-153
87	**N(alpha)-acetyltransferase 25, NatB auxiliary subunit (NAA25)** XM_021074209.1	3656-3936		2e-140
88	**nicotinate phosphoribosyltransferase isoform X2** XP_020946125.1	172-459	-	4e-160
115	**UMP-CMP kinase** Q29561.1	15-195	KIVP	4e-131

Nucleotides in red or amino acid region in black; note 5e-120 = $5x10^{-120}$. Proteins selected to take forward for further investigation were highlighted in green. Key: # – number; K – lysine; X – any amino acid; R – arginine; P – proline, Q – glutamine; L – Leucine; residues highlighted in blue are ubiquitinated. *In frame?* = Sequence was best match but not in frame with the HA tag.

Clones 116, 133 and 145 matched multiple porcine mRNAs, mRNAs identified in various porcine tissues that did not provide a protein match; clone 85 matched the prey plasmid vector pACT2 and therefore did not contain a cDNA insert.

The proteins were grouped based on function, and **Figure 3.9** shows an overview of the results and the numbers within each group.

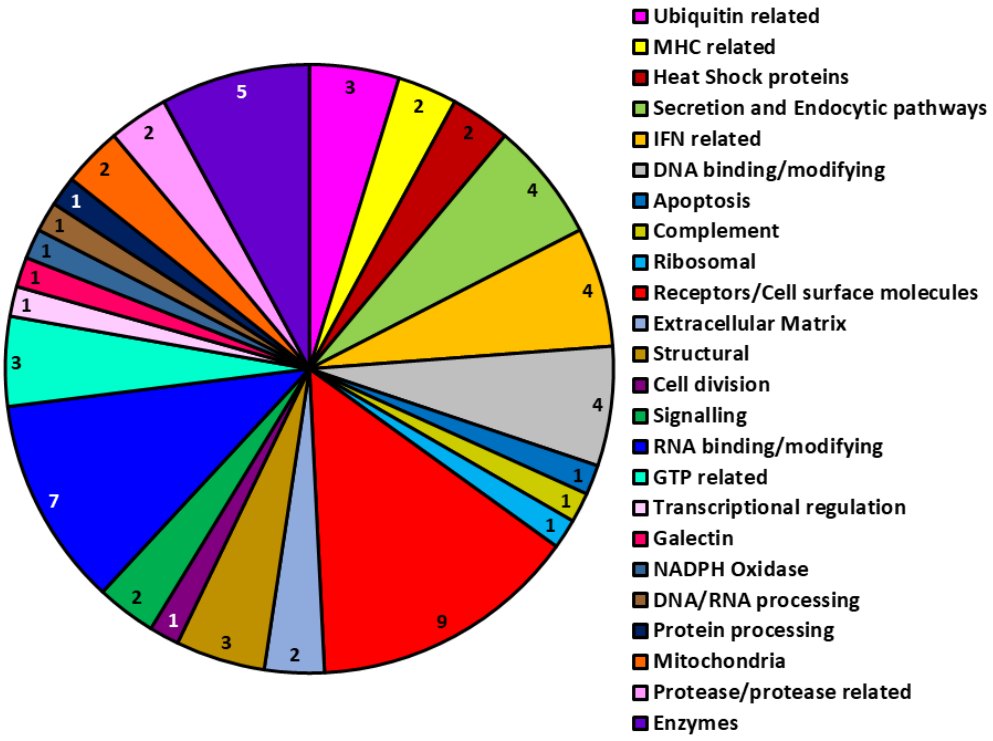

Figure 3.9: Proteins identified in the PRRSV-1 NSP1α y-2-h screen grouped by function. A y-2-h screen of NSP1α revealed 63 potentially interacting proteins, which were grouped broadly based on their cellular functions.

3.6.2.2 Sequence results from PRRSV-1 NSP1β screen

From the NSP1β screen, 233 sequences of cDNA inserts identified 126 potential binding partners for NSP1β. **Table 3.3** shows the results of the NSP1β screen. Proteins selected for further characterisation are highlighted in green and were selected based on the reported pathways that PRRSV is known to use or antagonise; residues

highlighted in blue are ubiquitinated. A more detailed table can be found in **Appendix 9.3**.

Table 3.3: Proteins identified in the NSP1β yeast-2-hybrid screen.

Clone #	Protein and NCBI Sequence ID	Region N or AA	Ubiquitin motifs: KXXP RXXXXLXK KQ	E value
IFN related				
78	**signal transducer and activator of transcription 3** NP_001038045.1	1-165	KPVP KPTP	9e-37
NF-κB				
51	**TGF-beta-activated kinase 1 and MAP3K7-binding protein 3** XP_020936488.1	414-701	KGSP	6e-61
GTP related				
63	**Rho GDP dissociation inhibitor alpha (ARHGDIA), transcript variant X3** XM_021066139.1	1543-2039		0
105	**putative GTP-binding protein 6 (LOC110257936)** XM_021080945.1	4558-4977		4e-104
229	**DENN domain-containing protein 4C isoform X1** XP_020918843.1	1-142	KRRP KPSP	3e-30
Complement				
268	**Sus scrofa complement C3 (C3), transcript variant X1, mRNA** XM_021080819.1	4257-4535		3e-144
Autophagy				
328	**beclin-1 isoform X1** XP_013836386.1	5-448		1e-85
Heat shock proteins				
290	**10 kDa heat shock protein, mitochondrial** NP_999472.1	1-102	KLPP	7e-65
350	**DNAJ homolog subfamily C member 10** XP_020931971.1	422-515 *In frame?*		4e-58
Transcriptional regulation				
323	**MyoD family inhibitor domain-containing protein isoform X2** XP_020934777.1	110-242		1e-61
Cell division				
37	**transmembrane protein 250 (TMEM250), transcript variant X2** XM_021081256.1	903-1469		4e-180

204	**cAMP regulated phosphoprotein 19 (ARPP19), transcript variant X3** XM_021082942.1	4650-4963		9e-164
216	**centromere-associated protein E isoform X5** XP_020956377.1	2223-2456		7e-134
240	**metalloproteinase inhibitor 2 isoform X3** XP_013845300.1	89-183 *In frame?*	KQ	5e-53
255	**centrosomal protein of 57 kDa isoform X2** XP_020918349.1	153-356	KSRP	2e-94
MHC related				
36 345	**MHC class II antigen, partial** AEX59168.1 AAP37552.1	9-98 175-249	36 - 345 - KEIP	2e-57 7e-34
348	**minor histocompatibility protein HA-1 isoform X3** XP_003354009.1	1-244	KQ RKKRELMK RFAEALEK	7e-101
RNA binding/modifying				
77	**methylosome subunit pICln** XP_003482618.1	43-218		5e-60
104	**pre-mRNA cleavage complex 2 protein Pcf11 isoform X1** XP_013834646.1	1163-1260		2e-60
126	**small nuclear ribonucleoprotein F** NP_001177142.1	1-85		4e-55
132	**cleavage and polyadenylation specificity factor subunit 4 isoform X1** XP_020941778.1	2-213	KQ	3e-77
190	**poly(rC)-binding protein 1** XP_003125105.1	122-281	KQ	2e-115
243	**clustered mitochondria protein homolog isoform X5** XP_020923287.1	435-571		2e-66
244	**RNA-binding protein 39 isoform X7** XP_020933927.1	195-310		2e-64
250	**RNA-binding protein 12** XP_003483994.1	395-623	KQ KGLP	2e-102
282	**ATP-dependent RNA helicase DDX18** XP_005654221.2	4-216 *In frame?*		9e-120
286	**RNA-binding protein 45 isoform X5** XP_020930624.1	1-220 *In frame?*		1e-111
295	**heterogeneous nuclear ribonucleoprotein K** NP_001254774.1	89-279	KIIP	4e-109

300	**heterogeneous nuclear ribonucleoprotein H isoform X4** XP_005654996.1	50-86 113-189 291-436		0.0032e-06 3e-74
Ribosomal				
67	**Sus scrofa ribosomal protein L28 (RPL28), transcript variant X6,** XM_021095014.1	52-600		2e-11
88	**60S ribosomal protein L27** NP_001090948.1	1-136 *In frame?*	88 - KKRP	2e-93
101	**40S ribosomal protein S20** AAS55928.1	18-105	KQ KKGP	1e-58
130 208 257	**40S ribosomal protein SA** NP_001032223.1	129-277 153-275 168-283	130 - KQ 208 - KFFP	5e-87 2e-82 6e-67
155	**40S ribosomal protein S18** NP_999105.1	1-152		7e-108
329	**fragile X mental retardation syndrome-related protein 1 isoform X8** XP_003358742.1	131-347		3e-124
Galectin				
19 20 21 156 205 267 304	**galectin 3 (LGALS3), transcript variant X1** XM_005659974.3 **galectin-3** NP_001090970.1	8-420 1-187 1-229 1-82 1-203 1-181 1-200	19 - 20 - KLSP, KPNP 21 - KPNP 156 - KIFP, KRLP, RYPWGLSK 205 - KPNP	8e-143 2e-86 1e-53 9e-31 1e-74 4e-80 7e-99
Apoptosis				
90	**serine protease HTRA2, mitochondrial** XP_020942985.1	204-443	-	1e-99
234	**NHL repeat-containing protein 2** NP_001230490.1	637-725	-	8e-39
Nuclear proteins				
112	**nucleoporin GLE1** XP_003122270.2	1-202		3e-142
164	**peroxisome proliferator-activated receptor-gamma 2** CAA07225.1	1-86		1e-32
227	**nucleoprotein TPR isoform X2** XP_013833352.2	458-554	-	2e-54
260	**nuclear pore membrane glycoprotein 210** XP_020925047.1	655-721		2e-38
Signalling				

66	**p21 (RAC1) activated kinase 1 (PAK1), transcript variant X9, mRNA** XM_021062561.1	557-869		1e-147
99	**A-kinase anchor protein 13 (AKAP13) isoform X2** XP_020955571.1	122-356	KQ	4e-153
119	**myoferlin isoform X4** XP_020929514.1	83-315		3e-76
133	**dedicator of cytokinesis protein 10 isoform X33** XP_020930475.1	601-714	KQ	1e-70
192	**Protein AF-17** XP_020922727.1	616-821	KQ	3e-109
199	**1-phosphatidylinositol 4,5-bisphosphate phosphodiesterase delta-1** NP_001230518.1	34-116		6e-115
PRRs				
69	**collectin-12 isoform X2** XP_020951815.1	533-737	KQ KGPP	8e-148
103 159	**toll-like receptor 4** ACL97681.1	24-100 24-100	103 - 159 -	2e-50 2e-47
Translation				
127	**eukaryotic translation initiation factor 3 subunit K isoform X2** XP_003127167.2	36-133 *In frame?*		2e-38
Intracellular transport				
141 184 320	**major vault protein** XP_020942083.1	1-179 1-157 589-706	141 - KQ 184 - KWWP 320 -	2e-117 7e-90 5e-39
Antibodies				
54 83 124 135 136 161	**IgG heavy chain precursor** BAM75557.1 BAM75568.1 BAM75543.1 BAM75562.1 BAM75552.1	130-459 14-240 19-342 20-241 103-333 20-311	54 – KTAP 83 - 124 - KTAP 135 - KTAP, KLLP 136 - KTAP, KTKP 161 - KQ, KTAP	6e-155 2e-103 1e-142 2e-93 2e-110 6e-141

340	BAM75568.1	14-275		2e-80
DNA binding/modifying				
43	**mortality factor 4-like protein 2** XP_003135315.1	75-237	2 KQ	3e-118
55 158	**E3 SUMO-protein ligase EGR2** NP_001090957.1	49-278 159-383	55 - KLYP 158 - KPFP	9e-93 3e-160
81	**DNA polymerase epsilon subunit 2 isoform X1** XP_003480516.1	229-483	KQ	0
89	**ATP-dependent DNA helicase Q1** NP_001240636.1	1-118	KQ KFRP	9e-66
97	**activator of transcription and developmental regulator AUTS2 (AUTS2)** NM_001246269.1	1755-2024		2e-136
108	**msx2-interacting protein** XP_020951052.1	2759-3015	KQ KPEP KLPP	1e-124
171	**mediator of RNA polymerase II transcription subunit 4** XP_013834181.1	1-104	KERP	4e-42
305 317	**endothelial PAS domain-containing protein 1** NP_001090889.1	104-558 207-422	317 -	4e-117 5e-92
342	**AT-rich interactive domain-containing protein 1A isoform X2** XP_020951290.1	2031-2119		4e-55
Secretion/Endocytic Pathways				
39	**glycosylated lysosomal membrane protein isoform X2** XP_005663352.1	191-320 *In frame?*	KQ	2e-87
138 230	**prolow-density lipoprotein receptor-related protein 1** XP_020947485.1	1157-1332 1157-1288	138 - 230 -	3e-110 2e-57
197	**protein transport protein Sec31A isoform X26** XP_020957515.1	626-796	KGRP	4e-111
308	**leucine-zipper-like transcriptional regulator 1** XP_003133045.2	826-985		2e-106
Protease/protease related				
96	**cathepsin B precursor** NP_001090927.1	44-327	-	0

172 222	**cathepsin D protein** AAV90625.1 AAY42145.2	451-1264 263-346	172 - 222 -	9e-142 2e-27
330	**cathepsin H transcript variant 3** ACB70169.1	19-235	KFQP	6e-139
Ubiquitin related				
195	**cullin-9 isoform X4** XP_001929303.2	296-458	KGGP	3e-105
259	**kelch-like protein 20** XP_005656773.1	1-193		1e-121
Mitochondria				
15 289	**fumarate hydratase, mitochondrial isoform X3** XP_020919702.1 **fumarate hydratase, mitochondrial isoform X2** XP_020919701.1	68-335 138-189		2e-120 2e-05
31	**NADH dehydrogenase [ubiquinone] 1 beta subcomplex subunit 9** XP_013851951.1	4-165	KQ	1e-104
32	**methyltransferase-like protein 17, mitochondrial** NP_001231255.1	342-461	KQ	3e-83
110	**iron-sulphur cluster assembly 2 homolog, mitochondrial** XP_003482336.1	5-154	-	8e-104
118	**histidine triad nucleotide-binding protein 2, mitochondrial isoform 1 precursor** NP_001231254.1	5-77	-	1e-42
297	**enoyl-CoA hydratase, mitochondrial** NP_001177104.1	1-228		1e-66
310	**citrate synthase, mitochondrial isoform X1** XP_020946802.1	3-262		4e-44
Cell migration/movement				
8	**absent in melanoma 1 protein isoform X3** XP_003121377.4	649-964	KKKP KLRP KDQP	3e-140
179	**neuroblast differentiation-associated protein AHNAK** XP_013849669.2	4475-4619	179 -	5e-83
237	**macrophage migration inhibitory factor** NP_001070681.1	1-67	KRKP	1e-41
239	**P-selectin glycoprotein ligand 1 propeptide precursor** CAO91826.1	96-161 *In frame?*	-	4e-35
Proteasome				
16	**proteasome subunit beta type-4** NP_001231384.1	1-264	16 – 2 KQ, KMNP	2e-172

82 117 254 256		1-248 1-258 1-81 1-226	82 – 2 KQ, KMNP 117 - KQ, KMNP 254 - 256 - KQ, KMNP	1e-154 2e-108 2e-46 6e-119
123	**proteasome subunit alpha type-1** XP_003123013.1	74-263	KAQP	2e-140
194	**proteasome (prosome, macropain) subunit, beta type, 8 (large multifunctional protease 7)** CAN13318.1	37-208	KKGP	2e-124
263	**proteasome maturation protein (POMP), ncRNA** XR_002336632.1	75-615		0
Receptors/cell surface molecules				
10	**C5a anaphylatoxin receptor 1** NP_001231144.1	219-347 *Not in frame*	KTLP	4e-82
22	**IGF-like family receptor 1** XP_020952886.1	79-122	KKIP	1e-18
25	**integrin beta-2 precursor** ABU86738.1	364-650	KITP	3e-164
64 106 122 303	**macrosialin isoform X1** XP_013834029.1	49-186 *In frame?* 49-194 *In frame?* 462-569 49-186 *Not in frame*	64 - 106 - 122 - 303 -	2e-66 2e-79 7e-41 3e-73
109	**V-set and immunoglobulin domain-containing protein 4 isoform X3** XP_013841676.1	45-143	-	7e-67
150 165 226 322	**Scavenger receptor cysteine-rich type 1 protein M130 isoform X1** XP_020946779.1 **CD163** ADM07458.1	97-370 74-258 111-245 95-246	150 - 2 KQ 165 - KQ 226 -	0 6e-127 4e-68 3e-101
251 306	**stabilin-1 isoform X7** XP_020924555.1	361-489 1480-1742		3e-70 6e-110

Structural				
24	**F-actin-capping protein subunit alpha-2** Q29221.3	178-286		2e-70
27	**Vimentin, partial** ABA39527.1	131-274	27 – KQ	1e-88
45		1-250	45 – KWNP, KRLP	6e-139
65	**Vimentin isoform X2** XP_005668164.1	1-198	65 - KNTP 74 - KQ	6e-63
74		126-393		2e-144
180		1-261	180 -	2e-140
224		1-124	224 -	9e-82
246		1-216 *In frame?*	246 - KSAP, KEEP	2e-101
258		1-81		1e-30
261		1-62		2e-32
264		82-222		5e-14
270		1-225		2e-57
272		1-176		7e-72
284		1-159		1e-63
333		1-222		4e-77
343		1-233	343 - KNTP, RTSCCLRK	1e-86
354	XP_005668163.1	213-415	354 –	4e-68

279		1-40	279 -	3e-16
80 115 236 220 344	**ferritin heavy chain isoform X1** XP_005660860.1 **ferritin heavy chain 1 (FTH1), transcript variant X1** XM_005660803.3	1-181 *In frame?* 1-156 118-556 1-84 108-405	80 – KQ, KNDP 115 - 236 – 220 –	7e-111 1e-79 4e-167 5e-55 1e-79
91	**WD repeat-containing protein 1** XP_020956671.1	285-588	KIVP	3e-166
193 252 274 337	**actin, cytoplasmic 2** XP_003357976.1 **beta actin** ABF19863.1 **beta actin** AAA17872.1	36-322 *In frame?* 52-532 *In frame?* 23-161 *In frame?* 14-229 *In frame?*	193 - 252 -	6e-176 4e-42 2e-115 2e-115
241 312	**macrophage-capping protein** XP_003124996.1 **capping actin protein, gelsolin like (CAPG), transcript variant X6** XM_003124949.4	27-191 813-1511	241 - KLKP, KCQP	8e-82 0
245	**PDZ and LIM domain protein 7 isoform X2** XP_020940036.1	109-367	KQ RAAHLLCK	3e-83
253	**Sus scrofa thymosin beta 4 X-linked (TMSB4X), mRNA** NM_001141991.2	52-532		0
324	**laminin subunit beta-1** XP_003130317.3	652-875		3e-76
Extracellular matrix				

23 183 206 223 247 334	**fibronectin** XP_003133690.2 **fibronectin** AAV88080.1	2152-2376 2121-2358 85-329 96-175 188-360 19-187 229-453	23 - KSEP 183 - KSEP 206 - KPEP 223 - KQ 247 - KPEP	1e-142 3e-132 5e-70 2e-121 2e-83 1e-72
33	**extracellular matrix protein 1 isoform X5** XP_020945568.1	126-280		1e-78
283	**granulins precursor** NP_001038043.1			5e-60
Enzymes				
40	**N(alpha)-acetyltransferase 40, NatD catalytic subunit (NAA40), transcript variant X2,** XM_013994174.2	2604-3479		0
61	**lon protease homolog 2, peroxisomal** XP_005664508.3	520-726	KQ	7e-85
71	**SH3 domain-binding glutamic acid-rich-like protein isoform X2** XP_020936361.1	1-85	4 KQ	5e-49
75 76	**L-xylulose reductase** XP_020922060.1	113-244 *In frame?* 134-199 *In frame?*	75 – KASP, RPATGLLK 76 - KAPP, KRTP, KKRP	1e-85 4e-13
107	**acyl-coenzyme A thioesterase 1-like** XP_020955153.1	306-464	KEKP	2e-111
131	**sodium/potassium-transporting ATPase subunit alpha-1 isoform X1** XP_020944376.1	805-946	KRQP	3e-95
145	**adenylate kinase isoenzyme 6 isoform X2** XP_003134069.1	41-138	145 -	3e-51
153	**aflatoxin B1 aldehyde reductase member 2** NP_001230751.1	151-369	KQ	1e-161
207	**pyruvate kinase PKM isoform X8**	401-525		5e-16

	XP_001929104.1			
210	**dual oxidase 2 precursor** NP_999164.2	65-252	RFGSNLMK	2e-62
265	**branched chain keto acid dehydrogenase E1, alpha polypeptide (BCKDHA)** NM_001123083.1	30-739		0
293	**glutathione peroxidase 1** AID58016.1	77-206		5e-94
302	**uridine-cytidine kinase-like 1 isoform X5** XP_020933287.1	29-100		9e-38
331	**glutamate-ammonia ligase** BAI47709.1	71-236		4e-74
332	**serine/threonine-protein phosphatase 2A catalytic subunit alpha isoform** NP_999531.1	134-309		2e-129
4 59 249 266	**L-lactate dehydrogenase B chain isoform X1** XP_013843801.1 **L-lactate dehydrogenase B chain** NP_001106758.1	16-306 13-297 12-231 18-40	KYSP KYSP	2e-176 0 3e-104 2e-05
Miscellaneous				
7	**uncharacterised protein C20orf96 homolog isoform X2** XP_013838676.1	28-187	KEGP	5e-61
181	**Sus scrofa mesoderm development candidate 2 (MESDC2)** XM_001928863.5	646-1488		0
182	**myotubularin related protein 14 (MTMR14), transcript variant X3,** XR_002337651.1	1941-2112	/	1e-84
269	**annexin A5** XP_003129266.2	69-181		3e-75
301	**neutrophil cytosol factor 2 isoform X1** XP_005667867.2	232-335	-	0.001

Nucleotides in red or amino acid region in black; note 5e-120 = $5x10^{-120}$. Proteins selected to take forward for further investigation were highlighted in green. Key: # – number; K – lysine; X – any amino acid; R – arginine; P – proline, Q – glutamine; L – Leucine; residues highlighted in blue are ubiquitinated. *In frame?* = Sequence was best match but not in frame with the HA tag.

Clones 30, 34, 46, 60, 79, 95, 151, 275, 277 matched various pig mRNAs, mRNAs identified in various porcine tissues that did not provide a protein match. Clones 48, 49, 50, 56, 68, 111, 149, 174, 175, 188, 203, 213, 217, 225, 232, 242, 248, 271, 273,

280, 294, 296, 315, 325, 326, 335, 336, 339, 341, 349, 352 matched the prey plasmid vector pACT2 and therefore did not contain a cDNA insert.

The proteins were grouped based on function, and **Figure 3.10** shows an overview of the results and the numbers within each group.

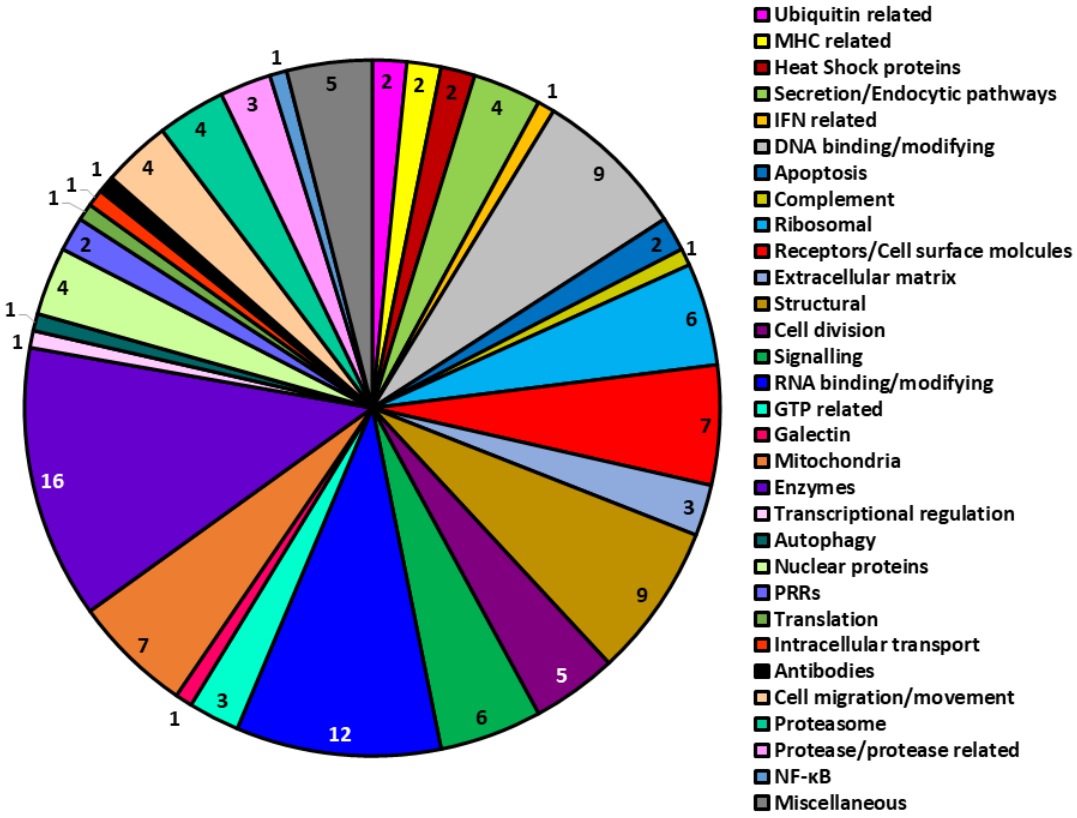

Figure 3.10: Proteins identified in the PRRSV-1 NSP1β y-2-h screen grouped by function. A y-2-h screen of NSP1β revealed 126 potentially interacting proteins, which were grouped broadly based on their cellular functions.

3.6.3 Proteins selected for characterisation

The proteins identified in both screens varied greatly in function. Proteins identified as putative interactors for both NSP1α and NSP1β included cathepsin D and NHL repeat-containing protein 2 (NHLRC2). Additionally, related proteins (both structurally and functionally) were identified in both screens, such as various HSPs (HSC70, HSP40/DNAJB1 and HSP10) and cathepsins (B, D, and H).

Due to time limitations, only 13 proteins from the NSP1α screen and 36 proteins from the NSP1β screen were selected to retest and characterise. These are highlighted in green in **Table 3.2** and **Table 3.3** and listed below in **Table 3.4**.

Table 3.4: Proteins selected to take forward and characterise from PRRSV-1 NSP1α and NSP1β yeast-2-hybrid screens.

Proteins selected from NSP1α screen	**Proteins selected from NSP1β screen**
Ubiquitin B	Integrin beta-2 precursor
E3 SUMO ligase PIAS1	Proteasome subunit beta type-4
E3 SUMO-protein ligase PIAS2 isoform 7	MHC class II antigen, partial
DNAJ homolog subfamily A member 3, mitochondrial isoform X2	TGF-beta-activated kinase 1 and MAP3K7-binding protein 3
Sialoadhesin precursor	IgG heavy chain precursor
Cathepsin D protein	TLR4
Heat shock cognate 71 kDa protein	Collectin-12 isoform X2
E3 ubiquitin-protein ligase MARCH7 isoform X8	Signal transducer and activator of transcription 3
Anaphase-promoting complex subunit 10	Cathepsin B precursor
Zinc finger MIZ domain-containing protein 1 (ZMIZ1)	Serine/threonine-protein kinase PAK 1
NHL repeat-containing protein 2	Nucleoporin GLE1
Interferon induced protein 35	Proteasome subunit alpha type-1

p21 (RAC1) activated kinase 2 (PAK2), transcript variant X4	Eukaryotic translation initiation factor 3 subunit K isoform X2
	CD163
	Mediator of RNA polymerase II transcription subunit 4
	Cathepsin D protein
	Proteasome (prosome, macropain) subunit, beta type, 8 (large multifunctional protease 7)
	Cullin-9 isoform X4
	Endothelial PAS domain-containing protein 1
	MyoD family inhibitor domain-containing protein isoform X2
	Beclin-1 isoform X1
	Cathepsin H transcript variant 3
	E3 SUMO-protein ligase EGR2
	Serine protease HTRA2, mitochondrial
	Cleavage and polyadenylation specificity factor subunit 4 isoform X1
	V-set and immunoglobulin domain-containing protein 4 isoform X3
	Nucleoprotein TPR isoform X2
	NHL repeat-containing protein 2
	Macrophage migration inhibitory factor
	Kelch-like protein 20
	Nuclear pore membrane glycoprotein 210
	Proteasome maturation protein (POMP)
	10 kDa heat shock protein, mitochondrial
	DNAJ homolog subfamily C member 10
	Major vault protein
	Dead box helicase 18

If PRRSV or other viruses had been previously shown to target a protein on the list (or a related protein) or its functional pathway, it was selected to take forward. Selected proteins were involved in the immune response, such as IFN signalling and the NF-κB pathway, protein expression, ubiquitination or nuclear transport and were selected as the mostly likely to be involved in immunomodulatory interactions. Proteins involved in transport across the nuclear membrane, such as nucleoporin (NUP) GLE1 (GLE1) and nucleoprotein translocated promoter region (TPR), were chosen as NSP1β functions in both the cytoplasm and nucleus (Han *et al.*, 2017), so it was deemed possible that they are involved in shuttling NSP1β. Ubiquitin and the ubiquitin ligase MARCH7 were selected as PRRSV clearly alters the ubiquitome of the cell (H. Zhang *et al.*, 2018). Various proteasome subunits were selected as PRRSV targets multiple proteins for proteasomal degradation (Du *et al.*, 2016; Yang *et al.*, 2017; H. Ke, Han, *et al.*, 2019) and some identified in the screen are part of the immunoproteasome, which is also targeted by PRRSV (Q. Liu *et al.*, 2020).

These proteins were taken forward to be further characterised using y-2-h with additional controls, immunoprecipitations, and confocal microscopy.

3.7 Discussion

To increase our understanding of the mechanisms by which the NSP1α and NSP1β proteins of PRRSV-1 carry out immunomodulation, and to identify novel functions, two high stringency y-2-h screens were conducted using NSP1α and NSP1β from a conventional low virulence PRRSV-1 subtype 1 strain 215-06 (Morgan *et al.*, 2013).

Both proteins were cloned into the bait plasmid, pGBKT7, and the expression of their respective fusion proteins confirmed, following transfection of BSR-T7 cells and subsequent infection with MVA-T7, by western blot analysis using a monoclonal antibody that recognises the Myc-tag situated between the DBD and the respective NSP1 ORF; indeed, proteins of the expected sizes were observed (**Figure 3.5**). However, there were unexpected differences in levels of expression: NSP1α and NSP1β from PRRSV-1 215-06 expressed significantly higher than PRRSV-1 SU1-Bel NSP1α and NSP1β (**Figure 3.5**). The reasons for differences in protein expression are unknown, but this difference has also been seen by other members of the Molecular Virology Group (The Pirbright Institute) in transfections using different vectors and cells. Further investigation is needed but this suggests different PRRSV-1 strains express NSP1 at different levels, which could affect protein function and strain virulence. Transformations to check for self-activation of y-2-h system confirmed that neither NSP1α nor NSP1β alone or in combination with pGADT7 plasmids self-activated the y-2-h system (**Figure 3.6**).

PRRSV-1 215-06 NSP1α and NSP1β were then screened for host protein interactions using the y-2-h system and a cDNA library generated from PAMs. Following the successful generation of colonies expressing putative NSP1-interacting proteins, the respective plasmids were isolated, and their inserts analysed by PCR prior to being sequenced. The screens successfully identified 63 and 126 potential binding partners for NSP1α and NSP1β, respectively.

The proteins identified were grouped by function manually, which although useful could be inaccurate or incomplete. Future analysis should include use of bioinformatic approaches to stratify and functionally analyse the data obtained from the y-2-h screens, such as Database for Annotation, Visualization and Integrated Discovery analysis. The potential binding proteins had a great range of functions; the

main functions of interest were immunomodulation, protein expression, nuclear transport, and ubiquitination. Both NSP1α and NSP1β modulate the immune response, between them targeting the innate and adaptive responses. NSP1α suppresses IFN-α (Song, Krell and Yoo, 2010) and the screen suggests it interacts with IFI35; therefore, NSP1α may target the same pathway at multiple stages. The NSP1β screen identified TAK1 binding protein 3 (TAB3) as a potential binding partner, a protein which functions in both the NF-κB pathway (Ishitani *et al.*, 2003) and autophagy (Takaesu, Kobayashi and Yoshimura, 2012). Given PRRSV targets the NF-κB pathway using NSP1α (Song, Krell and Yoo, 2010), NSP2 (Fang, Ying, Fang, et al., 2012) and N protein (H. Ke, Lee, et al., 2019), it is possible this interaction is another way of doing so. Additionally, PRRSV activates autophagy using NSP3, NSP5 and NSP9 to aid viral replication (Liu *et al.*, 2012; Zhang, Chen, *et al.*, 2019); NSP1β could also be involved.

In the NSP1β screen, components of the nuclear pore complex (NPC) and other nuclear proteins involved in nuclear-cytoplasmic transport, GLE1 and nuclear pore membrane glycoprotein 210 (also known as NUP210), were identified. NSP1β is a nucleocytoplasmic protein, dependant on KPNA6 for nuclear translocation (Yang *et al.*, 2018) and has previously been shown to interact with NUP62, causing NPC disintegration (H. Ke, Han, *et al.*, 2019). Based on this, it is feasible NSP1β interacts with and utilises other NPC proteins to transport itself and/or host proteins/RNA.

PRRSV has been shown to modify the ubiquitome of the cell and some PRRSV NSPs are themselves ubiquitinated, including NSP1β (H. Zhang *et al.*, 2018). Ubiquitin itself and the ubiquitin ligases MARCH7 and anaphase-promoting complex subunit 10 (ANAPC10) were identified in the NSP1α screen, implying that PRRSV NSP1α is involved in this. The ubiquitin-proteasomal pathway is used by PRRSV to degrade selected host proteins: E protein interacts with and causes the degradation of porcine cholesterol 25-hydroxylase (W. Ke *et al.*, 2019) and NSP1α targets SLA-1 for proteasomal degradation (Du *et al.*, 2016). The NSP1β screen identified multiple proteasomal subunits, including some that form the immunoproteasome. PRRSV has been shown to target the immunoproteasome (Q. Liu *et al.*, 2020), so it is possible

NSP1β is involved in this and/or targets the proteasome directly to either degrade or prevent degradation of specific proteins.

Some of the proteins identified have been shown previously to interact with either NSP1α or NSP1β or other PRRSV NSPs; identification of previously confirmed interactions validates the results of these y-2-h screens. The NSP1α y-2-h screen identified PIAS1 and PIAS2 as potential interactors; NSP1α interacting with PIAS1 has been previously reported but not published (Song *et al.*, 2010), which provides supporting evidence that these interactions are genuine. PIAS1 has also been shown to interact with N protein, leading to the release of p65 and NF-κB pathway activation (H. Ke, Lee, et al., 2019). STAT3, a transcription factor activated in response to IFN and other cytokines, is targeted for degradation by NSP5 but these proteins do not interact (Yang *et al.*, 2017), so perhaps NSP1β plays a role in this. Poly(rC)-binding protein (PCBP) 1 PCBP1 was found to interact with NSP1β, which has been previously confirmed and characterised: NSP1β interacts with both PCBP1 and PCBP2 to regulate RNA synthesis (Beura *et al.*, 2011).

PRRSV interferes with many of the pathways the proteins identified function in to enhance its own replication. If genuine, these interactions could provide mechanistic detail on how PRRSV NSP1α and NSP1β function. Thirteen putative interacting host proteins from the NSP1α screen and 36 from the NSP1β screen were selected based on their reported functions and were then retested to identify host proteins that self-activate the y-2-h system as described in **Chapter 4**.

Chapter 4: Confirmation of interactions with PRRSV-1 NSP1α and NSP1β

4.1 Introduction

The y-2-h screens identified a large list of potentially interacting PAM proteins for PRRSV-1 NSP1α and NSP1β. These needed to be confirmed, as non-specific interactions can occur in y-2-h leading to false positives, and then characterised using a combination of methods.

Confirmatory y-2-h with additional controls was the first approach used. This was to test the specificity of the reaction and to confirm that the identified putatively interacting proteins did not self-activate the y-2-h system. Thirteen proteins from the NSP1α screen and 36 from the NSP1β screen were retested (listed in **Table 3.4**). Three of the proteins selected were cloned into pGADT7 before re-testing, as the respective pACT2 plasmids could not be amplified by growth in bacteria. Additionally, using 3-AT, a competitive inhibitor of the *HIS3* gene product, the strength of interactions was investigated.

Eleven interactions confirmed by y-2-h retesting were subsequently selected for further investigation and characterisation using confocal immunofluorescence microscopy and co-immunoprecipitations, time permitting. For this, the cDNA sequences encoding the respective PAM proteins first needed to be cloned into a plasmid that facilitated expression in mammalian cells. To facilitate this and to enable the subsequent detection of expressed proteins with a single antibody, the respective cDNA inserts were cloned into the plasmid pEF-FLAG; this facilitated expression of the FLAG epitope tag as an N-terminal fusion on each protein. Other cloning approaches, involving cloning the T7 promoter into pACT2 and cloning the cDNA inserts into pGADT7, were attempted but cloning was unsuccessful. Another approach, using a primer containing the T7 promoter, HA tag, and KOZAK sequence to amplify the cDNA inserts for subsequent use in transfection, did not reliably give HA-tagged PAM protein expression.

Confocal immunofluorescence microscopy was performed to investigate the spatial expression of viral and host proteins. Max cells were used because previous work has

shown that their comparably larger size helps image acquisition and they can express high levels of viral proteins alone and following infection with MVA-T7 (Doceul *et al.*, 2008). For each experiment, Max cells were co-transfected or transfected alone with a plasmid encoding the respective FLAG-tagged PAM protein and/or a plasmid encoding Myc-tagged NSP1α or NSP1β. At 24 hours post transfection (hpt), cells were probed, stained, and imaged to detect protein location within the cell as described in **Section 2.15**.

4.2 Retesting identified interactions using y-2-h with additional controls

To confirm putative interactions, y-2-h with additional controls was performed. This was necessary to ensure the interaction was specific and to test for prey protein self-activation of the y-2-h system. Thirteen proteins from the NSP1α screen and 36 proteins from the NSP1β screen were selected to retest; these proteins were selected as the most likely to be involved in immune signalling and therefore immunomodulatory interactions (**Table 3.4**). The respective pACT2 prey plasmids were extracted (**Section 2.12.4**), amplified in bacteria (**Section 2.6**) and sequenced (**Section 2.10**) to confirm their identity. Three prey plasmids could not be amplified; the insert regions of these were therefore ordered and cloned into pGADT7 (**Section 4.2.1**). To retest putative viral-host protein interactions, yeast cells were co-transformed with the following plasmid combinations:

- the respective pACT2-prey plasmid (expressing the identified PAM protein) together with either the pGBKT7 or pGBKT7-53 control bait plasmid
- the respective pACT2-prey plasmid (expressing the identified PAM protein) in combination with either the pGBKT7-NSP1α or pGBKT7-NSP1β bait plasmid
- the pGBKT7-LAM and pGADT7-T negative control plasmids
- the pGBKT7-53 and pGADT7-T positive control plasmids.

Following the growth of yeast transformants on minimal drop out medium (SD agar -Trp, -Leu), five colonies from each plate were streaked onto a single plate containing the same medium (SD agar -Trp, -Leu) – this was carried out to confirm successful co-transformation. Following their growth, each yeast colony from this plate was then re-streaked onto a higher stringency medium containing X-α-gal (SD agar -Trp, -Leu, -Ade, -His, + X-α-gal). **Table 4.1** summarises the plasmid combinations that were transformed, the media used to test the yeast transformants and the purpose; **Figure 4.1** shows the test plate layout.

Table 4.1: Y-2-h retesting plasmid combinations and plates

Plasmid Combination	**SD Agar Plate**	**Purpose**
pGBKT7 & pACT2-prey protein	-Trp, -Leu	Confirm co-transformant
	-Trp, -Leu, -Ade, -His + X-α-gal	Negative interaction control for identified PAM protein.
pGBKT7-53 & pACT2-prey protein	-Trp, -Leu	Confirm co-transformant
	-Trp, -Leu, -Ade, -His + X-α-gal	Negative interaction control for identified PAM protein.
pGBKT7-NSP1α or pGBKT7-NSP1β & pACT2-prey protein	-Trp, -Leu	Confirm co-transformant
	-Trp, -Leu, -Ade, -His + X-α-gal	Test for interaction
pGADT7-T & pGBKT7-53	-Trp, -Leu	Confirm co-transformant
	-Trp, -Leu, -Ade, -His + X-α-gal	Y-2-h system positive control
pGADT7-T & pGBKT7-LAM	-Trp, -Leu	Confirm co-transformant
	-Trp, -Leu, -Ade, -His + X-α-gal	Y-2-h system negative control

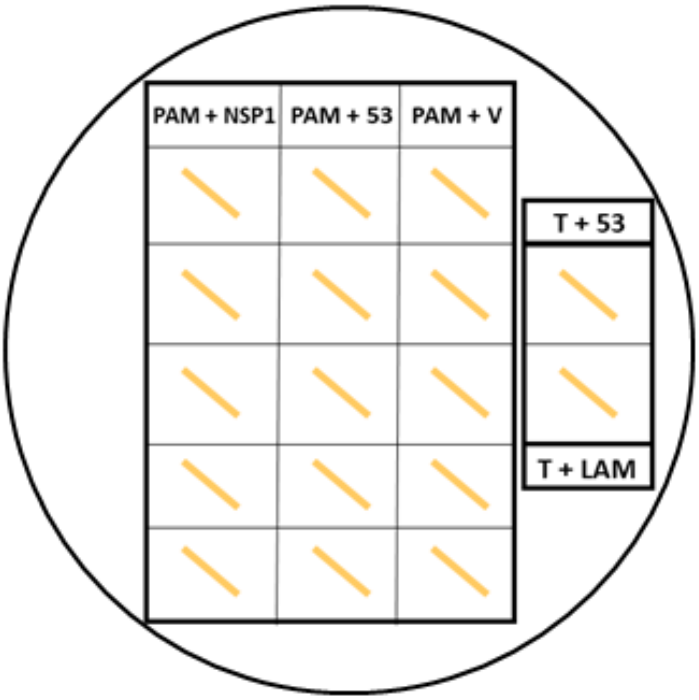

Figure 4.1: Y-2-h test plate layout. Key: PAM = selected PAM protein; pACT2-PAM cDNA; v = empty vector pGBKT7; T = pGADT7-T; 53 = pGBKT7-53; LAM = pGBKT7-LAM; NSP1 = pGBKT7-NSP1α or pGBKT7-NSP1β. In the y-2-h system, T+53 and T+LAM act as positive and negative controls, respectively.

The appearance of blue growth on the higher stringency medium by yeast transformants expressing NSP1α or NSP1β and the respective PAM protein suggested an interaction. However, the interaction was considered a possible false positive if blue growth was also observed for control transformants – these included yeast co-transformed with the respective pACT2-prey plasmid (expressing the identified PAM protein) together with either the empty pGBKT7 or pGBKT7-53 control bait plasmid. In such instances, the identified PAM protein may still have interacted with NSP1α or NSP1β, but it was not possible to confirm under these conditions.

4.2.1 Plasmid rescue and cloning into pGADT7

Despite repeated attempts, three prey plasmids, encoding IFI35, MVP and DDX18, could not be amplified. Therefore, cDNA sequences encoding the same portion of each protein identified in the y-2-h screen were obtained from NCBI (reference pig genome taxid: 9823) – these were synthesised with additional 5' *Nde*I and 3' *Bam*HI restriction sites and cloned into a standard vector plasmid pMA-RQ by GeneArt. The sequences ordered were not full-length genes, only the sections found in the original cDNA inserts were ordered, but any mismatches between these and the reference genes were corrected; additionally, the full-length IFI35 gene was ordered as it was of particular interest given its role in IFN signalling. The length of each cDNA insert is given in **Table 4.2** and agarose gel electrophoresis analyses of each plasmid following *Nde*I and *Bam*HI restriction digestion is shown in **Figure 4.2**.

Table 4.2: Expected size of each cDNA insert

Protein	**Insert length (bp)**
IFI35 partial	744
IFI35 full-length	864
MVP	544
DDX18	654

Each plasmid containing the insert, plus the target plasmid pGADT7, were sequentially digested with *Nde*I and *Bam*HI restriction enzymes (**Section 2.11.1**). The double-digests were then loaded onto an agarose gel (**Section 2.8**) to check the size of the inserts and to facilitate the extraction of the portion of gel containing the insert for subsequent purification (**Figure 4.2**).

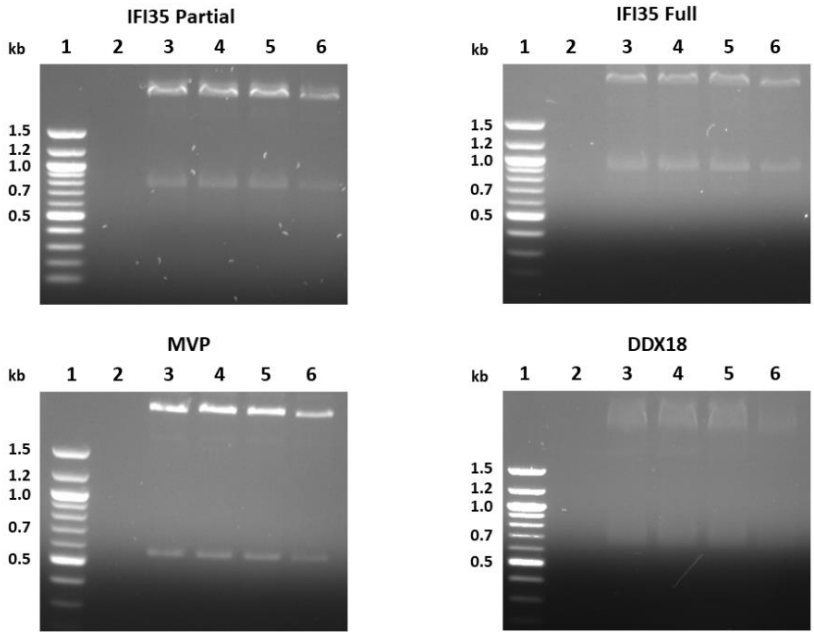

Figure 4.2: Double digests of each insert. Geneart plasmids containing the inserts for IFI35, MVP, and DDX18 were digested with *Nde*I and *Bam*HI and ran on an agarose gel to separate insert from plasmid.

*Nde*I and *Bam*HI restriction enzymes produced cDNA fragments of the expected sizes; double-digestion of pMA-IFI35 partial, pMA-IFI35 full-length, pMA-MVP and pMA-DDX18 released inserts of approximately 750 bp, 900 bp, 550 bp and 700 bp, respectively. The cDNA inserts were extracted and purified (**Section 2.9.2**), and then cloned into pGADT7 using *Nde*I and *Bam*HI restriction enzymes (**Section 2.11.2**). Following their amplification (**Section 2.6**), the respective plasmids were sequenced (**Section 2.10**) and found to be correct and in frame.

4.2.2 Retesting interactions from the PRRSV-1 NSP1α screen

Thirteen proteins from the NSP1α screen were selected to retest using y-2-h with additional controls. These were selected based on their functions and the pathways PRRSV-1 is known to antagonise; they are involved in either the immune response, such as IFN signalling and the NF-κB pathway, protein expression, ubiquitination, or nuclear transport. **Table 4.3** summarises the y-2-h retest results and **Figure 4.3** shows the retest plates for the proteins identified in the NSP1α screen.

Table 4.3: Proteins selected from the NSP1α screen to retest.

Protein	**Abbreviation**	**Result**
Cathepsin D	-	False positive
Ubiquitin B	-	False positive
Heat shock cognate 71 kDa protein	HSC70	False positive
Anaphase-promoting complex subunit 10	ANAPC10	False positive
E3 ubiquitin-protein ligase MARCH7 isoform X8	MARCH7	False positive
Zinc finger MIZ domain-containing protein 1	ZMIZ1	False positive
DNAJ homolog subfamily A member 3, mitochondrial isoform X2	DNAJA3	Genuine interaction
E3 SUMO-protein ligase PIAS2 isoform 7	PIAS2	Genuine interaction
Sialoadhesin precursor	-	False positive
NHL repeat-containing protein 2	NHLRC2	False positive
p21 (RAC1) activated kinase 2 (PAK2), transcript variant X4	PAK2	False positive
Interferon induced protein 35	IFI35	F – false positive P – no growth
E3 SUMO-protein ligase PIAS1	PIAS1	Genuine interaction*

Key: F – full-length; P – partial length. *Tested directly on SD agar containing 3AT.

A

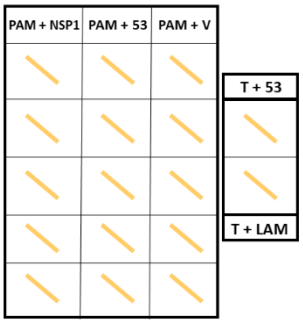

B

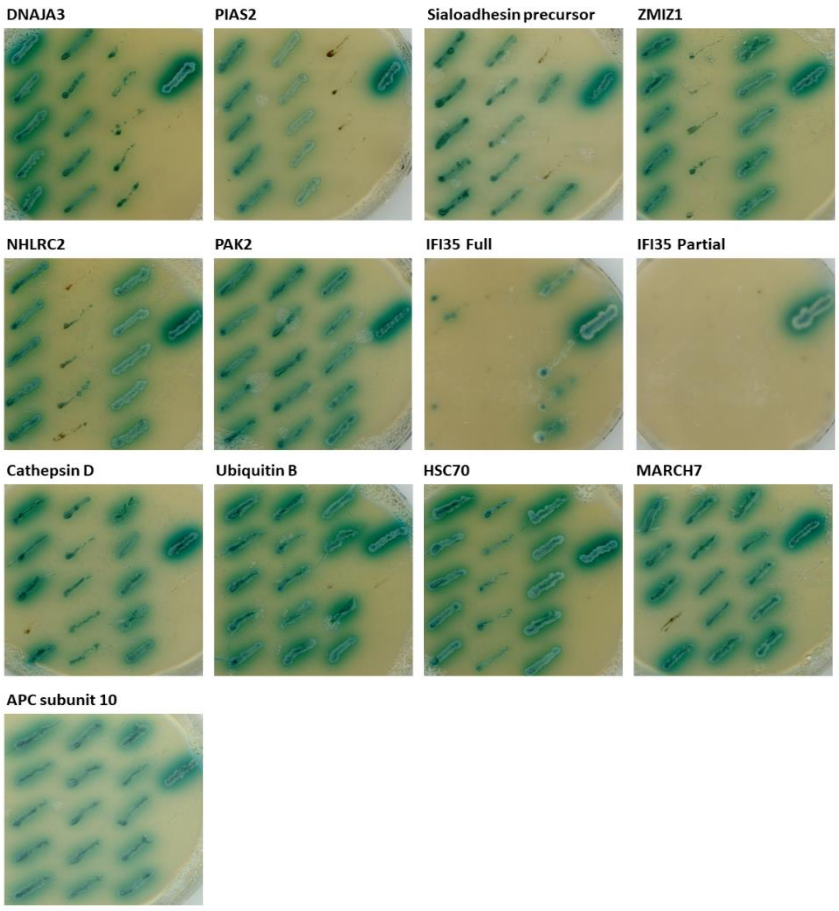

Figure 4.3: Y-2-h retest plates from NSP1α screen. Retest plate layout (**A**) and y-2-h retest plates (**B**). Yeast that had been co-transformed with combinations of the respective prey plasmid (termed "PAM protein" in (**A**)) and the bait plasmids NSP1α, pGBKT7-53 and pGBKT7 (termed "NSP1", "53" and "V" respectively in (**A**)) were plated on high stringency selection medium (SD agar -Trp, -Ade, -Leu and -His) containing X-α-Gal. The appearance of blue growth by yeast transformants expressing NSP1α and the respective PAM protein ("PAM protein + NSP1" in (**A**)) suggested an interaction. However, the interaction was considered a possible false positive if blue growth was also observed for the control transformants ("PAM protein + 53" and "PAM protein + V" in (**A**)). In the y-2-h system, T+53 and T+LAM act as positive and negative controls, respectively.

For all plates, blue growth was observed for the positive control yeast transformants (T+53) but not for the negative control (T+LAM) (**Figure 4.3**). Strong blue growth was observed for all yeast transformants expressing ubiquitin B, ANAPC10, MARCH7 and p21 (RAC1) activated kinase 2 (PAK2), regardless of the respective bait plasmid (pGBKT7-NSP1α, pGBKT7-53 or pGBKT7) that had been co-transformed. Strong blue growth was also observed for yeast co-transformed with prey plasmids encoding cathepsin D, HSC70, zinc finger MIZ-type containing 1 (ZMIZ1) or NHLRC2 in combination with either the NSP1α or empty pGBKT7 bait plasmid, whilst weaker or no growth was observed when the p53 bait plasmid had been co-transformed. Yeast co-transformed with the sialoadhesin precursor prey plasmid in combination with the NSP1α bait plasmid showed strong blue growth, weaker blue growth in combination with the p53 bait plasmid and limited growth with the empty pGBKT7 bait plasmid (two out of five colonies grew); sialoadhesin has not been previously shown to interact with p53. Therefore, 9 out of 13 retest plates appeared to be false positives. ANAPC10 has previously been shown to be a false positive in y-2-h screens carried out within the Molecular Virology Group (The Pirbright Institute) (unpublished data), which further validates the screen.

Yeast co-transformed with the PIAS2 prey plasmid in combination with either the NSP1α or p53 bait plasmid exhibited strong blue growth, although this was weaker with p53 in comparison to NSP1α. No growth was observed for yeast co-transformed with the PIAS2 prey and the empty pGBKT7 bait plasmid. PIAS2 has been shown previously to interact with p53, as has the related protein PIAS1 (Kahyo, Nishida and Yasuda, 2001; Schmidt and Müller, 2002). This suggests that the putative interaction between PIAS2 and NSP1α is genuine and not a false positive. Similarly, yeast co-transformed with the DNAJ homolog subfamily A member 3 (DNAJA3) prey plasmid together with either the NSP1α or p53 bait plasmids showed strong blue growth, but very weak or no growth with the empty pGBKT7 bait plasmid. DNAJA3 has previously been shown to interact with p53 (Trinh, Elwi and Kim, 2010); this suggests the interaction with NSP1α may also be genuine.

Yeast co-transformed with the partial IFI35 prey plasmid in combination with either the NSP1α, p53 or empty pGBKT7 bait plasmid exhibited no growth on the higher

stringency medium. In addition, only yeast co-transformed with the full-length IFI35 prey plasmid and the empty pGBKT7 bait plasmid grew on this medium, suggesting that NSP1α and IFI35 do not interact.

These results suggested that three interactions from the NSP1α screen were possibly genuine. PIAS1, PIAS2 and DNAJA3 were therefore selected to be retested in the presence of 3-AT, a competitive inhibitor of the *HIS3* gene product, to determine the strength of these interactions. Additionally, ubiquitin B, MARCH7, ZMIZ1, sialoadhesin precursor and NHLRC2 were also retested in the presence of 3-AT to confirm if these were false positives, or if the growth of yeast transformed with these proteins and empty pGBKT7 was background growth.

4.2.3 Retesting interactions from the PRRSV-1 NSP1β screen

Thirty-six proteins from the NSP1β screen were selected to retest using y-2-h with additional controls. **Table 4.4** summarises the y-2-h retest results and **Figure 4.4** shows the retest plates for the proteins identified in the NSP1β screen.

Table 4.4: Proteins selected from the NSP1β screen to retest.

Protein	Abbreviation	Result
Integrin beta-2 precursor	-	False positive
Proteasome subunit beta type-4	PSMB4	Genuine interaction
MHC class II antigen, partial	MHC class II	Genuine interaction
TGF-beta-activated kinase 1 and MAP3K7-binding protein 3	TAB3	Genuine interaction
IgG heavy chain precursor	-	Genuine interaction
Toll-like receptor 4	TLR4	Genuine interaction
Collectin-12 isoform X2	Collectin-12	Genuine interaction
Signal transducer and activator of transcription 3	STAT3	Genuine interaction
Cathepsin B precursor	-	Genuine interaction
p21 (RAC1) activated kinase 1	PAK1	Genuine interaction
Nucleoporin GLE1	GLE1	Genuine interaction
Proteasome subunit alpha type-1	PSMA1	Genuine interaction
Eukaryotic translation initiation factor 3 subunit K isoform X2	eIF-3 subunit K	Genuine interaction
CD163	-	Genuine interaction
Mediator of RNA polymerase II transcription subunit 4	MED4	Genuine interaction
Cathepsin D protein	Cathepsin D	Genuine interaction
Proteasome (prosome, macropain) subunit, beta type, 8 (large multifunctional protease 7)	PSMB8	Genuine interaction
Cullin-9 isoform X4	Cullin-9	Genuine interaction

Endothelial PAS domain-containing protein 1	EPAS-1	Genuine interaction
MyoD family inhibitor domain-containing protein isoform X2	MDFIC	Genuine interaction
Beclin-1 isoform X1	Beclin-1	Genuine interaction
Cathepsin H transcript variant 3	Cathepsin H	Genuine interaction
E3 SUMO-protein ligase early growth response 2	EGR2	-
Serine protease high temperature requirement protein A2, mitochondrial	HTRA2	False positive
Cleavage and polyadenylation specificity factor subunit 4 isoform X1	CPSF4	Genuine interaction
V-set and immunoglobulin domain-containing protein 4 isoform X3	VSIG4	False positive
Nucleoprotein TPR isoform X2	TPR	Genuine interaction
NHL repeat-containing protein 2	NHLRC2	-
Macrophage migration inhibitory factor	MIF	Genuine interaction
Kelch-like protein 20		Genuine interaction
Nuclear pore membrane glycoprotein 210	NUP210	Genuine interaction
Proteasome maturation protein (POMP)	POMP	False positive
10 kDa heat shock protein, mitochondrial	HSP10	Genuine interaction
DNAJ homolog subfamily C member 10	DNAJC10	No interaction
Major vault protein	MVP	Genuine interaction
Dead box helicase 18	DDX18	No interaction

A

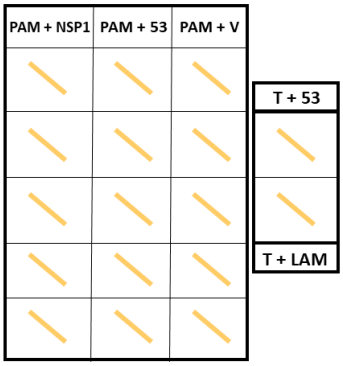
PAM + NSP1
PAM + 53
PAM + V
T + 53
T + LAM

B

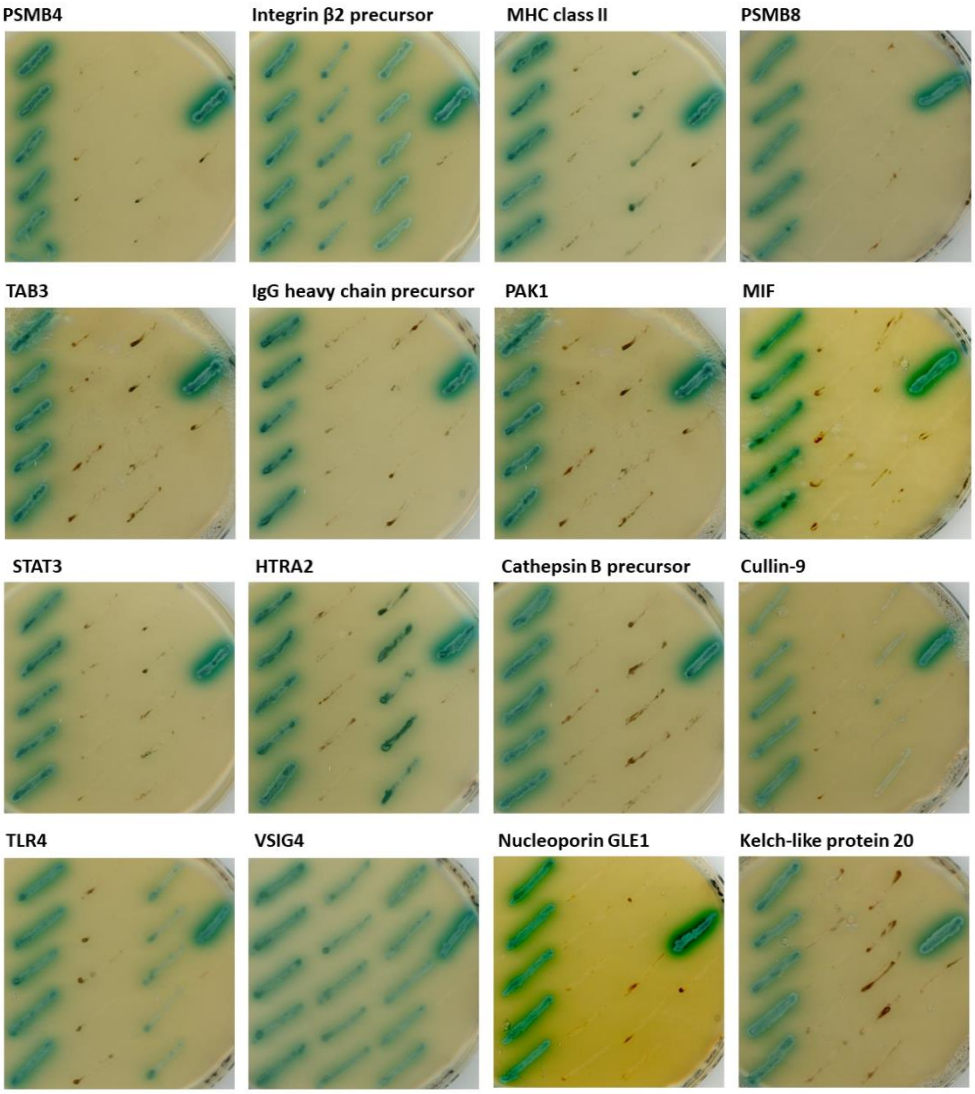
PSMB4
Integrin β2 precursor
MHC class II
PSMB8
TAB3
IgG heavy chain precursor
PAK1
MIF
STAT3
HTRA2
Cathepsin B precursor
Cullin-9
TLR4
VSIG4
Nucleoporin GLE1
Kelch-like protein 20

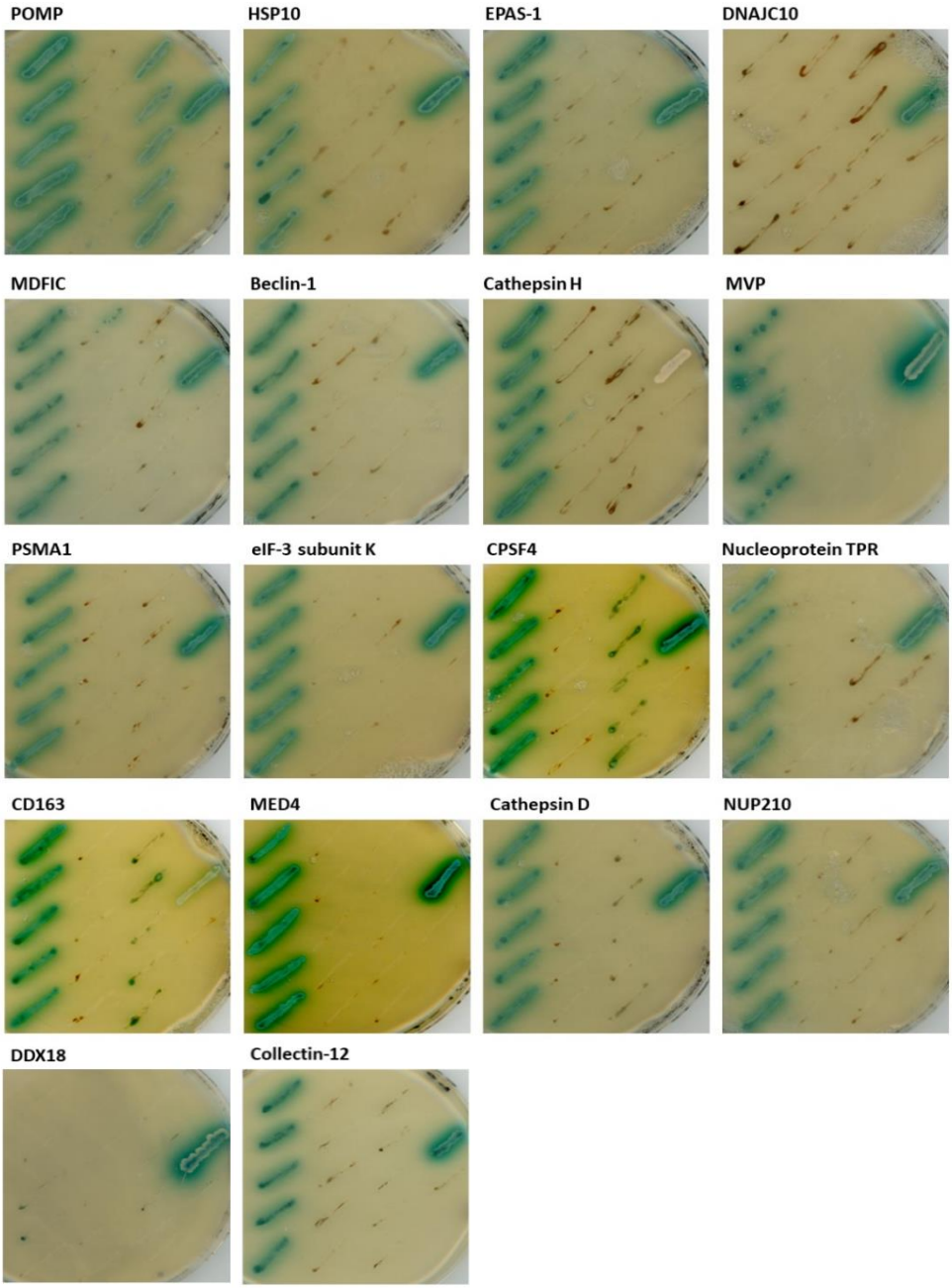

Figure 4.4: Y-2-h retest plates from NSP1β screen. Retest plate layout (**A**) and y-2-h retest plates (**B**). Yeast that had been co-transformed with combinations of the respective prey plasmid (termed "PAM protein" in (**A**)) and the bait plasmids NSP1β, pGBKT7-53 and pGBKT7 (termed "NSP1", "53" and "V" respectively in (**A**)) were plated on high stringency selection medium (SD agar -Trp, -Ade, -Leu and -His) containing X-α-Gal. The appearance of blue growth by yeast transformants expressing NSP1β and the respective PAM protein ("PAM protein + NSP1" in (**A**)) suggested an interaction. However, the interaction was considered a possible false positive if blue growth was also observed for the control transformants ("PAM protein + 53" and "PAM protein + V" in (**A**)). In the y-2-h system, T+53 and T+LAM act as positive and negative controls, respectively.

For all plates, strong blue growth was observed for the positive control (T+53) and no blue growth for the negative control (T+LAM) (**Figure 4.4**). The positive control transformed yeast on Cathepsin H and CD163 plates had strong growth but no blue; possibly because there was not enough X-α-Gal in the SD agar near those colonies.

Yeast colonies on two plates – V-set and immunoglobulin domain-containing protein 4 (VSIG4) and integrin β2 precursor – showed strong blue growth in all transformation combinations, suggesting that they were false positive interactions. Yeast co-transformed with the proteasome maturation protein (POMP) prey plasmid and either the NSP1β or empty pGBKT7 bait plasmid showed blue growth, however this was comparatively stronger in the presence of NSP1β. Similarly, yeast co-transformed with high temperature requirement protein A2 (HTRA2) prey plasmid and the NSP1β bait plasmid shown strong blue growth, but comparatively weaker growth with the empty pGBKT7 bait plasmid. These results suggested the interactions between NSP1β and either POMP or HTRA2 were likely false positives.

On five plates, testing the interaction of NSP1β with either MHC Class II, cullin-9, TLR4, cleavage and polyadenylation specificity factor subunit 4 (CPSF4) and CD163, yeast co-transformed with the respective PAM prey plasmid and NSP1β bait plasmid showed strong blue growth, but extremely weak or no growth when co-transformed with the respective PAM prey plasmid and the empty pGBKT7 bait plasmid. Given how much stronger the yeast grew when expressing NSP1β, these interactions appeared to be genuine and the growth with empty pGBKT7 bait plasmid was deemed as background. On 23 plates, including TAB3, STAT3 and beclin-1, yeast only exhibited strong blue growth when co-transformed with the PAM prey plasmid and the NSP1β bait plasmid; no blue growth was observed for the control transformants. Therefore, it appears 28 out of 36 interactions tested were genuine (**Table 4.4**).

There was no growth of yeast co-transformed with the either the DDX18 or DNAJ homolog subfamily C member 10 (DNAJC10) prey plasmids and any of the bait plasmids; therefore, these proteins did not interact with NSP1β.

After y-2-h retesting the proteins E3 small ubiquitin-like modifier (SUMO)-protein ligase early growth response 2 (EGR2) and NHLRC2 (plates not shown), sequencing

showed the plasmids for these proteins were incorrect. In the interests of time, and as NHLRC2 had already been shown to be a false positive in the NSP1α screen (**Figure 4.3**), interactions with these proteins were not investigated further.

Four proteins were selected for 3-AT retesting: TAB3, HTRA2, cullin-9 and CPSF4. TAB3 was selected to test the strength of the interaction, and cullin-9 and CPSF4 were retested to try and reduce the background activation of the system in yeast transformed with the empty pGBKT7 bait plasmid. HTRA2 was investigated further to confirm it was a false positive.

4.3 Testing the strength of interactions using 3-amino-1,2,4-triazole

3-AT was used to test the strength of interactions, as well as reduce background prey protein self-activation of the system. It is a competitive inhibitor of the *HIS3* gene product, an enzyme in the production pathway of His. In y-2-h, a yeast cell will only grow in the presence of 3-AT if the level of His is sufficient to overcome its inhibitory effect. The higher the 3-AT concentration, the stronger a prey-bait interaction must be to overcome it. Therefore, the presence of 3-AT helps to facilitate the selection of yeast transformants that produce high levels of His, because they exhibit strong bait and prey interactions. Proteins were tested using high stringency selection medium (-Trp, -Leu, -Ade, -His SD agar) containing multiple concentrations of 3-AT, ranging from 2.5-60 mM.

Yeast were transformed with individual bait and prey plasmids and plated on -Trp, -Leu SD agar to confirm double transformation. Five colonies were then streaked as previously described in **Section 4.2**, but this time onto quadruple dropout SD agar also containing 3-AT at the respective concentration. None of these plates contained X-α-Gal, so no colonies were blue.

4.3.1 Retesting interactions from the PRRSV-1 NSP1α screen with 3-amino-1,2,4-triazole

From the NSP1α screen, eight PAM proteins were retested using 3-AT: ubiquitin B, MARCH7, ZMIZ1, DNAJA3, PIAS2, sialoadhesin precursor, NHLRC2 and PIAS1. Yeast were tested on plates containing 10 mM 3-AT, 20 mM 3-AT and 60 mM 3-AT (**Figure 4.5**).

A

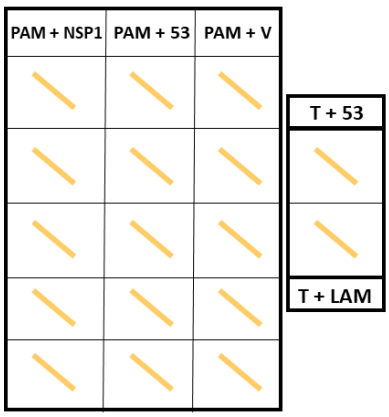

B

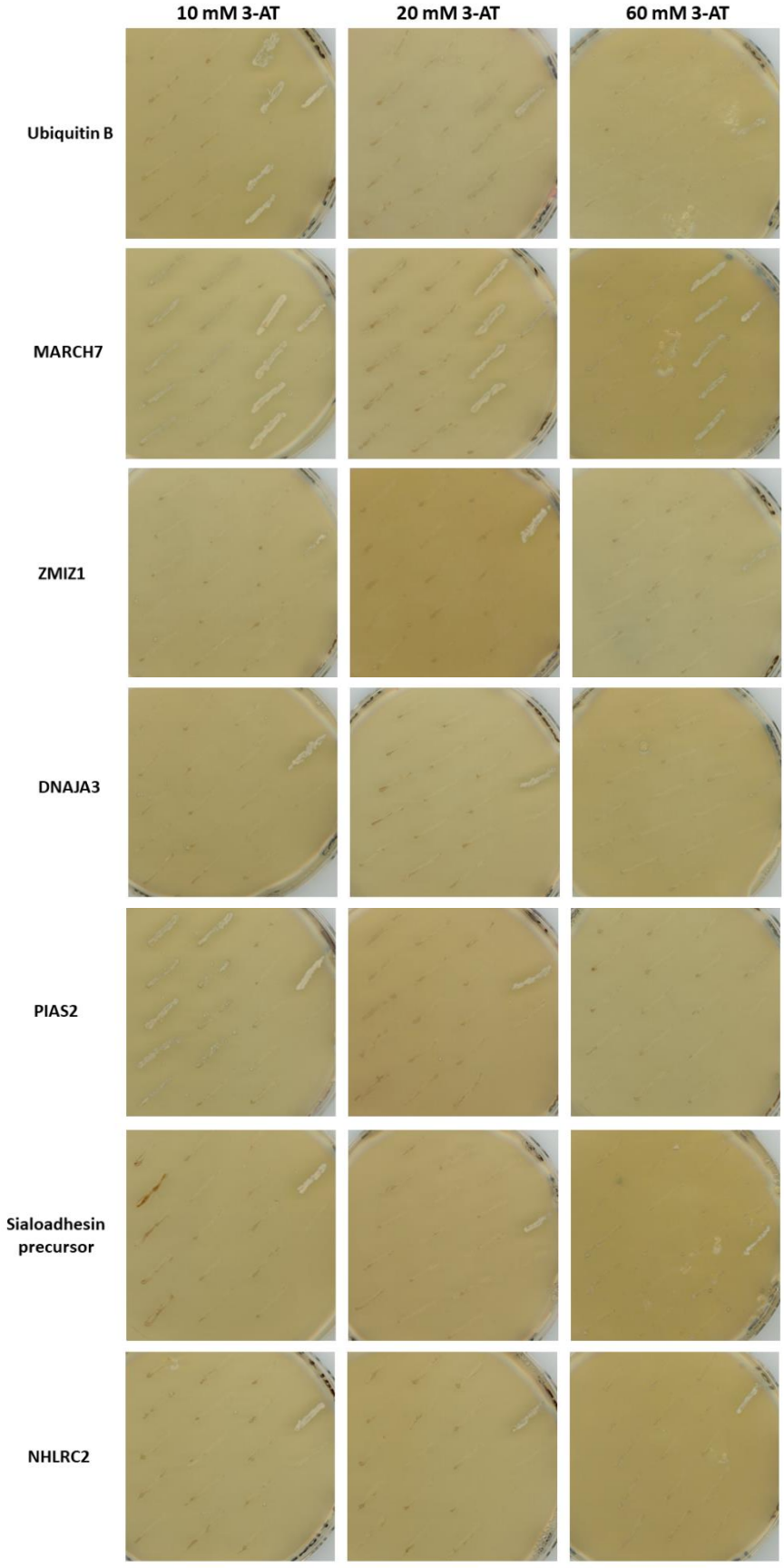
10 mM 3-AT
20 mM 3-AT
60 mM 3-AT
Ubiquitin B
MARCH7
ZMIZ1
DNAJA3
PIAS2
Sialoadhesin precursor
NHLRC2

Figure 4.5: Testing the strength of interactions with NSP1α using 3-AT. Retest plate layout (**A**) and y-2-h retest plates (**B**). Yeast that had been co-transformed with combinations of the respective prey plasmid (termed "PAM protein" in (**A**)) and the bait plasmids NSP1α, pGBKT7-53 and pGBKT7 (termed "NSP1", "53" and "V" respectively in (**A**)) were streaked on high stringency selection medium (SD agar -Trp, -Ade, -Leu and -His) containing either 10 mM, 20 mM or 60 mM 3-AT. The appearance of growth by yeast transformants expressing NSP1α and the respective PAM protein ("PAM protein + NSP1" in (**A**)) suggested an interaction; the higher the 3-AT concentration of the SD agar the yeast grew on, the stronger the interaction. In the y-2-h system, T+53 and T+LAM act as positive and negative controls, respectively.

Yeast expressing ubiquitin B and NSP1α did not grow in the presence of 3-AT (10-60 mM), but some growth was observed by yeast co-transformed with the Ubiquitin B prey plasmid and the empty pGBKT7 bait plasmid on 10 mM 3-AT SD agar. Yeast co-transformed with the MARCH7 prey plasmid and NSP1α bait plasmid showed minimal growth on the 10 mM 3-AT plate, but yeast co-transformed with MARCH7 prey plasmid and the empty vector plasmid pGBKT7 exhibited strong growth at every 3-AT concentration tested. These results confirmed those seen previously (**Figure 4.3**) and showed that the putative interactions identified between NSP1α and either ubiquitin B or MARCH7 were false positives.

Yeast co-transformed with PIAS2 prey plasmid and NSP1α bait plasmid grew on 10 mM 3-AT SD agar but not at higher 3-AT concentrations. As seen previously (**Figure 4.3**), there was also weak growth of yeast expressing PIAS2 and p53 on 10 mM 3-AT SD agar. These results confirmed that NSP1α strongly interacts with PIAS2. They also showed that PIAS2 strongly interacts with p53, albeit this interaction appeared comparatively weaker than the interaction between NSP1α and PIAS2.

Yeast transformed with either the ZMIZ1, sialoadhesin precursor, DNAJA3 and NHLRC2 prey plasmids and any of the bait plasmids showed no growth on any 3-AT SD agar. Based on these and previous results (**Figure 4.3**), ZMIZ1 and NHLRC2 were deemed to be false positives and were not investigated further.

Although no growth by transformants was seen in the presence of 10-60 mM 3-AT, it was postulated that based on the previous results (**Figure 4.3**) sialoadhesin precursor and DNAJA3 could both genuinely interact with NSP1α. To further investigate this,

respective transformants were retested using lower concentrations of 3-AT (2.5 mM and 5 mM), however, no growth was seen (**Figure 4.6**).

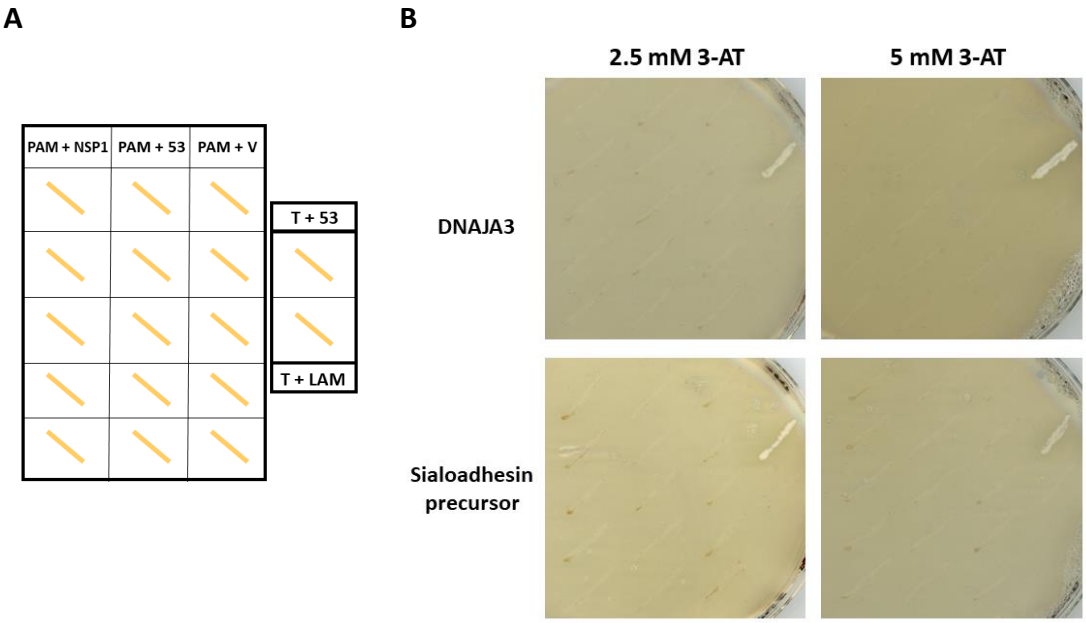

Figure 4.6: Testing the strength of interactions with NSP1α at lower concentrations of 3-AT. Retest plate layout (**A**) and y-2-h retest plates (**B**). Yeast were co-transformed with combinations of the respective prey plasmid (termed "PAM protein" in (**A**)) and the bait plasmids NSP1α, pGBKT7-53 and pGBKT7 (termed "NSP1", "53" and "V" respectively in (**A**)) and plated on high stringency selection medium (SD agar -Trp, -Ade, -Leu and -His) containing either 2.5 mM or 5 mM 3-AT. The appearance of growth by yeast transformants expressing NSP1α and the respective PAM protein ("PAM protein + NSP1" in (**A**)) suggested an interaction; the higher the 3-AT concentration of the SD agar the yeast grew on, the stronger the interaction. In the y-2-h system, T+53 and T+LAM act as positive and negative controls, respectively.

It could not be ruled out that NSP1α and DNAJA3 weakly interact. In contrast, the interaction between NSP1α and sialoadhesin precursor was suspected to be a false positive, as yeast co-transformed with the prey plasmid and either the empty pGBKT7 bait plasmid or p53 bait plasmid grew on Trp, Leu, Ade and His deficient SD agar (**Figure 4.6**). Retesting with 3-AT did not remove background activation but removed all growth, suggesting sialoadhesin was a false positive.

As well as transforming yeast with the PIAS1 prey plasmid and 215-06 NSP1α bait plasmid, PIAS1 was also re-tested with SU1-Bel NSP1α. Yeast were plated on -Trp -

Leu -Ade -His SD agar containing either 10 mM, 20 mM or 60 mM 3-AT as shown in **Figure 4.7**.

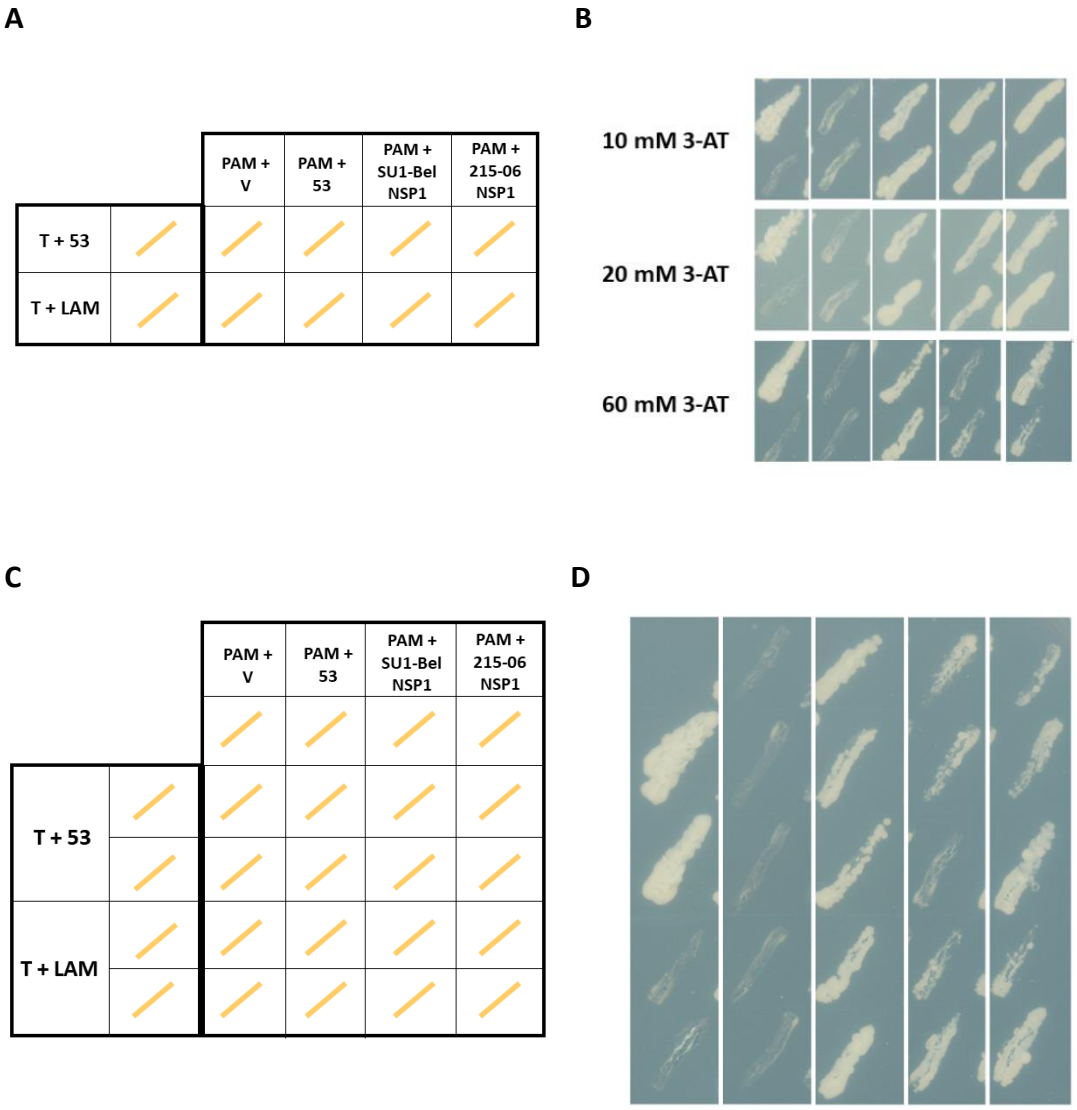

Figure 4.7: PIAS1 interacts very strongly with NSP1α. Test plate layout (**A**) for each yeast plate in (**B**). Test plate layout (**C**) for yeast plate (**D**). Yeast that had been co-transformed with combinations of the PIAS1 prey plasmid (termed "PAM protein" in (**A**) and (**C**)) and the bait plasmids NSP1α, pGBKT7-53 and pGBKT7 (termed "NSP1", "53" and "V" respectively in (**A**) and (**C**)) were plated on high stringency selection medium (SD agar -Trp, -Ade, -Leu and -His) containing either 10 mM, 20 mM or 60 mM 3-AT (**B**) or 60 mM 3-AT (**D**). The appearance of growth by yeast transformants expressing NSP1α and the respective PAM protein ("PAM protein + NSP1" in (**A**) and (**C**)) suggested an interaction; the higher the 3-AT concentration of the SD agar the yeast grew on, the stronger the interaction. In the y-2-h system, T+53 and T+LAM act as positive and negative controls, respectively.

At all 3-AT concentrations, strong growth was observed for the positive control, (T+53), and no growth for the negative control (T+LAM). Yeast expressing either 215-06 NSP1α and PIAS1, or SU1-Bel NSP1α and PIAS1, grew strongly on all plates (**Figure 4.7 B**), but less strongly as the 3-AT concentration increased to 60 mM. The same growth pattern was seen in yeast expressing PIAS1 with p53, a known verified interaction (Kahyo *et al.*, 2001). There was no growth in yeast colonies transformed with the PIAS1 bait plasmid and empty pGBKT7 bait plasmid on any plates. This confirmed that PIAS1 interacts very strongly with both 215-06 NSP1α and SU1-Bel NSP1α.

From the NSP1α screen, eight of the 13 proteins were investigated further using 3-AT plates. 3-AT retesting revealed PIAS2 strongly interacts with 215-06 NSP1α, as yeast could still grow in the presence of 10 mM 3-AT. PIAS1 interacts very strongly with both 215-06 and SU1-Bel NSP1α, as yeast growth and therefore the interaction could still be seen at 60 mM 3-AT. NSP1α has been reported previously to interact with PIAS1 (Song *et al.*, 2010).

Proteins identified in the NSP1α y-2-h screen were retested with 3-AT before NSP1β potential interactors. As yeast transformed with the positive control plasmid combination, 'T+53', struggled to grow on 60 mM 3-AT plates – with the exception of the PIAS1 plates – it was decided not to use this concentration in NSP1β retesting. Additionally, because minimal growth and therefore no interactions were seen at 10 mM and above, only 2.5 mM and 5 mM 3-AT plates were used to test NSP1β interactions.

4.3.2 Retesting interactions from the PRRSV-1 NSP1β screen with 3-amino-1,2,4-triazole

Four proteins from the NSP1β screen were retested on 3-AT plates: TAB3, HTRA2, CPSF4 and cullin-9. Yeast were co-transformed with one of these prey plasmids in combination with either the empty pGBKT7, pGBKT7-53 or pGBKT7-NSP1β bait plasmid, and re-streaked as described in **Section 4.2** onto SD agar deficient in Trp, Leu, Ade and His containing either 2.5 mM or 5 mM 3-AT (**Figure 4.8**).

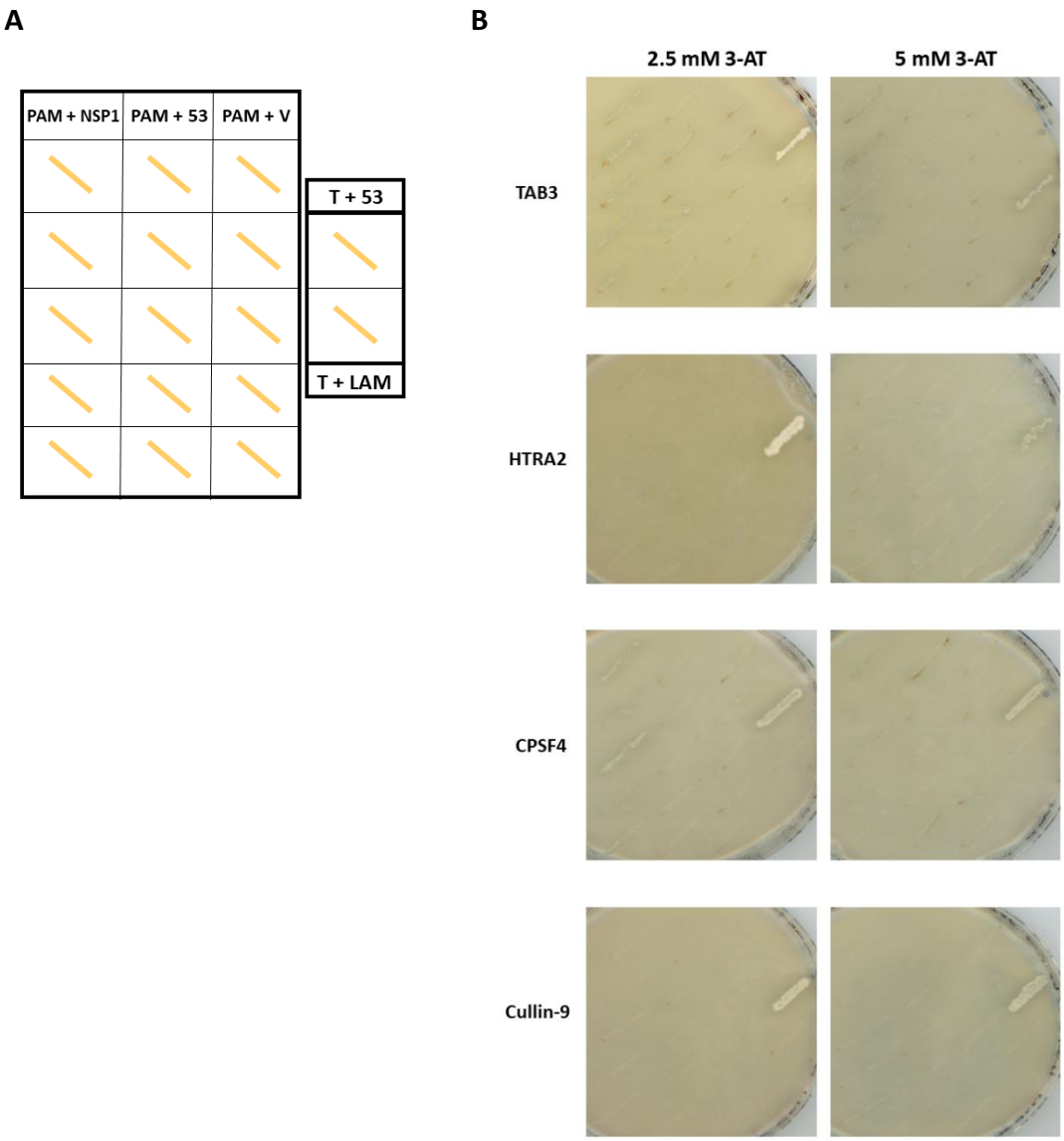

Figure 4.8: Testing the strength of interactions with NSP1ɓ using 3-AT. Test plate layout (**A**) for yeast plates (**B**). Yeast that had been co-transformed with combinations of the respective prey plasmid (termed "PAM protein" in (**A**)) and the bait plasmids NSP1β, pGBKT7-53 and pGBKT7 (termed "NSP1", "53" and "V" respectively in (**A**)) were plated on high stringency selection medium (SD agar -Trp, -Ade, -Leu and -His) containing either 2.5 mM or 5 mM 3-AT. The appearance of growth by yeast transformants expressing NSP1β and the respective PAM protein ("PAM protein + NSP1" in (**A**)) suggested an interaction; the higher the 3-AT concentration of the SD agar the yeast grew on, the stronger the interaction. In the y-2-h system, T+53 and T+LAM act as positive and negative controls, respectively.

Yeast transformed with the TAB3 prey plasmid and NSP1β bait plasmid grew on the 2.5 mM 3-AT SD agar plate, but not at the higher concentration of 5 mM 3-AT (**Figure**

4.8). This further confirmed that TAB3 interacts with NSP1β by y-2-h, but suggested the interaction is not strong.

Yeast expressing CPSF4 and NSP1β also grew in the presence of 2.5 mM but not 5 mM 3-AT (**Figure 4.8**). CPSF4 was retested to try and reduce background activation; given yeast only grew when expressing CPSF4 with NSP1β on the 3-AT plates, and that previous y-2-h re-test assays performed in the absence of 3-AT showed negligible growth of control transformants (**Figure 4.4**), the interaction between NSP1β and CPSF4 appeared genuine.

No growth was observed in the presence of 2.5 or 5 mM 3-AT by yeast co-transformed with either the HTRA2 or cullin-9 prey plasmid in combination with a bait plasmid (**Figure 4.8**). HTRA2 was found to be a false positive in the NSP1α screen (**Figure 4.3**). The fact yeast grew when co-transformed with the HTRA2 prey plasmid and either the NSP1β (strong growth) and empty pGBKT7 (medium growth) bait plasmids, suggests the interaction between NSP1β with HTRA2 is also a false positive. Given yeast co-transformed with the cullin-9 prey plasmid and NSP1β bait plasmid exhibited strong growth on higher stringency medium not containing 3-AT, whilst control transformants exhibited minimal growth (**Figure 4.4**), but no growth in the presence of 3-AT, it is likely that cullin-9 genuinely but weakly interacts with NSP1β.

Four out of 36 proteins were selected for 3-AT retesting; the results supported previous retest plates (**Figure 4.4**) that interactions between NSP1β and either TAB3 or CPSF4 are genuine. However, these interactions did not appear to be strong, as yeast expressing these combinations of proteins were unable to grow and overcome low levels of 3-AT in the SD agar.

4.4 Expression of FLAG-tagged PAM proteins

To further investigate confirmed y-2-h interactions, the PAM proteins needed to be expressed in mammalian cells for use in confocal microscopy and co-immunoprecipitations, time permitting. Eleven proteins were selected to take forward (**Table 4.5**) for this work. PIAS1, although of interest, was not taken forward as this interaction had already been referenced in an unpublished paper (Song *et al.*, 2010). Due to the respective number of putative interactions identified by each screen, only one NSP1α interactor and 10 NSP1β interactors were selected.

Table 4.5: Proteins selected to take forward and further characterise.

NSP1α interacting proteins	NSP1β interacting proteins
PIAS2	TAB3
	STAT3
	EPAS-1
	Beclin-1
	Cullin-9
	Nucleoprotein TPR
	Nucleoporin GLE1
	PSMB4
	PSMB8
	PSMA1

Multiple approaches were tested to achieve this expression. Members of the Molecular Virology Group (The Pirbright Institute) have previously used an MVA-T7 expression system, where plasmids such as pGBKT7 or pGADT7, which carry a T7 promoter, are transfected into BSR-T7 cells which are then infected with MVA-T7 (Doceul *et al.*, 2008). The combination of cells and virus both expressing the T7-polymerase induces protein expression. To achieve this, three approaches were used:

1. Cloning the T7 promoter into pACT2 to enable mammalian expression in the presence of exogenous T7-polymerase.

2. Cloning the cDNA inserts out of pACT2 into pGADT7, which has a T7 promoter, and would enable mammalian expression in the presence of exogenous T7-polymerase.
3. PCR amplification of cDNA encoding the respective portion of PAM protein using a forward primer that contains the T7 promoter, sequence encoding the HA-epitope tag and a KOZAK sequence (T7 pACT2 F, **Table 2.8**). This would enable mammalian expression in the presence of exogenous T7-polymerase.

For the first approach, the T7 promoter was ordered as a 5' phosphorylated DNA oligo (**Table 2.9**) with either the *Bam*HI or *Eco*RI restriction site at each end. The second approach involved using *Xho*I restriction site digestion and subsequent ligation. Neither of these approaches was successful. The third approach involved transfection of the resulting PCR product into BSR-T7 cells and subsequent infection with MVA-T7. This approach had initial success, with multiple proteins being expressed at their predicted sizes (**Figure 4.9**).

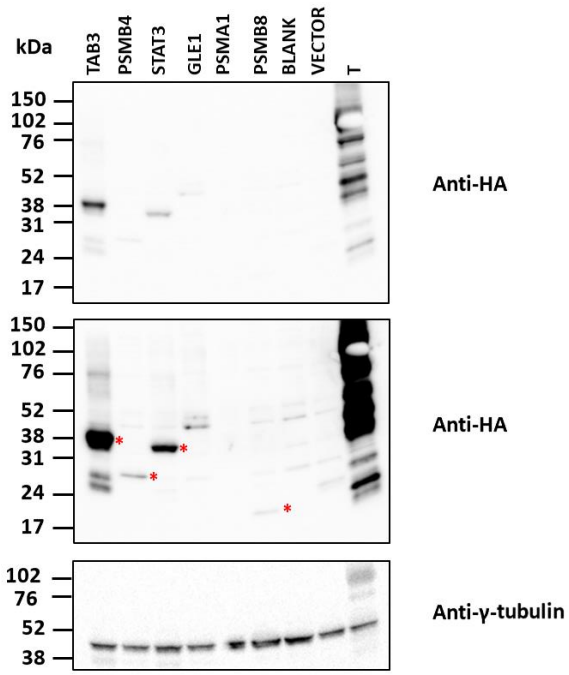

Figure 4.9: HA-tagged proteins were expressed in cells transfected with PCR products containing the T7 promoter and PAM cDNA insert. BSR-T7 cells were seeded in 6-well plates and when confluent transfected with 1 µg of PCR product containing the T7 promoter, HA-tag, KOZAK sequence and the cDNA insert coding for the specified PAM protein (from left to right): Lane 1 – TAB3; Lane 2 – PSMB4; Lane 3 – STAT3; Lane 4 – GLE1; Lane 5 – PSMA1; Lane 6 – PSMB8. Controls included untransfected cell lysate (Lane 7, BLANK), and cells transfected with either 1 µg of pGADT7 (Lane 8, VECTOR) or pGADT7-T (Lane 9, T). Twenty-four hpt, whole cell lysates were analysed via SDS-PAGE and western blotting. Membranes were probed with mouse anti-FLAG antibody, rabbit anti-γ-Tubulin antibody and mouse anti-Myc antibody. Blots were imaged using LI-COR Odyssey® CLx Imaging System. * indicates the specific band corresponding to the predicted size of HA-tagged protein in each lane.

In **Figure 4.9**, TAB3 (band at 38 kDa, **Lane 1**), PSMB4 (band at 28 kDa, **Lane 2**), STAT3 (band at 36 kDa, **Lane 3**) and PSMB8 (band at 20 kDa , **Lane 4**) were all expressed at approximately their predicted sizes. However, expression levels, as determined by western blot analysis of HA-tagged PAM proteins, appeared variable despite the respective PCR products being the correct predicted size. This was later found to be due to primer mis-priming due to the presence of pACT2 sequence encoding the HA-epitope tag upstream of the PAM cDNA insertion site. These three approaches were abandoned in favour of a fourth approach - cloning each PAM cDNA into the pEF-FLAG plasmid and subsequent expression in HEK-293-TLR3 cells.

4.4.1 Cloning cDNA inserts into pEF-FLAG

The respective cDNA sequence of the eleven interacting PAM proteins, situated between the two *Xho*I restriction sites of the pACT2 plasmid, was obtained by sequencing as described (**Section 2.10**) using the pGADT7 F and pGADT7 R primers. Primers (**Table 2.5**, **Table 2.8**) containing the appropriate combination of restriction sites, *Bam*HI, *Eco*RI, *Nco*I, *Xba*I and *Spe*I present in the multi cloning site of the pEF-FLAG plasmid, were then used to PCR amplify and clone each fragment. **Figure 4.10** shows the digested PCR products encoding each PAM protein, with all digested PCR products matching their predicted sizes (**Table 2.5**).

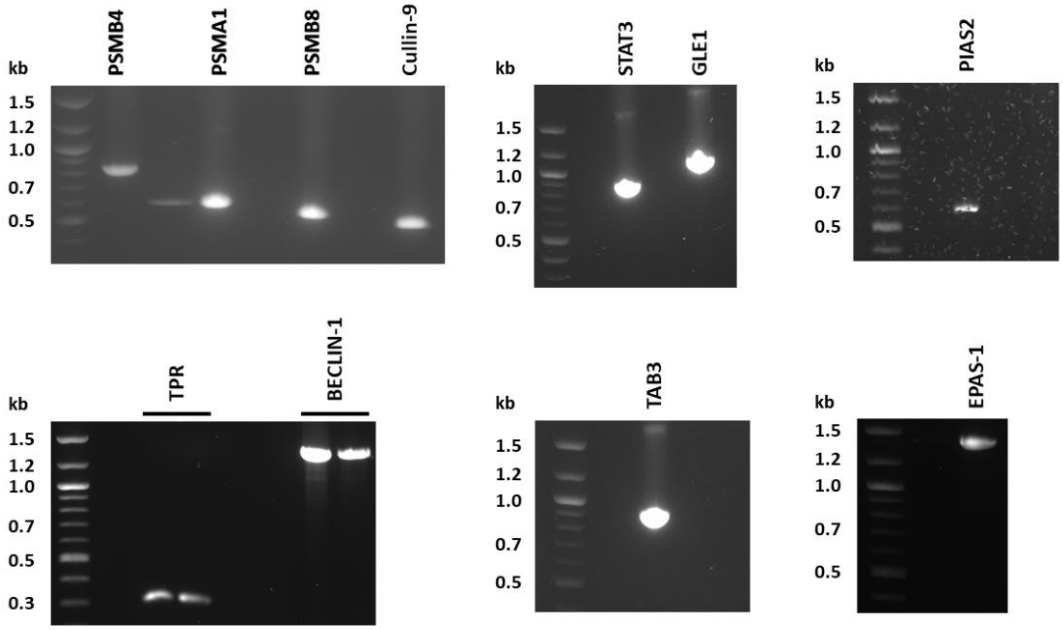

Figure 4.10: Digested PCR products for cloning into pEF-1. PCR products containing PAM cDNA inserts were digested with specific combinations of restriction enzymes and then analysed by agarose gel electrophoresis.

Colony numbers between control plates, bacteria transformed with digested vector only, and cloning plates, bacteria transformed with ligations, were compared. No/few colonies were observed on the control plates and many on the cloning plates; this indicated successful cloning. Every insert was successfully cloned into pEF-FLAG. The amplified plasmids were Sanger sequenced (**Section 2.10**), which confirmed they were in frame and encoded the correct PAM protein.

4.4.2 Checking protein expression of FLAG-tagged PAM proteins

Next, the expression of each fusion protein in immortalised mammalian cell lines was investigated. Each cDNA insert was translated using https://web.expasy.org/translate/, and the predicted protein size was calculated using the amino acid sequence on https://www.bioinformatics.org/sms/prot_mw.html. Each PAM protein was expressed with an N-terminal FLAG-epitope tag (DYKDDDDK (1.44 kDa)) fusion. The predicted size of each PAM protein, including the FLAG tag, is shown in **Table 4.6**.

Table 4.6: Predicted sizes and observed sizes of partial PAM proteins.

Protein	Predicted size (kDa)	Size on Western Blot (kDa)
TAB3	33.41	35
STAT3	33.87	36
EPAS-1	51.64	55
Beclin-1	52.79	52
Cullin-9	19.68	Not expressed
Nucleoprotein TPR	12.68	Not expressed
Nucleoporin GLE1	39.9	40
PSMB4	30.5	27
PSMB8	20.81	19
PSMA1	22.85	Not expressed
PIAS2	22.13	38

To check protein expression, HEK-293-TLR3 cells were transfected with pEF-FLAG-PAM proteins using the PEI/LBS method (**Section 2.13.1**).

The expression of FLAG-PSMB4 was first investigated, as this was the first protein successfully cloned. Cells were transfected with either 0.5 µg, 1 µg or 2 µg of pEF-FLAG-PSMB4 in combination with 0.5 µg or 1 µg of pcDNA-Myc-215-06-NSP1β; empty vector pEF-FLAG was used to keep the amount of DNA the same between transfections. Controls included untransfected cells and cells transfected with different amounts of pEF-FLAG empty vector, to check cell viability after transfecting

with different amounts of DNA. Following transfection, cells were incubated overnight and whole cell lysates collected the next day (**Section 2.13.3**). These whole cell lysates were then subjected to SDS-PAGE and western blot analysis (**Section 2.14**) for the expression of epitope-tagged PAM proteins. Duplicate western blot membranes were generated using the same whole cell lysates. One membrane was probed with mouse anti-Myc antibody, the other with mouse anti-FLAG antibody and rabbit anti-γ-tubulin antibody (**Table 2.7**). Blots were imaged using the LI-COR Odyssey® CLx Imaging System (**Figure 4.11**).

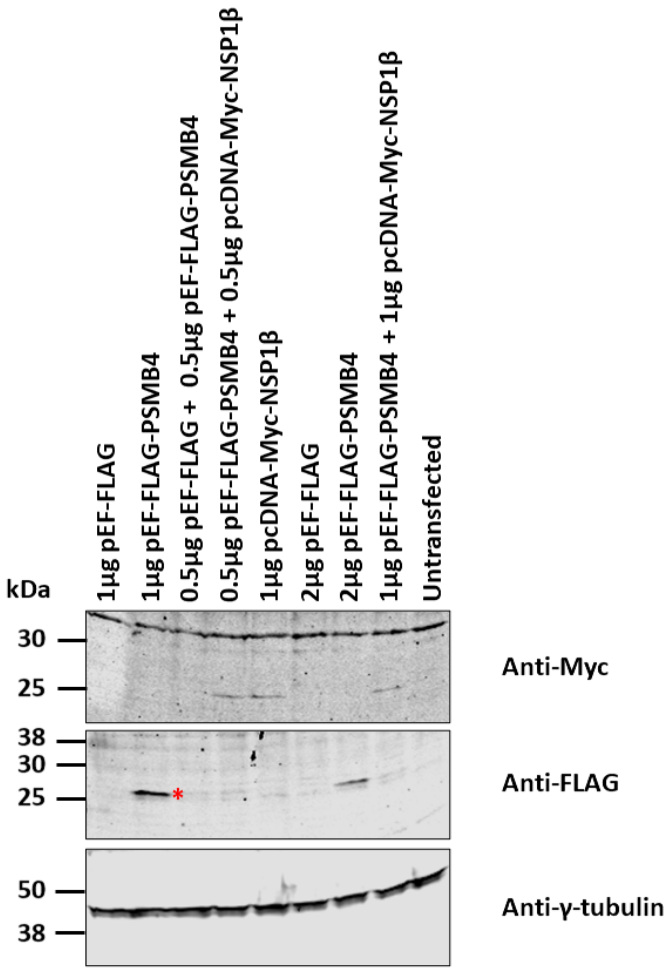

Figure 4.11: Expression of FLAG-PSMB4 with and without Myc-NSP1β. HEK-293-TLR3 cells were transfected with the following combinations of plasmids (from left to right): Lane 1 – 1 µg pEF-FLAG; Lane 2 – 1 µg pEF-FLAG-PSMB4; Lane 3 – 0.5 µg pEF-FLAG + 0.5 µg pEF-FLAG-PSMB4; Lane 4 – 0.5 µg pEF-FLAG-PSMB4 + 0.5 µg pcDNA-Myc-NSP1β; Lane 5 – 1 µg pcDNA-Myc-NSP1β; Lane 6 – 2 µg pEF-FLAG; Lane 7 – 2 µg pEF-FLAG-PSMB4; Lane 8 – 1 µg pEF-FLAG-PSMB4 + 1 µg pcDNA-Myc-NSP1β; 9 – untransfected control. Twenty-four hpt, whole cell lysates were analysed via SDS-PAGE and western blotting. Membranes were probed with mouse anti-FLAG antibody, rabbit anti-γ-Tubulin antibody and mouse anti-Myc antibody. Blots were imaged using LI-COR Odyssey® CLx Imaging System. * indicates the specific band corresponding to the FLAG-tagged protein in each lane. The expected protein sizes were: 30.5 kDa for FLAG-PSMB4, 27 kDa for Myc-NSP1β and 38-50 kDa for γ-tubulin.

Probing with the anti-Myc antibody identified weak bands corresponding to the predicted MW of Myc-NSP1β (25/26 kDa) in all samples prepared from cells that had been transfected with the pcDNA-Myc-NSP1β plasmid (**Figure 4.11, anti-Myc blot**).

On the FLAG blot (**Figure 4.11**), obvious bands were observed that corresponded to the predicted size (~27 kDa) of FLAG-PSMB4 (**Figure 4.11, anti-FLAG blot**); these bands correlated to whole cell lysates prepared following transfection with only the FLAG-PSMB4 plasmid. Weaker, less obvious bands corresponding to the predicted size of FLAG-PSMB4 were also observed in the whole cell lysates prepared from cells co-transfected with pEF-FLAG and pEF-FLAG-PSMB4 or pEF-FLAG-PSMB4 and pcDNA-Myc-NSP1β (**Figure 4.11, anti-FLAG blot**).

FLAG-PSMB4 expression level varied with the amount of plasmid used in transfection, and also if it was co-transfected with pcDNA-Myc-NSP1β. Cells transfected with 1 μg of pEF-FLAG-PSMB4 gave the highest FLAG-PSMB4 expression, even more than 2 μg; it is unclear why. Co-transfection of pcDNA-Myc-NSP1β in combination with pEF-FLAG-PSMB4 significantly reduced expression of FLAG-PSMB4, whilst Myc-NSP1β expression was unaffected. This was possibly because the two plasmids were competing for host transcription and translation machinery. γ-tubulin expression was comparable in every lane (**Figure 4.11**), showing equal loading in each lane. No FLAG- or Myc-epitope tag expression was observed for the non-transfected control sample. These results confirmed FLAG-PSMB4 can be expressed using pEF-FLAG-PSMB4 in HEK-293-TLR3 cells, with and without pcDNA-Myc-NSP1β. Based on these results, 1 μg of each plasmid was used in future co-transfections.

In the following experiments, HEK-293-TLR3 cells were transfected with either 1 μg of the respective pEF-FLAG-PAM plasmid, or 1 μg of pcDNA-Myc-NSP1α, or pcDNA-Myc-NSP1β, or co-transfected with both; pEF-FLAG was used to maintain an equivalent amount of DNA (2 μg) between transfections. Whole cell lysates were prepared and analysed as previously discussed. There was not enough untransfected sample to run on every gel (**Figure 4.12, A and D anti-Myc and anti γ-tubulin blots**) nor enough pcDNA-Myc-NSP1β cell lysate (**Figure 4.12 A anti-Myc and anti γ-tubulin blots**). One membrane was probed with mouse anti-FLAG antibody, the other with mouse anti-Myc tag antibody and rabbit anti γ-tubulin antibody (**Figure 4.12**).

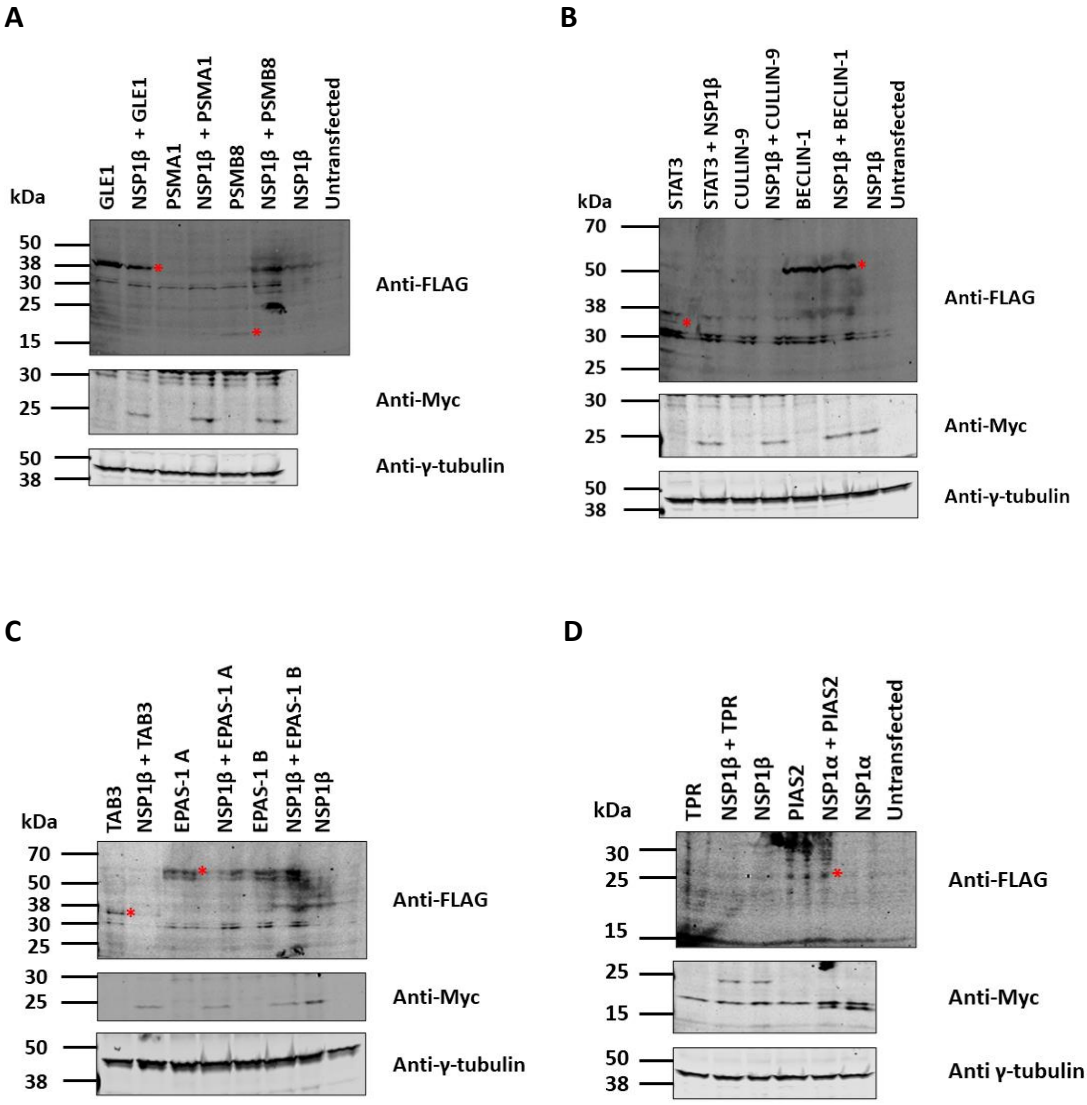

Figure 4.12: Expression of pEF-FLAG constructs. HEK-293-TLR3 cells were transfected with a combination of pEF-FLAG and pcDNA-Myc plasmids to investigate expression of FLAG-tagged PAM proteins with and without Myc-NSP1α or Myc-NSP1β (**A-D**). Twenty-four hpt, whole cell lysates were analysed by SDS-PAGE and western blot. Membranes were probed with mouse anti-FLAG antibody, rabbit anti-γ-Tubulin antibody and mouse anti-Myc antibody. * indicates the specific band corresponding to the FLAG-tagged protein in each lane.

FLAG-tagged nucleoprotein GLE1 was predicted to be ~40 kDa; an intense band matching this size was detected in cells transfected with pEF-FLAG-GLE1 (**Figure 4.12 A**). The intensity of this band decreased when transfected with pcDNA-Myc-NSP1β.

A band corresponding to the predicted MW of FLAG-PSMB8 (~19 kDa) was detected in whole cell lysates of cells transfected with pEF-FLAG-PSMB8, but not in whole cell lysates of cells co-transfected with pEF-FLAG-PSMB8 and pcDNA-Myc-NSP1β.

Flag-tagged STAT3 was predicted to be ~34 kDa; a putative band at 36 kDa was observed in cells transfected with pEF-FLAG-STAT3 with and without pcDNA-Myc-NSP1β. This band was present at a significantly lower intensity in cells co-transfected with pcDNA-Myc-NSP1β.

Obvious bands corresponding to the predicted MW of FLAG-beclin-1 (~53 kDa) were detected in whole cell lysates of cells transfected with pEF-FLAG-beclin-1 or co-transfected with pEF-FLAG-beclin-1 and pcDNA-Myc-NSP1β, however, FLAG-beclin-1 expression appeared comparatively lower in the latter.

A band of the predicted MW (~34 kDa) for FLAG-TAB3 was observed in the whole cell lysates of cells transfected with pEF-FLAG-TAB3 (**Figure 4.12 C**); this was also present in cells co-transfected with pcDNA-Myc-NSP1β but at a much lower intensity.

In all whole cell lysates prepared from cells transfected with pEF-FLAG-endothelial PAS domain-containing protein 1 (EPAS-1), there were multiple bands of the predicted MW (~52 kDa). Multiple bands were present, possibly because of sample entering the gel at too high voltage, affecting EPAS-1 as it is a large protein. Alternatively, post-translational modification of EPAS-1 could be the reason, as EPAS-1 can be methylated, ubiquitinated, acetylated, sumoylated and phosphorylated (Kristan, Debeljak and Kunej, 2021). In this case, the levels of FLAG-EPAS-1 expression appeared comparable in the presence and absence of NSP1β expression.

A putative band of the predicted MW (~25 kDa) for FLAG-PIAS2 was detected in whole cell lysates of cells transfected with pEF-FLAG-PIAS2; this band appeared at equal intensity with and without Myc-NSP1β. A bubble introduced during the transfer process made this band difficult to analyse.

The expression of proteasome subunit α type-1 (PSMA1), cullin-9 or nucleoprotein TPR was not detected in cells with or without Myc-NSP1β (**Figure 4.12 A, B & D**).

Following the probing of western blot membranes using an anti-Myc antibody, a band corresponding to the predicted MW (~25 kDa) of Myc-NSP1β was detected in all whole cell lysates prepared from cells transfected with pcDNA-Myc-NSP1β (**Figure 4.12**). The intensity of each band was comparable in cells transfected with pcDNA-Myc-NSP1β and either pEF-FLAG-TPR, pEF-FLAG-STAT3, pEF-FLAG-cullin-9 or pEF-

FLAG-beclin-1, to cells transfected with only pcDNA-Myc-NSP1β (**Figure 4.12 B & D**). However, in cells transfected with pcDNA-Myc-NSP1β and either pEF-FLAG-TAB3 or pEF-FLAG-EPAS-1, the Myc-NSP1β band was at a lower intensity compared to cells transfected with pcDNA-Myc-NSP1β alone (**Figure 4.12 C**).

In cell lysates transfected with pcDNA-Myc-NSP1α an expected band of ~20 kDa was detected following probing with an anti-Myc antibody (**Figure 4.12 D**). This band was more intense in whole cell lysates prepared from cells transfected with only pcDNA-Myc-NSP1α, rather pcDNA-Myc-NSP1α and pEF-FLAG-PIAS2.

Gamma tubulin (band at between 38-50 kDa, **Figure 4.12**) was expressed equally in all lysates on each gel, suggesting equal protein loading across the wells.

Of the 11 FLAG-tagged proteins tested, eight were detected by western blot. These were: PSMB4, GLE1, PSMB8, STAT3, beclin-1, TAB3, EPAS-1 and PIAS2. Of note, most FLAG-tagged proteins were expressed at a comparatively lower level when expressed in combination with Myc-NSP1α or Myc-NSP1β. Successfully expressed proteins were taken forward for use in confocal microscopy and coimmunoprecipitations, time permitting.

4.5 Analysing the co-localisation of identified PAM proteins with PRRSV-1 NSP1α and NSP1β by confocal immunofluorescence microscopy

Confocal immunofluorescence microscopy was performed to investigate the spatial expression of viral and host proteins. Max cells were preferred to HEK-293-TLR3, as previous work has shown that their comparably larger size helps image acquisition, they can express high levels of viral proteins, and as porcine cells they are more biologically relevant.

For each experiment, Max cells were seeded onto coverslips in 6-well plates and when 70% confluent, were transfected with 0.25 µg pEF-FLAG-PAM protein and/or pcDNA-Myc-NSP1α or pcDNA-Myc-NSP1β (**Section 2.13.1**). At 24 hpt, cells were fixed and probed with mouse anti-FLAG and rabbit anti-Myc antibodies (**Table 2.7**), followed by the corresponding secondaries to detect the tagged proteins (**Section 2.15**). Cells were then stained with DAPI, to visualise the nucleus, and imaged by confocal immunofluorescence microscopy (**Section 2.15**). Multiple images were taken per coverslip; the images presented best represent the images obtained from three experiments. Additionally, in co-transfected cells, Z stack series of images consisting of 6 successive levels of the cell were obtained to analyse protein location throughout the cell.

Only plasmids encoding PAM proteins whose expression had been confirmed (**Section 4.4**) were transfected into Max cells; these proteins were PIAS2, PSMB4, TAB3, GLE1, EPAS-1, beclin-1. The cellular localisation of exogenous PAM protein expression was analysed in the presence and absence of NSP1α or NSP1β. In all figures in **Section 4.5**, Myc-tagged NSP1α and NSP1β appear red, whereas FLAG-PAM proteins are shown in green. Areas of co-localisation between Myc-tagged NSP1α or NSP1β and a FLAG-tagged PAM protein appear yellow. Nuclei were stained with DAPI and appear blue.

4.5.1 Testing of different antibody dilutions to optimise imaging

To image transfected tagged proteins, the rabbit anti-Myc and mouse anti-FLAG primary antibodies (**Table 2.7**) were used to probe cells. The optimal antibody dilution for these antibodies was investigated, to maximise visualisation and reduce background. Two different primary antibody dilutions were tested for each antibody: 1:200 and 1:400 for the mouse anti-FLAG antibody and 1:100 and 1:200 for the rabbit anti-Myc; these dilutions were chosen based on manufacturer recommendations. Confluent Max cells seeded on coverslips, either untransfected or co-transfected with pcDNA-Myc-NSP1β and pEF-FLAG-PSMB4, were probed with either one or both primary antibodies at one of the two dilutions, then the corresponding secondaries, stained and imaged as described (**Figure 4.13**).

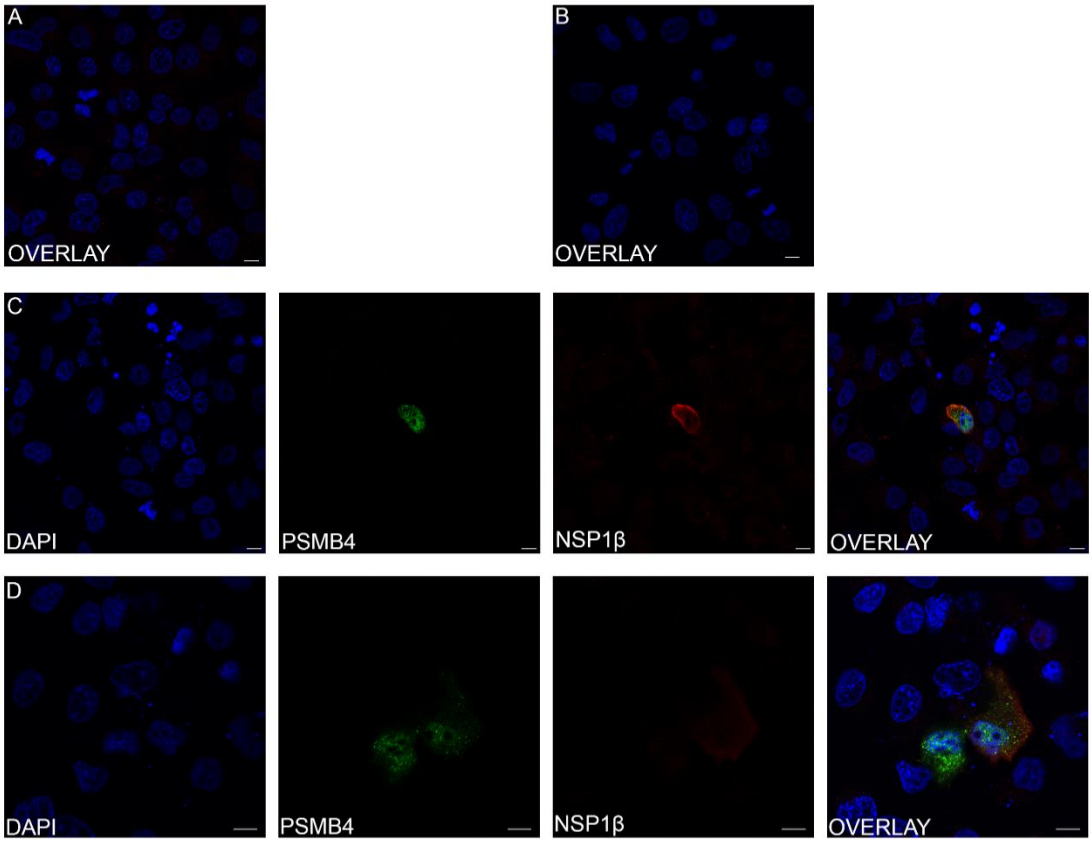

Figure 4.13: Primary antibody dilution optimisation. Max cells were seeded onto coverslips in 6-well plates. Cells were either not transfected (**A** and **B**) or co-transfected with pcDNA-Myc-NSP1β and pEF-FLAG-PSMB4 (**C** and **D**). At 24 hpt, cells were fixed and probed with either with a rabbit antibody recognising the Myc epitope tag, a mouse antibody recognising the FLAG epitope tag or both at different concentrations: (**A**) 1:100 anti-Myc antibody; (**B**) 1:200 anti-FLAG antibody; (**C**) 1:100 anti-Myc antibody and 1:200 anti-FLAG antibody; (**D**) 1:200 anti-Myc antibody and 1:400 anti-FLAG antibody. Probed cells were then stained with DAPI, to visualise nuclei, and imaged by confocal immunofluorescence microscopy. Nuclei are shown in blue, FLAG-tagged PSMB4 in green and Myc-tagged NSP1β in red. Scale bar = 10 µm.

Untransfected cells probed with 1:100 anti-Myc antibody, and therefore the higher antibody concentration, are shown in (**Figure 4.13 A**). Despite no Myc-tagged proteins being expressed, many red speckles and therefore high background was visible. Cells expressing Myc-tagged NSP1β are shown in (**Figure 4.13 C & D**), probed with 1:100 anti-Myc antibody and 1:200 anti-Myc antibody, respectively. Imaging with the higher antibody concentration again produced high background as red speckles were visible; this background was significantly reduced at the lower

antibody concentration. Myc-NSP1β was detected in the cytoplasm in both panels but appeared much brighter at the higher antibody concentration (**Figure 4.13 D**).

In contrast, in untransfected cells probed with higher concentration of 1:200 anti-FLAG antibody no green background staining was visible. Cell expressing FLAG-tagged PSMB4, are shown in (**Figure 4.13 C and D**). FLAG-PSMB4, shown in green, was brighter and therefore more visible when 1:200 is used rather than 1:400.

The rabbit anti-Myc was found to give high background at the higher antibody concentration of 1:100, but the lower antibody concentration reduced the intensity of the red Myc-NSP1β staining. As Myc-NSP1β could still be detected at the lower concentration and gave less background, 1:200 was chosen for subsequent experiments. Lower concentrations may have reduced background further but also would have reduced protein detection, and so were not tested. The mouse anti-FLAG, used at the higher concentration of 1:200, produced no to minimal background; therefore, to maximise protein visibility the higher antibody concentration of 1:200 was used going forward.

Therefore, these experiments led to the selection of a dilution of 1:200 for both antibodies.

4.5.2 PRRSV NSP1α

PRRSV NSP1α is a nucleocytoplasmic protein, shuttling between the two using its NES and the exportin chromosomal maintenance 1 (CRM-1) protein (Chen *et al.*, 2016). Previous confocal analysis has shown PRRSV-2 NSP1α to be distributed in both the nucleus and cytoplasm, with most of NSP1α concentrated to the nucleus (Yoo et al., 2010). **Figure 4.14** shows Max cells transfected with pcDNA-Myc-NSP1α.

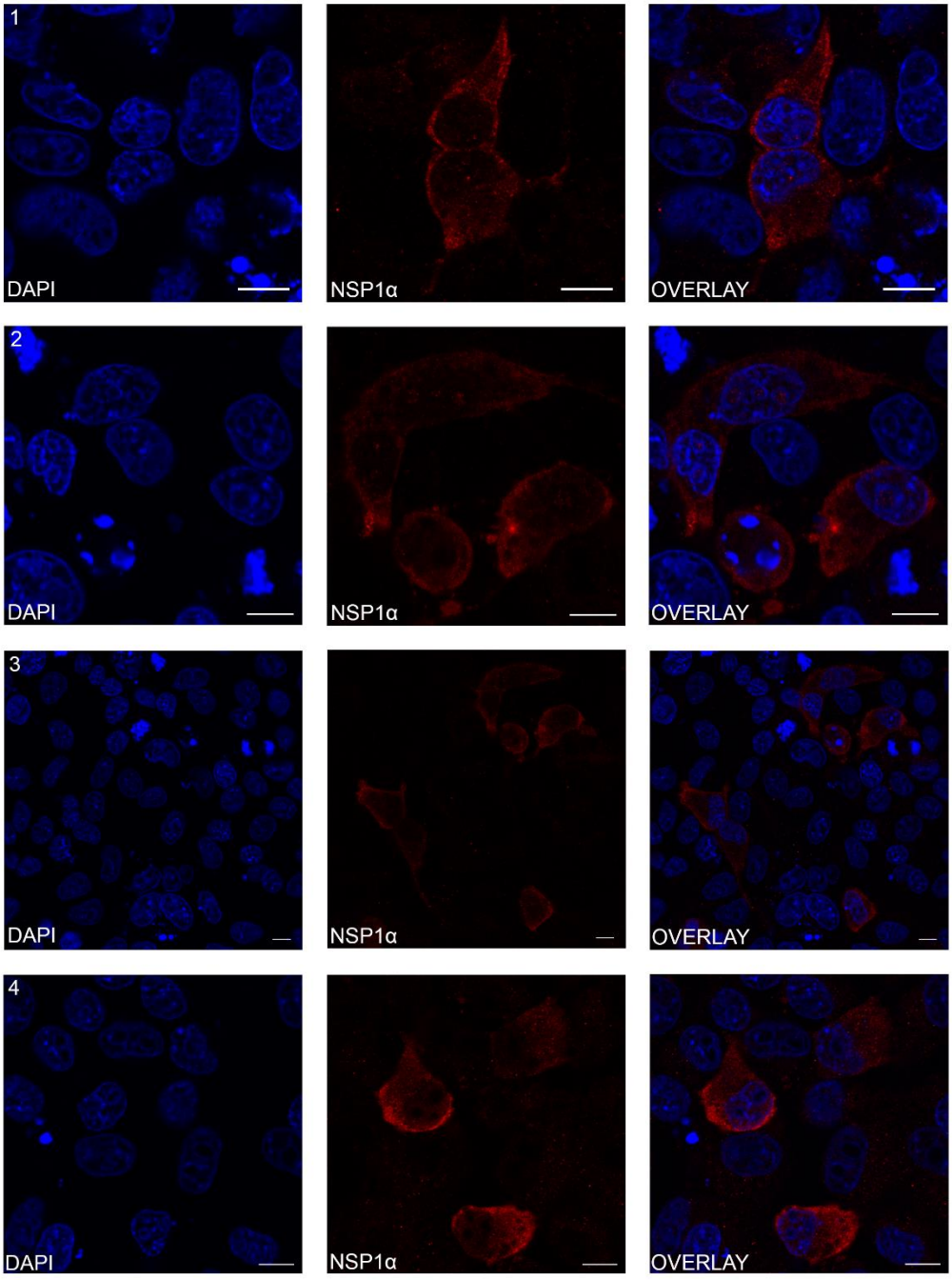

Figure 4.14: PRRSV NSP1α localises predominantly in the cytoplasm of Max cells. Max cells on coverslips in 6-well plates were transfected with pcDNA-Myc-NSP1α. At 24 hpt cells were probed with a rabbit antibody recognising the Myc epitope tag. Probed cells were then fixed and stained with DAPI, to visualise nuclei, and imaged by confocal immunofluorescence microscopy. Nuclei are shown in blue and Myc-NSP1α proteins are red. Multiple cells were imaged (**Rows 1-4**). Scale bar = 10 µm.

NSP1α localised almost exclusively to the cytoplasm of transfected cells (**Figure 4.14**). In some cells, low levels of NSP1α were detected in the nucleus (**Figure 4.14, Row 4**).

4.5.3 PIAS2

PIAS2, identified in the y-2-h screen, interacts with NSP1α (**Section 4.2**). PIAS2 is a SUMO E3 ligase that regulates the activity of multiple transcription factors, some of which are involved in the immune response (Kotaja *et al.*, 2002). PIAS2 has been shown to localise to the nucleus (Kong *et al.*, 2015; Adachi *et al.*, 2020). **Figure 4.15** shows Max cells transfected with pEF-FLAG-PIAS2 which showed, as expected, PIAS2 localised exclusively to the nucleus.

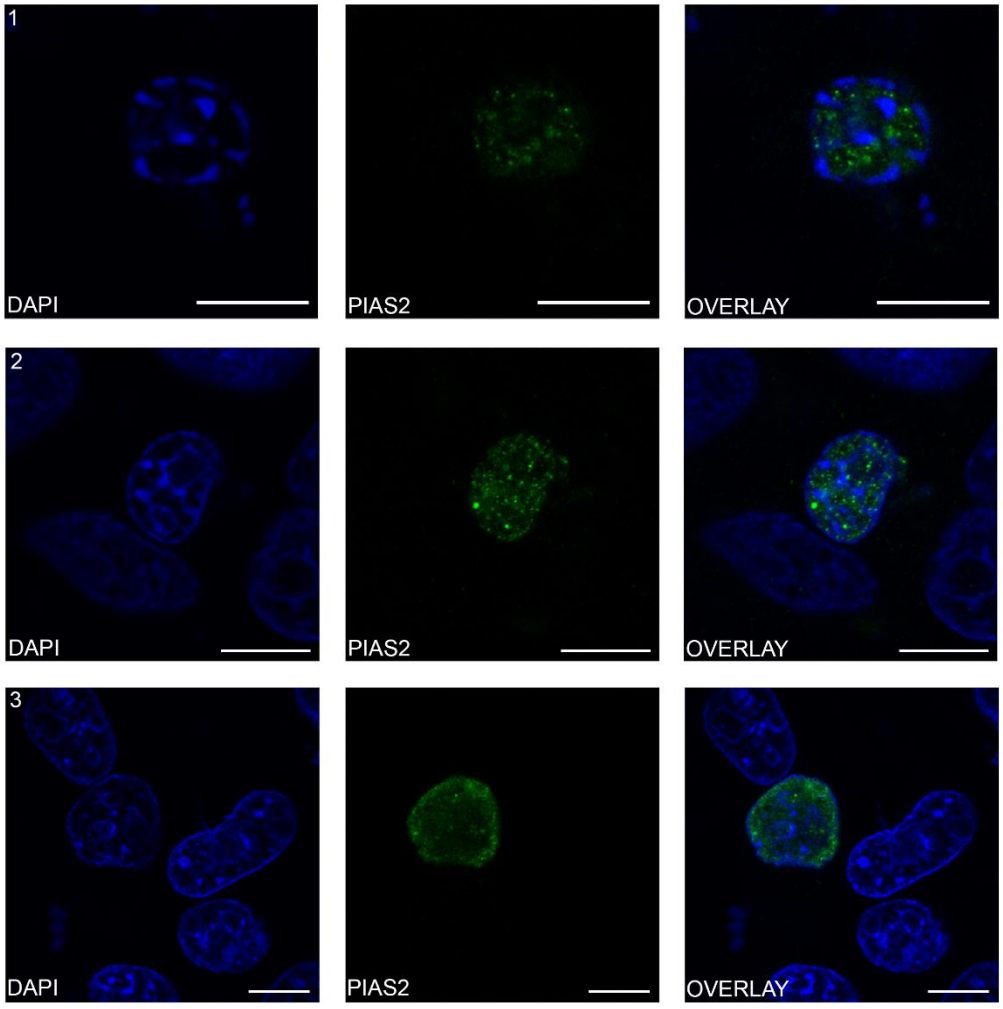

Figure 4.15: PIAS2 localises to the nucleus of Max cells. Max cells on coverslips in 6-well plates were transfected with pEF-FLAG-PIAS2. At 24 hpt cells were fixed and probed with a mouse antibody recognising the FLAG epitope tag. Probed cells were then stained with DAPI, to visualise nuclei, and imaged by confocal immunofluorescence microscopy. Multiple cells were imaged (**Rows 1-3**). Nuclei are shown in blue and FLAG-PIAS2 in green. Scale bar = 10 µm.

Max cells were then co-transfected with both pcDNA-Myc-NSP1α and pEF-FLAG-PIAS2 to determine if the localisation of PIAS2 changed in the presence of NSP1α and to determine if the two proteins co-localise. Only one cell was found. A Z stack series of images consisting of six successive levels of the cell was captured (**Figure 4.16**, **1-6**). Myc-NSP1α localised exclusively to the cytoplasm and FLAG-PIAS2 exclusively to the nucleus (**Figure 4.16**), and therefore behaved the same as when individually expressed. Moving through the levels of the cell their locations did not change and no obvious co-localisation was observed.

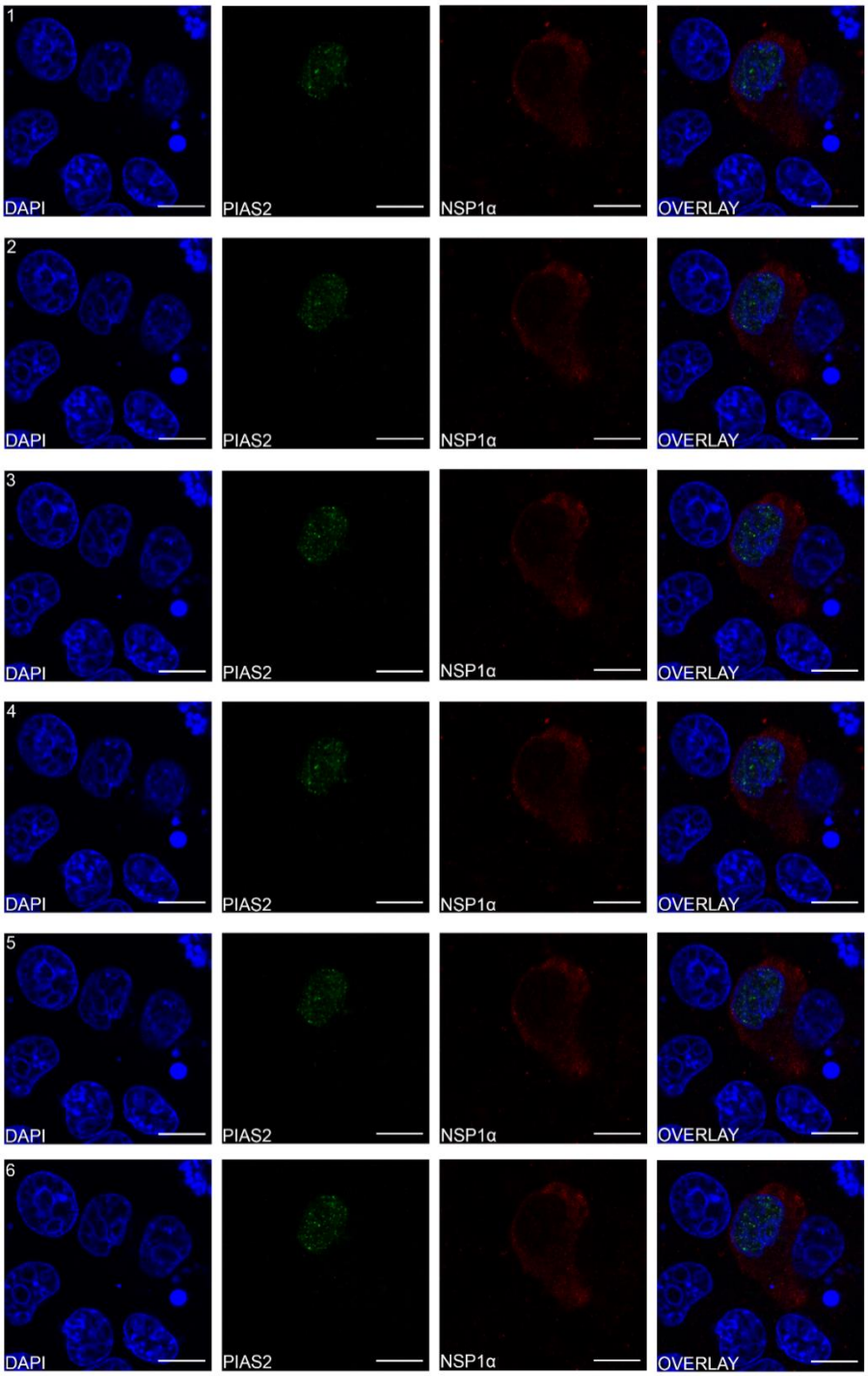

Figure 4.16: NSP1α and PIAS2 do not co-localise in Max cells. Max cells seeded on coverslips in 6-well plates were co-transfected with pcDNA-Myc-NSP1α and pEF-FLAG-PIAS2. At 24 hpt cells were probed with a rabbit antibody recognising the Myc epitope tag and a mouse antibody recognising the FLAG epitope tag. Probed cells were then stained with DAPI, to visualise nuclei, and imaged by confocal immunofluorescence microscopy. A Z stack series consisting of six successive levels is shown (**Rows 1-6**). Nuclei are shown in blue, Myc-NSP1α in red and FLAG-PIAS2 in green. Scale bar = 10 µm.

4.5.4 PRRSV NSP1β

NSP1β is also a nucleocytoplasmic protein (Beura *et al.*, 2010), but is found predominantly in the nucleus (Han *et al.*, 2014). NSP1β requires the soluble transport factor KPNA6 to move through the NPC into the nucleus (Yang *et al.*, 2018); no NES or method of import has been identified yet for NSP1β. **Figure 4.17** shows Max cells transfected with pcDNA-Myc-NSP1β.

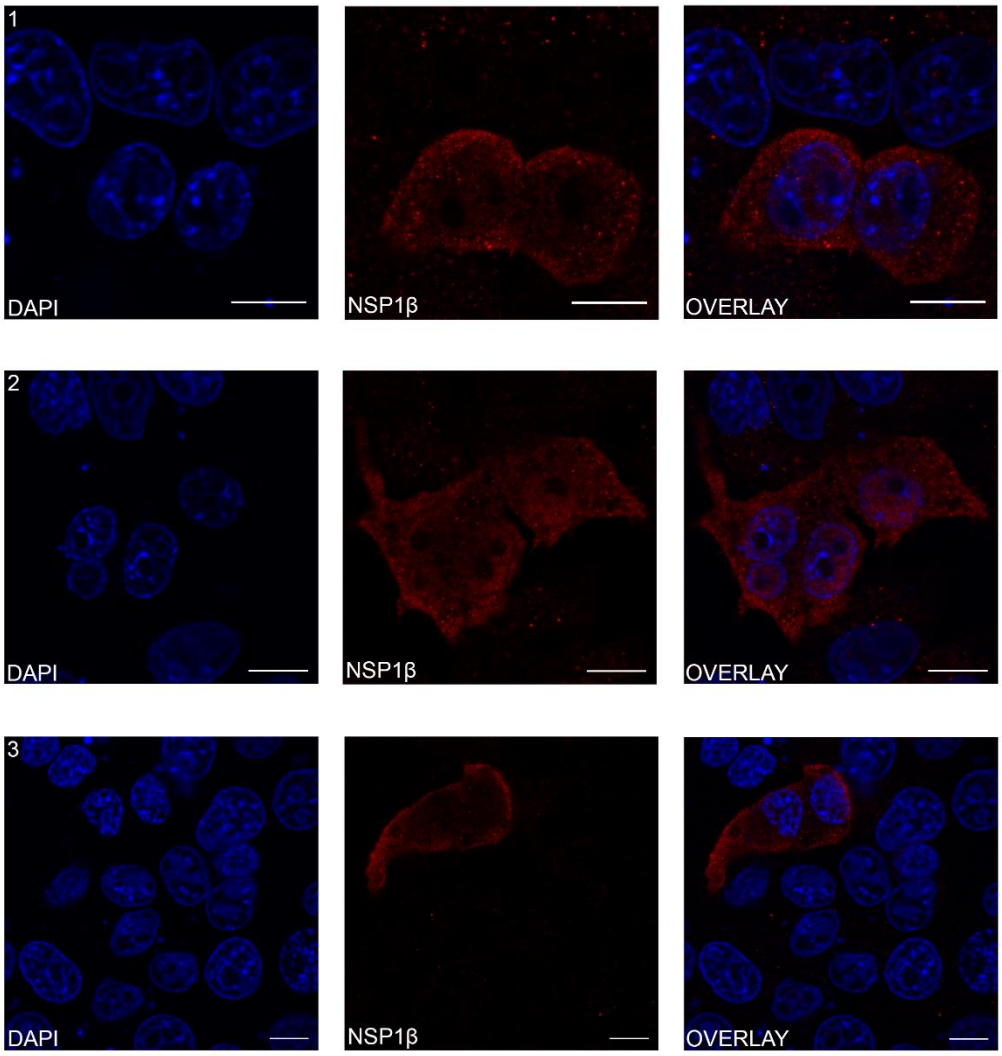

Figure 4.17: PRRSV NSP1β localises to both the cytoplasm and nucleus of Max cells. Max cells seeded on coverslips in 6-well plates were transfected with pcDNA-Myc-NSP1β. At 24 hpt cells were fixed and probed with a rabbit antibody recognising the Myc epitope tag. Probed cells were then stained with DAPI, to visualise nuclei, and imaged by confocal immunofluorescence microscopy. Nuclei are shown in blue and Myc-NSP1β in red. Multiple cells were imaged (**Rows 1-3**). Scale bar = 10 µm.

Myc-NSP1β distribution varied between cells. In some, NSP1β localised exclusively to the cytoplasm of transfected cells (**Figure 4.17, Row 1**). In others, NSP1β was detected in the both the nucleus and cytoplasm (**Figure 4.17, Row 2**).

4.5.5 Proteasome subunit β4

The interaction between PSMB4 and NSP1β was identified in the y-2-h screen (**Section 4.2**). The proteasome is large protein complex that regulates the degradation of proteins within the cell (Tanaka, 2009). PSMB4 is a non-catalytic part of the 20S proteasome complex. Proteasomes are found in the cytoplasm and nucleus (Brooks *et al.*, 2000); the 20s complex is found enriched in nuclear bodies known as clastosomes when proteasomes are stimulated (Lafarga *et al.*, 2002). **Figure 4.18** shows Max cells transfected with pEF-FLAG-PSMB4. FLAG-PSMB4 localised to both the nucleus and cytoplasm (**Figure 4.18**); its distribution between the two compartments varied cell to cell. In some cells, it was observed only in the nucleus (**Figure 4.18, Row 2**), in others it was predominantly nuclear (**Figure 4.18, Row 1**) and some evenly distributed (**Figure 4.18, Row 3**). Within the nucleus of some cells, bright green speckles were observed (**Figure 4.18, Rows 1 and 2**).

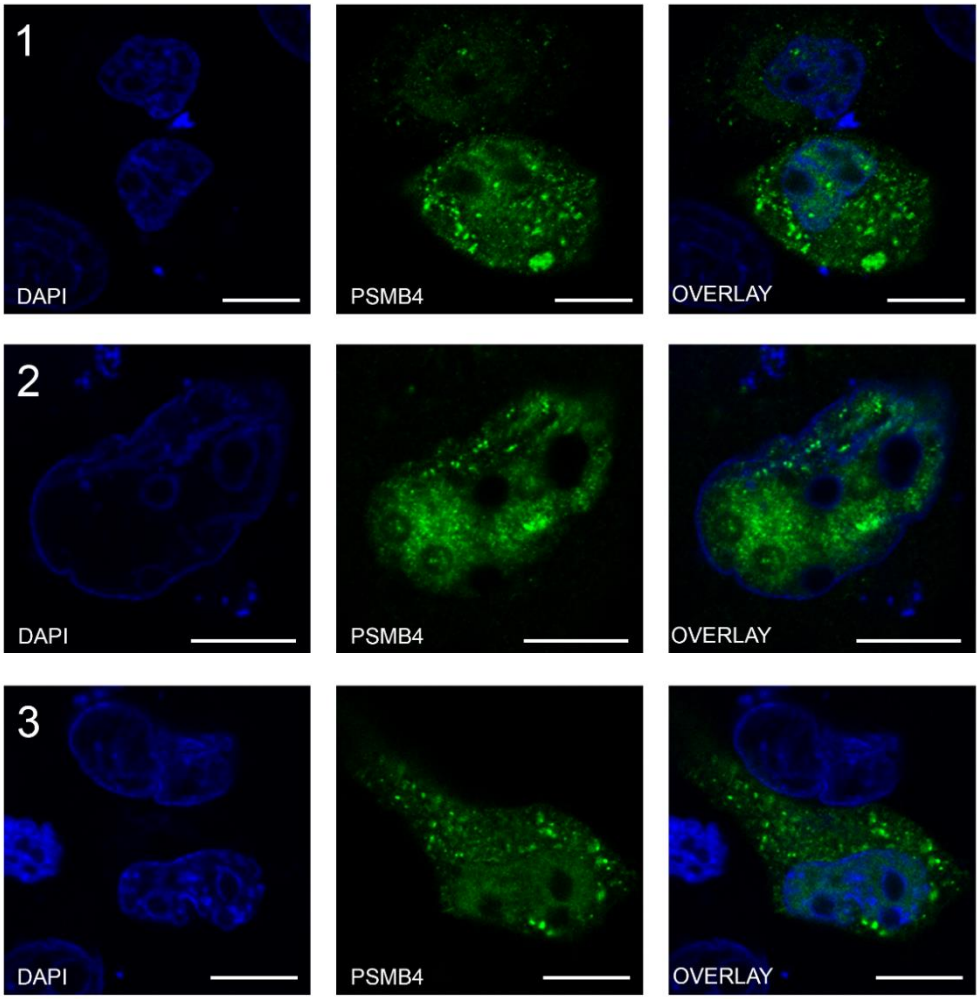

Figure 4.18: PSMB4 localises to both the nucleus and cytoplasm of Max cells. Max cells seeded on coverslips in 6-well plates were transfected with pEF-FLAG-PSMB4. At 24 hpt cells were probed with a mouse antibody recognising the FLAG epitope tag. Probed cells were then stained with DAPI, to visualise nuclei, and imaged by confocal immunofluorescence microscopy. Nuclei are shown blue and FLAG-PSMB4 in green. Multiple cells were imaged (**Rows 1-3**). Scale bar = 10 µm.

To observe PSMB4 localisation in the presence of its interacting partner NSP1β, Max cells were co-transfected with pcDNA-Myc-NSP1β and pEF-FLAG-PSMB4 (**Figure 4.19**); additionally, for Cell 1 (**Figure 4.19, Row 1**) a Z stack series of images consisting of six successive levels of the cell was captured (**Figure 4.20, Rows 1-6**).

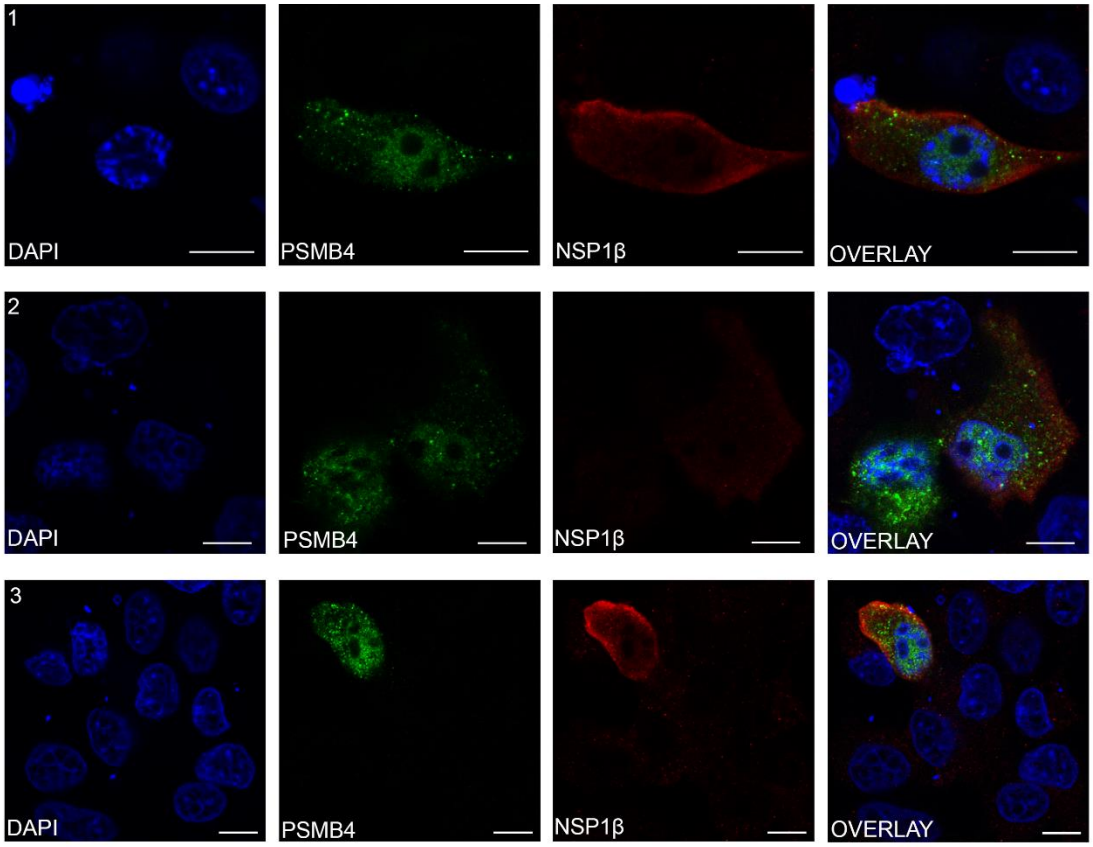

Figure 4.19: NSP1β and PSMB4 potentially co-localise in Max cells. Max cells seeded on coverslips in 6-well plates were co-transfected with pcDNA-Myc-NSP1β and pEF-FLAG-PSMB4. At 24 hpt cells were probed with a rabbit antibody recognising the Myc epitope tag and a mouse antibody recognising the FLAG epitope tag. Probed cells were then stained with DAPI, to visualise nuclei, and imaged by confocal immunofluorescence microscopy. Nuclei are shown in blue, Myc-NSP1β in red and FLAG-PSMB4 in green. Multiple cells were imaged (**Rows 1-3**). Scale bar = 10 µm.

FLAG-PSMB4 localised to both the nucleus and cytoplasm (**Figure 4.19**) in the presence of Myc-NSP1β. In **Figure 4.19, Row 2**, there was even distribution across the nucleus and the cytoplasm; in **Figure 4.19, Row 1 and 3** FLAG-PSMB4 appears to be concentrated in the nucleus. No bright speckles were observed in the nucleus, compared to cells expressing only FLAG-PSMB4. NSP1β was found exclusively in the cytoplasm but concentrated at the periphery of the cell (**Figure 4.19**). This contrasts

to cells solely expressing Myc-NSP1β, where it was evenly distributed throughout the cytoplasm (**Figure 4.19**). Some yellow labelling was observed at the cytoplasmic periphery in **Figure 4.19, Row 1 and 3**, suggesting possible co-localisation between FLAG-PSMB4 and Myc-NSP1β.

A Z stack series of images consisting of 6 successive levels of Cell 1 (**Figure 4.19**) was captured to investigate this further (**Figure 4.20**)**.** Moving through the levels, FLAG-PSMB4 remained distributed across the nucleus and cytoplasm, with more protein present in the nucleus. NSP1β was in the cytoplasm in every level, again more concentrated at the periphery throughout. A small number of yellow spots were observed in every level at the cell periphery, suggesting minimal co-localisation of FLAG-PSMB4 and Myc-NSP1β in the cytoplasm.

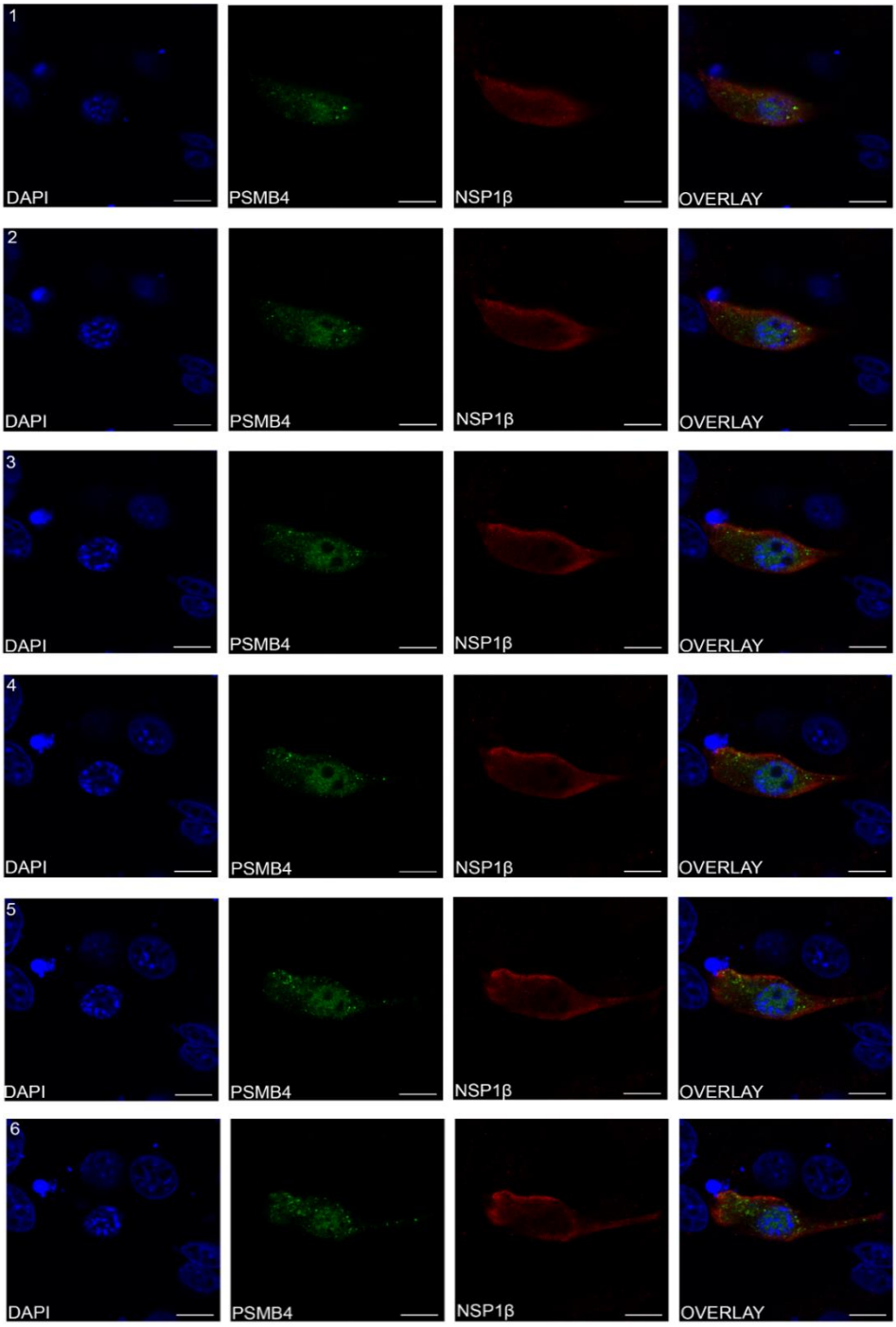

Figure 4.20: Minimal co-localisation of NSP1β and PSMB4 was observed throughout the cell. Max cells seeded on coverslips in 6-well plates were co-transfected with pcDNA-Myc-NSP1β and pEF-FLAG-PSMB4. At 24 hpt cells were probed with a rabbit antibody recognising the Myc epitope tag and a mouse antibody recognising the FLAG epitope tag. Probed cells were then stained with DAPI, to visualise nuclei, and imaged by confocal immunofluorescence microscopy. A Z stack series of images consisting of six successive levels of the cell was captured (**Rows 1-6**). Nuclei are shown in blue, Myc-NSP1β in red and FLAG-PSMB4 in green. Scale bar = 10 µm.

4.5.6 TAB3

TAB3, confirmed as interacting with NSP1β in the y-2-h screen, functions in both the NF-κB pathway (Cheung, Nebreda and Cohen, 2004; Kanayama *et al.*, 2004) and autophagy (Criollo et al., 2011; Takaesu, Kobayashi and Yoshimura, 2012), regulating the activity of both. TAB3 is normally located in the cytoplasm (Criollo et al., 2011). **Figure 4.21** shows Max cells transfected with pEF-FLAG-TAB3.

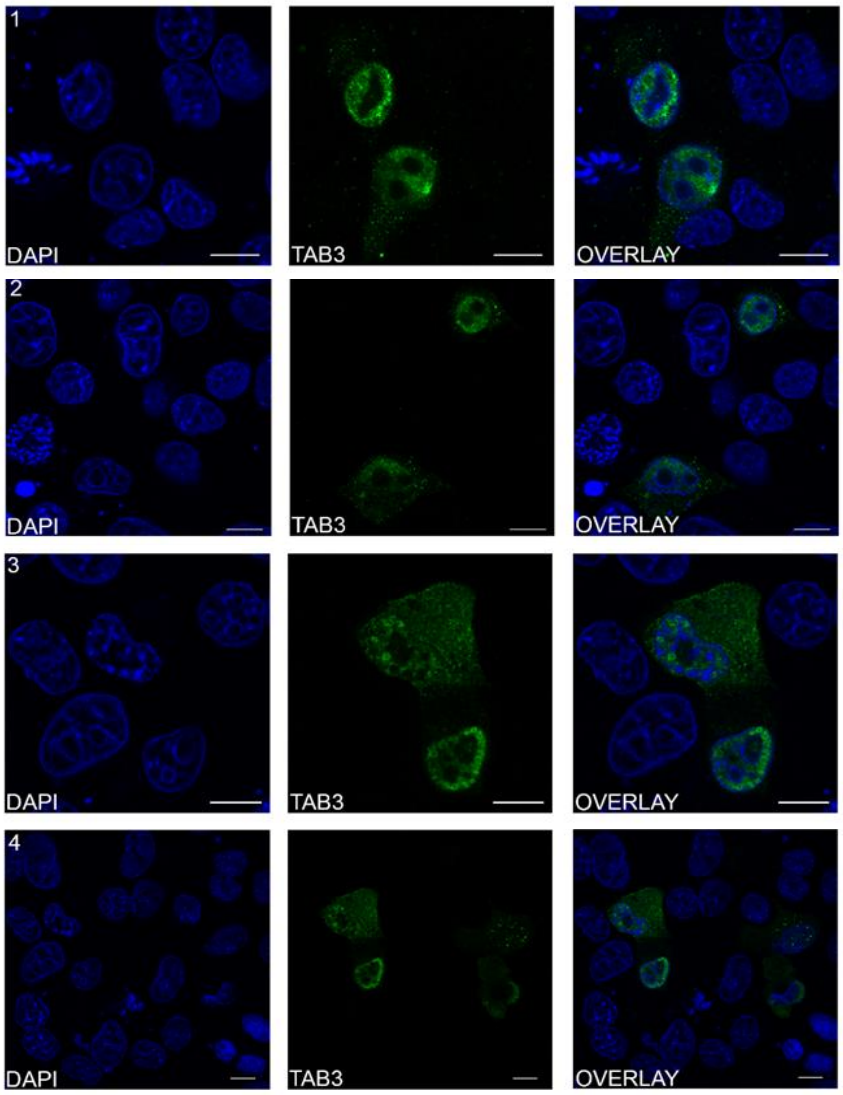

Figure 4.21: TAB3 is concentrated in the nuclei of Max cells. Max cells seeded on coverslips in 6-well plates were transfected with pEF-FLAG-TAB3. At 24 hpt cells were probed with a mouse antibody recognising the FLAG epitope tag. Probed cells were then stained with DAPI, to visualise nuclei, and imaged by confocal immunofluorescence microscopy. Nuclei are shown in blue and FLAG-TAB3 in green. Multiple cells were imaged (**Rows 1-4**). Scale bar = 10 µm.

FLAG-TAB3 localised to both the cytoplasm and nucleus in most cells (**Figure 4.21**), with most protein concentrated in the nucleus. Visible in the nucleus of multiple cells were small, bright rings of protein (**Figure 4.21, Panel 3**); it is unclear what these were.

Max cells were then co-transfected with pcDNA-Myc-NSP1β and pEF-FLAG-TAB3 to analyse co-localisation (**Figure 4.22**). Multiple patterns of localisation were observed for both proteins. In some cells, FLAG-TAB3 was exclusively in the nucleus, and Myc-NSP1β evenly distributed in the cytoplasm; no co-localisation was observed (**Figure 4.22, Row 1**). In other cells, FLAG-TAB3 was observed in both the nucleus and cytoplasm, with more concentrated in the nucleus. Myc-NSP1β was observed in the cytoplasm, again concentrated at the periphery of the cell (**Figure 4.22, panel 2**); no co-localisation was observed. And for other cells, FLAG-TAB3 was almost entirely in the cytoplasm (**Figure 4.22, panel 3**). Myc-NSP1β was observed in both the nucleus and cytoplasm and was evenly distributed throughout the latter. No co-localisation was observed.

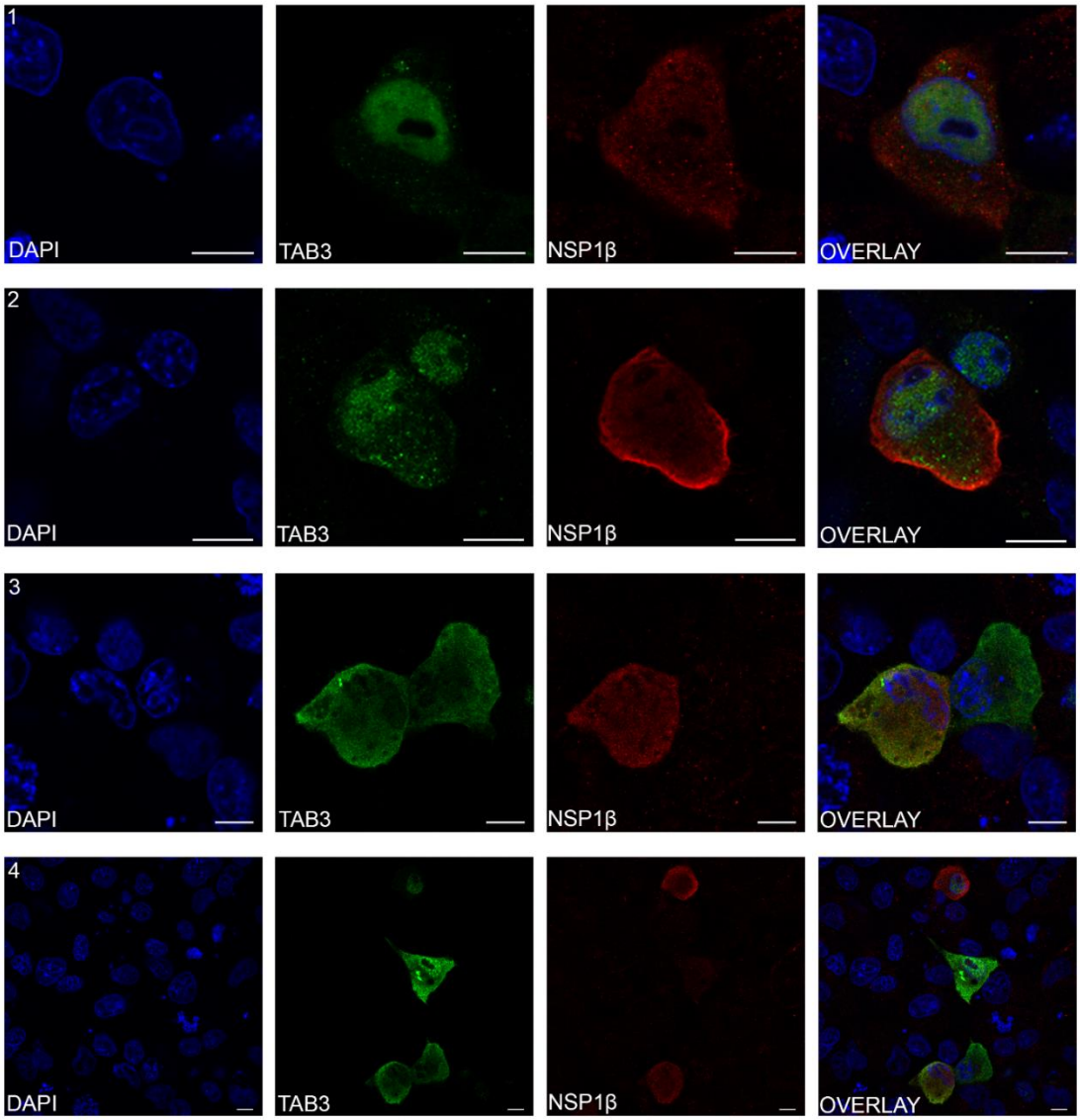

Figure 4.22: TAB3 localisation within Max cells varied in the presence of NSP1β. Max cells seeded on coverslips in 6-well plates were co-transfected with pcDNA-Myc-NSP1β and pEF-FLAG-TAB3. At 24 hpt cells were probed with a rabbit antibody recognising the Myc epitope tag and a mouse antibody recognising the FLAG epitope tag. Probed cells were then stained with DAPI, to visualise nuclei, and imaged by confocal immunofluorescence microscopy. Nuclei are shown in blue, Myc-NSP1β in red and FLAG-TAB3 in green. Multiple cells were imaged (**Rows 1-4**). Scale bar = 10 µm.

Additionally, to further investigate co-localisation, 2 Z stack series of images consisting of six successive levels of 2 co-transfected cells (**Figure 4.23 and 4.24**).

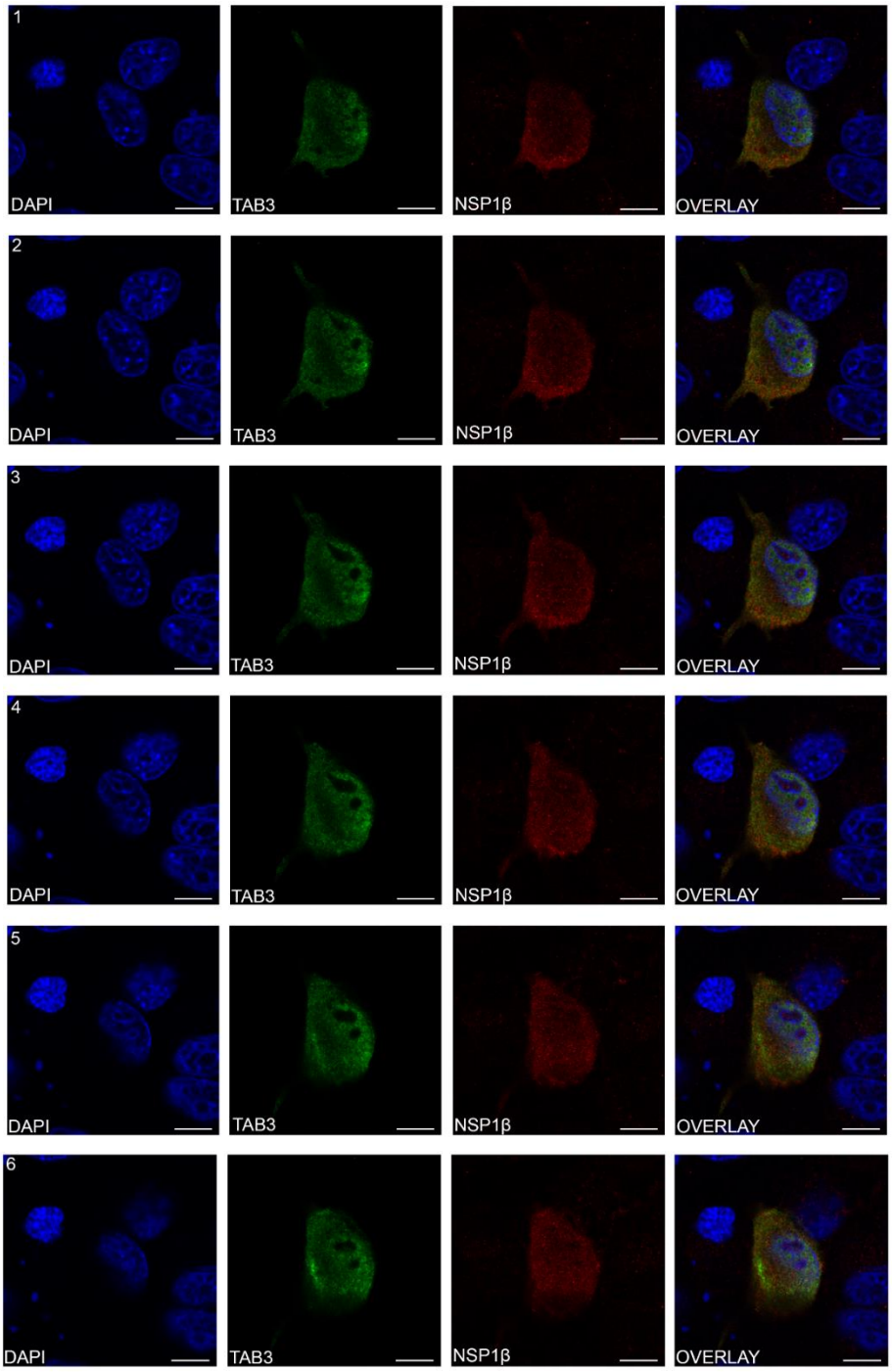

Figure 4.23: TAB3 did not co-localise with NSP1β in Max cells. Max cells seeded on coverslips in 6-well plates were co-transfected with pcDNA-Myc-NSP1β and pEF-FLAG-TAB3. At 24 hpt cells were probed with a rabbit antibody recognising the Myc epitope tag and a mouse antibody recognising the FLAG epitope tag. Probed cells were then stained with DAPI, to visualise nuclei, and imaged by confocal immunofluorescence microscopy. A Z stack series of images consisting of six successive levels of the cell was captured (**Rows 1-6**). Nuclei are shown in blue, Myc-NSP1β in red and FLAG-TAB3 in green. Scale bar = 10 µm.

In **Figure 4.23**, FLAG-TAB3 was observed in both the cytoplasm and nucleus. It was more concentrated in the nucleus, where bright small rings of protein are visible; these became less visible from **panel 4** onwards. Myc-NSP1β was found in both the nucleus and cytoplasm, although more protein was in the cytoplasm, and this was slightly more concentrated at the cell periphery (**Figure 4.23**). Despite both being in the cytoplasm, no co-localisation was observed on any level.

In contrast, in **Figure 4.24**, some co-localisation (yellow in the overlay) was visible at the cell periphery in the top cell. The top cell expressed both FLAG-TAB3 and Myc-NSP1β; it was unclear if the bottom cell expressed Myc-NSP1β or if this was background. FLAG-TAB3 was observed in both the cytoplasm and the nucleus (**Figure 4.24**); again, small bright rings were observed within the nucleus. Myc-NSP1β was observed predominantly in the cytoplasm, with most protein concentrated at the cell periphery. Co-localisation was visible but minimal, as there were a few yellow regions in the overlay image at the cell periphery. This supports the data from the y-2-h screen that NSP1β and TAB3 interact.

It was not possible to say with certainty if TAB3 and NSP1β co-localised, as different cells displayed different patterns of localisation and minimal co-localisation was observed.

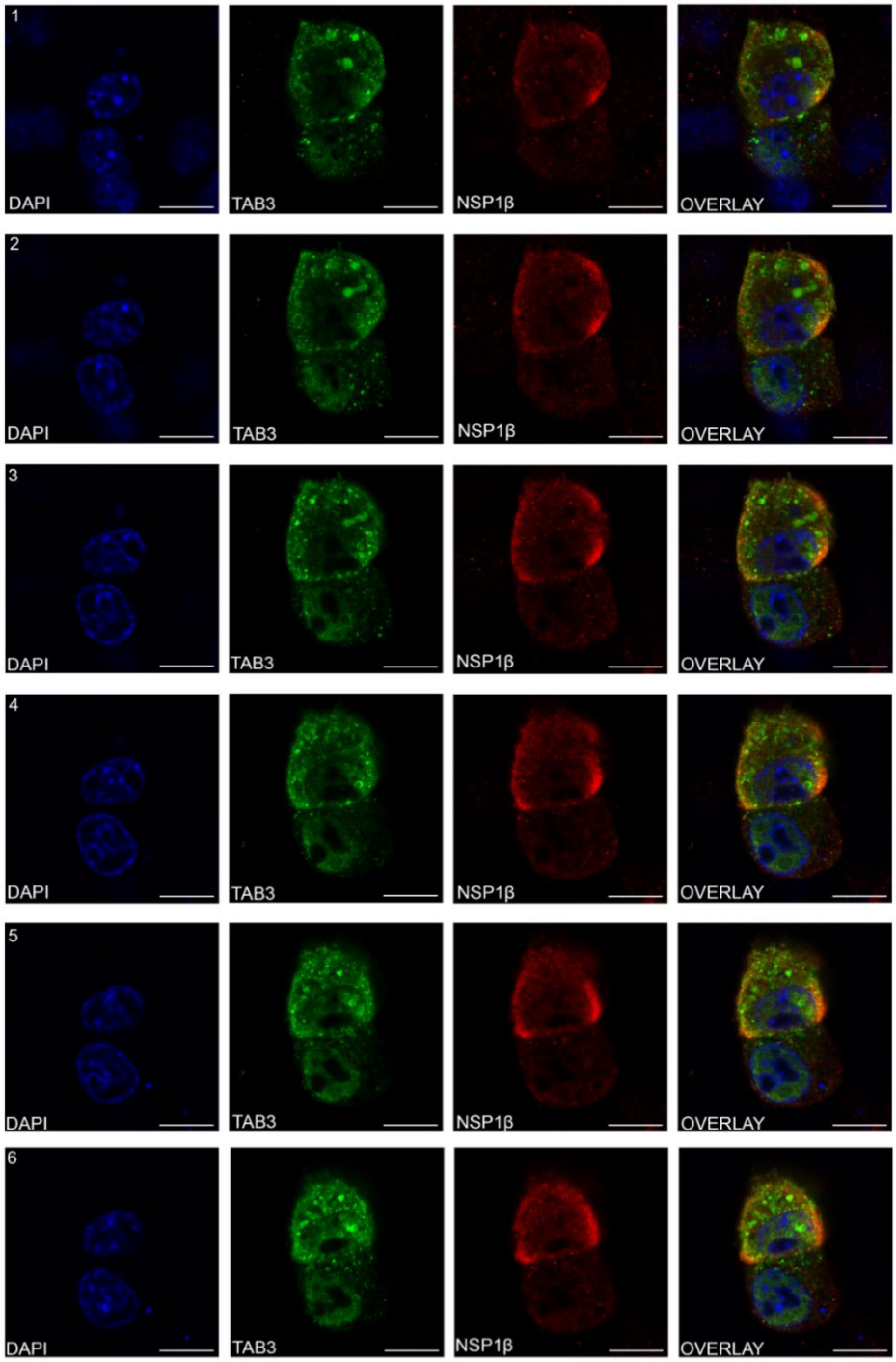

Figure 4.24: TAB3 potentially co-localised with NSP1β in the cytoplasm of Max cells. Max cells seeded on coverslips in 6-well plates were co-transfected with pcDNA-Myc-NSP1β and pEF-FLAG-TAB3. At 24 hpt cells were probed with a rabbit antibody recognising the Myc epitope tag and a mouse antibody recognising the FLAG epitope tag. Probed cells were then stained with DAPI, to visualise nuclei, and imaged by confocal immunofluorescence microscopy. A Z stack series of images consisting of six successive levels of the cell was captured (**Rows 1-6**). Nuclei are shown in blue, Myc-NSP1β in red and FLAG-TAB3 in green. Scale bar = 10 µm.

4.5.7 Nucleoporin GLE1

GLE1 was one of multiple nuclear transport proteins identified in the y-2-h screen of NSP1β (**Section 4.2**) GLE1 is an mRNA export factor, transporting mRNA from the nucleus to the cytoplasm (Murphy and Wente, 1996), possibly through its interaction with NUP155 in the NPC (Rayala *et al.*, 2004). It shuttles between the nucleus and cytoplasm (Kendirgi *et al.*, 2003), modulating adenosine triphosphate (ATP)-dependent DEAD-box RNA helicases (Sharma and Wente, 2020) and translation initiation and termination (Bolger *et al.*, 2008). **Figure 4.25** shows Max cells transfected with pcDNA-FLAG-GLE1.

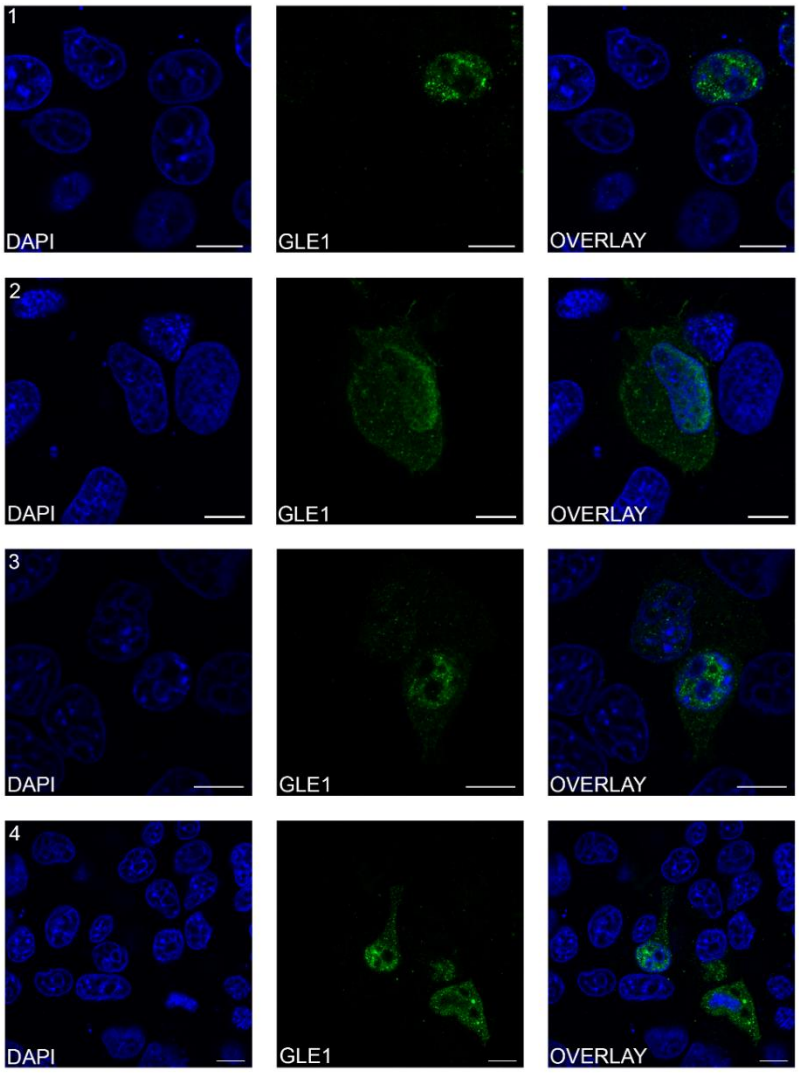

Figure 4.25: GLE1 localises predominantly to the nucleus of Max cells. Max cells seeded on coverslips in 6-well plates were transfected with pEF-FLAG-GLE1. At 24 hpt cells were probed with a mouse antibody recognising the FLAG epitope tag. Probed cells were then stained with DAPI, to visualise nuclei, and imaged by confocal immunofluorescence microscopy. Nuclei are shown in blue and FLAG-GLE1 in green. Multiple cells were imaged (**Rows 1-4**). Scale bar = 10 µm.

FLAG-GLE1 was detected in both the nucleus and cytoplasm of transfected cells, with more protein found in the nucleus (**Figure 4.25**). This matches the cellular distribution previously seen in confocal immunofluorescence images by Sharma and colleagues (Sharma and Wente, 2020). In one cell (**Figure 4.25, Row 4**), FLAG-GLE1 was exclusively in the cytoplasm.

Cells were then co-transfected with pEF-FLAG-GLE1 and pcDNA-Myc-NSP1β to look for co-localisation (**Figure 4.26**).

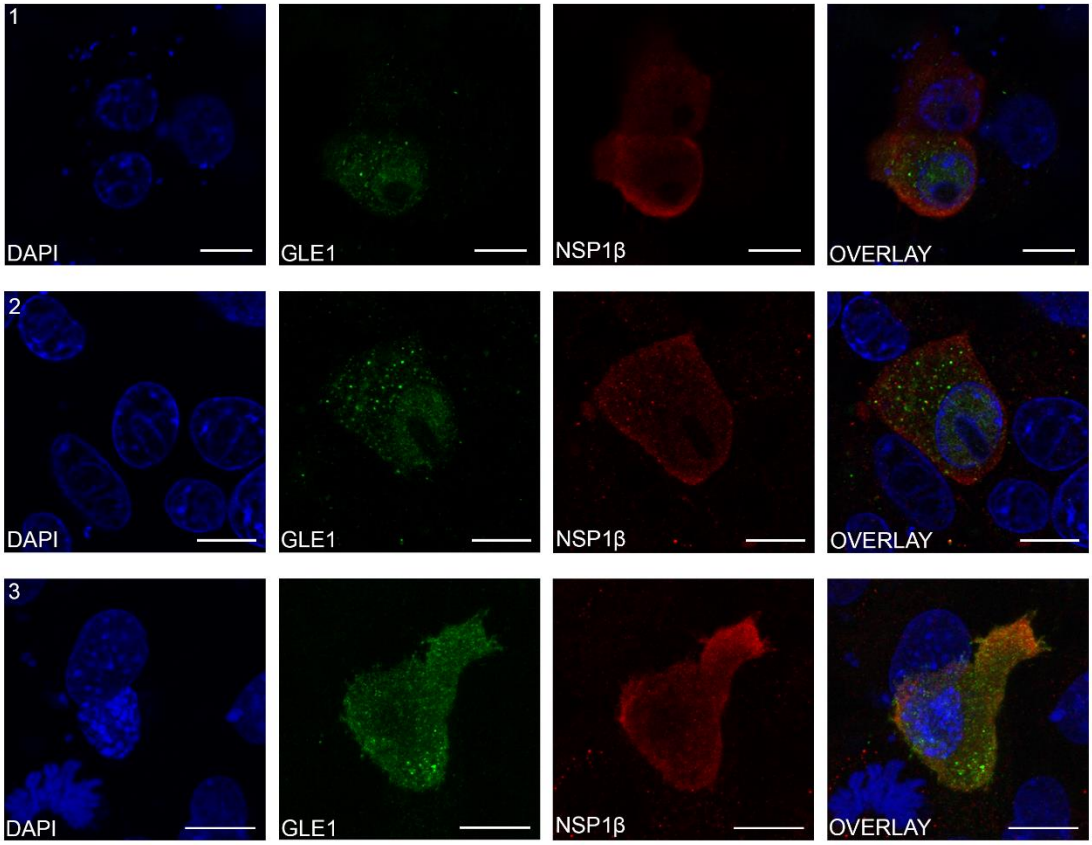

Figure 4.26: NSP1β and GLE1 do not co-localise in Max cells. Max cells seeded on coverslips in 6-well plates were co-transfected with pcDNA-Myc-NSP1β and pEF-FLAG-GLE1. At 24 hpt cells were probed with a rabbit antibody recognising the Myc epitope tag and a mouse antibody recognising the FLAG epitope tag. Probed cells were then stained with DAPI, to visualise nuclei, and imaged by confocal immunofluorescence microscopy. Nuclei are shown in blue, FLAG-GLE1 is green and Myc-NSP1β is red. Multiple cells were imaged (**Rows 1-3**). Scale bar = 10 µm.

In cells co-expressing Myc-NSP1β, FLAG-GLE1 localised to both the nucleus and cytoplasm (**Figure 4.26**). In one cell, (**Figure 4.26, row 3**), minimal FLAG-GLE1 was found in the nucleus. However, the nucleus of this cell did not look like a normal healthy nucleus as it was globular in appearance rather than defined. NSP1β localised exclusively to the cytoplasm, concentrating at the periphery of the cell (**Figure 4.26**). No co-localisation was observed.

To further investigate protein cellular distribution, a Z stack series of images consisting of six successive levels of a co-transfected cell was obtained (**Figure 4.27**).

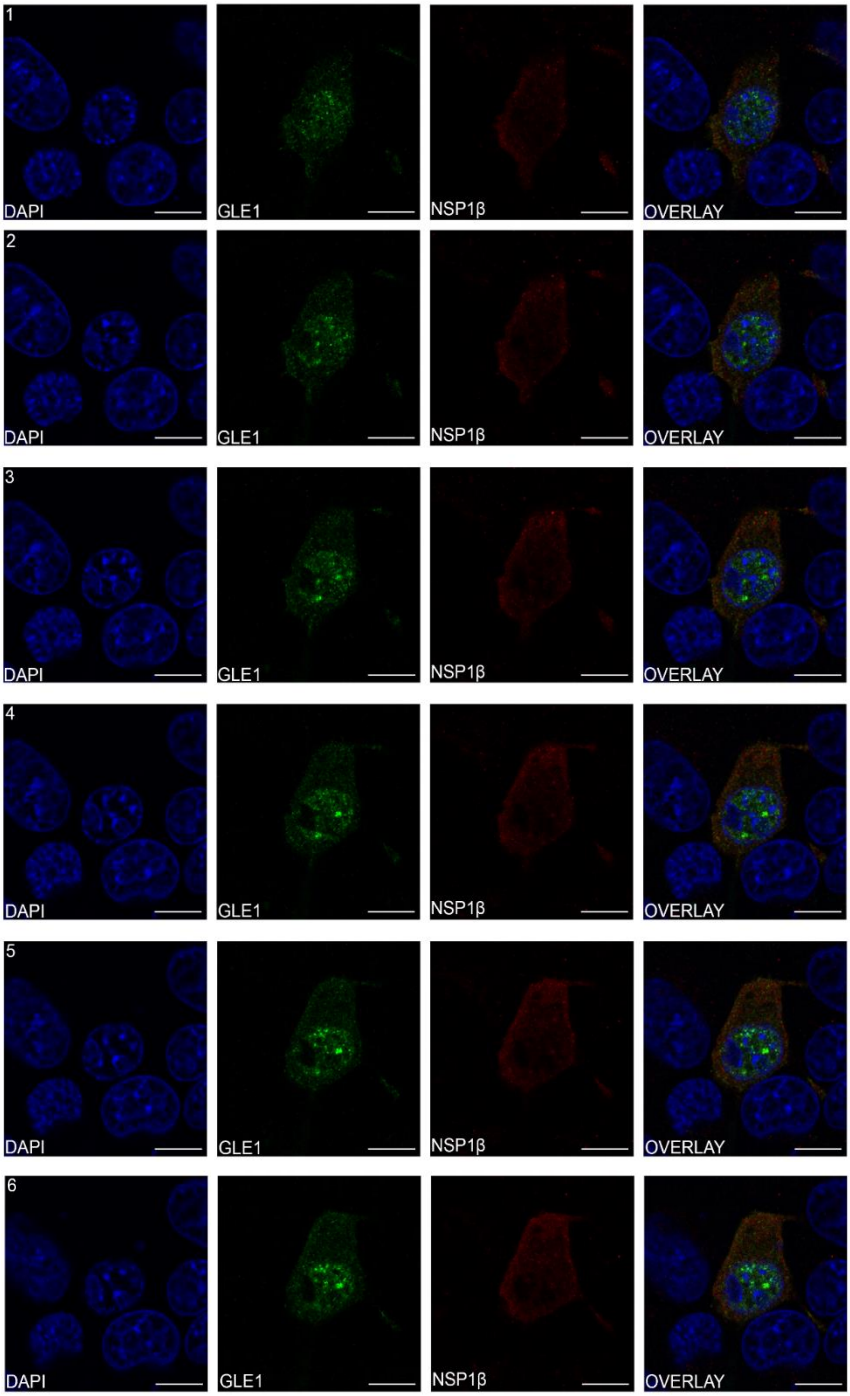

Figure 4.27: No co-localisation of NSP1β and GLE1 was observed throughout the cell. Max cells seeded on coverslips in 6-well plates were co-transfected with pcDNA-Myc-NSP1β and pEF-FLAG-GLE1. At 24 hpt cells were probed with a rabbit antibody recognising the Myc epitope tag and a mouse antibody recognising the FLAG epitope tag. Probed cells were then stained with DAPI, to visualise nuclei, and imaged by confocal immunofluorescence microscopy. A Z stack series of images consisting of six successive levels of the cell was captured (**Rows 1-6**). Nuclei are shown in blue, FLAG-GLE1 is green and Myc-NSP1β is red. Scale bar = 10 µm.

FLAG-GLE1 was located primarily in the nucleus through the cell, concentrated at puncta throughout the nucleus (**Figure 4.27**). Myc-NSP1β again exclusively remained in the cytoplasm and no co-localisation was observed. This does not match the results predicted based on the observations in the y-2-h screen.

4.5.8 EPAS-1

EPAS-1, also known as hypoxia inducible factor (HIF) 2α (HIF2α), is a hypoxia induced transcription factor (Tian, McKnight and Russell, 1997) identified in the NSP1β y-2-h screen (**Section 4.2**). HIFs regulate expression of genes involved in cell proliferation, angiogenesis, apoptosis, and metabolism (Koh and Powis, 2012). Under normal physiological conditions within the cell, EPAS-1 is degraded; whereas, in mild hypoxic conditions, it becomes activated and stable, translocating into the nucleus (Tian, McKnight and Russell, 1997; Koh and Powis, 2012). **Figure 4.28** shows Max cells transfected with pEF-FLAG-EPAS-1.

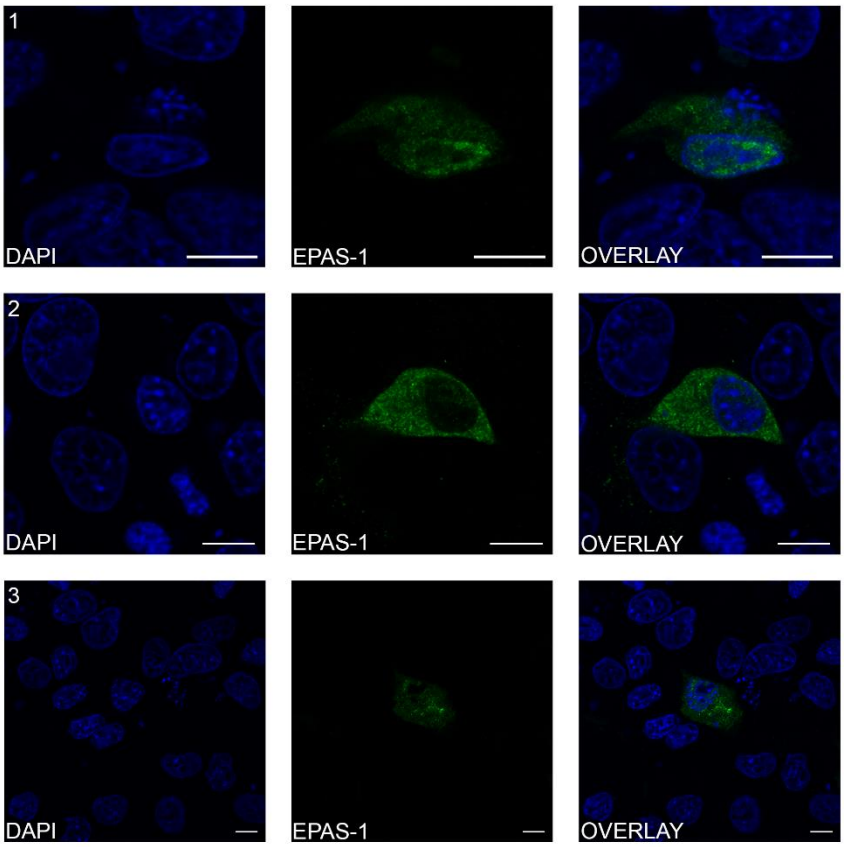

Figure 4.28: EPAS-1 cellular localisation varied between Max cells. Max cells seeded on coverslips in 6-well plates were transfected with pEF-FLAG-EPAS-1. At 24 hpt cells were probed with a mouse antibody recognising the FLAG epitope tag. Probed cells were then stained with DAPI, to visualise nuclei, and imaged by confocal immunofluorescence microscopy. Nuclei are shown in blue and FLAG-EPAS-1 in green. Multiple cells were imaged (**Rows 1-3**). Scale bar = 10 μm.

In singly transfected cells, FLAG-EPAS-1 was observed in both the nucleus and the cytoplasm (**Figure 4.28, Row 1 and 3**). FLAG-EPAS-1 was predominantly in the nucleus in one cell (**Figure 4.28, Row 1**), but evenly distributed in another (**Figure 4.28, Row**

3). These cells match the expectation for EPAS-1 localisation. However, high levels of EPAS-1 were seen exclusively in the cytoplasm of one cell (**Figure 4.28, Row 2**). The high levels of EPAS-1 detected in the cytoplasm in this does not match expectations unless the cell has become hypoxic and protein is unable to enter the nucleus.

To analyse EPAS-1 localisation in the presence of NSP1β, cells were co-transfected with pEF-FLAG-EPAS-1 and pcDNA-Myc-NSP1β (**Figure 4.29**).

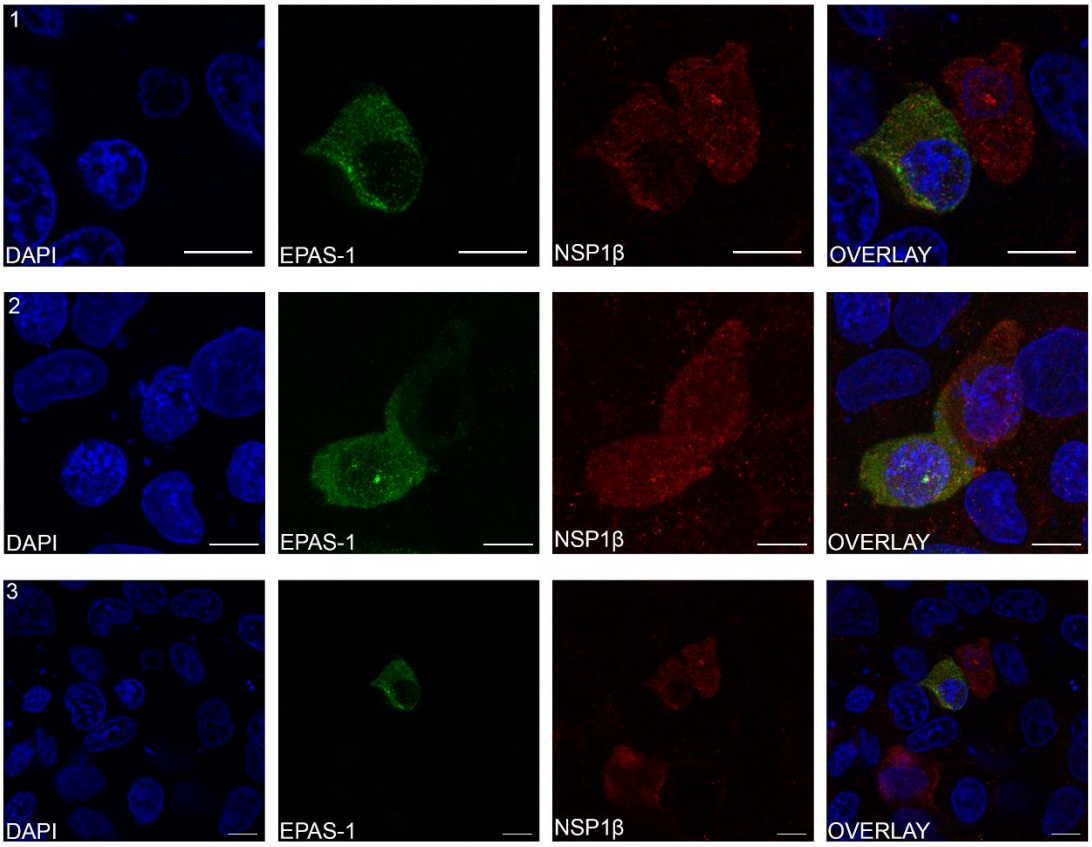

Figure 4.29: EPAS-1 and NSP1β do not co-localise in Max cells. Max cells seeded on coverslips in 6-well plates were co-transfected with pcDNA-Myc-NSP1β and pEF-FLAG-EPAS-1. At 24 hpt cells were probed with a rabbit antibody recognising the Myc epitope tag and a mouse antibody recognising the FLAG epitope tag. Probed cells were then stained with DAPI, to visualise nuclei, and imaged by confocal immunofluorescence microscopy. Multiple cells were imaged (**Rows 1-3**). Nuclei are shown in blue, FLAG-EPAS-1 is green and Myc-NSP1β is red. Scale bar = 10 µm.

In cells expressing FLAG-EPAS-1 and Myc-NSP1β, FLAG-EPAS-1 was observed almost exclusively in the cytoplasm, with minimal protein seen in the nucleus (**Figure 4.29**). This is different to when FLAG-EPAS-1 is expressed alone (**Figure 4.29**). Myc-NSP1β

was only present in the cytoplasm of most cells (**Figure 4.29**) but was observed in the nucleus in (**Figure 4.29, Row 2**). No co-localisation was observed.

To further investigate EPAS-1 cellular distribution in the presence of NSP1β, a Z stack series of images consisting of six successive levels of a co-transfected cell was obtained (**Figure 4.30*,* Rows 1-6**). FLAG-EPAS-1 remained exclusively in the cytoplasm in the cell, as did NSP1β; but again, no co-localisation was observed. These results do not support the y-2-h data.

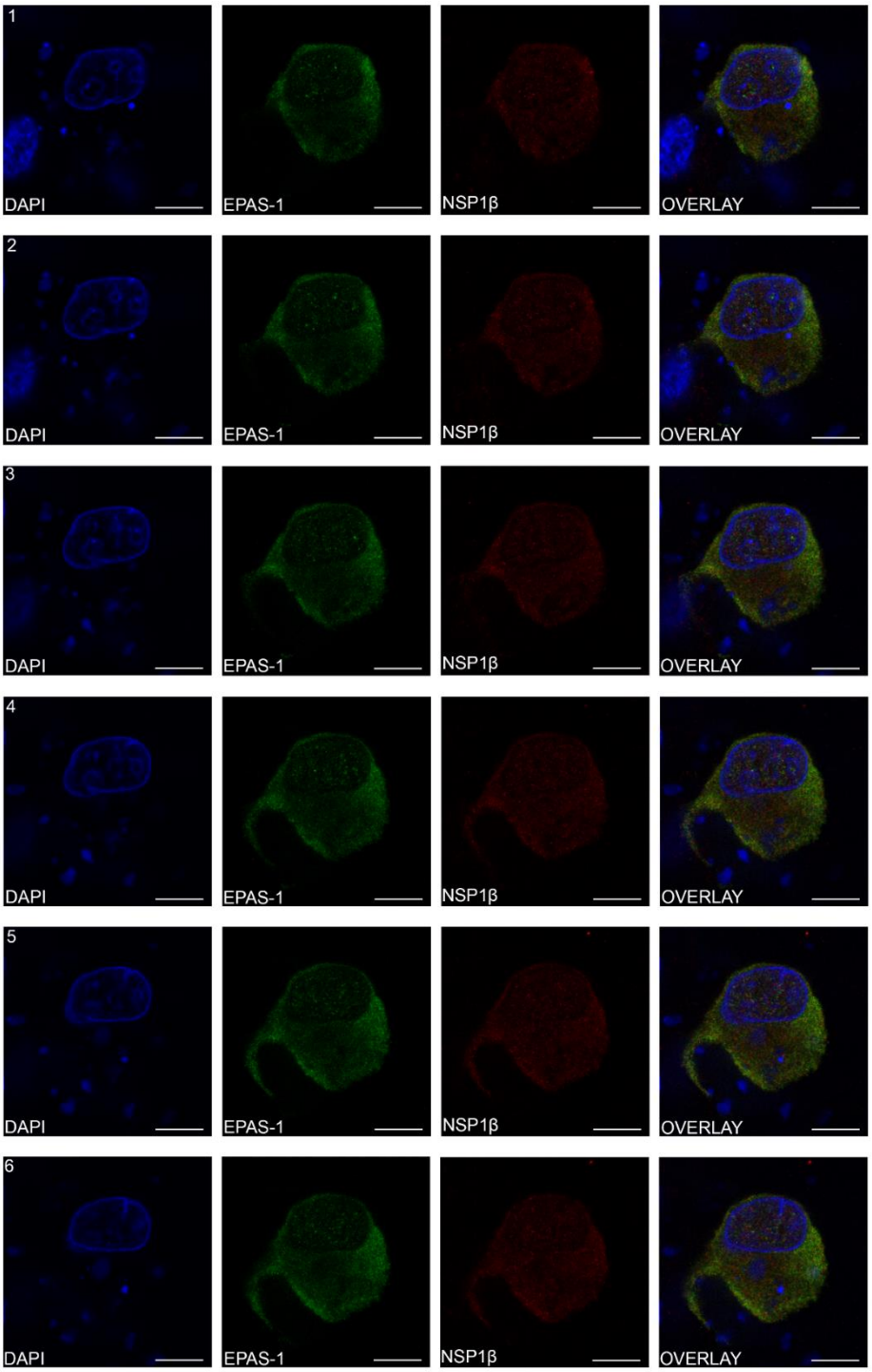

Figure 4.30: NSP1ɓ and EPAS-1 do not co-localise throughout the cell. Max cells seeded on coverslips in 6-well plates were co-transfected with pcDNA-Myc-NSP1β and pEF-FLAG-EPAS-1. At 24 hpt cells were probed with a rabbit antibody recognising the Myc epitope tag and a mouse antibody recognising the FLAG epitope tag. Probed cells were then stained with DAPI, to visualise nuclei, and imaged by confocal immunofluorescence microscopy. A Z stack series of images consisting of six successive levels of the cell was captured (**Rows 1-6**). Nuclei are shown in blue, FLAG-EPAS-1 is green and Myc-NSP1β is red. Scale bar = 10 µm.

4.5.9 Beclin-1

The NSP1β γ-2-h screen identified beclin-1 as an interacting protein (**Section 4.2**). Beclin-1 is involved in the regulation of autophagy and apoptosis (Wirawan *et al.*, 2010; Kang *et al.*, 2011). It is required for autophagosome formation, interacting with multiple proteins to induce autophagy (He and Levine, 2010; Kang *et al.*, 2011). **Figure 4.31** shows Max cells transfected with pEF-FLAG-beclin-1.

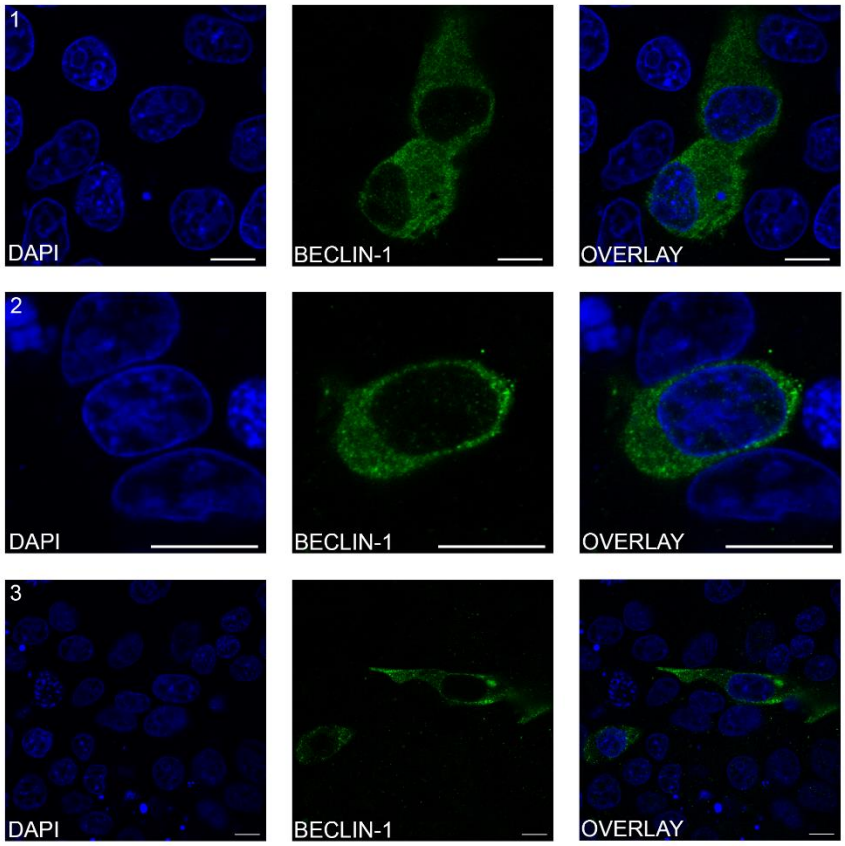

Figure 4.31: Beclin-1 localises exclusively to the cytoplasm of Max cells. Max cells seeded on coverslips in 6-well plates were transfected with pEF-FLAG-beclin-1. At 24 hpt cells were probed with a mouse antibody recognising the FLAG epitope tag. Probed cells were then stained with DAPI, to visualise nuclei, and imaged by confocal immunofluorescence microscopy. Multiple cells were imaged (**Rows 1-3**). Nuclei are shown in blue, and FLAG-beclin-1 in green. Scale bar = 10 µm.

FLAG-beclin-1 was observed exclusively in the cytoplasm of all cells observed (**Figure 4.31**). It was evenly distributed throughout, occupying the entire cytoplasm up to the nuclear membrane. This matches the previously observed cellular distribution of the full-length protein (Pattingre *et al.*, 2005).

To observe beclin-1 localisation in the presence of NSP1β, Max cells were co-transfected with pEF-FLAG-beclin-1 and pcDNA-NSP1β (**Figure 4.32**).

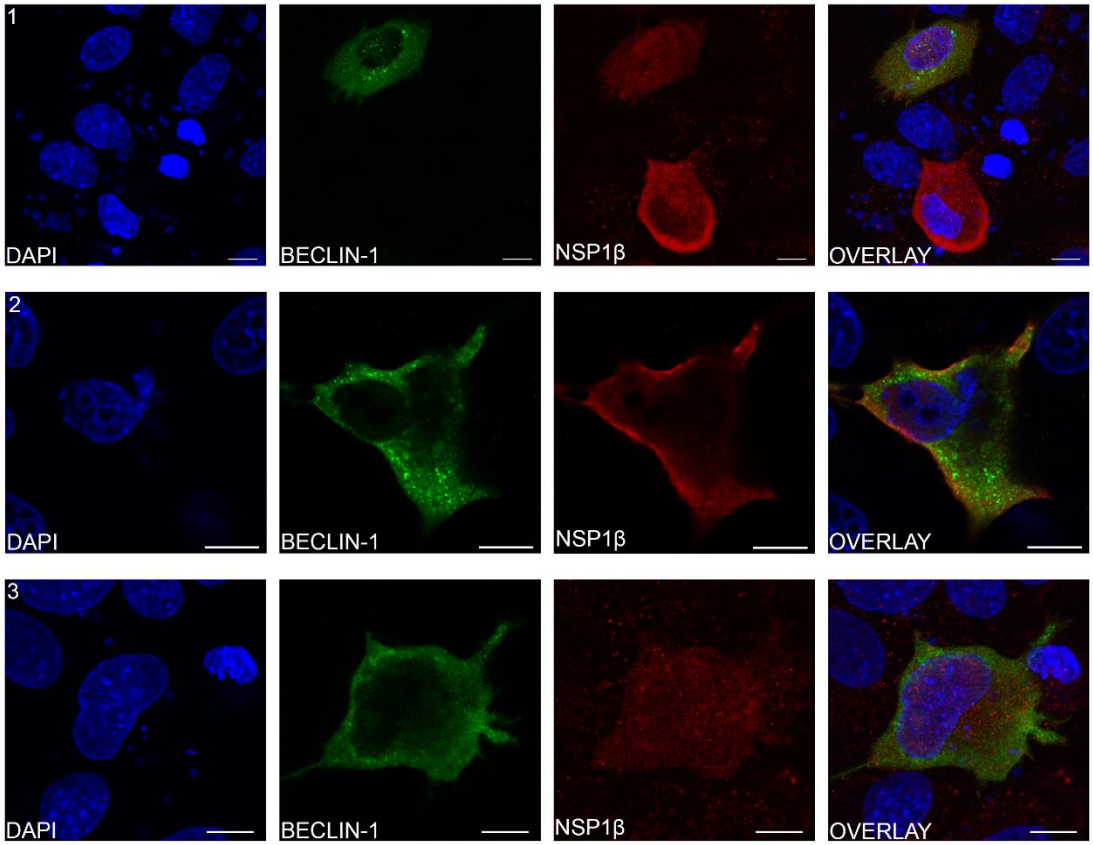

Figure 4.32: NSP1β and beclin-1 do not co-localise in Max cells. Max cells seeded on coverslips in 6-well plates were co-transfected with pcDNA-Myc-NSP1β and pEF-FLAG-beclin-1. At 24 hpt cells were probed with a rabbit antibody recognising the Myc epitope tag and a mouse antibody recognising the FLAG epitope tag. Probed cells were then stained with DAPI, to visualise nuclei, and imaged by confocal immunofluorescence microscopy. Multiple cells were imaged (**Rows 1-3**). Nuclei are shown in blue, FLAG-beclin-1 in green and Myc-NSP1β in red. Scale bar = 10 µm.

FLAG-beclin-1 was observed exclusively in the cytoplasm in the presence of Myc-NSP1β (**Figure 4.32**). Myc-NSP1β distribution was variable: it was evenly distributed between the nucelus and cytoplasm in some cells (**Figure 4.32, Row 1 and 3**) and exclusively cytoplasm and concentrated at the periphery in others (**Figure 4.32, Row 2**). No co-localisation was observed.

In (**Figure 4.32, row 3**) beclin-1 does not occupy the cytoplasm up to the nuclear membrane like previously observed in cells expressing only FLAG-beclin-1 (**Figure**

4.31). Myc-NSP1β instead occupied the space surrounding the nucleus and FLAG-beclin-1 was restricted to the cell periphery. To investigate this further, a Z stack series of images consisting of six successive levels of a co-transfected cell was obtained (**Figure 4.33, rows 1-6**).

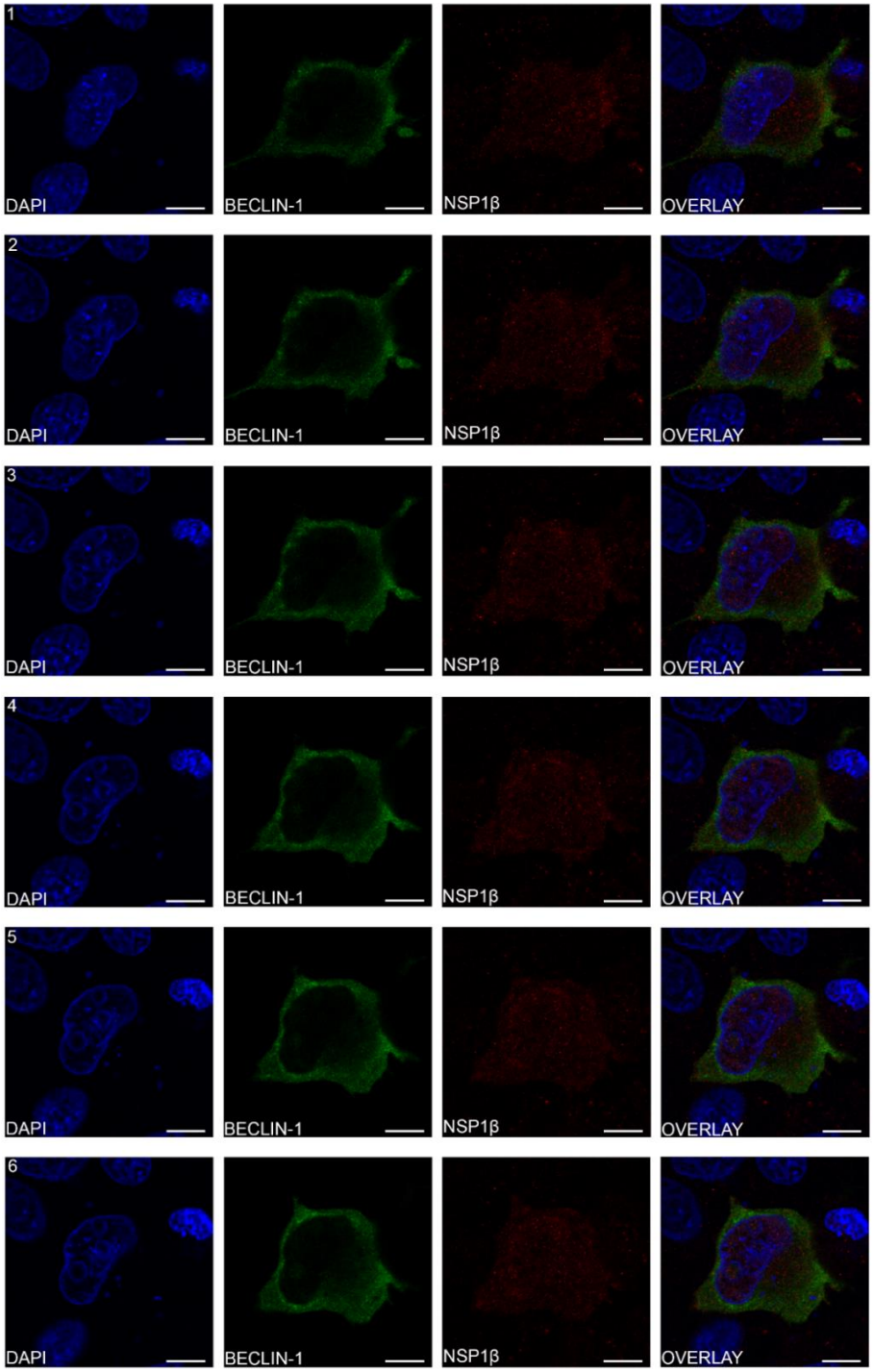

Figure 4.33: Beclin-1 distribution changes in the presence of NSP1β in Max cells. Max cells seeded on coverslips in 6-well plates were co-transfected with pcDNA-Myc-NSP1β and pEF-FLAG-beclin-1. At 24 hpt cells were probed with a rabbit antibody recognising the Myc epitope tag and a mouse antibody recognising the FLAG epitope tag. Probed cells were then stained with DAPI, to visualise nuclei, and imaged by confocal immunofluorescence microscopy. A Z stack series of images consisting of six successive levels of the cell was captured (**Rows 1-6**). Nuclei are shown in blue, FLAG-beclin-1 is green and Myc-NSP1β is red. Scale bar = 10 µm.

Throughout the cell, FLAG-beclin-1 remained in the cytoplasm (**Figure 4.33**) and was concentrated at the periphery. Myc-NSP1β was also in the cytoplasm, occupying the centre of the cell adjacent to the nucleus. FLAG-beclin-1 and Myc-NSP1β did not co-localise, however beclin-1 appeared unable to enter the centre of the cell, as previously seen in cells expressing FLAG-beclin-1 alone (**Figure 4.31**). This suggests Myc-NSP1β had altered the beclin-1 distribution.

4.6 Characterisation of interactions summary

A summary of the results from y-2-h using 3-AT (**Section 4.3**) and confocal immunofluorescence microscopy (**Section 4.5**) for selected confirmed interacting proteins is shown below (**Table 4.7**); false positives are not shown. The porcine protein, whether it interacts with NSP1α or NSP1β, the highest concentration of 3-AT yeast co-expressing this protein grew on, and the protein localisation results are shown.

Table 4.7: Summary of results from y-2-h with 3-AT and confocal immunofluorescence microscopy for confirmed interacting proteins.

NSP1 α/β	PAM protein	3-AT results (mM)	Subcellular localisation expected	Subcellular localisation observed	Co-localisation with NSP1α/β	Change in localisation in the presence of NSP1α/β
α*	PIAS1	60	/	/	/	/
α	PIAS2	10	Nucleus	Nucleus	X	X
α	DNAJA3	0	/	/	/	/
β	Cullin-9	0	/	/	/	/
β	CPSF4	2.5	/	/	/	/
β	PSMB4	/	Cytoplasm Nucleus	Cytoplasm Nucleus	Cell periphery	Loss of nuclear speckles
β	TAB3	2.5	Cytoplasm	Cytoplasm Nucleus	Cell periphery	X
β	GLE1	/	Cytoplasm Nucleus	Cytoplasm Nucleus	X	X
β	EPAS-1	/	Nucleus	Cytoplasm Nucleus	X	Exclusively cytoplasmic
β	Beclin-1	/	Cytoplasm	Cytoplasm	X	Excluded from cytoplasm surrounding nucleus

Key: / – untested; X – no; * – NSP1α from both 215-06 and SU1-Bel.

4.7 Discussion

Interactions identified in the y-2-h screen had to be validated and characterised using a combination of methods. Y-2-h with additional controls was used to check the PAM proteins identified as potential interactors did not self-activate the y-2-h system. Yeast were transformed to express the selected protein in combination with either empty pGBKT7 plasmid, p53 and NSP1α or NSP1β and plated on quadruple dropout SD agar containing X-α-Gal. Genuine interactions, and therefore proteins that did not self-activate the y-2-h system, were identified as those where the yeast only grew when expressing the prey protein with NSP1α or NSP1β. Retesting interactions using the y-2-h system identified 3 putative interactions from the NSP1α screen (**Figure 4.3**) and 28 from the NSP1β screen (**Figure 4.4**).

From the interactions confirmed with NSP1α, two were involved in the immune response – PIAS1 and PIAS2 – and the other in protein folding and the regulation of apoptosis, DNAJA3. PIAS1 and PIAS2 are related proteins, with more than 40% sequence identity, sharing several domains and motifs (Shuai & Liu, 2005); so it is unsurprising both of them were able to interact with NSP1α. Testing the strength of the interaction of NSP1α with PIAS1 used the bait plasmid pGBKT7-NSP1α/β, whereas with PIAS2 the bait plasmid pGBKT7-NSP1α. This difference could account for the difference observed in interaction strengths, as NSP1β could be involved in the interaction. The interaction between PIAS1 and an unspecified PRRSV strain NSP1α has been shown previously in unpublished work (Song *et al.*, 2010); further supporting that these interactions are genuine. Given the roles of PIAS1 and PIAS2 in the regulation of transcription factors involved in the immune response (Shuai and Liu, 2005), including STATs and NF-κB (Liu *et al.*, 2005; Shuai, 2006), it is logical that these would be targeted by PRRSV to enhance viral replication. DNAJA3, also known as tumorous imaginal disc 1 (TID-1), is a member of the DNAJ/HSP40 family of proteins, functioning both in the mitochondria and cytoplasm (Ng, Baird and Screaton, 2014), with roles in protein folding and degradation (Duncan *et al.*, 2015). DNAJA3/TID-1 functions as a co-chaperone when complexed with HSP70 to regulate NF-κB activity (Kumada *et al.*, 2019), and can interact with the IFN-γ receptor subunit 2 to modulate downstream transcriptional activity (Sarkar *et al.*, 2001). Additionally,

through its DNAJ domain, it complexes with p53, translocating it to the cytoplasm to initiate apoptosis (Ahn *et al.*, 2010; Trinh, Elwi and Kim, 2010). Given the multiple functions of DNAJA3/TID-1, and how manipulating or hijacking these pathways might benefit PRRSV, it seems reasonable for NSP1α to bind this protein.

The interactions confirmed from the NSP1β screen (**Figure 4.4**) included TAB3, STAT3, beclin-1 and GLE1. These proteins fell into multiple functional categories including the immune response, nuclear transport, the proteasome and transcription and translation. It is logical proteins with these functions were identified as PRRSV NSP1α and NSP1β inhibit the immune response in multiple ways (Wang *et al.*, 2013; Jing *et al.*, 2016), are nucleocytoplasmic (Beura *et al.*, 2010; Chen *et al.*, 2016), cause the degradation of cellular proteins (Du *et al.*, 2016) and are involved in viral replication (Kroese *et al.*, 2008; Y. Li, Treffers, *et al.*, 2014). No previously identified interactions were confirmed in the y-2-h retesting of NSP1β interactions as none were retested, but the published interaction with PCBP1 (Beura *et al.*, 2011) was identified in the NSP1β y-2-h screen (**Table 9.2**).

The retesting identified multiple false positives (**Table 4.3, Table 4.4**), including ANAPC10, PAK2, sialoadhesin precursor and cathepsin D (in the NSP1α screen only). ANAPC10 has appeared in previous y-2-h screens conducted by the Molecular Virology Group (The Pirbright Institute) as a false positive (unpublished data), so this result was expected. Cathepsin D was identified as a genuine interaction in the NSP1β screen (**Figure 4.4**), but as false positive in the NSP1α screen (**Figure 4.3**). It is unclear why this occurred, but the clone identified in the NSP1β screen contained a shorter region of the protein, amino acids 263-346 (**Table 3.3**), than the clone in the NSP1α screen, amino acids 81-395 (**Table 3.2**). The two related proteins PAK2 and PAK1, were identified in the NSP1α and NSP1β, respectively, but PAK2 was a false positive and PAK1 was genuine. Despite being related and structurally similar, there are sequence differences and have non-redundant functions, which could explain the different y-2-h results (Grebeňová *et al.*, 2019). Sialoadhesin, the precursor of which was identified in the NSP1α screen, is an entry receptor used by PRRSV (van Gorp *et al.*, 2008). It was therefore surprising this interaction was a false positive, as I proposed PRRSV might target this protein to alter its expression at the cell surface to

enhance infection. Additionally, the ubiquitin ligase, MARCH7, and ubiquitin itself were false positives (**Figure 4.3**); suggesting these proteins are not how PRRSV alters the ubiquitome of the cell (H. Zhang *et al.*, 2018). However, in the NSP1α y-2-h screen the bait plasmid pGBKT7-NSP1α/β was used, not pGBKT7-NSP1α like in the y-2-h retesting. Therefore, it is possible NSP1β was also involved in the identified interactions in NSP1α screen, either bridging the interaction between NSP1α and the PAM protein (which don't interact) or facilitating it. PRRSV NSP1α and NSP1β have not been shown to interact previously (Nan *et al.*, 2018; Song *et al.*, 2018). The y-2-h retesting experiments would therefore need to be repeated using the pGBKT7-NSP1α/β bait plasmid to investigate this.

To investigate the strength of certain interactions, and double check some false positives, y-2-h using plates containing 3-AT was performed. 3-AT is a competitive inhibitor of the *HIS3* gene product, so yeast will only grow in the presence of 3-AT if the level of His is sufficient to overcome the inhibitory effect of 3-AT, which is dependent on the strength of the interaction. Yeast transformed with either TAB3 or CPSF4 and NSP1β transformed yeast grew on 2.5 mM 3-AT plates (**Figure 4.8**), and yeast with PIAS2 and NSP1α were able to grow on 10 mM 3-AT (**Figure 4.5**); this supports that these interactions are genuine but they vary in strength. PIAS1 and NSP1α from SU1-Bel and 215-06 transformed yeast were able to still grow on 60 mM plates (**Figure 4.7**), showing this was a genuine very strong interaction. Further work using 3-AT could be carried out to determine the strength of the other interactions identified.

Of the confirmed interactions, 11 were selected to take forward and further confirm and characterise using confocal immunofluorescence microscopy and co-immunoprecipitations, time permitting (**Table 4.5**). Eleven proteins were selected, rather focusing on one, to maximise the chances of successfully cloning at least one for subsequent analysis. These were selected based on their function and what pathways PRRSV and other viruses are known or suspected to target and use; investigating these interactions could provide insight into how PRRSV-1 manipulates these processes. PIAS2, TAB3, STAT3, beclin-1, EPAS-1 were selected as they are involved in the immune response (IFN signalling, NF-κB pathway, autophagy,

apoptosis etc), TPR and GLE1 as they are involved nucleocytoplasmic transport, PSMB4, PSMB8 and PSMA1 as they are subunits of the proteasome and cullin-9 as it is a ubiquitin ligase scaffold protein.

To do this, the selected proteins along with NSP1α and NSP1β had to be expressed in mammalian cells (BSR-T7, HEK-293-TLR-3 and MAX); however, pACT2 did not have a suitable promoter for eukaryotic expression. Multiple approaches, previously used successfully by others, were tested including: cloning the T7 promoter into pACT2 using DNA oligos; cloning the cDNA inserts out of pACT2 into pGADT7; and using a primer containing the T7 promoter to amplify the cDNA insert and using the resulting PCR product to transfect cells. Two cloning strategies were tested: cDNA inserts were excised from pACT2 using *Xho*I and ligated into pGADT7, the restriction enzyme used to clone them into pACT2; alternatively, the pACT2-PAM protein plasmids were digested with either *Bam*HI or *Eco*RI, and the cloning of DNA oligo containing the T7 promoter into this was attempted. Neither of these cloning approaches attempts were successful. It is unclear why these approaches did not work. Both strategies involved digestions with one restriction enzyme, approach one with either *Bam*HI or *Eco*RI and approach two with *Xho*I; this possibly led to inserts being cloned in the wrong orientation or high levels of vector self-ligation. The third approach involved using a primer containing the T7 promoter, an HA tag and KOZAK sequence in PCR with pACT2-PAM protein as the template to amplify the cDNA insert and introduce the promoter and tag upstream. This had initial success, with expression of some of the HA-tagged PAM proteins (**Figure 4.9**) at their predicted sizes in BSR-T7 cells. However, this could not always be replicated; analysis of the pACT2 primer sequence revealed potential mispriming to the pACT2 vector. After multiple unsuccessful attempts, these approaches were abandoned.

A new approach, using the vector pEF-FLAG and HEK-293-TLR3, was tried. Forward and reverse primers each containing restriction sites specific to each insert (**Table 2.5**, **Table 2.8**) were designed and used to amplify each insert. These were digested and cloned into pEF-FLAG; all 11 proteins were successfully cloned into pEF-FLAG. However, only 8 of the 11 tagged partial proteins were expressed in HEK-293-TLR3 cells (**Figure 4.11, Figure 4.12**). These were: PIAS2, PSMB4, TAB3, STAT3, GLE1,

PSMB8, EPAS-1 and beclin-1; with PIAS2 and STAT3 being putative bands. TPR, cullin-9 and PSMA1 could not be detected (**Figure 4.12**). This is possibly because these partial proteins were less stable. All 3 proteins were small, between 12-23 kDa for predicted sizes (**Table 4.6**), which could have affected their stability as maybe the amino acids and bonds normally present in the full-length protein which stabilise the protein were not all present.

Additionally, expression of most of the tagged partial proteins decreased if they were expressed with NSP1α or NSP1β in HEK-293-TLR3 cells (**Figure 4.11, Figure 4.12**). It is unclear why this occurred; it is possible in co-transfections the two plasmids were competing for transcription and translation machinery so individual protein expression was reduced compared to single transfections. Different plasmid ratios and quantities in transfection were trialled (**Figure 4.11**), however further optimisation of transfections could be performed, including altering plasmid ratios for each specific pEF-FLAG plasmid, varying transfection timings and testing alternative cell types. Additionally, NSP1α or NSP1β may target proteins for degradation as both have been shown to previously (Han *et al.*, 2013; Wang *et al.*, 2013). This could be investigated by treating cells with inhibitors of protein turnover pathways, such as the proteasomal inhibitor MG132 or lysosomal inhibitor leupeptin.

Confocal immunofluorescence microscopy was used to analyse protein localisation within the cell and check for co-localisation. Only FLAG-tagged proteins previously expressed in HEK-293-TLR3 cells were tested in Max cells. Max cells were preferred due their bigger size, which enhance imaging, and because they are porcine cells, so are more biologically relevant in the context of PRRSV. These proteins were PIAS2, PSMB4, TAB3, GLE1, EPAS-1 and beclin-1. Due to time constraints, PSMB8 and STAT3 were not tested. Antibody concentration was optimised (**Figure 4.13**) to reduce background. Future work building on this could optimise imaging further, including trying alternative antibodies to detect Myc or varying the blocking buffer composition.

PRRSV NSP1α is nucleocytoplasmic protein (Kroese *et al.*, 2008) but was observed predominantly in the cytoplasm (**Figure 4.14**), with low levels of NSP1α seen in the nucleus of few cells (**Figure 4.14, Row 4**). PRRSV NSP1β is also nucleocytoplasmic but

its distribution varied between cells: in some it was only observed in the cytoplasm (**Figure 4.17, Row 1**) but in others in both compartments (**Figure 4.17**, **Row 2**). In almost all cells co-transfected with either pcDNA-Myc-NSP1α or pcDNA-Myc-NSP1β and pEF-FLAG-PAM protein, both NSP1α and NSP1β were cytoplasmic. However, in the presence of beclin-1 (**Figure 4.32**) and TAB3 (**Figure 4.22 and Figure 4.23**), Myc-NSP1β was observed in the nucleus of some cells. The nuclear presence of NSP1β in cells expressing beclin-1 and TAB3 could be a consequence of their interaction, but this would need to be investigated further.

The cellular localisation of PRRSV NSP1α and NSP1β in Max cells differed to what has been seen previously using confocal microscopy. NSP1α has been observed present in both cytoplasm and nucleus, with some showing it to be predominantly nuclear (Yoo *et al.*, 2010; Chen *et al.*, 2016), others concentrated in the cytoplasm (Han *et al.*, 2017). NSP1β was present in both the nucleus and cytoplasm, but where was it most concentrated varied with time post infection (Han et *al.*, 2017). It is unclear why neither NSP1α nor NSP1β when expressed alone were rarely present in the nucleus, given some of their functions rely on this (Song, Krell and Yoo, 2010; Han *et al.*, 2017).

The cells were all fixed 24 hpt, so at that time point it was possible both NSP1α and NSP1β were predominantly cytoplasmic. Imaging the cells at different time points post transfection or infection might show the proteins with different distribution patterns; this have been seen previously, with NSP1β overtime moving into the nucleus (Han *et al.*, 2017). NSP1α shuttles repeatedly between the nucleus and cytoplasm, so at the time of imaging could have been moving out of the nucleus (Chen *et al.*, 2016).

As well as timing being a factor, NSP1β might require the presence of other viral proteins. The translocation of NSP1β into the nucleus is not well characterised – no nuclear localisation sequence (NLS) has been identified – but it requires the presence of KPNA6, a soluble transport factor that moves proteins into the nucleus through the NPC (Yang *et al.*, 2018). The levels of KPNA6 increase during infection as PRRSV NSP12 increases the protein half-life; knocking out KPNA6 prevented NSP1β translocation into the nucleus and reduced viral replication (Yang *et al.*, 2018). Therefore, it is possible NSP1β needed more KPNA6 present in the cell, and therefore

NSP12, to move into the nucleus. NSP1α may also require other PRRSV proteins only present in infected cells, however, it does not require KPNA6 (Yang *et al.*, 2018). Therefore, whether cells are transfected or infected could affect NSP1α and NSP1β cellular distribution. Additionally, it would be worth co-transfecting cells with both NSP1α and NSP1β to see if they interact and/or depend on each other for correct localisation.

The interaction between NSP1α and PIAS2 was identified and verified using the y-2-h system (**Figure 4.3**). In Max cells transfected with pEF-FLAG-PIAS2, FLAG-PIAS2 localised to the nucleus (**Figure 4.15**) behaving like the full-length protein (Kong *et al.*, 2015; Adachi *et al.*, 2020). No co-localisation was observed between PIAS2 and NSP1α (**Figure 4.16**). However, only one co-transfected cell was identified when using the pEF-FLAG-PIAS2 plasmid (**Figure 4.16**). This transfection needs to be repeated and optimised to maximise protein expression. The partial PIAS2 may not be very stable so retesting full-length protein might improve expression levels. Alternatively, NSP1α could target PIAS2 for degradation, as it does with CREB-binding protein (CBP) and SLA-1 (Han *et al.*, 2013; Du *et al.*, 2016). This could be investigated by treating cells with inhibitors of protein turnover pathways, such as the proteasomal inhibitor MG132 or lysosomal inhibitor leupeptin.

PSMB4, TAB3, GLE1, EPAS-1 and beclin-1 were proven to interact with NSP1β (**Figure 4.4**). In Max cells transfected with pEF-FLAG-PSMB4, PMSB4 localised to both the nucleus and cytoplasm (**Figure 4.18**), with most protein concentrated in the nucleus in some cells (**Figure 4.18, Rows 1 and 2**) and equal distribution in others (**Figure 4.18, Row 3**). Proteasomes, and therefore proteasome units are found in both subcellular locations (Brooks *et al.*, 2000). Bright speckles observed in the nuclei of cells (**Figure 4.18, Rows 1 and 2**) could possibly be clastosomes, where proteasomes and therefore this subunit are found enriched (Lafarga *et al.*, 2002). In the presence of NSP1β, localisation of PSMB4 was unchanged and minimal co-localisation was observed (**Figures 4.19 & 4.20**). Clastosomes are part of the antiviral response against varicella zoster virus (Reichelt *et al.*, 2011), sequestering the viral ORF23 capsid surface protein and preventing nucleocapsids leaving the nucleus. Although varicella zoster virus is a DNA virus that replicates in the nucleus, this could be an antiviral

strategy to sequester PRRSV NSPs, or conversely a method used by PRRSV to sequester cellular antiviral proteins.

In cells expressing TAB3 alone, it was observed in both the nucleus and cytoplasm with most protein concentrated in the nucleus (**Figure 4.21**). TAB3 was expected to be solely in the cytoplasm (Criollo et al., 2011); it is unclear why TAB3 was regularly observed in the nucleus. Criollo and colleagues expressed full-length TAB3 in HeLa cells, whereas here TAB3 was expressed as a partial protein in Max cells, so this could explain the differences. TAB3 undergoes numerous post-translational modifications (Ishitani *et al.*, 2003; Mendoza *et al.*, 2008), which the partial length TAB3 may have not, which could have affected protein behaviour. TAB3 functions in the cytoplasm in both the NF-κB pathway (Kanayama *et al.*, 2004; Shinohara, Yasuda and Kurosaki, 2016) and autophagy regulation (Criollo et al., 2011), but has been detected in the nucleus but not nucleoli using confocal microscopy, https://www.proteinatlas.org/ENSG00000157625-TAB3/antibody#ICC. TAB3 binds and regulates the activity of transforming growth factor-β (TGF-β) activated kinase 1 (TAK1) in the cytoplasm (Cheung, Nebreda and Cohen, 2004), but TAK1 complexed with TAB1, TAB2, TAB4 and IκB kinase α/β (IKKα/β) has been detected in the nucleus (Ear *et al.*, 2010); TAB3 was not detected at all in cells in this paper. TAK1 is also neddylated by Nedd8, which promotes TAK1 nuclear import (Li *et al.*, 2020). Therefore, it cannot be ruled out TAB3 is also found in the nucleus complexed with TAK1 and IKKα/β, or that TAB3 binding neddylated TAK1 imports TAB3 into the nucleus. This would need to be investigated further, possibly by probing for TAK1 and/or inhibiting neddylation using MLN4924 and then analysing protein localisation. Splice variants of TAB3 have also been reported but not fully investigated, so it is possible these function in the nucleus (Jin *et al.*, 2003).

TAB3 appeared to form rings of protein in the nucleus when expressed alone (**Figure 4.21, Row 3**) and with NSP1β (**Figure 4.23**); this was observed in multiple cells but it was unclear what these were or why they were in the nucleus. In the presence of NSP1β (**Figure 4.22**), TAB3 was again predominantly nuclear and no co-localisation was observed. However, in one cell (**Figure 4.22, Row 3**) it was entirely cytoplasmic with Myc-NSP1β occupying the nucleus instead; either the proteins were behaving as

expected or possibly altered each other's subcellular distribution. This could be investigated further by fixing cells at different time points to observe how protein localisation changes over time, or by mutating the proteins to inhibit the interaction and observing the effect on subcellular distribution.

A Z stack obtained of another cell revealed minimal co-localisation of TAB3 and NSP1β at the cell periphery (**Figure 4.24**). This was the only potential co-localisation observed; analysis using confocal immunofluorescence microscopy would need to be repeated to confirm this. Activation of the NF-κB pathway or autophagy, pathways which TAB3 functions in, may be required to see correct subcellular localisation.

The nuclear protein GLE1 was observed in both the nucleus and cytoplasm of transfected cells, with more protein concentrated into the nucleus (**Figure 4.25**), as previously observed (Sharma and Wente, 2020). No co-localisation between GLE1 and NSP1β was observed (**Figure 4.26, Figure 4.27**). NSP1β interacts with another NPC protein NUP62, an interaction which has been observed using confocal immunofluorescence microscopy (H. Ke, Han, *et al.*, 2019); therefore, it is surprising no co-localisation was observed here.

In cells expressing FLAG-EPAS-1, EPAS-1 was observed in the both the cytoplasm and nucleus of transfected cells (**Figure 4.28**). The presence of EPAS-1 at a high level exclusively in the cytoplasm of one cell was surprising (**Figure 4.28, Row 2**), as EPAS-1 is degraded in the cytoplasm, only becoming stable and moving to the nucleus in hypoxic conditions (Tian, McKnight and Russell, 1997). This suggests the partial EPAS-1 was not behaving like the full-length protein. In cells expressing FLAG-EPAS-1 and Myc-NSP1β, EPAS-1 cellular distribution changed: FLAG-EPAS-1 was observed almost exclusively in the cytoplasm, with minimal protein seen in the nucleus (**Figure 4.29**). No co-localisation was observed. To properly investigate interactions between NSP1β and EPAS-1, a hypoxic environment may need to be induced in the cell, using $CoCl_2$ solution (Wu and Yotnda, 2011), to activate and stabilise EPAS-1.

In transfected Max cells, beclin-1 localised exclusively and consistently to the cytoplasm, occupying up to the nuclear membrane (**Figure 4.31**). In the presence of NSP1β, beclin-1 remained in the cytoplasm (**Figure 4.32**). However, in one cell for

which a Z stack was obtained (**Figure 4.33**), beclin-1 was restricted to the periphery of the cell. Throughout the cell, NSP1β instead occupied the space surrounding the nucleus; this suggests NSP1β has potentially displaced beclin-1 within the cell, which could impair its ability to function in autophagy and apoptosis.

The low levels of NSP1α and NSP1β in the nucleus could explain the lack of or minimal co-localisation with the FLAG-PAM proteins that co-localise there (PIAS2, PSMB4, GLE1). As discussed earlier, there could be multiple reasons for this, one of which being the need for cells to be infected with PRRSV for NSP1α and NSP1β to localise properly. The lack of infection could also affect the subcellular distribution of the PAM proteins, as some may require activation of certain pathways or certain cellular conditions (e.g. EPAS-1 and hypoxia) to become active. Some of the PAM proteins, which are partial, did also not behave as expected like their full-length versions (such as TAB3); this could have prevented their interactions with NSP1. The interactions identified also varied in strength (**Section 4.3**) and may be transient, making it difficult to image cells at the exact moment of interaction. Different porcine cells should also be used, ideally PAMs the main target cell of PRRSV, to test the effect of cell type on protein localisation. Co-localisation was not quantified, so proteins that did not appear to co-localise might in fact do. In future work, image analysis software could be used to empirically quantify the degree of co-localisation on confocal images. Therefore, to investigate further co-localisation using confocal immunofluorescence microscopy: expressing full-length PAM proteins, infecting cells, transfecting both NSP1α and NSP1β together, fixing at different timepoints, and using alternative porcine cells, should be tested.

Further work is needed to test by co-immunoprecipitation the interactions between the FLAG-tagged PAM proteins with either NSP1α or NSP1β. Expressing the full-length tagged proteins, rather partial may also improve their stability and therefore expression, allowing testing of other proteins. Additionally, use of primary antibodies against the specific PAM proteins, if available, could be used to detect if endogenously expressed proteins interact with PRRSV NSP1α and NSP1β. An alternative pull-down method, GFP-Trap combined with mass spectrometry, was planned, but due to time constraints and the COVID-19 pandemic this could not be

attempted. Future experiments using GFP-tagged NSP1α and NSP1β in this approach could be used to identify a list of interacting proteins, which could be subsequently compared to the y-2-h data.

Y-2-h retesting confirmed 3 interactions with PRRSV-1 NSP1α and 28 interactions with NSP1β (**Section 4.2**); further work is needed to re-test the other proteins identified in the screen. Investigating the strength of selected interactions using 3-AT revealed NSP1α from 215-06 and SU1-Bel interacts very strongly with PIAS1 (**Figure 4.7**), whereas 215-06 NSP1α interacts strongly with PIAS2 (**Figure 4.5**). 215-06 NSP1β interacts weakly with TAB3 and CPSF4 (**Figure 4.8**). Although y-2-h confirmed the interactions, most could not be observed using confocal immunofluorescence microscopy. However, some co-localisation was observed between TAB3 and NSP1β (**Figure 4.24**). Interestingly, NSP1β appeared to alter beclin-1 localisation in the cytoplasm (**Figure 4.33**). Optimisation and alterations of both confocal immunofluorescence microscopy and co-immunoprecipitations, discussed above, are required.

The proteins identified and the potential consequences of their interactions with PRRSV-1 NSP1α and NSP1β are discussed in detail in **Chapter 5**.

Chapter 5: Discussion

5.1 Overview

PRRSV is endemic in most swine producing countries, with the PRRS panzootic costing the swine industry millions every year (Holtkamp *et al.*, 2013; Paz, 2015). This demonstrates the urgent need for safer and more effective PRRSV vaccines (Nan *et al.*, 2017). To achieve this, a deeper understanding of virus-host interactions involved in immunomodulation is required. Studies carried out previously and throughout the course of this project have sought to understand these interactions, with most focussing on NSPs including NSP1α and NSP1β (Song et al., 2018; H. Ke, Han, et al., 2019; Li et al., 2019). PRRSV NSP1α and NSP1β have been shown to modulate the immune response to PRRSV in multiple ways, including inhibiting NF-κB activation, blocking type I IFN signalling pathways, and downregulating SLA expression to reduce antigen presentation (Du *et al*., 2016; Jing *et al.*, 2016; Wang *et al.*, 2013), as well as having crucial roles in viral replication (Kroese *et al.*, 2008; Y. Li, Treffers, *et al.*, 2014). However, despite these recent studies, the mechanistic details underlying immunomodulation are yet to be fully elucidated (**Section 1.3**), and given the multifunctional nature of viral NSPs, it is likely they have other unidentified roles. NSP1α and NSP1β from the PRRSV-1 strain 215-06 were chosen to study since most previous work has focussed on PRRSV-2 strains (**Table 1.3, Table 1.4**), and 215-06 is a subtype 1 strain representative of the PRRSV-1 strains that predominate in Western, Central and Southern Europe, North America and Asia.

This project aimed to elucidate the PRRSV-1 215-06 NSP1α and NSP1β interactomes and characterise the identified interactions. Using the y-2-h method, 63 putative interactions with NSP1α (in the presence of NSP1β) and 126 interactions with NSP1β were identified (**Section 3.6**). Due to time constraints, only a combined total of 39 proteins from both y-2-h screens were selected to take forward and retest. In future work, all these proteins should be retested using y-2-h with additional controls (**Section 4.2**) to confirm whether they are genuine interactions. The proteins selected for confirmation and further characterisation were deemed the most likely to be involved in immunomodulation; this decision was based on their functions and previously known interactions with viral proteins. They were involved in either

immune signalling, nuclear transport, ubiquitination and transcription and translation, or shown to be previously targeted by PRRSV or other viruses.

Retesting proteins using y-2-h with additional controls (**Section 4.2**) confirmed three interactions from the NSP1α screen and 28 from the NSP1β screen. From these, a total of 12 proteins were retested using 3-AT to either determine the strength of the interactions or confirm false positives (**Section 4.3**). This revealed that NSP1α interacts very strongly with PIAS1 (**Figure 4.7**) and strongly with PIAS2 (**Figure 4.5)**; in comparison, NSP1β was found to weakly interact with TAB3 and CPSF4 (**Figure 4.8**). In future work, the strength of other putative interactions could be investigated using y-2-h with 3-AT. The results of the y-2-h screen are discussed in **Section 3.7** and **Section 4.7**.

To further investigate the confirmed interactions using confocal immunofluorescence microscopy, the selected proteins had to be cloned into a vector containing a suitable promoter for mammalian cell expression. Three approaches (**Section 4.4**) were attempted to try to introduce a T7 promoter upstream of the cDNA insert, which would allow the expression of the HA-tagged PAM proteins when transfected into BSR-T7 cells infected with MVA-T7. This method of protein expression had been used successfully previously within the Molecular Virology Group (The Pirbright Institute) (Doceul *et al.*, 2008). The two strategies involving cloning were never successful and the third, using a primer containing the T7 promoter to amplify the cDNA insert, had limited success (**Figure 4.9**). A fourth approach yielded better success: this involved cloning the cDNA inserts in the vector pEF-FLAG, which contains a CMV promoter instead, and transfecting these plasmids into HEK-293-TLR3 cells (**Section 4.4**). This part of the project was a significant bottleneck; unsuccessful cloning and lack of protein expression prevented the project moving forward as anticipated.

Upon reflection, the approach of cloning cDNA inserts into pEF-FLAG should have been tested earlier to allow more time for confocal immunofluorescence microscopy and co-immunoprecipitations, as well as other experiments such as luciferase assays and GFP-trap pulldowns. Additionally, fewer proteins or even one from each y-2-h screen, could have been selected for further analysis. With fewer proteins to work

with and clone, their sequences could have potentially been ordered and synthesised by GeneArt (Thermofisher), with restriction sites introduced to facilitate cloning. However, if these proteins had failed to express, this would have wasted time and money; therefore, it was beneficial to work with more proteins. Rather than attempting to clone the cDNA inserts for use in confocal immunofluorescence and coimmunoprecipitations, it may have been better in hindsight to instead try GFP-Trap pulldowns first, as this would only have involved cloning NSP1α and NSP1β rather than the partial PAM proteins. However, this would have delayed the confocal microscopy and if the proteins identified by y-2-h had not been identified by GFP-Trap and mass spectrometry, it would not have supported that data further. There were pros and cons to both strategies.

Confocal immunofluorescence microscopy was used to analyse subcellular localisation of NSP1α, NSP1β and the selected PAM proteins, as well as to check for co-localisation (**Section 4.5**). NSP1α and NSP1β, which are nucleocytoplasmic (Yoo et al., 2010; Chen et al., 2016; Han et al., 2017), were rarely detected in the nucleus with or without the presence of the PAM proteins (**Section 4.5**). TAB3 and EPAS-1 did not follow their expected cellular distribution (**Figure 4.21 and Figure 4.28**, respectively), whereas PIAS2, PSBM4, GLE1 and beclin-1 did (**Figure 4.15, Figure 4.18, Figure 4.25, Figure 4.31,** respectively). Co-localisation was only observed between NSP1β and TAB3 (**Figure 4.24**), but this was minimal. Notably, beclin-1 distribution within the cytoplasm was altered in the presence of NSP1β (**Figure 4.33**). Given the y-2-h confirmed these interactions, the lack of co-localisation observed is more likely to be due to experimental conditions. The lack of expected subcellular distribution, small number of co-transfected cells and the absence of infection, amongst other factors, as discussed in **Section 4.7**, could explain this.

Full characterisation of the interactions was not achieved due to issues expressing proteins in mammalian cells (**Section 4.4**) and time constraints. Future work that could be performed to achieve this is discussed in **Chapter 6**, as well as **Section 4.7**.

Although the potential consequences of the confirmed interactions have not yet been investigated, we can postulate what they could be based on previously

identified NSP1α and NSP1β functions, the pathways PRRSV targets and knowledge from related viruses.

5.2 Potential consequences of identified interactions

5.2.1 Nuclear transport

Proteins are translated in the cytoplasm of cells, but some function in the nucleus and therefore need to be imported. Additionally, to function, some proteins may need to shuttle between the nucleus and cytoplasm, and so need to be exported from the nucleus. Proteins are transported in and out of the nucleus through NPCs in the nuclear envelope, macromolecular structures composed of ~30 multicopy proteins called NUPs (**Figure 5.1**) (Strambio-De-Castillia, Niepel and Rout, 2010). These make up the cytoplasmic filaments, cytoplasmic ring, internal pore ring, nuclear ring, and nuclear basket (Schwartz, 2016; de Jesús-González *et al.*, 2021).

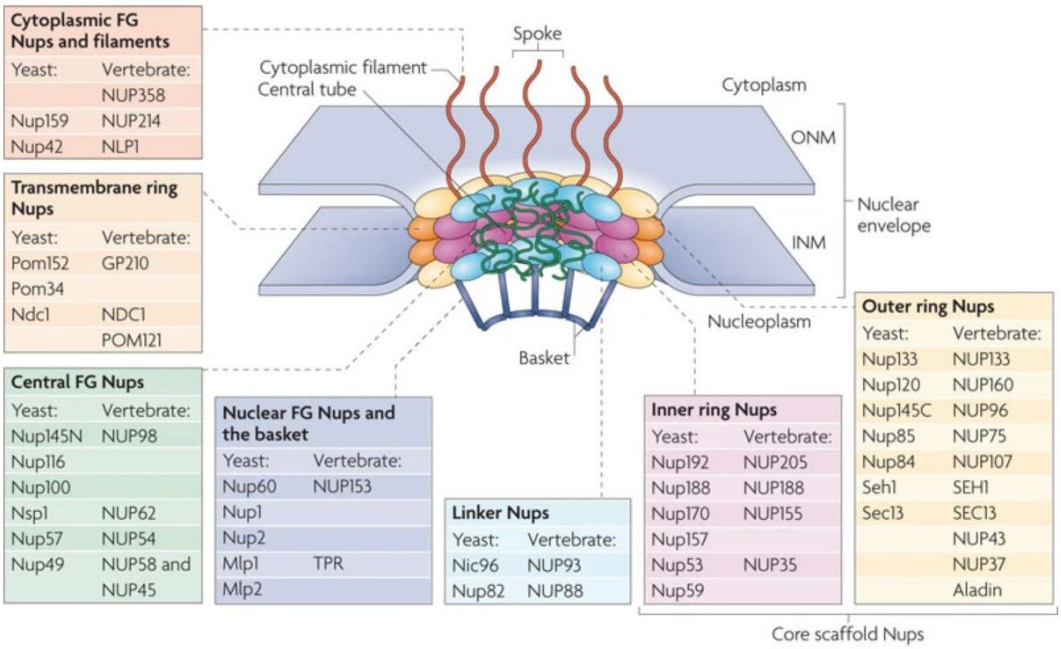

Figure 5.1: Structure of the nuclear pore complex. The structure of the nuclear pore complex and locations of each nucleoporin (NUP) with the complex are shown. The yeast and vertebrate annotations for each protein are listed. Key: GP210 – glycoprotein 210; Mlp – myosin-like protein; Ndc1 – nuclear division cycle protein 1; Nic96 – Nup-interacting component of 76 kDa; NLP1 – Nup-like protein 1; Pom – pore membrane protein; Seh1 – SEC13 homologue 1; TPR – translocated promoter region. *Figure 1 reprinted by permission from Springer Nature* (Strambio-De-Castillia, Niepel and Rout, 2010).

Proteins less than 40 kDa can diffuse passively through the NPC, whereas bigger proteins need to interact with the NPC or carrier molecules in an energy dependent process (Becskei and Mattaj, 2003; Stewart, 2007). Most of the transport is mediated

by a family of carrier molecules called β-karyopherins (Yuh and Blobel, 2001), with import carriers known as importins and export carriers known as exportins.

There are different import pathways which use different importins and different NLSs (Macara, 2001; Stewart, 2007). The classical pathway of nuclear transport is the most characterised and uses importin-β in combination with the adaptor protein importin-α (Stewart, 2007). Importin-α, bound to importin-β, recognises the NLS sequence in the cargo (Fontes, Teh and Kobe, 2000), but some proteins can directly bind importin-β (Lee *et al.*, 2003). Through interactions between the importins and the NPC, the complex is transported into the nucleus, where cargo is released when importin-β interacts with Ran-GTP (Lee *et al.*, 2005; Stewart, 2007).

Most nuclear export of proteins is mediated by the β-karyopherin CRM-1 (Hutten and Kehlenbach, 2007; Thakar *et al.*, 2013), with microRNA (miRNA) instead exported by exportin-5 and transfer RNA (tRNA) being exported by both exportin-5 and exportin-t (Arts *et al.*, 1998; Bohnsack *et al.*, 2002; Lund *et al.*, 2004). In contrast, mRNA export uses the unrelated protein heterodimer nuclear RNA export factor 1 (NXF1) and nuclear transport factor 2 like export factor 1 (NXT1) (Strabetaer, 2000; Stewart, 2007). CRM-1, complexed with Ran-GTP, recognises an NES in target proteins, and the complex moves through the NPC; hydrolysis of GTP in the cytoplasm releases the cargo (de Jesús-González *et al.*, 2021). CRM-1 independent export using the protein B-23 has also been observed for both cellular (Gao *et al.*, 2005) and viral proteins (Adachi *et al.*, 1993; Li, 1997). **Figure 5.2** shows an overview of classical nuclear import and export.

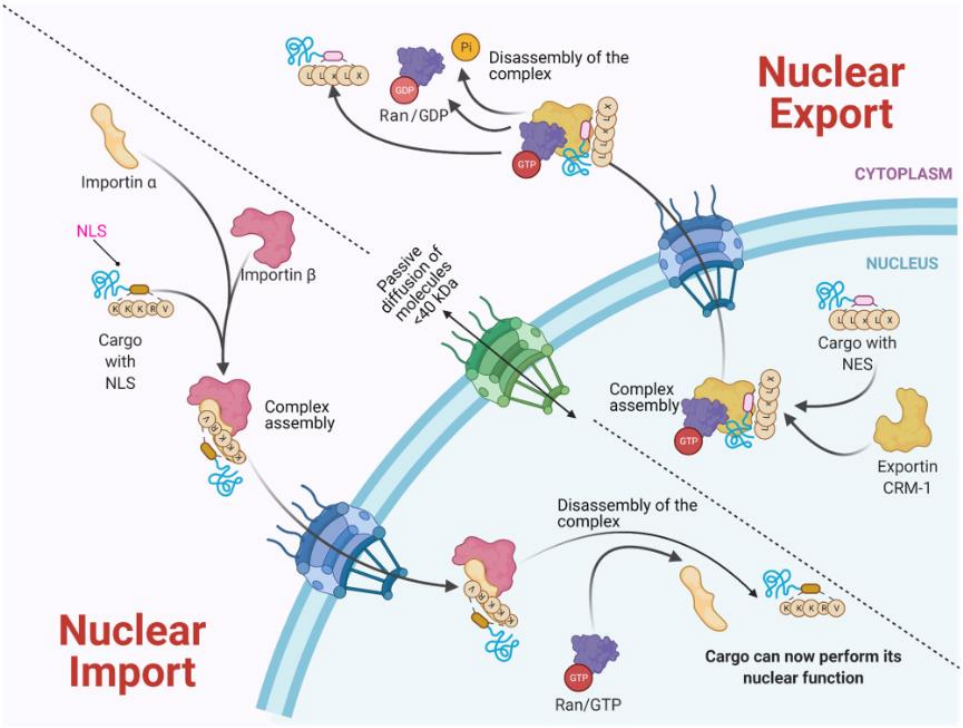

Figure 5.2: Overview of nuclear import and export. In the classical pathway of nuclear import, importin-α and importin-β form a complex with the cargo protein through recognition of a nuclear localisation sequence (NLS). In nuclear export via CRM-1, the cargo protein contains a nuclear export sequence (NES). In both cases, a GTP gradient is required. Molecules less than 40 kDa diffuse passively through the NPC. *Figure 2 used with permission from Multidisciplinary Digital Publishing Institute (MDPI) Journals* (de Jesús-González *et al.*, 2021).

PRRSV replicates in the cytoplasm of infected cells (W. Zhang *et al.*, 2018), but some of its proteins – NSP1α, NSP1β and N protein – also function in the nucleus (Han *et al.*, 2013, 2017; H. Ke, Lee, *et al*., 2019). For example, PRRSV-2 NSP1α inhibits IFN-β production in two different ways depending on its location: in the cytoplasm NSP1α prevents IκBα degradation to inhibit NF-κB activation (Song, Krell and Yoo, 2010), whereas in the nucleus it causes CBP degradation, thereby preventing IRF-3 signalling (Han *et al.*, 2013). Therefore, PRRSV needs to manipulate host nuclear transport machinery to shuttle these proteins between the two subcellular compartments.

The PRRSV nucleoprotein N contains an NLS, nucleolar localisation sequence and NES, and undergoes a *C*-*N*-*C*-1 shuttling scheme, when *C* is cytoplasm and *N* is the nucleus (Rowland and Yoo, 2003; Lee *et al.*, 2006). N interacts with both importin-α and importin-β, using the classical import pathway to enter the nucleus (Rowland and

Yoo, 2003). However, an alternative pathway of transport from cytoplasm to nucleolus using nucleolin, the most abundant protein in nucleoli, has also been postulated (Rowland and Yoo, 2003) as this has been used by other viruses. Both the human T-lymphotropic virus 1 Rex protein and human immunodeficiency virus (HIV) 1 (HIV-1) Tat proteins interact with the cellular protein B-23, which shuttles them from the cytoplasm to the nucleolus (Adachi *et al.*, 1993; Li, 1997). N protein binds to the exportin CRM-1 to leave the nucleus (Rowland and Yoo, 2003).

It is not known how NSP1α translocates into the nucleus, but it contains a classical NES that interacts with CRM-1, and shuttles continuously between the nucleus and cytoplasm (Chen *et al.*, 2016). This NES is highly conserved between PRRSV strains, and mutating or deleting it alters NSP1α subcellular distribution, thereby preventing NSP1α from degrading CBP in the nucleus and therefore inhibiting NF-κB activation (Han *et al.*, 2013; Chen *et al.*, 2016). The NES in 215-06 NSP1α does not completely match the consensus; however, neither do the NESs in two other PRRSV-1 strains, Lelystad and Lena (Chen *et al.*, 2016). No proteins were identified in the y-2-h screen of NSP1α with roles in nuclear transport (**Figure 3.9**).

No NLS or NES to date has been identified in NSP1β. However, NSP1β translocation into the nucleus is dependent on KPNA6, as in KPNA6 knock out cells NSP1β is restricted to the cytoplasm (Yang *et al.*, 2018). In infected cells, NSP12 reduces the poly-ubiquitination of KPNA6, increasing the half-life and therefore levels of KPNA6; other NSPs are also able to do this but to a lesser extent (Yang *et al.*, 2018). It is possible that a lack of NSP12 in transfected Max cells (**Section 4.5**) could explain the low levels of NSP1β that were detected in the nucleus. NSP12 and NSP1β interact (Song *et al.*, 2018), but no interaction between either KPNA6 and NSP1β or KPNA6 and NSP12 has been observed (Yang *et al.*, 2018). The y-2-h screens confirmed STAT3 as an interacting protein with NSP1β (**Figure 4.4**), and STAT3 is known to use KPNA6 to move into the nucleus (Ma and Cao, 2006). Therefore, perhaps this interaction acts as a bridge between the importin and NSP1β, allowing NSP1β to be imported despite not having an NLS.

NSP1β contains an SAP motif (Han *et al.*, 2017), which is essential for IFN suppression (Han *et al.*, 2017; Ke *et al.*, 2018). SAP motifs are found in multiple cellular proteins,

including PIAS family proteins (Tan *et al.*, 2002). SAP affects the nuclear localisation pattern of Acinus protein isoforms (F. Wang *et al.*, 2014) and is thought to target PIAS proteins to the nuclear scaffold (Sachdev *et al.*, 2001; Shuai and Liu, 2005); SAP also binds to DNA (Aravind and Koonin, 2000; Okubo *et al.*, 2004). Therefore, it is possible this motif is involved in the localisation of NSP1β to the nucleus in host cells; this idea is supported by the fact the SAP motif is required for NSP1β to retain mRNA in the nucleus (Han *et al.*, 2017).

Additionally, interfering with the nuclear transport of cellular proteins and mRNA could aid viral replication, either by reducing competition for translation machinery in the cytoplasm or by preventing the production of anti-viral proteins. PRRSV NSP1β causes nuclear retention of host mRNA by interacting with NUP62 in the NPC, leading to NPC disintegration, with the SAP motif being crucial for this (Han *et al.*, 2017; H. Ke, Han, *et al.*, 2019). In turn, this leads to an increase in viral protein production and a decrease in the synthesis of cellular proteins, in particular antiviral proteins including type I IFN and ISGs (H. Ke, Han, *et al.*, 2019). NSP1β also inhibits JAK-STAT signalling by causing degradation of the importin KPNA1 (Wang *et al.*, 2013), however, the interactions involved have not been elucidated as NSP1β does not bind KPNA1. It is interesting that NSP1β causes KPNA1 degradation yet relies on the related protein KPNA6 for nuclear import (Yang *et al.*, 2018), and that STAT3 uses KPNA6 for nuclear import (Ma and Cao, 2006). These interactions and functions of NSP1β do not explain how NSP1β moves into the nucleus; therefore, it is feasible that NSP1β interacts with other NPC components or importins. Given the predicted size of NSP1β of ~23 kDa, it could diffuse passively in and out of the nucleus. However, given NSP1β has numerous important nuclear roles; is dependent on KPNA6 for nuclear import (Yang *et al.*, 2018); and has been observed to be concentrated within the nucleus (Han *et al.*, 2017), it is likely that NSP1β is targeted to the nucleus.

Interestingly, the NSP1β y-2-h screen identified three proteins involved in nuclear transport: GLE1, TPR and NUP210; y-2-h retesting (**Section 4.2**) suggested all three interactions were genuine.

GLE1 is a nucleocytoplasmic shuttling protein (Kendirgi *et al.*, 2003). It is an mRNA export factor, transporting mRNA from the nucleus to the cytoplasm (Murphy and

Wente, 1996). During export, GLE1 interacts with inositol hexakisphosphate to activate DEAD-box protein 5 (Dbp5), which in turn remodels complexes of RNA and RNA-binding proteins (Folkmann *et al.*, 2011). It is disputed whether the interaction of GLE1-IP with Dbp5 promotes RNA binding or release (Folkmann *et al.*, 2011; Montpetit *et al.*, 2011; Noble *et al.*, 2011).

Additionally, GLE1 interacts with NUP155 in the NPC, which has also been proposed as a step in mRNA export (Rayala *et al.*, 2004). This interaction is necessary but not sufficient to target GLE1 to the NPC, as GLE1 also needs to interact with the NUP NPL1 for NPC localisation (Kendirgi *et al.*, 2005). More recently, NUP42, (in vertebrates known as NPL1) has been confirmed to interact with GLE1 and enhance its ability to activate Dbp5 ATPase activity; this interaction has been shown to be crucial for mRNA export (Adams *et al.*, 2017).

PRRSV targets NUP62 and KPNA6 (Wang *et al.*, 2013; Yang *et al.*, 2018) which are involved in nuclear transport, so it is feasible it also targets GLE1. In influenza A virus (IAV) infected patients, the GLE1 gene was found to be upregulated, but it was unclear if this was part of the host response or deliberate targeting by the virus (Peng *et al.*, 2016). Therefore, it would be interesting to investigate whether GLE1 expression is also altered during PRRSV-1 infection using western blot analysis. No other interactions between other viruses and GLE1 have been reported.

Indeed, it is common for viruses to target the NPC and carrier proteins (de Jesús-González *et al.*, 2021). PRRSV-related viruses from the *Coronaviridae* family, SARS-CoV and SARS-CoV-2, both target NUPs. SARS-CoV NSP1 targets NUP93, causing it to delocalise from the NPC (Gomez *et al.*, 2019), whereas SARS-CoV-2 dislocates NUP98 (Kato *et al.*, 2021). Additionally, HIV-1 Rev protein targets multiple importins and transportin to enter the nucleus (Arnold *et al.*, 2006), supporting the idea that PRRSV NSP1β may target more than one NUP or carrier molecule.

The nucleoprotein TPR forms part of the nuclear pore basket (Krull *et al.*, 2004) (**Figure 5.1**) and binds to NUP153 in the NPC (Hase and Cordes, 2003). It regulates NPC numbers within the cell, providing a scaffold for extracellular signal-regulated kinase to phosphorylate NUP153 to begin NPC biogenesis (McCloskey, Ibarra and

Hetzer, 2018). TPR is involved in mRNA export (Frosst *et al.*, 2002) and regulates mRNA export via the NXF1:NXT1 pathway (Coyle *et al.*, 2011), helping to prevent export of incorrectly spliced mRNAs. Given the role of TPR in mRNA export, this could be another method used by NSP1β to mediate mRNA retention in the nucleus. Additionally, TPR is involved in perinuclear organisation, with a role in the formation of heterochromatin exclusion zones near the NPC (Krull *et al.*, 2010). This role in heterochromatin exclusion zone formation potentially impacts HIV-1 integration sites (Marini *et al.*, 2015; Wong, Mamede and Hope, 2015). TPR is a large protein, 267 kDa (Cordes *et al.*, 1997), but the region identified in the NSP1β y-2-h screen was much smaller (**Table 3.3**); this could explain difficulties in protein stability and expression. The cytoplasmic tail of TPR has been shown to interact with the exportin CRM-1 (Zhao *et al.*, 2014), which is used by NSP1α to exit the nucleus (Chen *et al.*, 2016); so NSP1β could influence CRM-1 nuclear export via TPR. This paper also identified an interaction between TPR and the importin snurportin, implying a role for TPR in nuclear import (Zhao *et al.*, 2014); therefore, the interaction between NSP1β and TPR could lead to NSP1β translocating into the nucleus. No other specific interactions between any other viruses and TPR have been identified.

NUP210, also known as nuclear glycoprotein 210 (GP210 in **Figure 5.1**), is a major transmembrane glycosylated protein of the NPC (Greber, Senior and Gerace, 1990), present as an array of dimers (Favreau *et al.*, 2001). It consists of a large cisternal domain; a single transmembrane segment; and a COOH-terminal, 58-amino acid residue cytoplasmic tail, with the transmembrane domain being sufficient for localisation to the NPC (Wozniak and Blobel, 1992). In myoblasts and embryonic stem cells, NUP210 is absent from NPCs of dividing cells but present in fully differentiated cells and is essential for the induction of genes involved in cell differentiation (D'Angelo *et al.*, 2012). The exact role of NUP210 in nuclear transport has not been identified, but its interaction with NSP1β suggests it could have an important function. No interaction between PRRSV or any other viral proteins and NUP210 have been reported.

The heterogeneous nuclear ribonucleoprotein H was also identified in the NSP1α y-2-h screen (**Table 9.1**). Detailed knowledge of protein function is limited, but it

complexes with both heterogeneous nuclear RNA and pre-mRNAs in the nucleus (Geuens, Bouhy and Timmerman, 2016), and is involved in regulation of alternative splicing of human epidermal growth factor receptor 2 in breast cancer cells (Gautrey *et al.*, 2015). It is interesting that NSP1β interacts with both this protein and GLE1, as both are involved in the regulation of mRNA export. Some heterogeneous nuclear ribonucleoproteins shuttle between the cytoplasm and nucleus (Geuens, Bouhy and Timmerman, 2016), so it is possible that this protein could be involved in transporting NSP1β.

The interactions between NSP1β and the proteins identified could shed light on how NSP1β shuttles between the nucleus and cytoplasm or provide mechanistic detail to known NSP1β functions. Further experiments, including some listed in **Chapter 6**, using NSP1β and components of the NPC and shuttling proteins, need to be carried out to elucidate how NSP1β interacts with the NPC.

If we could impair nuclear translocation of NSP1α and NSP1β or imprison them within the nucleus in PRRSV vaccine strains, this could inhibit their immunomodulatory functions and potentially increase vaccine efficacy.

5.2.2 Protein expression

Protein expression involves the transcription of mRNA from DNA, mRNA processing and export, translation, and protein folding. Viruses target host cell protein expression, either to prevent expression of antiviral proteins or to hijack transcription and translation machinery to enhance their own viral protein expression (Walsh, Mathews and Mohr, 2013; Jaafar and Kieft, 2018; X. Liu *et al.*, 2020).

Multiple proteins involved in the regulation or the process of transcription and translation were identified in the y-2-h screens (**Table 9.1** and **Table 9.2**); these fall under the categories of nuclear proteins, heat shock proteins, DNA binding/modifying, transcriptional regulation, ribosomal and RNA related/binding/splicing. PRRSV downregulates and upregulates the expression of specific genes during infection (Zhang *et al.*, 2009), so it is expected that PRRSV interacts with the groups of proteins identified.

Transcription factors and machinery were identified in both y-2-h screens (DNA binding/modifying, transcriptional regulation section in **Table 9.1** and **Table 9.2**). Notably, mediator of RNA polymerase II transcription subunit 4 (MED4) and EPAS-1 (also known as HIF2α) were confirmed to interact with NSP1β (**Figure 4.4**), however the NSP1α screen also contained an RNA polymerase subunit, TATA box-binding protein-associated factor RNA polymerase I subunit B (**Table 9.1**). HIFs regulate expression of genes involved in cell proliferation, angiogenesis, apoptosis, and metabolism (Koh and Powis, 2012). The interaction between EPAS-1 and NSP1β was investigated further using confocal microscopy, given the role of HIFs in the immune response (Palazon *et al.*, 2014); no co-localisation was observed (**Figure 4.29**). EPAS-1 requires a hypoxic environment to be stable (Tian, McKnight and Russell, 1997), this confocal immunofluorescence should be repeated following induction of hypoxia. The transcriptional activator, myoblast determination protein 1 (MyoD) family inhibitor domain-containing protein (MDFIC), also known as HIC, was confirmed to interact with NSP1β (**Figure 4.4**). MDFIC interacts with PRRSV N (Song *et al.*, 2009). It is unclear what the consequences of this interaction are, but it is postulated to be a method of regulating host gene expression (Song *et al*., 2009). Therefore, NSP1β interacting with the identified transcription factors may allow PRRSV to control

expression of specific host or viral genes, whereas targeting the machinery gives PRRSV general control of protein expression.

Splicing of mRNA involves the removal of introns from the sequence. In both screens, a range of proteins involved in the regulation of splicing and alternative splicing were identified (RNA related/binding/splicing section in **Table 9.1** and **Table 9.2**). In the NSP1β screen, CPSF4 was identified and confirmed as a weak interactor with NSP1β (**Figure 4.8**). CPSF4 is a member of the CPSF complex (Barabino *et al.*, 1997), which is involved in polyadenylation and pre-mRNA cleavage (Schönemann *et al.*, 2014; Misra and Green, 2016). IAV non-structural protein 1 binds to CPSF4 specifically to inhibit nuclear export of host mRNAs (Nemeroff *et al.*, 1998) and to regulate alternative splicing of the p53 gene (Dubois *et al.*, 2019) in order to control the cellular innate response. To date, PRRSV has not been reported to target this complex or splicing machinery but does mediate host cell shut off by retaining mRNA in the nucleus (Han *et al.*, 2017). This could be another method of retaining host mRNA or given its complex protein expression system (**Section 1.2.3.2**), PRRSV may possibly require these proteins for replication.

GLE1, discussed earlier (**Section 5.2.1**), is also involved in transcription termination (Sharma and Wente, 2020) and in translation initiation and termination (Bolger *et al.*, 2008; Bolger and Wente, 2011). As well as Dbp5, GLE1 has been implicated in the regulation of another ATP-dependent DEAD-box RNA helicase, DDX1, and together they are involved in transcription termination (Sharma and Wente, 2020). Additionally, GLE1 interacts with the DEAD box protein Ded1, which unwinds RNA, to inhibit its ATPase activity, thereby inhibiting translation initiation (Bolger and Wente, 2011). Ded1 has been shown to suppress tomato bushy stunt virus RNA recombination and maintain viral genome integrity (Chuang, Prasanth and Nagy, 2015); therefore, PRRSV NSP1β could use GLE1 to target Ded1 for similar purposes. GLE1 also interacts with the eukaryotic translation initiation factor (eIF) 3 (eIF3) complex (Bolger *et al.*, 2008), and is required for efficient translation termination and interacts with translation termination factors, such as Sup45 and Sup35 in yeast (Bolger *et al.*, 2008). The multiple roles occupied by GLE1 in transcription and

termination make it a likely target for PRRSV, as interacting with GLE1 would help it to control host protein expression and could help viral replication.

Proteins functioning in translation, including eIF-3 subunit K, which like GLE1 is involved in translation initiation (Hinnebusch, 2006), were confirmed to interact with NSP1β (**Figure 4.4**) and multiple ribosomal subunits, including 40S subunits, were identified in both y-2-h screens (ribosomal section in **Table 9.1** and **Table 9.2**). Interestingly, the eIF-3 complex binds to the ribosomal 40s subunit (Kolupaeva *et al.*, 2005). PRRSV interacting with host cell translational machinery could be a strategy to maximise PRRSV protein expression. Given NSP1α and NSP1β are the first two viral proteins translated during infection (den Boon et al., 1995; Fang and Snijder, 2010), it is feasible to suggest that they would target ribosomes and replication machinery to influence production of the other viral NSPs and structural proteins. The interactions between NSP1α and NSP1β with the ribosomal subunits need to be confirmed, but it should be noted that ribosomal proteins have been identified in previous y-2-h screens conducted by the Molecular Virology Group (The Pirbright Institute) and shown to be false positives (unpublished data). PRRSV targets host translation machinery to induce host translation shut off through eIF2α phosphorylation-dependent pathways and, using NSP2, eIF2α phosphorylation-independent pathways (Li, Fang, et al., 2018). Additionally, PRRSV-2 induces phosphorylation of eIF2α, leading to formation of stress granules (Zhou *et al.*, 2017), which have been shown to be in close proximity to the RTC and are associated with host translation shut off (Catanzaro and Meng, 2019). NSP1α and NSP1β have not been implicated in any of this, but the interactions identified in this study, and the importance of host translation shut off to viral replication, suggest they may also manipulate translation. PRRSV translation has not been shown previously to require eIF2α, but given eIF2α complexes with eIF-3 and this complex is involved in translation initiation (Asano *et al.*, 2000; Jivotovskaya *et al.*, 2006), it is possible that PRRSV does use it. Other viruses target the eIF-3 complex: Hepatitis C virus uses an internal ribosome entry site (IRES) to prevent eIF-3 binding to the 40S ribosomal subunit, and therefore enhance translation of viral mRNAs (Hashem *et al.*, 2013). Classical swine fever virus non-structural protein 5A binds eIF-3 subunit E to increase

translational efficiency of the viral IRES, as well as decrease cellular translational efficiency (X. Liu *et al.*, 2018).

HSPs are molecular chaperones involved in protein folding and protein quality control (Mayer and Bukau, 2005; Qiu *et al.*, 2006). Multiple HSP family members were identified in both the NSP1α and NSP1β y-2-h screens (heat shock proteins section **Table 9.1** and **Table 9.2**). NSP1α interacted with HSC70 and DNAJA3 (**Table 9.1**), but only the latter was deemed a genuine interaction (**Figure 4.3**). NSP1β interacted with HSP10 and DNAJC10, but only the interaction with HSP10 was confirmed (**Figure 4.4**). Given that PRRSV has been shown previously to upregulate expression levels of 2 HSPs, HSP27 and the HSC70 ATPase domain (which was identified in the NSP1α y-2-h screen) (Zhang *et al.*, 2009), it is logical PRRSV would interact with these proteins.

DNAJA3, also known as HSP40 member A3 and TID-1, interacted genuinely but weakly with NSP1α (**Figure 4.3, Figure 4.6**). DNAJA3, like other HSP40 proteins, acts as a co-chaperone, binding and activating members of the HSP70 protein family for protein folding and complex assembly (Qiu *et al.*, 2006). DNAJA3 is also involved in maintaining mitochondrial membrane potential homogeneity as well as mitochondrial DNA integrity, by using its function as co-chaperone to prevent complex I accumulation (Ng, Baird and Screaton, 2014). It also binds to p53, resulting in translocation of p53 to the mitochondria, which induces intrinsic apoptosis (Trinh, Elwi and Kim, 2010).

To date PRRSV has not been reported to target DNAJA3, but HSP40 family members are used by other viruses. DNAJA3 is part of the antiviral response against foot-and-mouth disease virus (FMDV) by interacting with LC3 to induce degradation of the capsid virus protein (VP) 1 (VP1) to overcome VP1 suppression of IFN-β signalling (Zhang, Yang, *et al.*, 2019). HIV-1 Nef protein interacts with and induces expression of HSP40; this interaction increases translocation of HSP40 into the nucleus where it is involved in viral gene expression (Kumar and Mitra, 2005). Additionally, HSP40 member B1 interacts with IAV nucleoprotein in viral ribonucleoproteins and is required for efficient binding of IAV nucleoprotein and importin-α (Batra *et al.*, 2016); therefore, HSP40 is involved in nuclear import of viral ribonucleoproteins. As DNAJA3 and related proteins have both antiviral functions and roles in viral replication, PRRSV

NSP1α could target it to inhibit the antiviral response and/or facilitate viral replication.

It is worth noting PRRSV has recently been shown to interact with and use HSC70, not for protein folding but for virus internalisation and attachment (Wang *et al.*, 2022). HSC70, also referred to as HSPA8, interacts with GP4 and inhibiting this interaction inhibits attachment; HSC70 also functions in the latter stages of viral entry as it is involved in clathrin mediated endocytosis of the virus (Wang *et al.*, 2022).

HSP10 is involved in protein folding and sorting in the mitochondria (Höhfeld and Hartl, 1994); however, it has been observed elsewhere within the cell when performing alternate functions (Jia *et al.*, 2011). Deformed wing virus VP2 protein interacts with HSP10 to reduce HSP10 expression (Huang *et al.*, 2020).

Multiple HSPs, including HSP70 and HSP10, have functions in the mitochondria (Herrmann *et al.*, 1994; Höhfeld and Hartl, 1994). Although PRRSV NSP1α and NSP1β do not appear to localise to the mitochondria, it is possible that they influence the translocation of these HSPs to the mitochondria and/or target their functions in the cytoplasm.

PRRSV has been shown to interfere with host cell protein expression (Zhang *et al.*, 2009; Han *et al.*, 2017; Li, Fang, *et al.*, 2018). The interactions identified could reveal novel roles of NSP1α and NSP1β in the regulation of both host and viral transcription and translation.

5.2.3 Ubiquitination and the proteasome

Ubiquitination is an intracellular protein modification that leads to either protein degradation by the 26S proteasome or regulates protein activity in many pathways (Bednash and Mallampalli, 2016; Chen and Chen, 2012; Hicke, 2001; Tanaka, 2009). Ubiquitin itself has seven lysine (K) residues, K6, K11, K27, K29, K33, K48, K63, which along with an N-terminus M1, are used to link ubiquitin to target proteins (Komander and Rape, 2012).

The 26S proteasome is a large protein complex, made up of a 20S core particle and two 19S regulatory particles (**Figure 5.3**) (Groll *et al.*, 1997; Huang *et al.*, 2016), that regulates the degradation of proteins within the cell (Tanaka, 2009). Proteasomes are found in the cytoplasm and nucleus (Peters, Franke and Kleinschmidt, 1994; Brooks *et al.*, 2000) but are also found enriched in clastosomes (a type of nuclear body) when proteasome dependent proteolysis is stimulated by osmotic stress, infection or serum (Lafarga *et al.*, 2002).

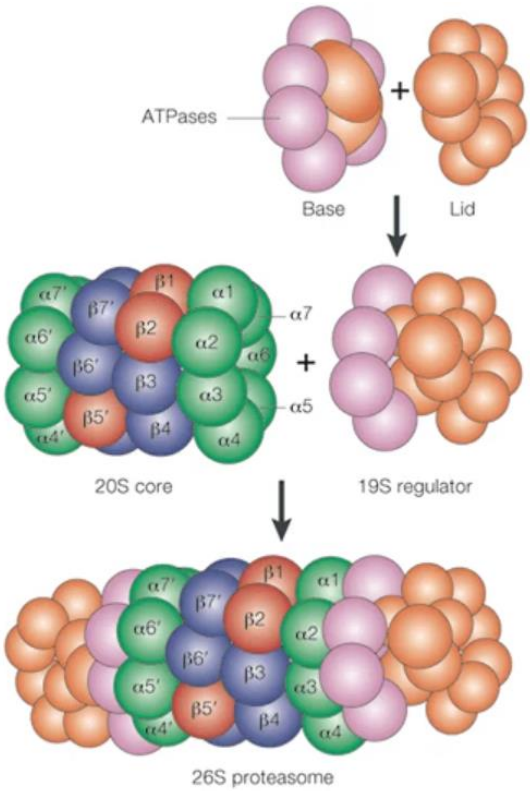

Figure 5.3: Proteasome structure. The outer rings in green are composed of α subunits (1-7), with the inner rings in purple and red made of β subunits (1-7); β1, β2 and β5 in red are catalytically active. In the immunoproteasome, these are replaced with β1i, β2i and β5i. *Figure 1, reprinted by permission from Springer Nature* (Kloetzel, 2001).

The 26S proteasome subunit S5a/Rpn10 (part of the regulatory 19S particle, **Figure 5.3**) recognises proteins with lysine-48 linked ubiquitin (Deveraux *et al.*, 1994), with the proteasome catalytic subunits cleaving the proteins into smaller peptides (Heinemeyer *et al.*, 1997; Kloetzel, 2001). Both monoubiquitination and polyubiquitination have been shown to be involved in protein activity regulation (Hicke, 2001). Monoubiquitination is key to histone regulation and therefore to gene expression (Robzyk, Recht and Osley, 2000; Hicke, 2001), as well as endocytosis (Shih, Sloper-Mould and Hicke, 2000). In the NF-κB pathway, TAB2 and TAB3 through their ZF domains bind lysine-63 polyubiquitin chains on target proteins, such as TNF receptor-associated factor 6, which is required to subsequently phosphorylate and activate TAK1 and IKK (Kanayama *et al.*, 2004).

PRRSV alters the ubiquitome of the cell, with 983 ubiquitination sites on 717 proteins shown to be altered (H. Zhang *et al.*, 2018); additionally, NSP1β is ubiquitinated. NSP1α has since been shown to be ubiquitinated by the E3 ubiquitin ligase ankyrin repeat and SOCS box-containing 8 (ASB8), which increases NSP1α stability (Li *et al.*, 2019). More recently, NSP1α, NSP7 and NSP9 together have been shown to upregulate expression of the E3 ubiquitin ligase RNF122, which ubiquitinates and stabilises NSP4 to promote PRRSV infection (Sun *et al.*, 2022). The NSP1α screen identified 3 proteins involved in ubiquitination: ubiquitin itself, the E3 ubiquitin ligase MARCH7 and ANAPC10; using y-2-h, all were confirmed as false positives (**Figure 4.3**). Y-2-h identified and confirmed that cullin-9 interacts with NSP1β (**Figure 4.4**). The cullin ring ligase family of proteins, of which cullin-9 or PARC is a member, are E3 ubiquitin ligases which transfer ubiquitin onto target proteins (Sarikas, Hartmann and Pan, 2011). Cullin-9 has only two identified substrates and its mechanism of ubiquitination is unknown (Ortolano *et al.*, 2021); its structure and complexes have also not been elucidated (Sarikas, Hartmann and Pan, 2011). Cullin-9 binds p53 and regulates its subcellular localisation (Nikolaev *et al.*, 2003). To date, no viruses have been shown to target cullin-9, however other cullin ligases have been shown to be targeted (Liu and Tan, 2020). Simian virus 5 V protein hijacks the DDB1-Cul4A ubiquitin ligase complex to degrade STATs and block interferon signalling (Li *et al.*, 2006), and HIV-1 Vpu, Vpr, Vif, and HIV-2 Vpx act as scaffold proteins to recruit and

hijack between them cullin 1, cullin 4 and cullin 5 complexes (Jäger *et al.*, 2012; Mahon *et al.*, 2014). Therefore, although all the mechanisms and proteins involved in how PRRSV modifies ubiquitination within the cell have yet to be identified, it is possible that cullin-9 is utilised and hijacked by NSP1β to achieve this.

Analysis has revealed three ubiquitinated motifs in proteins that are targeted by PRRSV: $K^{ub}XXP$, $RXXXXLXK^{ub}$ and $K^{ub}Q$, (where K = lysine; X = any amino acid; R = arginine; P = proline, Q = glutamine; L = Leucine) (H. Zhang *et al.*, 2018). The sequences of the proteins identified in both y-2-h screens were examined for these motifs (**Table 9.1**, **Table 9.2**). Motifs were observed in multiple proteins, notably DNAJA3 from the NSP1α screen (**Table 9.1**) and STAT3, TAB3 and proteasome subunits from the NSP1β screen (**Table 9.2**). Identification of these motifs in interacting proteins could provide mechanistic insight into interactions and their consequences.

The NSP1β y-2-h screen identified and confirmed interactions with multiple proteasome subunits: PSMA1, PSMB4 and PSMB8 (**Table 9.2**; α1, β4 and β5 in **Figure 5.3**); no subunits were identified in the NSP1α y-2-h screen using pGBKT7-NSP1α/β. All three subunits form part of the 20s core particle with PSMA1 part of the outer ring and PSMB4 and PSMB8 part of the inner rings (Groll *et al.*, 1997). PSMA1 and PSMB4 are non-catalytic, whereas PSMB8, also known as PSMB5i, is catalytic and only present in the immunoproteasome (Kloetzel, 2001; Tanaka, 2009).

Previous analysis has shown that PRRSV upregulates expression of PSMA1 in infected cells (Zhang *et al.*, 2009), but that PRRSV suppresses the immunoproteasome by reducing expression of the inducible subunits (Q. Liu *et al.*, 2020). The immunoproteasome processes peptides more efficiently for antigen presentation (Kloetzel, 2001; Murata *et al.*, 2018). It has the same structure as the normal proteasome, except the three catalytic subunits within the core particle are replaced with three additional β subunits (Kloetzel, 2001), one of which is PSMB8/PSMB5i. The expression of these subunits is induced by IFN-γ and TNFα (Aki *et al.*, 1994; McCarthy and Weinberg, 2015).

The PSMB8/PSMB5i active site differs to PSMB5 in the normal proteasome (Huber *et al.*, 2012). As a result, the induced proteasome subunit produces more antigenic peptides with C-terminal hydrophobic residues, which fit better in the cleft of the MHC class I molecules for antigen presentation (Huber *et al.*, 2012; Murata *et al.*, 2018).

It is interesting that immunoproteasome 20S core assembly is assisted by HSC70 and POMP (Witt *et al.*, 2000; Kloetzel, 2001), which were identified in the NSP1α and NSP1β y-2-h screens, respectively, but both were confirmed as false positives.

Given the importance of ubiquitin to many processes within the cell, the ubiquitome of the cell is altered by viruses to enhance their own replication (Gustin *et al.*, 2011). PRRSV NSP1α interacts with the ubiquitin ligase ABS8, resulting in K-63 linked polyubiquitination of NSP1α; this increases NSP1α stability, enhancing NSP1α ability to inhibit NF-κB and therefore promotes viral replication (Li *et al.*, 2019). This does not explain the altered ubiquitome of PRRSV-infected cells, implying that there are other methods and interactions between PRRSV and ubiquitin ligases that are still unidentified. Although y-2-h suggested the interaction between NSP1α and MARCH7 was a false positive (**Figure 4.3**), other methods may show the interaction to be genuine, so this could be investigated further.

The NSP1β y-2-h screen identified kelch-like protein 20, component of the BCR (BTB-CUL3-RBX1) E3 ubiquitin-protein ligase complex (Furukawa *et al.*, 2003; Wimuttisuk *et al.*, 2014). Therefore, this interaction could be how PRRSV hijacks a ubiquitin ligase to alter the ubiquitome of the cell. However, kelch-like protein 20 also negatively regulates death-associated protein kinase, which is involved in IFN-induced cell death (Lee *et al.*, 2010); so this could be a method to interfere with IFN signalling and prevent host cell death to enhance replication.

PRRSV-related nidovirus, SARS-CoV, relies on the ubiquitin-proteasome system (UPS) for entry, RNA synthesis and protein expression (Raaben *et al.*, 2010), whereas murine coronavirus uses the UPS to move from endosome to cytoplasm during entry. More recently, it has been shown PRRSV also requires the UPS for successful replication, as inhibiting proteasomes inhibited PRRSV replication (Pang *et al.*, 2021).

Given the roles of proteasomes and immunoproteasomes in protein degradation and antigen presentation, they are both utilised and targeted by viruses. PRRSV targets multiple proteins for proteasomal degradation to promote its own replication. PRRSV-2 NSP1α targets SLA-1 for degradation to reduce antigen presentation (Du *et al.*, 2016), and NSP5 from both PRRSV species mediates an increase in STAT3 polyubiquitination, resulting in STAT3 degradation (Yang *et al.*, 2017).

PRRSV interfering with ubiquitination in cells (H. Zhang *et al.*, 2018) could allow it to regulate the activation of multiple immune pathways, host gene expression and protein degradation. The additional binding of NSP1β to proteasome subunits (**Table 9.1**), in particular the immunoproteasome subunit PSMB8, could provide mechanistic detail on how PRRSV causes cellular protein degradation (Han *et al.*, 2013; Wang *et al.*, 2013; Du *et al.*, 2016; Yang *et al.*, 2017) and suppresses the immunoproteasome (Q. Liu *et al.*, 2020). Increasing our knowledge of the link between PRRSV and ubiquitination could help us to develop interventions that possibly reduce or prevent PRRSV replication.

5.2.4 Immune signalling pathways

Immune signalling pathways incorporate all the proteins: from receptors on the cell surface/within the cell which detect pathogens; to the mediator proteins involved in intracellular signalling; to the proteins expressed as a consequence of that signalling. Particularly important pathways in the antiviral response are the IFN pathway and the NF-κB pathway, as demonstrated by the numerous viruses and strategies used by viruses to manipulate these (J. Zhao *et al.*, 2015; García-Sastre, 2017). The IFN proteins are cytokines produced during viral infection that activate expression of ISGs (Schneider, Chevillotte and Rice, 2014) to limit viral replication and spread (Samuel, 2001; Takaoka *et al.*, 2003; Schmeisser, Bekisz and Zoon, 2014), as well as activating immune cells (Siegel, 1988; Lee *et al.*, 2017) and upregulating antigen presentation (Zhou, 2009). The NF-κB family of transcription factors are involved in the regulation of the immune response, inflammation, cell survival and proliferation (Oeckinghaus and Ghosh, 2009; Liu *et al.*, 2017). In particular, NF-κB is involved in the induction of inflammatory cytokines in macrophages (Wang, Liang and Zen, 2014), regulating T cell differentiation (Oh and Ghosh, 2013) and in inflammasome activation (Qiao *et al.*, 2012).

PRRSV targets both the innate and adaptive immune response using its NSPs and structural proteins (Huang, Zhang and Feng, 2015). The y-2-h screens identified multiple interactions with components of immune signalling pathways; those discussed are listed under IFN signalling pathway, NF-κB pathway, autophagy, MHC related, PRRs and intracellular transport in **Table 9.1** and **Table 9.2**.

Immune signalling pathways begin with the detection of PAMPs by PRRs (Mogensen, 2009) which ultimately leads to activation of the type I IFN and NF-κB pathways. The NSP1β screen identified and confirmed interactions with two PRRs, TLR4 and Collectin-12 (**Figure 4.4**).

TLR4 is a transmembrane PRR that recognises bacterial lipopolysaccharide (LPS) (Chow *et al.*, 1999), leading to production of type I IFNs and inflammatory cytokines (Chow *et al.*, 1999; Lu, Yeh and Ohashi, 2008). However, TLR4 has been implicated in the antiviral response against respiratory syncytial virus (Kurt-Jones *et al.*, 2000). Recently, TLR4 has been shown to be bound and activated by SARS-CoV-2 spike

protein, which increases expression of the SARS-CoV-2 entry receptor angiotensin converting enzyme-2 (Aboudounya and Heads, 2021). Using LPS to stimulate TLR4 signalling pathways reduces PRRSV infection (Zhu *et al.*, 2020). Therefore, it is possible TLR4 has an unknown antiviral function against PRRSV or a role in PRRSV entry.

The TLR4 interacting protein IFI35 (Xiahou *et al.*, 2017) was identified twice in the NSP1α screen (IFN related in **Table 9.1**). The interaction between secreted IFI35 and TLR4 leads to NF-κB activation in macrophages and promotes the inflammatory response (Xiahou *et al.*, 2017). In IFN-α stimulated cells, IFI35 interacts with N-Myc and STAT interactor, which inhibits proteasomal degradation of IFI35 (Chen *et al.*, 2000; Zhou *et al.*, 2000). IFI35 can suppress activation of the IFN-β and ISG56 promoters and interacts with RIG-I, causing its degradation (Das *et al.*, 2014). Vesicular stomatitis virus (VSV) requires IFI35 for replication because of its regulatory functions, but no direct interaction between VSV and IFI35 has yet been identified (Das *et al.*, 2014).

Y-2-h retesting suggested the interaction between NSP1α and full-length IFI35 protein was possibly a false positive, although no growth was observed using the partial IFI35 (**Figure 4.3**). This was a surprise, given the role of IFI35 is regulating NF-κB activation and IFN signalling. However, the retesting used the pGBKT7-NSP1α bait plasmid, but the pGBKT7-NSP1α/β bait plasmid was used in the original screen, so it is possible the interaction is genuine and NSP1β could be involved. Therefore, it is worth retesting the partial IFI35 prey plasmid with the pGBKT7-NSP1α/β bait plasmid in y-2-h. If PRRSV could control the activity of IFI35, it could possibly prevent IFN production and NF-κB signalling in macrophages during infection.

Collectin-12 recognises yeast and bacterial PAMPs leading to phagocytosis (Ohtani *et al.*, 2001), and can activate the alternative pathway of complement (Ma *et al.*, 2015). No interactions between PRRSV or any other viruses and collectin-12 have been reported. However, 5 members of the collectin family of proteins, mannan-binding protein, conglutinin, CL-43, and the lung-associated proteins surfactant protein (SP) A (SP-A) and SP-D bind to IAV and reduce its infectivity (Malhotra *et al.*, 1994; Malhotra and Sim, 1995). SP-A and SP-D also bind to and inhibit neuraminidase (Tecle

et al., 2007). Therefore, it is possible that collectin-12 reduces PRRSV infectivity and the interaction with NSP1β prevents this.

Some endosomal TLRs are proteolytically cleaved by cathepsins into their functional forms (Ewald *et al.*, 2011; Garcia-Cattaneo *et al.*, 2012). It is interesting that PRRSV NSP1β bound to 3 cathepsins (B, D and H) (Protease/protease related in **Table 9.2**), of which B and H cleave TLR3 (Garcia-Cattaneo *et al.*, 2012). TLR3 detects dsRNA in the cell (Alexopoulou *et al.*, 2001), which is an intermediate in PRRSV replication that persists in prolonged infections (Knoops *et al.*, 2012; Guo *et al.*, 2018). PRRSV also downregulates Cathepsin D expression during infection (Zhang *et al.*, 2009). Therefore, this could be a strategy by PRRSV to prevent the formation of functional TLRs and avoid detection.

An activator of type I IFN production, MVP, was confirmed to interact with NSP1β in y-2-h (**Figure 4.4**). MVP induces type I IFN production (Steiner *et al.*, 2006), which reduces PRRSV replication, so PRRSV in turn reduces MVP expression (Wu *et al.*, 2021). Therefore, perhaps this interaction between NSP1β and MVP explains how PRRSV targets MVP.

Proteins involved in the type I IFN and NF-κB signalling pathways, PIAS1, PIAS2 and STAT3, were identified in the y-2-h screens. NSP1α was confirmed to interact very strongly with PIAS1 (**Figure 4.7**) and strongly with PIAS2 (**Figure 4.5**). PIAS1 and PIAS2 are SUMO ligases that regulate transcription factors involved in the immune response (Shuai and Liu, 2005), including STATs and NF-κB (Liu *et al.*, 2005; Shuai, 2006). IFNs activate JAK-STAT signalling pathways, so by regulating STAT activity PIAS proteins can in turn affect IFN signalling (Liu *et al.*, 2004).

The interaction between NSP1α and PIAS1 has been reported in an unpublished paper (Song *et al.*, 2010) but no interaction with PIAS2 has been previously described. NSP1α interacting with PIAS1 was observed using two PRRSV-1 strains (215-06 and SU1-Bel, **Figure 4.7**) so it would be interesting to see if this interaction is conserved in more virulent strains and with PRRSV-2 NSP1α. PRRSV N has also been shown to bind PIAS1 in the nucleus, leading to NF-κB activation (H. Ke, Lee, *et al.*, 2019). PRRSV NSP1α has been shown to inhibit NF-κB signalling in numerous ways (Song, Krell and

Yoo, 2010; Jing *et al.*, 2016; Li *et al.*, 2019). NSP1α hijacks ASB8 which ubiquitinates IKKβ leading to its degradation (Li *et al.*, 2019), as well as inhibiting IκBα phosphorylation and degradation, thereby preventing NF-κB nuclear translocation (Song, Krell and Yoo, 2010); both of which prevent NF-κB activation. NSP1α also suppresses type I IFN induction through causing degradation of CBP (Han *et al.*, 2013). Therefore, it is likely that the interactions with PIAS1 and PIAS2 are another method of NSP1α inhibiting NF-κB activation or IFN signalling.

NSP1β was observed to interact with STAT3 (**Figure 4.4**), a transcription factor whose activity is regulated by PIAS proteins (Chung *et al.*, 1997; Shuai and Liu, 2005). STAT3 is activated in response to numerous cytokines (Niemand *et al.*, 2003; Stout *et al.*, 2004; Kuchipudi, 2015) and regulates the activity of genes involved in many functions including cell survival, the immune response and cell proliferation (Hirano, Ishihara and Hibi, 2000; Levy and Lee, 2002; Kuchipudi, 2015). Specific roles in the immune response include negatively regulating the type I IFN response activated by STAT1 (Ho and Ivashkiv, 2006), regulating inflammatory Th cell differentiation (Yang *et al.*, 2007) and promoting T cell proliferation by preventing apoptosis (Takeda *et al.*, 2015). Therefore, targeting STAT3 would give PRRSV the potential to regulate multiple cellular processes. PRRSV NSP5 causes STAT3 degradation but does not interact with it (Yang *et al.*, 2017), so it is possible that NSP1β is involved in this.

Neither PIAS1 or PIAS2 (also known as PIASx) have been shown to interact with STAT3, instead they regulate STAT1 and STAT4, respectively (B Liu et al., 1998; Arora et al., 2003; Shuai and Liu, 2005). PRRSV NSP1β has been shown to prevent STAT1 and STAT2 nuclear translocation by causing importin KPNA1 degradation (Patel *et al.*, 2010). Therefore, perhaps PRRSV uses NSP1β to control STAT3 activity directly (through binding STAT3), as well as regulating STAT1 and STAT2 indirectly (through KPNA1). Additionally, NSP1α interacting with both PIAS1 and PIAS2 may enable PRRSV to control STAT1 and STAT4 proteins indirectly. Therefore, PRRSV could use NSP1α and NSP1β to maximise its control over JAK-STAT signalling.

A regulator of both NF-κB activation and autophagy, TAB3 was identified and confirmed as a weak interactor of NSP1β (**Figure 4.4, Figure 4.8**). TAB3 functions in the NF-κB pathway and together with TAB2 binds and activates TAK1 (Cheung,

Nebreda and Cohen, 2004), resulting in downstream activation of the NF-κB pathway (Jin *et al.*, 2003; Kanayama *et al.*, 2004). Additionally, TAB3 negatively regulates autophagy through its interaction with beclin-1 (Criollo *et al.*, 2011; Takaesu, Kobayashi and Yoshimura, 2012) .

PRRSV has not been shown to target TAB3 previously but multiple PRRSV proteins, including NSP1α (discussed previously), NSP4 (Chen *et al.*, 2019) and NSP11 (Shi *et al.*, 2011) manipulate NF-κB signalling. Other viruses target the TAK1-TAB2-TAB3 complex, with enterovirus 71 3C protein binding to and cleaving the components (including TAB3) (Lei *et al.*, 2014) to inhibit NF-κB signalling. Therefore, inhibiting this transcription factor is important to PRRSV, and other viruses, so it is likely this interaction with TAB3 could be another strategy to prevent NF-κB activation.

The TAB3 interacting protein beclin-1 was also confirmed to interact with NSP1β (**Figure 4.4**), and its cytoplasmic distribution was potentially altered in the presence of NSP1β in Max cells (**Figure 4.33**), which could impair its ability to function. Beclin-1 regulates autophagy (Kihara *et al.*, 2001; Kang *et al.*, 2011), the lysosomal degradation pathway of cellular components (Dunn, 1994), as part of the class III phosphatidylinositol 3-kinase complex involved in inducing autophagosome formation (Kihara *et al.*, 2001; Kang *et al.*, 2011). Beclin-1 also interacts with the anti-apoptotic protein Bcl-2 (Liang *et al.*, 1998), which prevents beclin-1 activating autophagy (Pattingre *et al.*, 2005) but does not affect the ability of Bcl-2 to inhibit apoptosis (Ciechomska *et al.*, 2009). However, this interaction demonstrates a possible link between autophagy and apoptosis (Kang *et al.*, 2011), as beclin-1 has also been shown to have anti-apoptotic functions and is cleaved by caspases during apoptosis (Djavaheri-Mergny, Maiuri and Kroemer, 2010). In PRRSV-infected cells, autophagy postpones apoptosis through beclin-1 binding to the pro-apoptotic protein Bcl 2 associated agonist of cell death (Bad), both of which are upregulated by PRRSV, but no change in beclin-1 binding to Bcl-2 was observed (Zhou *et al.*, 2016). Given NSP1β binds beclin-1, it is possible NSP1β helps to promote the interaction between beclin-1 and Bad or is involved in regulating their expression. PRRSV has also been shown to delay apoptosis during the early stages of infection, then later to induce apoptosis (Costers *et al.*, 2008; Yuan *et al.*, 2016), with NSP4 and NSP10

inducing apoptosis but not through targeting Bcl-2 (Yuan *et al.*, 2016); GP5 has also been shown to be pro-apoptotic (Suárez *et al.*, 1996). However, Bcl-2 expression has been shown previously to be reduced in PRRSV infection during apoptosis (Lee and Kleiboeker, 2007) in a time dependent manner (Yin *et al.*, 2012). Therefore, perhaps NSP1β binding beclin-1 is a novel approach to target the anti-apoptotic Bcl-2, either to inhibit apoptosis early in infection or to reduce its expression and induce apoptosis later in infection.

TAB3 binds to beclin-1 and negatively regulates autophagy (Criollo *et al.*, 2011; Takaesu, Kobayashi and Yoshimura, 2012). Activation of autophagy causes TAB2 and TAB3 to dissociate from beclin-1 and bind to TAK-1 in the cytoplasm instead (Niso-Santano *et al.*, 2012). Autophagy is an important pathway to PRRSV, as NSP2, NSP3 and NSP5 together induce incomplete autophagy in infected cells to increase viral replication (Sun *et al.*, 2012; Zhang, Chen, *et al.*, 2019). PRRSV NSP1β binding to both TAB3 and beclin-1 could promote their interaction, which would therefore prevent TAB3 activating TAK-1 and NF-κB, whilst simultaneously inhibiting autophagy. This is interesting, as PRRSV has been shown to induce autophagy (Sun *et al.*, 2012) rather than inhibit it. FMDV virus 2C protein binds to beclin-1 and prevents it from causing fusion of the autophagosome and lysosome, which enhances viral replication (Gladue *et al.*, 2012). It is postulated that the autophagosome provides a replication site for PRRSV and during infection incomplete autophagy (no autophagosome and lysosome fusion) has been observed (Sun *et al.*, 2012); therefore, perhaps NSP1β behaves similarly to FMDV 2C.

As well as the innate response, PRRSV interferes with the adaptive: PRRSV NSP1α and NSP4 have both been shown to target SLA-I (porcine MHC) for degradation (Du *et al.*, 2016; Qi *et al.*, 2017) to reduce antigen presentation. This project confirmed NSP1β interacts with porcine MHC class II in a section containing the α domain (**Figure 4.4**). This therefore could be another strategy of PRRSV to avoid detection and reduce antigen presentation by degrading MHC class II, especially as NSP1β also binds proteasomal subunits, so could target this protein for proteasomal degradation.

Given the importance of the IFN and NF-κB pathways in the antiviral response, it is logical for PRRSV to target these in numerous ways. What we currently know about

PRRSV immunomodulation is not enough, given the lack of effective vaccines (Nan *et al.*, 2017). Therefore, this analysis and the interactions identified could be used to elucidate novel mechanisms of PRRSV immunomodulation.

5.3 Conclusion

Although the pathways have been discussed individually, many of the proteins identified in the y-2-h screen are multifunctional and are involved in multiple processes, such as GLE1. Therefore, by interacting with one of these PAM proteins, PRRSV can target multiple cellular pathways, but this does make it more difficult to unravel the true function of an interaction.

This analysis will be used to correlate identified interactions with known NSP functions, or to speculate new ones, and to identify their role in the PRRSV life cycle as well as to establish their relevance to immunomodulation. Using this information, we can design specific future experiments to further our understanding of PRRSV. Increasing our understanding of how PRRSV modulates the immune response will aid vaccine and antiviral design.

Chapter 6: Future Work

This project identified a large list of putative interacting proteins for PRRSV-1 NSP1α (**Table 9.1**) and NSP1β (**Table 9.2**) and confirmed a selection of these (**Figure 4.3, Figure 4.4**). Only NSP1s from a single PRRSV-1 strain, except for testing the interaction between SU1-Bel NSP1α and PIAS1 (**Figure 4.7**), were tested. Therefore, y-2-h retesting could be repeated using NSP1α and NSP1β from PRRSV-1 SU1-Bel, as well from PRRSV-2 strains, to see if the interaction is conserved across subtypes and species. If different strains interact differently with specific proteins, this could be a factor affecting their virulence. Additionally, y-2-h retesting of proteins identified in the NSP1α screen using the pGBKT7-NSP1α/β bait plasmid, or yeast-3-hybrid using NSP1α and NSP1β individual plasmids, needs to be performed to see if the results differ to using pGBKT7-NSP1α alone; this is to test if NSP1β is involved in those interactions.

The PAM proteins identified in the y-2-h were not full-length proteins, as the cDNAs from the PAM library cloned into pACT2 were not all full-length. This was for 2 reasons: the in vitro reverse transcription process during cDNA synthesis produced a high proportion of incomplete negative RNA strands, and the cDNA library was size fractionated to "standardise" ligation. Although this is useful, as it helps to identify the region of the PAM proteins involved in the interaction, it can affect protein stability, expression, and subcellular localisation. Therefore, confocal immunofluorescence microscopy and co-immunoprecipitations along with other characterisation experiments should be tried with full-length proteins as well.

All the work in this project involved investigating interactions in transformed or transfected cells; no work was carried out in PRRSV-infected cells. To investigate the interactions in the context of infection, and potentially see their role in the viral life cycle, confocal immunofluorescence microscopy and co-immunoprecipitations should be tried in infected cells. This would be harder to do, as specific antibodies against NSP1α, NSP1β and PAM proteins would be required, which are either not commercially available or not good enough. Using human cells, such as HEK-293-TLR3, could solve the issue of detecting PAM proteins as there are better antibodies available against specific human proteins than pig proteins. However, the

interactions between NSP1α or NSP1β and the human orthologue would need to be confirmed first. Additionally, within our group, a reverse genetic system for PRRSV has been developed; current research is trying to clone tags onto NSP1α and NSP1β within the genome. If successful, this would generate an infectious PRRSV clone with tagged NSPs; this would be extremely useful for detecting and pulling down NSP1α and NSP1β in infected cells.

Although the interacting regions of the PAM proteins have been broadly deduced, it is still unknown which regions or motifs within NSP1α and NSP1β are involved in interactions. This information is extremely important, as it could be used to mutate NSP1 and abolish the interactions, which may help rationally attenuate PRRSV. Therefore, any/all of the approaches to identify the interactions could be performed using specific tagged domains of NSP1α or NSP1β or using NSP1 sequence mutants e.g., mutate the SAP motif in NSP1β (Ke *et al.*, 2018). Once the region or residues involved have been identified, deletions or mutations could be introduced into the infectious PRRSV clone to see the consequence of abolishing the interaction on viral replication.

Further experiments to confirm the interactions identified by other methods should be tried. GFP-Trap pulldowns partnered with mass spectrometry, used previously by other members of the group (Jourdan, Osorio and Hiscox, 2012), could be used to screen for NSP1α and NSP1β interactions. The resulting list would then be compared to the y-2-h data to see if the same proteins appear, as well as additional novel unidentified interactions. Co-immunoprecipitations using Myc-NSP1α and Myc-NSP1β and the FLAG-tagged PAM proteins could also be performed; both Myc and FLAG pulldowns should be trialled to identify the interaction in HEK-293-TLR3 cells. Unfortunately, due to time constraints, these approaches could not be tested, but they could provide more evidence to support the interactions identified or confirmed by y-2-h.

The effect of the interactions on specific pathways should also be investigated. NSP1α interacts with PIAS1 and PIAS2, which both regulate IFN signalling (Shuai and Liu, 2005) and the protein TAB3, which interacts with NSP1β (**Figure 4.4**), functions in the NF-κB pathway (Kanayama *et al.*, 2004). Luciferase assays use reporter genes from

different signalling pathways. Therefore, an NF-κB luciferase reporter could be used with NSP1β, and an IFN luciferase reporter with NSP1α, to see the effect on NF-κB activation and IFN signalling, respectively, and identify the parts of the pathways targeted. Additionally, western blotting and reverse transcription PCR could be used to analyse protein expression of components of the pathway in transfected or infected cells. This would help to elucidate the consequences of the interaction and help to provide mechanistic detail.

Possible alterations could include trialling different amounts and ratios of DNA in transfections, altering incubation times for transfections, infecting cells, activating/inhibiting certain pathways, or inducing specific cell environments (e.g., hypoxia) and testing new antibodies.

This project has provided the groundwork for the future work needed to further investigate immunomodulation by PRRSV-1 NSP1α and NSP1β.

Chapter 7: Conclusion

The interactions identified and investigated in this study between PAM proteins and PRRSV NSP1α or NSP1β have increased our knowledge of PRRSV NSPs. This list, in combination with the future work described, could help to reveal novel functions of the respective PRRSV proteins, as well as provide mechanistic detail to previously published immunomodulatory functions. This information would be crucial in rationally attenuating PRRSV for use in vaccines, and therefore in combating one of the economically most important infectious diseases affecting the global pig industry.

Chapter 8: References

Aboudounya, M.M. and Heads, R.J. (2021) "COVID-19 and Toll-Like Receptor 4 (TLR4): SARS-CoV-2 May Bind and Activate TLR4 to Increase ACE2 Expression, Facilitating Entry and Causing Hyperinflammation," *Mediators Inflammation*, 2021. doi:10.1155/2021/8874339.

Adachi, A., Liu, W., James, J., Jiao, P., Liao, M., Zu, S., Xue, Q., He, Z., Shi, C., Zhang, J., Wu, W., Li, W., Liu, Z. and Huang, J. (2020) "Duck PIAS2 Promotes H5N1 Avian Influenza Virus Replication Through Its SUMO E3 Ligase Activity," *Front. Microbiol*, 11, p. 1246. doi:10.3389/fmicb.2020.01246.

Adachi, Y., Copeland, T.D., Hatanaka, M. and Oroszlan, S. (1993) "Nucleolar targeting signal of Rex protein of human T-cell leukemia virus type I specifically binds to nucleolar shuttle protein B-23.," *J. Biochem*, 268(19), pp. 13930–4.

Adams, R.L., Mason, A.C., Glass, L., Aditi and Wente, S.R. (2017) "Nup42 and IP6 coordinate Gle1 stimulation of Dbp5/DDX19B for mRNA export in yeast and human cells," *Traffic*, 18(12), pp. 776–790. doi:10.1111/tra.12526.

Ahmed, A.U. (2011) 'An overview of inflammation: mechanism and consequences', *Front. Biol*, 6(4), p. 274. Available at: https://doi.org/10.1007/s11515-011-1123-9.

Ahn, B.Y., Trinh, D.L.N., Zajchowski, L.D., Lee, B., Elwi, A.N. and Kim, S.W. (2010) "Tid1 is a new regulator of p53 mitochondrial translocation and apoptosis in cancer," *Oncogene*, 29(8), pp. 1155–1166. doi:10.1038/onc.2009.413.

Aki, M., Shimbara, N., Takashina, M., Akiyama, K., Kagawa, S., Tamura, T., Tanahashi, N., Yoshimura, T., Tanaka, K. and Ichihara, A. (1994) "Interferon-γ Induces Different Subunit Organizations and Functional Diversity of Proteasomes1," *J. Biochem*, 115(2), pp. 257–269. doi:10.1093/oxfordjournals.jbchem.a124327.

Ala, A., Dhillon, A.P. and Hodgson, H.J. (2003) 'Role of cell adhesion molecules in leukocyte recruitment in the liver and gut', *Int. J. Exp. Pathol.*, 84(1), p. 1. Available at: https://doi.org/10.1046/J.1365-2613.2003.00235.X.

Albina, E., Carrat, C. and Charley, B. (1998) "Interferon-α response to swine arterivirus (PoAV), the porcine reproductive and respiratory syndrome virus," *J. Interferon Cytokine Res*, 18(7), pp. 485–490. doi:10.1089/jir.1998.18.485.

Alexopoulou, L., Holt, A.C., Medzhitov, R. and Flavell, R.A. (2001) "Recognition of double-stranded RNA and activation of NF-kappaB by Toll-like receptor 3," *Nature*, 413(6857), pp. 732–738. doi:10.1038/35099560.

An, T.-Q., Li, J.-N., Su, C.-M. and Yoo, D. (2020) "Molecular and Cellular Mechanisms for PRRSV Pathogenesis and Host Response to Infection," *Virus Res*, p. 197980. doi:10.1016/j.virusres.2020.197980.

Aravind, L. and Koonin, E. v. (2000) "SAP - a putative DNA-binding motif involved in chromosomal organization," *Trends Biosci*, 25(3), pp. 112–114. doi:10.1016/S0968-0004(99)01537-6.

Arnold, M., Nath, A., Hauber, J. and Kehlenbach, R.H. (2006) “Multiple Importins Function as Nuclear Transport Receptors for the Rev Protein of Human Immunodeficiency Virus Type 1 *,” *J. Biol. Chem*, 281(30), pp. 20883–20890. doi:10.1074/jbc.m602189200.

Arora, T., Liu, B., He, H., Kim, J., Murphy, T.L., Murphy, K.M., Modlin, R.L. and Shuai, K. (2003) “PIASx is a transcriptional co-repressor of signal transducer and activator of transcription 4,” *J. Biol. Chem*, 278(24), pp. 21327–21330. doi:10.1074/JBC.C300119200.

Article, E., Liu, R.Z., Wu, S.-W., Lei, C.-Q., Zhou, Q., Li, S., Shu, H.-B. and Wang, Y.-Y. (2013) “Protein Cell & Protein Cell Heat shock cognate 71 (HSC71) regulates cellular antiviral response by impairing formation of VISA aggregates,” *Protein Cell*, 4(5), pp. 373–382. doi:10.1007/s13238-013-3902-3.

Arts, G.J., Kuersten, S., Romby, P., Ehresmann, B. and Mattaj, I.W. (1998) “The role of exportin-t in selective nuclear export of mature tRNAs.,” *EMBO J*, 17(24), p. 7430. doi:10.1093/EMBOJ/17.24.7430.

Asano, K., Clayton, J., Shalev, A. and Hinnebusch, A.G. (2000) “A multifactor complex of eukaryotic initiation factors, eIF1, eIF2, eIF3, eIF5, and initiator tRNA(Met) is an important translation initiation intermediate in vivo,” *Genes Dev*, 14(19), pp. 2534–2546. doi:10.1101/GAD.831800.

Ashraf, M.A. and Nookala, V. (2022) ‘Biochemistry of Platelet Activating Factor’, *StatPearls* [Preprint]. Available at: https://www.ncbi.nlm.nih.gov/books/NBK557392/ (Accessed: 26 August 2022).

Balka, G., Podgórska, K., Brar, M.S., Bálint, Á., Cadar, D., Celer, V., Dénes, L., Dirbakova, Z., Jedryczko, A., Márton, L., Novosel, D., Petrović, T., Sirakov, I., Szalay, D., Toplak, I., Leung, F.C.-C. and Stadejek, T. (2018) “Genetic diversity of PRRSV 1 in Central Eastern Europe in 1994–2014: origin and evolution of the virus in the region,” *Sci. Rep*, 8(1), p. 7811. doi:10.1038/s41598-018-26036-w.

Barabino, S.M.L., Hübner, W., Jenny, A., Minvielle-Sebastia, L. and Keller, W. (1997) “The 30-kD subunit of mammalian cleavage and polyadenylation specificity factor and its yeast homolog are RNA-binding zinc finger proteins.,” *Genes Dev*, 11(13), pp. 1703–1716. doi:10.1101/GAD.11.13.1703.

Bartel, P., Chien, C.T., Sternglanz, R. and Fields, S. (1993) “Elimination of false positives that arise in using the two-hybrid system,” *Biotechniques*, 14(6), pp. 920–924.

Bassaganya-Riera, J., Thacker, B.J., Yu, S., Strait, E., Wannemuehler, M.J. and Thacker, E.L. (2004) “Impact of Immunizations with Porcine Reproductive and Respiratory Syndrome Virus on Lymphoproliferative Recall Responses of CD8+ T Cells,” *Viral Immunol*, 17(1), pp. 25–37. doi:10.1089/088282404322875430.

Batra, J., Tripathi, S., Kumar, A., Katz, J.M., Cox, N.J., Lal, R.B., Sambhara, S. and Lal, S.K. (2016) “Human Heat shock protein 40 (Hsp40/DnaJB1) promotes influenza A virus replication by assisting nuclear import of viral ribonucleoproteins,” *Sci. Rep, 2016 6:1*, 6(1), pp. 1–15. doi:10.1038/srep19063.

Baumann, A., Mateu, E., Murtaugh, M.P. and Summerfield, A. (2013) “Impact of genotype 1 and 2 of porcine reproductive and respiratory syndrome viruses on interferon-α responses

by plasmacytoid dendritic cells," *Vet. Res.*, 44(1), pp. 1–10. Available at: https://doi.org/10.1186/1297-9716-44-33/FIGURES/5.

Bautista, E.M., Faaberg, K.S., Mickelson, D. and McGruder, E.D. (2002) "Functional properties of the predicted helicase of porcine reproductive and respiratory syndrome virus," *Virology*, 298(2), pp. 258–270. doi:10.1006/viro.2002.1495.

Becskei, A. and Mattaj, I.W. (2003) "The strategy for coupling the RanGTP gradient to nuclear protein export," *PNAS*, 100(4), pp. 1717–1722. doi:10.1073/pnas.252766999

Beltrame, M.H., Catarino, S.J., Goeldner, I., Boldt, A.B.W. and Reason, I.J. de M. (2014) 'The Lectin Pathway of Complement and Rheumatic Heart Disease', *Front. Pediatr.*, 2(JAN), p. 21. Available at: https://doi.org/10.3389/FPED.2014.00148.

Benfield, D.A. and Nelson, E. (1992) "Characterization of swine infertility and respiratory syndrome (SIRS) virus (isolate ATCC VR-2332)," *J. Vet. Diagn. Invest*, 4(2), pp. 127–133. doi:10.1177/104063879200400202.

Beura, L.K., Dinh, P.X., Osorio, F.A. and Pattnaik, A.K. (2011) "Cellular Poly(C) Binding Proteins 1 and 2 Interact with Porcine Reproductive and Respiratory Syndrome Virus Nonstructural Protein 1 and Support Viral Replication," *J. Virol*, 85(24), pp. 12939–12949. doi:10.1128/JVI.05177-11.

Beura, L.K., Sarkar, S.N., Kwon, B., Subramaniam, S., Jones, C., Pattnaik, A.K. and Osorio, F.A. (2010) "Porcine reproductive and respiratory syndrome virus nonstructural protein 1beta modulates host innate immune response by antagonizing IRF3 activation.," *J. Virol*, 84(3), pp. 1574–84. doi:10.1128/JVI.01326-09.

Biterova, E., Ignatyev, A., Uusimaa, J., Hinttala, R. and Ruddock, L.W. (2018) "Structural analysis of human NHLRC2, mutations of which are associated with FINCA disease," *PLoS One*, 13(8), p. e0202391. doi:10.1371/journal.pone.0202391.

Blanchette, J., Jaramillo, M. and Olivier, M. (2003) 'Signalling events involved in interferon-γ-inducible macrophage nitric oxide generation', *Immunology*, 108(4), p. 513. Available at: https://doi.org/10.1046/J.1365-2567.2003.01620.X.

Bohnsack, M.T., Regener, K., Schwappach, B., Saffrich, R., Paraskeva, E., Hartmann, E. and Görlich, D. (2002) "Exp5 exports eEF1A via tRNA from nuclei and synergizes with other transport pathways to confine translation to the cytoplasm," *EMBO J*, 21(22), p. 6205. doi:10.1093/EMBOJ/CDF613.

Bolger, T.A., Folkmann, A.W., Tran, E.J. and Wente, S.R. (2008) "The mRNA Export Factor Gle1 and Inositol Hexakisphosphate Regulate Distinct Stages of Translation," *Cell*, 134(4), pp. 624–633. doi:10.1016/j.cell.2008.06.027.

Bolger, T.A. and Wente, S.R. (2011) "Gle1 Is a Multifunctional DEAD-box Protein Regulator That Modulates Ded1 in Translation Initiation," *J. Biol. Chem.*, 286(46), p. 39750. doi:10.1074/JBC.M111.299321.

den Boon, J.A., Faaberg, K.S., Meulenberg, J.J., Wassenaar, A.L., Plagemann, P.G., Gorbalenya, A.E. and Snijder, E.J. (1995) "Processing and evolution of the N-terminal region of the arterivirus replicase ORF1a protein: identification of two papainlike cysteine proteases.," *J. Virol*, 1995;69(7):4500-4505. doi:10.1128/JVI.69.7.4500-4505.1995

den Boon, J.A., Snijder, E.J., Chirnside, E.D., de Vries, A.A., Horzinek, M.C. and Spaan, W.J. (1991) "Equine arteritis virus is not a togavirus but belongs to the coronaviruslike superfamily.," *J. Virol*, 65(6), pp. 2910–2920. doi:10.1128/jvi.65.6.2910-2920.1991.

Bøtner, A., Strandbygaard, B., Sørensen, K.J., Have, P., Madsen, K.G., Madsen, E.S. and Alexandersen, S. (1997) "Appearance of acute PRRS-like symptoms in sow herds after vaccination with a modified live PRRS vaccine," *Vet. Rec*, 141(19), pp. 497–499. doi:10.1136/vr.141.19.497.

van Breedam, W., Delputte, P.L., van Gorp, H., Misinzo, G., Vanderheijden, N., Duan, X. and Nauwynck, H.J. (2010) "Porcine reproductive and respiratory syndrome virus entry into the porcine macrophage," *J. Gen. Virol,* Jul;91(Pt 7):1659-67. doi: 10.1099/vir.0.020503-0.

Brooks, P., Fuertes, G., Murray, R.Z., Bose, S., Knecht, E., Rechsteiner, M.C., Hendil, K.B., Tanaka, K., Dyson, J. and Rivett, A.J. (2000) "Subcellular localization of proteasomes and their regulatory complexes in mammalian cells.," *Biochem. J*, 346(Pt 1), p. 155. doi:10.1042/0264-6021:3460155.

Brown, J.R., Conn, K.L., Wasson, P., Charman, M., Tong, L., Grant, K., McFarlane, S. and Boutell, C. (2016) "SUMO Ligase Protein Inhibitor of Activated STAT1 (PIAS1) Is a Constituent Promyelocytic Leukemia Nuclear Body Protein That Contributes to the Intrinsic Antiviral Immune Response to Herpes Simplex Virus 1," *J. Virol*, 90(13), pp. 5939–5952. doi: 10.1128/JVI.00426-16.

Brückner, A., Polge, C., Lentze, N., Auerbach, D. and Schlattner, U. (2009) "Yeast two-hybrid, a powerful tool for systems biology," *Int. J. Mol. Sci*, pp. 2763–2788. doi:10.3390/ijms10062763.

Buchholz, U.J., Finke, S. and Conzelmann, K.-K. (1999) "Generation of Bovine Respiratory Syncytial Virus (BRSV) from cDNA: BRSV NS2 Is Not Essential for Virus Replication in Tissue Culture, and the Human RSV Leader Region Acts as a Functional BRSV Genome Promoter," *J. Virol*, 73(1), p. 251. doi:10.1128/jvi.73.1.251-259.1999.

Burkard, C., Lillico, S.G., Reid, E., Jackson, B., Mileham, A.J., Ait-Ali, T., Whitelaw, C.B.A. and Archibald, A.L. (2017) "Precision engineering for PRRSV resistance in pigs: Macrophages from genome edited pigs lacking CD163 SRCR5 domain are fully resistant to both PRRSV genotypes while maintaining biological function," *PLoS Pathog*, 13(2). doi:10.1371/journal.ppat.1006206.

Calvert, J.G., Slade, D.E., Shields, S.L., Jolie, R., Mannan, R.M., Ankenbauer, R.G. and Welch, S.-K.W. (2007) "CD163 Expression Confers Susceptibility to Porcine Reproductive and Respiratory Syndrome Viruses," *J. Virol*, 81(14), pp. 7371–7379. doi:10.1128/jvi.00513-07.

Catanzaro, N. and Meng, X.J. (2019) "Porcine reproductive and respiratory syndrome virus (PRRSV)-induced stress granules are associated with viral replication complexes and suppression of host translation," *Virus Res*, 265, pp. 47–56. doi: 10.1016/j.virusres.2019.02.016

Cavanagh, D. (1997) "Nidovirales: a new order comprising Coronaviridae and Arteriviridae.," *Arch. Virol*, 142(3), pp. 629–633.

Chang, X.B., Yang, Y.Q., Gao, J.C., Zhao, K., Guo, J.C., Ye, C., Jiang, C.G., Tian, Z.J., Cai, X.H., Tong, G.Z. and An, T.Q. (2018) "Annexin A2 binds to vimentin and contributes to porcine

reproductive and respiratory syndrome virus multiplication," *Vet. Res*, 49(1), pp. 1–12. doi:10.1186/S13567-018-0571-5

Charerntantanakul, W. (2012) "Porcine reproductive and respiratory syndrome virus vaccines: Immunogenicity, efficacy and safety aspects," *World J Virol*, 1(1), p. 23. doi:10.5501/wjv.v1.i1.23.

Chen, J. and Chen, Z.J. (2012) "Regulation of NF-κB by Ubiquitination." *Curr. Opin. Immunol*, 2013 Feb;25(1):4-12. doi:10.1016/j.coi.2012.12.005.

Chen, J., Shpall, R.L., Meyerdierks, A., Hagemeier, M., Bottger, E.C. and Naumovski, L. (2000) "Interferon-inducible Myc/STAT-interacting Protein Nmi Associates with IFP 35 into a High Molecular Mass Complex and Inhibits Proteasome-mediated Degradation of IFP 35 *," *J. Biol. Chem*, 275(46), pp. 36278–36284. doi:10.1074/jbc.m006975200.

Chen, J., Wang, D., Sun, Z., Gao, L., Zhu, X., Guo, J., Xu, S., Fang, L., Li, K. and Xiao, S. (2019) "Arterivirus nsp4 Antagonizes Interferon Beta Production by Proteolytically Cleaving NEMO at Multiple Sites," *J. Virol*, 93(12), pp. 385–404. doi:10.1128/jvi.00385-19.

Chen, Z., Lawson, S., Sun, Z., Zhou, X., Guan, X., Christopher-Hennings, J., Nelson, E.A. and Fang, Y. (2010) "Identification of two auto-cleavage products of nonstructural protein 1 (nsp1) in porcine reproductive and respiratory syndrome virus infected cells: nsp1 function as interferon antagonist," *Virology*, 398(1), pp. 87–97. doi:10.1016/j.virol.2009.11.033.

Chen, Z., Liu, S., Sun, W., Chen, L., Yoo, D., Li, F., Ren, S., Guo, L., Cong, X., Li, J., Zhou, S., Wu, J., Du, Y. and Wang, J. (2016) "Nuclear export signal of PRRSV NSP1α is necessary for type I IFN inhibition," *Virology*, 499, pp. 278–287. doi:10.1016/j.virol.2016.07.008.

Cheung, P.C.F., Nebreda, A.R. and Cohen, P. (2004) "TAB3, a new binding partner of the protein kinase TAK1," *Biochem. J*, 378(1), pp. 27–34. doi:10.1042/BJ20031794.

Chiu, M.L., Goulet, D.R., Teplyakov, A. and Gilliland, G.L. (2019) 'Antibody Structure and Function: The Basis for Engineering Therapeutics', *Antibodies*, 8(4), p. 55. Available at: https://doi.org/10.3390/ANTIB8040055.

Choi, K., Lee, J., Park, C., Jeong, J. and Chae, C. (2015) "Comparison of the Pathogenesis of Single or Dual Infections with Type 1 and Type 2 Porcine Reproductive and Respiratory Syndrome Virus," *J. Comp. Pathol*, 152(4), pp. 317–324. Available at: https://doi.org/10.1016/j.jcpa.2015.03.002.

Chow, J.C., Young, D.W., Golenbock, D.T., Christ, W.J. and Gusovsky, F. (1999) "Toll-like receptor-4 mediates lipopolysaccharide-induced signal transduction," *J. Biol. Chem*, 274(16), pp. 10689–10692. doi:10.1074/JBC.274.16.10689.

Chu, J.J.H. and Ng, M.L. (2004) "Interaction of West Nile Virus with αvβ3 Integrin Mediates Virus Entry into Cells *," *J. Biol. Chem*, 279(52), pp. 54533–54541. doi:10.1074/JBC.M410208200.

Chuang, C., Prasanth, K.R. and Nagy, P.D. (2015) "Coordinated Function of Cellular DEAD-Box Helicases in Suppression of Viral RNA Recombination and Maintenance of Viral Genome Integrity," *PLoS Pathog*, 11(2), p. e1004680. doi:10.1371/journal.ppat.1004680.

Chung, C.D., Liao, J., Liu, B., Rao, X., Jay, P., Berta, P. and Shuai, K. (1997) "Specific inhibition of Stat3 signal transduction by PIAS3.," *Science*, 278(5344), pp. 1803–5. doi:10.1126/science.278.5344.1803.

Ciechomska, I.A., Goemans, G.C., Skepper, J.N. and Tolkovsky, A.M. (2009) "Bcl-2 complexed with Beclin-1 maintains full anti-apoptotic function," *Oncogene, 2009 28:21*, 28(21), pp. 2128–2141. doi:10.1038/onc.2009.60.

Cordes, V.C., Reidenbach, S., Rackwitz, H.-R., Franke, W.W., Byrd, D.A., Sweet, D.J., Pante, N., Konstan-Tinov, K.N., Guan, T. and Saphire, A.C.S. (1997) "Identification of Protein p270/Tpr as a Constitutive Component of the Nuclear Pore Complex–attached Intranuclear Filaments," *J. Cell Biol*, 136(3), pp. 515–529. doi:10.1083/JCB.136.3.515.

Costers, S., Lefebvre, D.J., Delputte, P.L. and Nauwynck, H.J. (2008) "Porcine reproductive and respiratory syndrome virus modulates apoptosis during replication in alveolar macrophages," *Arch. Virol*, 153(8), pp. 1453–1465. doi:10.1007/S00705-008-0135-5/TABLES/4.

Coyle, J.H., Bor, Y.C., Rekosh, D. and Hammarskjold, M.L. (2011) "The Tpr protein regulates export of mRNAs with retained introns that traffic through the Nxf1 pathway," *RNA*, 17(7), pp. 1344–1356. doi:10.1261/RNA.2616111.

Criollo, A., Niso-Santano, M., Malik, S.A., Michaud, M., Morselli, E., Mariño, G., Lachkar, S., Arkhipenko, A. v, Harper, F., Pierron, G., Rain, J.C., Ninomiya-Tsuji, J., Fuentes, J.M., Lavandero, S., Galluzzi, L., Maiuri, M.C. and Kroemer, G. (2011) "Inhibition of autophagy by TAB2 and TAB3," *EMBO J*, 30(24), pp. 4908–4920. doi:10.1038/emboj.2011.413.

Crotty, S. (2015) 'A brief history of T cell help to B cells', *Nat. Rev. Immunol.,* 15(3), pp. 185–189. Available at: https://doi.org/10.1038/nri3803.

Cullen, S.P. and Martin, S.J. (2008) 'Mechanisms of granule-dependent killing', *Cell Death Differ.*, 15(2), pp. 251–262. Available at: https://doi.org/10.1038/SJ.CDD.4402244.

D'Angelo, M.A., Gomez-Cavazos, J.S., Mei, A., Lackner, D.H. and Hetzer, M.W. (2012) "A Change in Nuclear Pore Complex Composition Regulates Cell Differentiation," *Dev. Cell*, 22(2), pp. 446–458. doi:10.1016/j.devcel.2011.11.021

Darwich, L., Gimeno, M., Sibila, M., Diaz, I., de la Torre, E., Dotti, S., Kuzemtseva, L., Martin, M., Pujols, J. and Mateu, E. (2011) "Genetic and immunobiological diversities of porcine reproductive and respiratory syndrome genotype I strains," *Vet. Microbiol*, 150(1–2), pp. 49–62. doi:10.1016/j.vetmic.2011.01.008.

Das, A., Dinh, P.X., Panda, D. and Pattnaik, A.K. (2014) "Interferon-inducible protein IFI35 negatively regulates RIG-I antiviral signaling and supports vesicular stomatitis virus replication," *J. Virol*, 88(6), pp. 3103–3113. doi:10.1128/JVI.03202-13.

Das, P.B., Dinh, P.X., Ansari, I.H., de Lima, M., Osorio, F.A. and Pattnaik, A.K. (2010) "The Minor Envelope Glycoproteins GP2a and GP4 of Porcine Reproductive and Respiratory Syndrome Virus Interact with the Receptor CD163," *J. Virol*, 84(4), pp. 1731–1740. doi:10.1128/jvi.01774-09.

Dea, S., Sawyer, N., Alain, R. and Athanassious, R. (1995) "Ultrastructural characteristics and morphogenesis of porcine reproductive and respiratory syndrome virus propagated in the

highly permissive MARC-145 cell clone," *Adv. Exp. Med. Biol*, 380, pp. 95–98. doi:10.1007/978-1-4615-1899-0_13.

Delputte, P.L., Costers, S. and Nauwynck, H.J. (2005) "Analysis of porcine reproductive and respiratory syndrome virus attachment and internalization: Distinctive roles for heparan sulphate and sialoadhesin," *J. Gen. Virol*, 86(5), pp. 1441–1445. doi:10.1099/vir.0.80675-0.

Delputte, P.L. and Nauwynck, H.J. (2004) "Porcine Arterivirus Infection of Alveolar Macrophages Is Mediated by Sialic Acid on the Virus," *J. Virol*, 78(15), pp. 8094–8101. doi:10.1128/jvi.78.15.8094-8101.2004.

Delputte, P.L., Vanderheijden, N., Nauwynck, H.J. and Pensaert, M.B. (2002) "Involvement of the Matrix Protein in Attachment of Porcine Reproductive and Respiratory Syndrome Virus to a Heparinlike Receptor on Porcine Alveolar Macrophages," *J. Virol*, 76(9), pp. 4312–4320. doi:10.1128/jvi.76.9.4312-4320.2002.

Dempsey, P.W., Vaidya, S.A. and Cheng, G. (2003) 'The Art of War: Innate and adaptive immune responses', *Cell. Mol. Life Sci., 60:12*, 60(12), pp. 2604–2621. Available at: https://doi.org/10.1007/S00018-003-3180-Y.

Deveraux, Q., Ustrell, V., Pickart, C. and Rechsteiner, M. (1994) "A 26 S protease subunit that binds ubiquitin conjugates.," *J. Biol. Chem*, 269(10), pp. 7059–7061. doi:10.1016/S0021-9258(17)37244-7.

Dienz, O. and Rincon, M. (2009) 'The effects of IL-6 on CD4 T cell responses', *Clin. Immunol.*, 130(1), pp. 27–33. Available at: https://doi.org/10.1016/j.clim.2008.08.018.

Dinarello, C.A. (2018) 'Overview of the IL-1 family in innate inflammation and acquired immunity', *Immunol. Rev.*, 281(1), pp. 8–27. Available at: https://doi.org/10.1111/imr.12621.

Djavaheri-Mergny, M., Maiuri, M.C. and Kroemer, G. (2010) "Cross talk between apoptosis and autophagy by caspase-mediated cleavage of Beclin 1," *Oncogene*, 29, pp. 1717–1719. doi:10.1038/onc.2009.519.

Doceul, V., Charleston, B., Crooke, H., Reid, E., Powell, P.P. and Seago, J. (2008) "The Npro product of classical swine fever virus interacts with IκBα, the NF-κB inhibitor," *J. Gen. Virol*, 89(8), pp. 1881–1889. doi:10.1099/vir.0.83643-0.

Dokland, T. (2010) "The structural biology of PRRSV," *Virus Res*, pp. 86–97. doi:10.1016/j.virusres.2010.07.029.

Drappier, M. and Michiels, T. (2015) 'Inhibition of the OAS/RNase L pathway by viruses', *Curr. Opin. Virol.*, 15, pp. 19–26. Available at: https://doi.org/10.1016/j.coviro.2015.07.002.

Du, J., Ge, X., Liu, Y., Jiang, P., Wang, Z., Zhang, R., Zhou, L., Guo, X., Han, J. and Yang, H. (2016) "Targeting Swine Leukocyte Antigen Class I Molecules for Proteasomal Degradation by the nsp1α Replicase Protein of the Chinese Highly Pathogenic Porcine Reproductive and Respiratory Syndrome Virus Strain JXwn06," *J. Virol*, 90(2), pp. 682–693. doi:10.1128/jvi.02307-15.

Duarte, J.H. (2016) 'Functional switching', *Nat. Immunol.*, 17(S1), pp. S12–S12. Available at: https://doi.org/10.1038/ni.3607.

Dubois, J., Traversier, A., Julien, T., Padey, B., Lina, B., Bourdon, J.-C., Marcel, V., Boivin, G., Rosa-Calatrava, M. and Terrier, O. (2019) " The Nonstructural NS1 Protein of Influenza Viruses Modulates TP53 Splicing through Host Factor CPSF4 ," *J. Virol*, 93(7), pp. 2168–2186. doi:10.1128/jvi.02168-18.

Duncan, Emma J, Cheetham, Michael E, Chapple, J Paul, van der Spuy, Jacqueline, Chapple, J P, Duncan, E J, van der Spuy, J, Cheetham, · M E and Cheetham, M E (2015) "The Role of HSP70 and Its Co-chaperones in Protein Misfolding, Aggregation and Disease," *Sub-Cell. Biochem*, 78, pp. 243–273. doi:10.1007/978-3-319-11731-7_12.

Dunkelberger, J.R. and Song, W.C. (2009) 'Complement and its role in innate and adaptive immune responses', *Cell Res., 20:1*, 20(1), pp. 34–50. Available at: https://doi.org/10.1038/cr.2009.139.

Dunn, W.A. (1994) "Autophagy and related mechanisms of lysosome-mediated protein degradation," *Trends Cell Biol*, 4(4), pp. 139–143. doi:10.1016/0962-8924(94)90069-8.

Durfee, T., Becherer, K., Chen, P.L., Yeh, S.H., Yang, Y., Kilburn, A.E., Lee, W.H. and Elledge, S.J. (1993) "The retinoblastoma protein associates with the protein phosphatase type 1 catalytic subunit," *Genes Dev*, 7(4), pp. 555–569. doi:10.1101/gad.7.4.555.

Ear, T., Fortin, C.F., Simard, F.A. and McDonald, P.P. (2010) "Constitutive Association of TGF-β–Activated Kinase 1 with the IκB Kinase Complex in the Nucleus and Cytoplasm of Human Neutrophils and Its Impact on Downstream Processes," *J. Immunol*, 184(7), pp. 3897–3906. doi:10.4049/jimmunol.0902958.

El-Radhi, A.S. (2018) 'Pathogenesis of Fever', in *Clinical Manual of Fever in Children*. Cham: Springer International Publishing, pp. 53–68. Available at: https://doi.org/10.1007/978-3-319-92336-9_3.

Ettinger, R., Sims, G.P., Fairhurst, A.-M., Robbins, R., da Silva, Y.S., Spolski, R., Leonard, W.J. and Lipsky, P.E. (2005) 'IL-21 induces differentiation of human naive and memory B cells into antibody-secreting plasma cells', *J. Immunol., (Baltimore, Md. : 1950)*, 175(12), pp. 7867–7879. Available at: https://doi.org/10.4049/JIMMUNOL.175.12.7867.

Ewald, S.E., Engel, A., Lee, J., Wang, M., Bogyo, M. and Barton, G.M. (2011) "Nucleic acid recognition by Toll-like receptors is coupled to stepwise processing by cathepsins and asparagine endopeptidase.," *J. Exp. Med*, 208(4), pp. 643–51. doi:10.1084/jem.20100682.

Fang, Ying, Fang, L., Wang, Y., Lei, Y., Luo, R., Wang, D., Chen, H. and Xiao, S. (2012) "Porcine reproductive and respiratory syndrome virus nonstructural protein 2 contributes to NF-κB activation," *Virol. J*, 9(1), p. 83. doi:10.1186/1743-422X-9-83.

Fang, Y, Fang, L.R., Wang, Y., Lei, Y.Y., Luo, R., Wang, D., Chen, H.C. and Xiao, S.B. (2012) "Porcine reproductive and respiratory syndrome virus nonstructural protein 2 contributes to NF-kappa B activation," *Virol J*, 9, p. 83. doi:10.1186/1743-422X-9-83.

Fang, Y. and Snijder, Eric J (2010) "The PRRSV replicase: Exploring the multifunctionality of an intriguing set of nonstructural proteins," *Virus Res*, pp. 61–76. doi:10.1016/j.virusres.2010.07.030.

Fang, Ying, Treffers, E.E., Li, Y., Tas, A., Sun, Z., van der Meer, Y., de Ru, A.H., van Veelen, P.A., Atkins, J.F., Snijder, E.J. and Firth, A.E. (2012) "Efficient - 2 Frameshifting by mammalian

ribosomes to synthesize an additional arterivirus protein," *PNAS*, 109(43), pp. E2920–E2928. doi:10.1073/pnas.1211145109.

Favreau, C., Bastos, R., Cartaud, J., Courvalin, J.C. and Mustonen, P. (2001) "Biochemical characterization of nuclear pore complex protein gp210 oligomers," *Eur. J. Biochem*, 268(14), pp. 3883–3889. doi:10.1046/J.1432-1327.2001.02290.X.

Fehr, A.R. and Yu, D. (2013) "Control the Host Cell Cycle: Viral Regulation of the Anaphase-Promoting Complex," *J. Virol*, 87(16), pp. 8818–8825. doi:10.1128/jvi.00088-13.

Fields, S. (1993) "The Two-Hybrid System to Detect Protein-Protein Interactions," *Methods*, 5(2), pp. 116–124. doi:10.1006/meth.1993.1016.

Fields, S. and Song, O.K. (1989) "A novel genetic system to detect protein-protein interactions," *Nature*, 340(6230), pp. 245–246. doi:10.1038/340245a0.

Folkmann, A.W., Noble, K.N., Cole, C.N. and Wente, S.R. (2011) "Dbp5, Gle1-IP6 and Nup159: a working model for mRNP export," *Nucleus*, 2(6), pp. 540–548. doi:10.4161/NUCL.2.6.17881.

Fontes, M.R.M., Teh, T. and Kobe, B. (2000) "Structural basis of recognition of monopartite and bipartite nuclear localization sequences by mammalian importin-α11," *J. Mol. Biol*, 297(5), pp. 1183–1194. doi:10.1006/jmbi.2000.3642.

Forthal, D.N. (2015) 'Functions of Antibodies', *Microbiol. Spectrum.*, 2(4), p. 1. Available at: https://doi.org/10.1128/9781555817411.ch2.

Frosst, P., Guan, T., Subauste, C., Hahn, K. and Gerace, L. (2002) "Tpr is localized within the nuclear basket of the pore complex and has a role in nuclear protein export," *J. Cell Biol*, 156(4), pp. 617–630. doi:10.1083/JCB.200106046.

Frydas, I.S., Verbeeck, M., Cao, J. and Nauwynck, H.J. (2013) "Replication characteristics of porcine reproductive and respiratory syndrome virus (PRRSV) European subtype 1 (Lelystad) and subtype 3 (Lena) strains in nasal mucosa and cells of the monocytic lineage: Indications for the use of new receptors of PRRSV (Lena)," *Vet. Res.*, 44(1), pp. 1–14. Available at: https://doi.org/10.1186/1297-9716-44-73/FIGURES/8.

Furukawa, M., He, Y.J., Borchers, C. and Xiong, Y. (2003) "Targeting of protein ubiquitination by BTB–Cullin 3–Roc1 ubiquitin ligases," *Nat. Cell Biol, 2003 5:11*, 5(11), pp. 1001–1007. doi:10.1038/ncb1056.

Galliher-Beckley, A.J. (2013) 'Caspase-1 activation and mature interleukin-1β release are uncoupled events in monocytes', *World J. Biol. Chem.*, 4(2), p. 30. Available at: https://doi.org/10.4331/wjbc.v4.i2.30.

Gallo, R.L. and Nizet, V. (2008) 'Innate barriers against infection and associated disorders', *Drug Discov. Today Dis. Mech.*, 5(2), p. 145. Available at: https://doi.org/10.1016/J.DDMEC.2008.04.009.

Gao, H., Jin, S., Song, Y., Fu, M., Wang, M., Liu, Z., Wu, M. and Zhan, Q. (2005) "B23 Regulates GADD45a Nuclear Translocation and Contributes to GADD45a-induced Cell Cycle G2-M Arrest *," *J. Biol. Chem*, 280(12), pp. 10988–10996. doi:10.1074/jbc.m412720200.

Gao, J., Xiao, S., Liu, X., Wang, L., Ji, Q., Mo, D. and Chen, Y. (2014) “Inhibition of HSP70 reduces porcine reproductive and respiratory syndrome virus replication in vitro,” *BMC Microbiol*, 14(1), pp. 1–11. doi:10.1186/1471-2180-14-64.

Gao, J., Xiao, S., Xiao, Y., Wang, X., Zhang, C., Zhao, Q., Nan, Y., Huang, B., Liu, H., Liu, N., Lv, J., Du, T., Sun, Y., Mu, Y., Wang, G., Syed, S.F., Zhang, G., Hiscox, J.A., Goodfellow, I. and Zhou, E.M. (2016) “MYH9 is an Essential Factor for Porcine Reproductive and Respiratory Syndrome Virus Infection,” *Sci Rep, 2016 6:1*, 6(1), pp. 1–13. doi:10.1038/srep25120.

Garcia-Cattaneo, A., Gobert, F.X., Müller, M., Toscano, F., Flores, M., Lescure, A., Nery, E. del and Benaroch, P. (2012) “Cleavage of Toll-like receptor 3 by cathepsins B and H is essential for signaling,” *PNAS*, 109(23), pp. 9053–9058. doi:10.1073/PNAS.1115091109

García-Sastre, A. (2017) “Ten Strategies of Interferon Evasion by Viruses,” *Cell Host Microbe*, 22(2), p. 176. doi:10.1016/j.chom.2017.07.012.

Gautier, V.W., Sheehy, N., Duffy, M., Hashimoto, K. and Hall, W.W. (2005) “Direct interaction of the human I-mfa domain-containing protein, HIC, with HIV-1 Tat results in cytoplasmic sequestration and control of Tat activity,” *PNAS*, 102(45), pp. 16362–16367. doi:10.1073/PNAS.0503519102.

Gautrey, H., Jackson, C., Dittrich, A.L., Browell, D., Lennard, T. and Tyson-Capper, A. (2015) “SRSF3 and hnRNP H1 regulate a splicing hotspot of HER2 in breast cancer cells,” *RNA Biol*, 12(10), pp. 1139–1151. doi:10.1080/15476286.2015.1076610.

Geuens, T., Bouhy, D. and Timmerman, V. (2016) “The hnRNP family: insights into their role in health and disease,” *Hum. Genet, 2016 135:8*, 135(8), pp. 851–867. doi:10.1007/S00439-016-1683-5.

Gladue, D.P., O’Donnell, V., Baker-Branstetter, R., Holinka, L.G., Pacheco, J.M., Fernandez-Sainz, I., Lu, Z., Brocchi, E., Baxt, B., Piccone, M.E., Rodriguez, L. and Borca, M. v. (2012) “Foot-and-Mouth Disease Virus Nonstructural Protein 2C Interacts with Beclin1, Modulating Virus Replication,” *J. Virol*, 86(22), pp. 12080–12090. doi:10.1128/JVI.01610-12

Gomez, G.N., Abrar, F., Dodhia, M.P., Gonzalez, F.G. and Nag, A. (2019) “SARS coronavirus protein nsp1 disrupts localization of Nup93 from the nuclear pore complex.,” *Biochem. Cell Biol*, 97(6), pp. 758–766. doi:10.1139/bcb-2018-0394.

van Gorp, H., van Breedam, W., Delputte, P.L. and Nauwynck, H.J. (2008) “Sialoadhesin and CD163 join forces during entry of the porcine reproductive and respiratory syndrome virus,” *J. Gen. Virol*, 89(12), pp. 2943–2953. doi:10.1099/vir.0.2008/005009-0.

van Gorp, H., van Breedam, W., van Doorsselaere, J., Delputte, P.L. and Nauwynck, H.J. (2010) “Identification of the CD163 Protein Domains Involved in Infection of the Porcine Reproductive and Respiratory Syndrome Virus,” *J. Virol*, 84(6), pp. 3101–3105. doi:10.1128/jvi.02093-09.

Grebeňová, D., Holoubek, A., Röselová, P., Obr, A., Brodská, B. and Kuželová, K. (2019) “PAK1, PAK1Δ15, and PAK2: similarities, differences and mutual interactions,” *Sci Rep 2019 9:1*, 9(1), pp. 1–18. doi:10.1038/s41598-019-53665-6.

Greber, U.F., Senior, A. and Gerace, L. (1990) “A major glycoprotein of the nuclear pore complex is a membrane-spanning polypeptide with a large lumenal domain and a small cytoplasmic tail.,” *EMBO J*, 9(5), p. 1495. doi:10.1002/j.1460-2075.1990.tb08267.x.

Groll, M., Ditzel, L., Löwe, J., Stock, D., Bochtler, M., Bartunik, H.D. and Huber, R. (1997) “Structure of 20S proteasome from yeast at 2.4Å resolution,” *Nature, 1997 386:6624*, 386(6624), pp. 463–471. doi:10.1038/386463a0.

Groscurth, P. and Filgueira, L. (1998) ‘Killing mechanisms of cytotoxic T lymphocytes’, *News Physiol. Sci.*, 13(1), pp. 17–21. Available at: https://doi.org/10.1152/PHYSIOLOGYONLINE.1998.13.1.17

Guerrero, C.A., Bouyssounade, D., Zárate, S., Iša, P., López, T., Espinosa, R., Romero, P., Méndez, E., López, S. and Arias, C.F. (2002) “Heat Shock Cognate Protein 70 Is Involved in Rotavirus Cell Entry,” *J. Virol*, 76(8), pp. 4096–4102. doi:10.1128/jvi.76.8.4096-4102.2002.

Guo, J., Chen, D., Gao, X., Hu, X., Zhou, Y., Wu, C., Wang, Y., Chen, J., Pei, R. and Chen, X. (2017) “Protein Inhibitor of Activated STAT2 Restricts HCV Replication by Modulating Viral Proteins Degradation,” *Viruses, 2017, Vol. 9, Page 285*, 9(10), p. 285. doi:10.3390/v9100285.

Guo, H., Callaway, J.B. and Ting, J.P.-Y. (2015) ‘Inflammasomes: mechanism of action, role in disease, and therapeutics’, *Nat. Med.*, 21(7), pp. 677–687. Available at: https://doi.org/10.1038/nm.3893.

Guo, R., Shang, P., Carrillo, C.A., Sun, Z., Lakshmanappa, Y.S., Yan, X., Renukaradhya, G.J., McGill, J., Jaing, C.J., Niederwerder, M.C., Rowland, R.R.R. and Fang, Y. (2018) “Double-stranded viral RNA persists in vitro and in vivo during prolonged infection of porcine reproductive and respiratory syndrome virus,” *Virology*, 524, pp. 78–89. doi:10.1016/j.virol.2018.08.006.

Gustin, J.K., Moses, A. v., Früh, K. and Douglas, J.L. (2011) “Viral takeover of the host ubiquitin system,” *Front. Microbiol*, 2(JULY), p. 161. doi:10.3389/fmicb.2011.00161.

Han, J., Rutherford, M.S. and Faaberg, K.S. (2009) “The Porcine Reproductive and Respiratory Syndrome Virus nsp2 Cysteine Protease Domain Possesses both trans- and cis-Cleavage Activities,” *J. Virol*, 83(18), pp. 9449–9463. doi:10.1128/jvi.00834-09.

Han, K., Seo, H.W., Oh, Y., Kang, I., Park, C. and Chae, C. (2013) “Comparison of the virulence of European and North American genotypes of porcine reproductive and respiratory syndrome virus in experimentally infected pigs,” *Vet. J. VET*, 195(3), pp. 313–318. Available at: https://doi.org/10.1016/J.TVJL.2012.06.035.

Han, M., Du, Y., Song, C. and Yoo, D. (2013) “Degradation of CREB-binding protein and modulation of type I interferon induction by the zinc finger motif of the porcine reproductive and respiratory syndrome virus nsp1alpha subunit,” *Virus Res*, 172(1–2), pp. 54–65. doi:10.1016/j.virusres.2012.12.012.

Han, M., Ke, H., Zhang, Q. and Yoo, D. (2017) “Nuclear imprisonment of host cellular mRNA by nsp1β protein of porcine reproductive and respiratory syndrome virus,” *Virology*, 505, pp. 42–55. doi:10.1016/j.virol.2017.02.004.

Han, M., Kim, C.Y., Rowland, R.R.R., Fang, Y., Kim, D. and Yoo, D. (2014) "Biogenesis of non-structural protein 1 (nsp1) and nsp1-mediated type I interferon modulation in arteriviruses," *Virology*, 458–459(1), pp. 136–150. doi:10.1016/j.virol.2014.04.028.

Hanada, K., Suzuki, Y., Nakane, T., Hirose, O. and Gojobori, T. (2005) "The origin and evolution of porcine reproductive and respiratory syndrome viruses," *Mol. Biol. Evol*, 22(4), pp. 1024–1031. doi:10.1093/molbev/msi089.

Hannoodee, S. and Nasuruddin, D.N. (2021) 'Acute Inflammatory Response', *Nature*, 206(4979), p. 20. Available at: https://doi.org/10.1038/206020a0.

Harada, A., Sekido, N., Akahoshi, T., Wada, T., Mukaida, N. and Matsushima, K. (1994) 'Essential involvement of interleukin-8 (IL-8) in acute inflammation', *J. Leukocyte Biol.*, 56(5), pp. 559–564. Available at: https://doi.org/10.1002/jlb.56.5.559.

Hase, M.E. and Cordes, V.C. (2003) "Direct interaction with Nup153 mediates binding of Tpr to the periphery of the nuclear pore complex," *Mol. Biol. Cell*, 14(5), pp. 1923–1940. doi:10.1091/MBC.E02-09-0620.

Hashem, Y., des Georges, A., Dhote, V., Langlois, R., Liao, H.Y., Grassucci, R.A., Pestova, T. v., Hellen, C.U.T. and Frank, J. (2013) "Hepatitis-C-virus-like internal ribosome entry sites displace eIF3 to gain access to the 40S subunit," *Nature, 2013 503:7477*, 503(7477), pp. 539–543. doi:10.1038/nature12658.

Hassin, D., Garber, O.G., Meiraz, A., Schiffenbauer, Y.S. and Berke, G. (2011) 'Cytotoxic T lymphocyte perforin and Fas ligand working in concert even when Fas ligand lytic action is still not detectable', *Immunology*, 133(2), p. 190. Available at: https://doi.org/10.1111/J.1365-2567.2011.03426.X.

Hatzi, K., Philip Nance, J., Kroenke, M.A., Bothwell, M., Haddad, E.K., Melnick, A. and Crotty, S. (2015) 'BCL6 orchestrates Tfh cell differentiation via multiple distinct mechanisms', *J. Exp. Med.*, 212(4), pp. 539–553. Available at: https://doi.org/10.1084/JEM.20141380.

He, C. and Levine, B. (2010) "The Beclin 1 interactome," *Curr. Opin. Cell Biol*, 22(2), p. 140. doi:10.1016/j.ceb.2010.01.001.

He, Q., Li, Y., Zhou, L., Ge, X., Guo, X. and Yang, H. (2015) "Both Nsp1beta and Nsp11 are responsible for differential TNF-alpha production induced by porcine reproductive and respiratory syndrome virus strains with different pathogenicity in vitro," *Virus Res*, 201, pp. 32–40. doi:10.1016/j.virusres.2015.02.014.

Heinemeyer, W., Fischer, M., Krimmer, T., Stachon, U. and Wolf, D.H. (1997) "The Active Sites of the Eukaryotic 20 S Proteasome and Their Involvement in Subunit Precursor Processing*," *J. Biol. Chem*, 272(40), pp. 25200–25209. doi:10.1074/jbc.272.40.25200.

Van Hemert, M.J., De Wilde, A.H., Gorbalenya, A.E. and Snijder, E.J. (2008) "The in vitro RNA synthesizing activity of the isolated arterivirus replication/transcription complex is dependent on a host factor," *J. Biol. Chem*, 283(24), pp. 16525–16536. doi:10.1074/jbc.M708136200.

Herrmann, J.M., Stuart, R.A., Craig, E.A. and Neupert, W. (1994) "Mitochondrial heat shock protein 70, a molecular chaperone for proteins encoded by mitochondrial DNA," *J. Cell Biol*, 127(4), pp. 893–902. doi:10.1083/JCB.127.4.893.

Hicke, L. (2001) “Protein regulation by monoubiquitin,” *Nat. Rev. Mol. Cell Biol, 2001 2:3*, 2(3), pp. 195–201. doi:10.1038/35056583.

Hinnebusch, A.G. (2006) “eIF3: a versatile scaffold for translation initiation complexes,” *Trends Biochem. Sci*, 31(10), pp. 553–562. doi:10.1016/j.tibs.2006.08.005.

Hirano, T., Ishihara, K. and Hibi, M. (2000) “Roles of STAT3 in mediating the cell growth, differentiation and survival signals relayed through the IL-6 family of cytokine receptors,” *Oncogene*, 19(21), pp. 2548–2556. doi:10.1038/sj.onc.1203551.

Ho, H.H. and Ivashkiv, L.B. (2006) “Role of STAT3 in type I interferon responses. Negative regulation of STAT1-dependent inflammatory gene activation,” *J. Biol. Chem*, 281(20), pp. 14111–14118. doi:10.1074/JBC.M511797200.

van der Hoeven, B., Oudshoorn, D., Koster, A.J., Snijder, E.J., Kikkert, M. and Bárcena, M. (2016) “Biogenesis and architecture of arterivirus replication organelles,” *Virus Res*, pp. 70–90. doi:10.1016/j.virusres.2016.04.001.

Höhfeld, J. and Hartl, F.U. (1994) “Role of the chaperonin cofactor Hsp10 in protein folding and sorting in yeast mitochondria,” *J. Cell Biol*, 126(2), pp. 305–315. doi:10.1083/jcb.126.2.305.

Holtkamp, D.J., Kliebenstein, J.B., Neumann, E.J., Zimmerman, J.J., Rotto, H.F., Yoder, T.K., Wang, C., Yeske, P.E., Mowrer, C.L. and Haley, C.A. (2013) “Assessment of the economic impact of porcine reproductive and respiratory syndrome virus on United States pork producers,” *J. Swine Health Prod*, 21(2), pp. 72–84.

Holtz, A.E. and Zhu, L. (1995) “Clontechniques,” X(3), p. 20.

Huang, C., Zhang, Q. and Feng, W.-H. (2015) “Regulation and evasion of antiviral immune responses by porcine reproductive and respiratory syndrome virus.,” *Virus Res*, 202, pp. 101–111. doi:10.1016/j.virusres.2014.12.014.

Huang, C., Zhang, Q., Guo, X. -k., Yu, Z. -b., Xu, A.-T., Tang, J. and Feng, W. -h. (2014) “Porcine Reproductive and Respiratory Syndrome Virus Nonstructural Protein 4 Antagonizes Beta Interferon Expression by Targeting the NF-kappaB Essential Modulator,” *J. Virol*, 88(18), pp. 10934–10945. doi:10.1128/JVI.01396-14.

Huang, S., Fei, D., Ma, Y., Wang, C., Shi, D., Liu, K., Li, M. and Ma, M. (2020) “Identification of a novel host protein interacting with the structural protein VP2 of deformed wing virus by yeast two-hybrid screening,” *Virus Res*, 286, p. 198072. doi:10.1016/j.virusres.2020.198072.

Huang, X., Luan, B., Wu, J. and Shi, Y. (2016) “An atomic structure of the human 26S proteasome,” *Nat. Struct. Mol. Biol,* 23, 778–785. doi:10.1038/nsmb.3273.

Huang, Y.W., Dryman, B.A., Li, W. and Meng, X.J. (2009) “Porcine DC-SIGN: Molecular cloning, gene structure, tissue distribution and binding characteristics,” *Dev. Comp. Immunol*, 33(4), pp. 464–480. doi:10.1016/J.DCI.2008.09.010.

Huber, E.M., Basler, M., Schwab, R., Heinemeyer, W., Kirk, C.J., Groettrup, M. and Groll, M. (2012) “Immuno- and constitutive proteasome crystal structures reveal differences in substrate and inhibitor specificity,” *Cell*, 148(4), pp. 727–738. doi:10.1016/J.CELL.2011.12.030.

Hutten, S. and Kehlenbach, R.H. (2007) “CRM1-mediated nuclear export: to the pore and beyond,” *Trends Cell Biol*, 17(4), pp. 193–201. doi:10.1016/j.tcb.2007.02.003.

Ishitani, T., Takaesu, G., Ninomiya-Tsuji, J., Shibuya, H., Gaynor, R.B. and Matsumoto, K. (2003) “Role of the TAB2-related protein TAB3 in IL-1 and TNF signaling,” *EMBO J*, 22(23), pp. 6277–6288. doi:10.1093/emboj/cdg605.

Iwabuchi, K., Li, B., Bartel, P. and Fields, S. (1993) “Use of the two-hybrid system to identify the domain of p53 involved in oligomerization,” *Oncogene*, 8(6), pp. 1693–1696.

Jaafar, Z.A. and Kieft, J.S. (2018) “Viral RNA structure-based strategies to manipulate translation,” *Nat. Rev. Microbiol, 2018 17:2*, 17(2), pp. 110–123. doi:10.1038/s41579-018-0117-x.

Jackson, T., Mould, A.P., Sheppard, D. and King, A.M.Q. (2002) “Integrin αvβ1 Is a Receptor for Foot-and-Mouth Disease Virus,” *J. Virol*, 76(3), pp. 935–941. doi:10.1128/jvi.76.3.935-941.2002

Jäger, S., Kim, D.Y., Hultquist, J.F., Shindo, K., Larue, R.S., Kwon, E., Li, M., Anderson, B.D., Yen, L., Stanley, D., Mahon, C., Kane, J., Franks-Skiba, K., Cimermancic, P., Burlingame, A., Sali, A., Craik, C.S., Harris, R.S., Gross, J.D. and Krogan, N.J. (2012) “Vif hijacks CBF – β to degrade APOBEC3G and promote HIV–1 infection,” *Nature*, 481(7381), p. 371. doi:10.1038/nature10693.

Jain, S., Gautam, V. and Naseem, S. (2011) ‘Acute-phase proteins: As diagnostic tool’, *J. Pharm. Bioallied Sci.*, 3(1), p. 118. Available at: https://doi.org/10.4103/0975-7406.76489.

James, P., Halladay, J. and Craig, E.A. (1996) “Genomic libraries and a host strain designed for highly efficient two-hybrid selection in yeast.,” *Genetics*, 144(4), pp. 1425–36. doi:10.1093/genetics/144.4.1425.

de Jesús-González, L.A., Palacios-Rápalo, S., Reyes-Ruiz, J.M., Osuna-Ramos, J.F., Cordero-Rivera, C.D., Farfan-Morales, C.N., Gutiérrez-Escolano, A.L. and del Ángel, R.M. (2021) “The Nuclear Pore Complex Is a Key Target of Viral Proteases to Promote Viral Replication,” *Viruses*, 13(4). doi:10.3390/v13040706.

Jia, H., Halilou, A.I., Hu, L., Cai, W., Liu, J. and Huang, B. (2011) “Heat shock protein 10 (Hsp10) in immune-related diseases: one coin, two sides.,” *Int. J. Biochem. Mol.*, 2(1), pp. 47–57.

Jiang, W., Jiang, P., Wang, Xinglong, Li, Y., Wang, Xianwei and Du, Y. (2007) “Influence of porcine reproductive and respiratory syndrome virus GP5 glycoprotein N-linked glycans on immune responses in mice,” *Virus Genes*, 35(3), pp. 663–671. doi:10.1007/s11262-007-0131-y.

Jiang, Y., Li, G., Yu, L., Li, L., Zhang, Y., Zhou, Y., Tong, W., Liu, C., Gao, F. and Tong, G. (2020) “Genetic Diversity of Porcine Reproductive and Respiratory Syndrome Virus (PRRSV) From 1996 to 2017 in China,” *Front. Microbiol.*, 11, p. 618. Available at: https://doi.org/10.3389/FMICB.2020.00618/BIBTEX.

Jin, G., Klika, A., Callahan, M., Faga, B., Danzig, J., Jiang, Z., Li, X., Stark, G.R., Harrington, J. and Sherf, B. (2003) “Identification of a human NF-κB-activating protein, TAB3,” *PNAS*, 2004;101(7):2028-2033. doi:10.1073/pnas.0307314101.

Jin, H., Zhou, L., Ge, X., Zhang, H., Zhang, R., Wang, C., Wang, L., Zhang, Z., Yang, H. and Guo, X. (2017) "Cellular DEAD-box RNA helicase 18 (DDX18) Promotes the PRRSV Replication via Interaction with Virus nsp2 and nsp10," *Virus Res*, 238, pp. 204–212. doi:10.1016/j.virusres.2017.05.028.

Jing, H., Fang, L., Ding, Z., Wang, D., Hao, W., Gao, L., Ke, W., Chen, H. and Xiao, S. (2016) "Porcine reproductive and respiratory syndrome virus nsp1α inhibits NF-κB activation by targeting linear ubiquitin chain assembly complex (LUBAC)," *J. Virol*, 91(November), p. JVI.01911-16. doi:10.1128/jvi.01911-16.

Jivotovskaya, A. v., Valášek, L., Hinnebusch, A.G. and Nielsen, K.H. (2006) "Eukaryotic translation initiation factor 3 (eIF3) and eIF2 can promote mRNA binding to 40S subunits independently of eIF4G in yeast," *Mol. Cell. Biol*, 26(4), pp. 1355–1372. doi:10.1128/MCB.26.4.1355-1372.2006.

Jourdan, S.S., Osorio, F. and Hiscox, J.A. (2012) "An interactome map of the nucleocapsid protein from a highly pathogenic North American porcine reproductive and respiratory syndrome virus strain generated using SILAC-based quantitative proteomics," *Proteomics*, 12, pp. 1015–1023. doi:10.1002/pmic.201100469.

Kahyo, T., Nishida, T. and Yasuda, H. (2001) "Involvement of PIAS1 in the sumoylation of tumor suppressor p53," *Mol. Cell*, 8(3), pp. 713–718. doi:10.1016/S1097-2765(01)00349-5.

Kanayama, A., Seth, R.B., Sun, L., Ea, C.-K., Hong, M., Shaito, A., Chiu, Y.-H., Deng, L. and Chen, Z.J. (2004) "TAB2 and TAB3 Activate the NF-κB Pathway through Binding to Polyubiquitin Chains," *Mol. Cell*, 15(4), pp. 535–548. doi:10.1016/j.molcel.2004.08.008.

Kang, R., Zeh, H.J., Lotze, M.T. and Tang, D. (2011) "The Beclin 1 network regulates autophagy and apoptosis," *Cell Death Differ*, 18, pp. 571–580. doi:10.1038/cdd.2010.191.

Kappes, M.A. and Faaberg, K.S. (2015) "PRRSV structure, replication and recombination: Origin of phenotype and genotype diversity," *Virology*, pp. 475–486. doi:10.1016/j.virol.2015.02.012.

Karniychuk, U.U., Geldhof, M., Vanhee, M., van Doorsselaere, J., Saveleva, T.A. and Nauwynck, H.J. (2010) "Pathogenesis and antigenic characterization of a new East European subtype 3 porcine reproductive and respiratory syndrome virus isolate," *BMC Vet. Res*, 6, p. 30. doi:10.1186/1746-6148-6-30.

Kato, K., Ikliptikawati, D.K., Kobayashi, A., Kondo, H., Lim, K., Hazawa, M. and Wong, R.W. (2021) "Overexpression of SARS-CoV-2 protein ORF6 dislocates RAE1 and NUP98 from the nuclear pore complex.," *Biochem. Biophys. Res. Commun*, 536, pp. 59–66. doi:10.1016/j.bbrc.2020.11.115.

Ke, H., Han, M., Kim, J., Gustin, K.E. and Yoo, D. (2019) "Porcine Reproductive and Respiratory Syndrome Virus Nonstructural Protein 1 Beta Interacts with Nucleoporin 62 To Promote Viral Replication and Immune Evasion," *J. Virol*, 93(14). doi:10.1128/JVI.00469-19.

Ke, H., Han, M., Zhang, Q., Rowland, R., Kerrigan, M. and Yoo, D. (2018) "Type I interferon suppression-negative and host mRNA nuclear retention-negative mutation in nsp1β confers attenuation of porcine reproductive and respiratory syndrome virus in pigs," *Virology,* 2018;517:177-187. doi:10.1016/j.virol.2018.01.016.

Ke, H., Lee, S., Kim, J., Liu, H.C. and Yoo, D. (2019) “Interaction of PIAS1 with PRRS virus nucleocapsid protein mediates NF-κB activation and triggers proinflammatory mediators during viral infection,” *Sci Rep, 2019 9:1*, 9(1), pp. 1–17. doi:10.1038/s41598-019-47495-9.

Ke, W., Fang, L., Tao, R., Li, Y., Jing, H., Wang, D. and Xiao, S. (2019) “Porcine Reproductive and Respiratory Syndrome Virus E Protein Degrades Porcine Cholesterol 25-Hydroxylase via the Ubiquitin-Proteasome Pathway,” *J. Virol*, 93(20), pp. 767–786. doi:10.1128/jvi.00767-19

Keffaber, K.K. (1989) “Reproductive failure of unknown etiology,” *Am. Assoc. Swine Prac. News*.

Kendirgi, F., Barry, D.M., Griffis, E.R., Powers, M.A. and Wente, S.R. (2003) “An essential role for hGle1 nucleocytoplasmic shuttling in mRNA export,” *J. Cell Biol*, 160(7), pp. 1029–1040. doi:10.1083/jcb.200211081.

Kendirgi, F., Rexer, D.J., Alcázar-Román, A.R., Onishko, H.M. and Wente, S.R. (2005) “Interaction between the Shuttling mRNA Export Factor Gle1 and the Nucleoporin hCG1: A Conserved Mechanism in the Export of Hsp70 mRNA,” *Mol. Biol. Cell*, 16(9), p. 4304. doi:10.1091/mbc.e04-11-0998.

Kihara, A., Kabeya, Y., Ohsumi, Y. and Yoshimori, T. (2001) “Beclin–phosphatidylinositol 3-kinase complex functions at the trans-Golgi network,” *EMBO Rep*, 2(4), p. 330. doi:10.1093/embo-reports/kve061.

Kim, H., Kim, H.K., Jung, J.H., Choi, Y.J., Kim, J., Um, C.G., Hyun, S. bin, Shin, S., Lee, B., Jang, G., Kang, B.K., Moon, H.J. and Song, D.S. (2011) “The assessment of efficacy of porcine reproductive respiratory syndrome virus inactivated vaccine based on the viral quantity and inactivation methods,” *Virol. J*, 8. doi:10.1186/1743-422x-8-323.

Kim, J.-K., Fahad, A.-M., Shanmukhappa, K. and Kapil, S. (2006) “Defining the cellular target(s) of porcine reproductive and respiratory syndrome virus blocking monoclonal antibody 7G10,” *J. Virol*, 80(2), pp. 689–696. doi:10.1128/jvi.80.2.689-696.2006.

Kim, O., Sun, Y., Lai, F.W., Song, C. and Yoo, D. (2010) “Modulation of type I interferon induction by porcine reproductive and respiratory syndrome virus and degradation of CREB-binding protein by non-structural protein 1 in MARC-145 and HeLa cells,” *Virology*, 402(2), pp. 315–326. doi:10.1016/j.virol.2010.03.039.

Kimman, T.G., Cornelissen, L.A., Moormann, R.J., Rebel, J.M.J. and Stockhofe-Zurwieden, N. (2009) “Challenges for porcine reproductive and respiratory syndrome virus (PRRSV) vaccinology,” *Vaccine*, pp. 3704–3718. doi:10.1016/j.vaccine.2009.04.022.

Klein, L., Kyewski, B., Allen, P.M. and Hogquist, K.A. (2014) ‘Positive and negative selection of the T cell repertoire: what thymocytes see (and don’t see)’, *Nat. Rev. Immunol.*, 14(6), pp. 377–391. Available at: https://doi.org/10.1038/nri3667.

Kloetzel, P.M. (2001) “Antigen processing by the proteasome,” *Nat. Rev. Mol. Cell Biol, 2001 2:3*, 2(3), pp. 179–188. doi:10.1038/35056572.

Knoops, K., Barcena, M., Limpens, R.W.A.L., Koster, A.J., Mommaas, A.M. and Snijder, E.J. (2012) “Ultrastructural Characterization of Arterivirus Replication Structures: Reshaping the Endoplasmic Reticulum To Accommodate Viral RNA Synthesis,” *J. Virol*, 86(5), pp. 2474–2487. doi:10.1128/jvi.06677-11.

Koh, M.Y. and Powis, G. (2012) “Passing the baton: the HIF switch,” *Trends Biochem. Sci* , 37(9), pp. 364–372. doi:10.1016/j.tibs.2012.06.004.

Kolupaeva, V.G., Unbehaun, A., Lomakin, I.B., Hellen, C.U.T. and Pestova, T. v (2005) “Binding of eukaryotic initiation factor 3 to ribosomal 40S subunits and its role in ribosomal dissociation and anti-association.” *RNA*, 2005;11(4):470-486.doi:10.1261/rna.7215305.

Komander, D. and Rape, M. (2012) “The Ubiquitin Code,” *Annu. Rev. Biochem*, 81(1), pp. 203–229. doi:10.1146/annurev-biochem-060310-170328.

Kong, X., Ma, S., Guo, J., Ma, Y., Hu, Y., Wang, J. and Zheng, Y. (2015) “Ubiquitously expressed transcript is a novel interacting protein of protein inhibitor of activated signal transducer and activator of transcription 2,” *Mol. Med. Rep*, 11(4), p. 2443. doi:10.3892/mmr.2014.3023.

Kotaja, N., Karvonen, U., Jänne, O.A. and Palvimo, J.J. (2002) “PIAS Proteins Modulate Transcription Factors by Functioning as SUMO-1 Ligases,” *Mol. Cell. Biol*, 22(14), pp. 5222–5234. doi:10.1128/mcb.22.14.5222-5234.2002

Kranich, J. and Krautler, N.J. (2016) ‘How follicular dendritic cells shape the B-cell antigenome’, *Front. Immunol.*, 7(JUN), p. 225. Available at: https://doi.org/10.3389/FIMMU.2016.00225/XML/NLM.

Kristan, A., Debeljak, N. and Kunej, T. (2021) “Integration and Visualization of Regulatory Elements and Variations of the EPAS1 Gene in Human,” *Genes*, 12(11), p. 1793. Available at: https://doi.org/10.3390/genes12111793.

Kroese, M. v., Zevenhoven-Dobbe, J.C., Bos-de Ruijter, Judy N. A., Peeters, B.P.H., Meulenberg, J.J.M., Cornelissen, L.A.H.M. and Snijder, E.J. (2008) “The nsp 1alpha and nsp 1beta papain-like autoproteinases are essential for porcine reproductive and respiratory syndrome virus RNA synthesis,” *J. Gen. Virol*, 89(2), pp. 494–499. doi:10.1099/vir.0.83253-0.

Krull, S., Dörries, J., Boysen, B., Reidenbach, S., Magnius, L., Norder, H., Thyberg, J. and Cordes, V.C. (2010) “Protein Tpr is required for establishing nuclear pore-associated zones of heterochromatin exclusion,” *EMBO J*, 29(10), pp. 1659–1673. doi:10.1038/EMBOJ.2010.54.

Krull, S., Thyberg, J., Björkroth, B., Rackwitz, H.R. and Cordes, V.C. (2004) “Nucleoporins as components of the nuclear pore complex core structure and Tpr as the architectural element of the nuclear basket,” *Mol. Biol. Cell*, 15(9), pp. 4261–4277. doi:10.1091/mbc.e04-03-0165

Kuchipudi, S. v. (2015) “The Complex Role of STAT3 in Viral Infections,” *J. Immunol. Res*, 2015, pp. 1–9. doi:10.1155/2015/272359.

Kumada, K., Fuse, N., Tamura, T., Okamori, C. and Kurata, S. (2019) “HSP70/DNAJA3 chaperone/cochaperone regulates NF-κB activity in immune responses,” *Biochem. Biophys. Res. Commun*, 513(4), pp. 947–951. doi:10.1016/j.bbrc.2019.04.077.

Kumar, M. and Mitra, D. (2005) “Heat shock protein 40 is necessary for human immunodeficiency virus-1 Nef-mediated enhancement of viral gene expression and replication,” *J. Biol. Chem*, 280(48), pp. 40041–40050. doi:10.1074/jbc.m508904200.

Kurosaki, T., Kometani, K. and Ise, W. (2015) ‘Memory B cells’, *Nat. Rev. Immunol.*, 15(3), pp. 149–159. Available at: https://doi.org/10.1038/nri3802.

Kurt-Jones, E.A., Popova, L., Kwinn, L., Haynes, L.M., Jones, L.P., Tripp, R.A., Walsh, E.E., Freeman, M.W., Golenbock, D.T., Anderson, L.J. and Finberg, R.W. (2000) "Pattern recognition receptors TLR4 and CD14 mediate response to respiratory syncytial virus," *Nat. Immunol, 2000 1:5*, 1(5), pp. 398–401. doi:10.1038/80833.

Lafarga, M., Berciano, M.T., Pena, E., Mayo, I., Castaño, J.G., Bohmann, D., Rodrigues, J.P., Tavanez, J.P. and Carmo-Fonseca, M. (2002) "Clastosome: A subtype of nuclear body enriched in 19S and 20S proteasomes, ubiquitin, and protein substrates of proteasome," *Mol. Biol. Cell*, 13(8), pp. 2771–2782. doi:10.1091/mbc.e02-03-0122

Lanzavecchia, A., Iezzi, G. and Viola, A. (1999) 'From TCR Engagement to T Cell Activation: A Kinetic View of T Cell Behavior', *Cell*, 96, pp. 1–4.

Lauber, C., Goeman, J.J., de Parquet, M.C., Thi Nga, P., Snijder, E.J., Morita, K. and Gorbalenya, A.E. (2013) "The Footprint of Genome Architecture in the Largest Genome Expansion in RNA Viruses," *PLoS Pathog*, 9(7), p. e1003500. doi:10.1371/journal.ppat.1003500.

Lee, A.J., Chen, B., Chew, M. v., Barra, N.G., Shenouda, M.M., Nham, T., van Rooijen, N., Jordana, M., Mossman, K.L., Schreiber, R.D., Mack, M. and Ashkar, A.A. (2017) "Inflammatory monocytes require type I interferon receptor signaling to activate NK cells via IL-18 during a mucosal viral infection," *J. Exp. Med*, 214(4), pp. 1153–1167. doi:10.1084/jem.20160880.

Lee, C., Hodgins, D., Calvert, J.G., Welch, S.K.W., Jolie, R. and Yoo, D. (2006) "Mutations within the nuclear localization signal of the porcine reproductive and respiratory syndrome virus nucleocapsid protein attenuate virus replication," *Virology*, 346(1), p. 238. doi:10.1016/j.virol.2005.11.005.

Lee, S.J., Matsuura, Y., Liu, S.M. and Stewart, M. (2005) "Structural basis for nuclear import complex dissociation by RanGTP," *Nature, 2005 435:7042*, 435(7042), pp. 693–696. doi:10.1038/nature03578.

Lee, S.J., Sekimoto, T., Yamashita, E., Nagoshi, E., Nakagawa, A., Imamoto, N., Yoshimura, M., Sakai, H., Chong, K.T., Tsukihara, T. and Yoneda, Y. (2003) "The structure of importin-beta bound to SREBP-2: nuclear import of a transcription factor.," *Science*, 302(5650), pp. 1571–5. doi:10.1126/science.1088372.

Lee, S.M. and Kleiboeker, S.B. (2007) "Porcine reproductive and respiratory syndrome virus induces apoptosis through a mitochondria-mediated pathway," *Virology*, 365(2), pp. 419–434. doi:10.1016/j.virol.2007.04.001.

Lee, Y.R., Yuan, W.C., Ho, H.C., Chen, C.H., Shih, H.M. and Chen, R.H. (2010) "The Cullin 3 substrate adaptor KLHL20 mediates DAPK ubiquitination to control interferon responses," *EMBO J*, 29(10), pp. 1748–1761. doi:10.1038/emboj.2010.62.

Lehmann, K.C., Gulyaeva, A., Zevenhoven-Dobbe, J.C., Janssen, G.M.C., Ruben, M., Overkleeft, H.S., Van Veelen, P.A., Samborskiy, D. V, Kravchenko, A.A., Leontovich, A.M., Sidorov, I.A., Snijder, E.J., Posthuma, C.C. and Gorbalenya, A.E. (2015) "Discovery of an essential nucleotidylating activity associated with a newly delineated conserved domain in the RNA polymerase-containing protein of all nidoviruses," *Nucleic Acids Res*, 43(17), pp. 8416–8434. doi:10.1093/nar/gkv838.

Lei, X., Han, N., Xiao, X., Jin, Q., He, B. and Wang, J. (2014) "Enterovirus 71 3C Inhibits Cytokine Expression through Cleavage of the TAK1/TAB1/TAB2/TAB3 Complex," *J. Virol*, 88(17), pp. 9830–9841. doi:10.1128/jvi.01425-14.

Levy, D.E. and Lee, C. (2002) "What does Stat3 do?," *J Clin Invest*, 109(9), p. 1143. doi:10.1172/jci15650.

Li, B. and Fields, S. (1993) "Identification of mutations in p53 that affect its binding to SV40 large T antigen by using the yeast two-hybrid system," *FASEB J*, 7(10), pp. 957–963. doi:10.1096/fasebj.7.10.8344494.

Li, J., Guo, D., Huang, L., Yin, M., Liu, Q., Wang, Y., Yang, C., Liu, Y., Zhang, L., Tian, Z., Cai, X., Yu, L. and Weng, C. (2014) "The interaction between host Annexin A2 and viral Nsp9 is beneficial for replication of porcine reproductive and respiratory syndrome virus," *Virus Res*, 189, pp. 106–113. doi:10.1016/j.virusres.2014.05.015.

Li, L., Jay, S.M., Wang, Y., Wu, S.W. and Xiao, Z. (2017) 'IL-12 stimulates CTLs to secrete exosomes capable of activating bystander CD8+ T cells', *Sci. Rep.*, 7(1), pp. 1–10. Available at: https://doi.org/10.1038/s41598-017-14000-z.

Li, L., Zhao, Q., Ge, X., Teng, K., Kuang, Y., Chen, Y., Guo, X. and Yang, H. (2012) "Chinese highly pathogenic porcine reproductive and respiratory syndrome virus exhibits more extensive tissue tropism for pigs," *Virol. J.*, 9(1), pp. 1–6. Available at: https://doi.org/10.1186/1743-422X-9-203/FIGURES/3.

Li, R., Chen, C., He, J., Zhang, Lilin, Zhang, Lei, Guo, Y., Zhang, W., Tan, K. and Huang, J. (2019) "E3 ligase ASB8 promotes porcine reproductive and respiratory syndrome virus proliferation by stabilizing the viral Nsp1α protein and degrading host IKKβ kinase," *Virology*, 532, pp. 55–68. doi:10.1016/j.virol.2019.04.004.

Li, S., Fang, W., Cui, Y., Shi, H., Chen, J., Li, L., Zhang, L. and Zhang, X. (2020) "Neddylation promotes protein translocation between the cytoplasm and nucleus," *Biochem. Biophys. Res. Commun*, 529(4), pp. 991–997. doi:10.1016/j.bbrc.2020.07.012.

Li, S., Zhou, A., Wang, J. and Zhang, S. (2016) "Interplay of autophagy and apoptosis during PRRSV infection of Marc145 cell," *Infect. Genet. Evol.*, 39, pp. 51–54. doi:10.1016/j.meegid.2016.01.011.

Li, T., Chen, X., Garbutt, K.C., Zhou, P. and Zheng, N. (2006) "Structure of DDB1 in complex with a paramyxovirus V protein: Viral Hijack of a propeller cluster in ubiquitin ligase," *Cell*, 124(1), pp. 105–117. doi:10.1016/j.cell.2005.10.033

Li, Yang, Fang, L., Zhou, Y., Tao, R., Wang, D. and Xiao, S. (2018) "Porcine Reproductive and Respiratory Syndrome Virus Infection Induces both eIF2α Phosphorylation-Dependent and -Independent Host Translation Shutoff," *J. Virol*, 92(16). doi:10.1128/JVI.00600-18.

Li, X., Galliher-Beckley, A., Wang, L., Nietfeld, J., Feng, W. and Shi, J. (2017) "Comparison of Immune Responses in Pigs Infected with Chinese Highly Pathogenic PRRS Virus Strain HV and North American Strain NADC-20," *Open Virol J.*, 11(1), pp. 73–82. Available at: https://doi.org/10.2174/1874357901711010073.

Li, Y., Shang, P., Shyu, D., Carrillo, C., Naraghi-Arani, P., Jaing, C.J., Renukaradhya, G.J., Firth, A.E., Snijder, E.J. and Fang, Y. (2018) "Nonstructural proteins nsp2TF and nsp2N of porcine

reproductive and respiratory syndrome virus (PRRSV) play important roles in suppressing host innate immune responses," *Virology*, 517, pp. 164–176. doi:10.1016/j.virol.2017.12.017.

Li, Y., Treffers, E.E., Napthine, S., Tas, A., Zhu, L., Sun, Z., Bell, S., Mark, B.L., van Veelen, P.A., van Hemert, M.J., Firth, A.E., Brierley, I., Snijder, E.J. and Fang, Y. (2014) "Transactivation of programmed ribosomal frameshifting by a viral protein," *PNAS*, 111(21), pp. E2172–E2181. doi:10.1073/pnas.1321930111.

Li, Y., Wang, X., Bo, K., Wang, X., Tang, B., Yang, B., Jiang, W. and Jiang, P. (2007) "Emergence of a highly pathogenic porcine reproductive and respiratory syndrome virus in the Mid-Eastern region of China," *Transbound Emerg Dis,* 2017;64(6):2059-2074. doi:10.1111/tbed.12617.

Li, Y.-P. (1997) "Protein B23 is an important human factor for the nucleolar localization of the human immunodeficiency virus protein Tat," *J. Virol*, 71(5), pp. 4098–4102. doi:10.1128/jvi.71.5.4098-4102.1997.

Li, Y., Xue, C., Wang, L., Chen, X., Chen, F. and Cao, Y. (2010) "Genomic analysis of two Chinese strains of porcine reproductive and respiratory syndrome viruses with different virulence," *Virus Genes*, 40(3), pp. 374–381. Available at: https://doi.org/10.1007/S11262-010-0453-Z/FIGURES/4.

Li, Y., Zhou, L., Zhang, J., Ge, X., Zhou, R., Zheng, H., Geng, G., Guo, X. and Yang, H. (2014) "Nsp9 and Nsp10 Contribute to the Fatal Virulence of Highly Pathogenic Porcine Reproductive and Respiratory Syndrome Virus Emerging in China," *PLoS Pathog.*, 10(7), p. e1004216. Available at: https://doi.org/10.1371/JOURNAL.PPAT.1004216.

Li, Z. and Srivastava, P. (2003) "Heat-Shock Proteins," *Curr. Protoc. Immunol*, 58(1), p. A.1T.1-A.1T.6. doi:10.1002/0471142735.ima01ts58.

Liang, X.H., Kleeman, L.K., Jiang, H.H., Gordon, G., Goldman, J.E., Berry, G., Herman, B., And, † and Levine, B. (1998) "Protection against Fatal Sindbis Virus Encephalitis by Beclin, a Novel Bcl-2-Interacting Protein," *J. Virol*, 72(11), pp. 8586–8596. doi:10.1128/jvi.72.11.8586-8596.1998.

Liu, B, Liao, J., Rao, X., Kushner, S.A., Chung, C.D., Chang, D.D. and Shuai, K. (1998) "Inhibition of Stat1-mediated gene activation by PIAS1.," *PNAS*, 95(18), pp. 10626–31. doi:10.1073/pnas.95.18.10626.

Liu, B., Mink, S., Wong, K.A., Stein, N., Getman, C., Dempsey, P.W., Wu, H. and Shuai, K. (2004) "PIAS1 selectively inhibits interferon-inducible genes and is important in innate immunity," *Nat. Immunol 2004 5:9*, 5(9), pp. 891–898. doi:10.1038/ni1104.

Liu, B., Yang, R., Wong, K.A., Getman, C., Stein, N., Teitell, M.A., Cheng, G., Wu, H. and Shuai, K. (2005) "Negative regulation of NF-kappaB signaling by PIAS1.," *Mol. Cell. Biol*, 25(3), pp. 1113–23. doi:10.1128/mcb.25.3.1113-1123.2005.

Liu, L., Tian, J., Nan, H., Tian, M., Li, Y., Xu, X., Huang, B., Zhou, E., Hiscox, J.A. and Chen, H. (2016) "Porcine Reproductive and Respiratory Syndrome Virus Nucleocapsid Protein Interacts with Nsp9 and Cellular DHX9 To Regulate Viral RNA Synthesis," *J. Virol*, 90(11), pp. 5384–5398. doi:10.1128/jvi.03216-15.

Liu, Q., Qin, Y., Zhou, L., Kou, Q., Guo, X., Ge, X., Yang, H. and Hu, H. (2012) "Autophagy sustains the replication of porcine reproductive and respiratory virus in host cells," *Virology*, 429(2), pp. 136–147. doi:10.1016/j.virol.2012.03.022.

Liu, Q., Yu, Y.-Y., Wang, H.-Y., Wang, J.-F. and He, X.-J. (2020) "The IFN-γ-induced immunoproteasome is suppressed in highly pathogenic porcine reproductive and respiratory syndrome virus-infected alveolar macrophages," *Vet. Immunol. Immunopathol*, 226, p. 110069. doi:10.1016/j.vetimm.2020.110069.

Liu, T., Zhang, L., Joo, D. and Sun, S.C. (2017) "NF-κB signaling in inflammation," *Signal Transduct. Target. Ther,* 2(1), pp. 1–9. doi:10.1038/sigtrans.2017.23.

Liu, X., Hong, T., Parameswaran, S., Ernst, K., Marazzi, I., Weirauch, M.T. and Fuxman Bass, J.I. (2020) "Human Virus Transcriptional Regulators," *Cell*, 182(1), pp. 24–37. doi:10.1016/j.cell.2020.06.023.

Liu, X., Wang, X., Wang, Q., Luo, M., Guo, H., Gong, W., Tu, C. and Sun, J. (2018) "The eukaryotic translation initiation factor 3 subunit E binds to classical swine fever virus NS5A and facilitates viral replication," *Virology*, 515, pp. 11–20. doi:10.1016/j.virol.2017.11.019.

Liu, Y., Hu, Y., Chai, Y., Liu, L., Song, J., Zhou, S., Su, J., Zhou, L., Ge, X., Guo, X., Han, J. and Yang, H. (2018) "Identification of Nonstructural Protein 8 as the N-Terminus of the RNA-Dependent RNA Polymerase of Porcine Reproductive and Respiratory Syndrome Virus," *Virol. Sin, 2018 33:5*, 33(5), pp. 429–439. doi:10.1007/s12250-018-0054-x.

Liu, Y. and Tan, X. (2020) "Viral Manipulations of the Cullin-RING Ubiquitin Ligases," *Adv. Exp. Med. Biol*, 1217, pp. 99–110. doi:10.1007/978-981-15-1025-0_7.

Liu, Z. and Roche, P.A. (2015) 'Macropinocytosis in phagocytes: Regulation of MHC class-II-restricted antigen presentation in dendritic cells', *Front. Physiol.,* 6(JAN), p. 1. Available at: https://doi.org/10.3389/FPHYS.2015.00001/XML/NLM.

Lu, G., Reinert, J.T., Pitha-Rowe, I., Okumura, A., Kellum, M., Knobeloch, K.P., Hassel, B. and Pitha, P.M. (2006) 'ISG15 enhances the innate antiviral response by inhibition of IRF-3 degradation.', *Cell. Mol. Biol. (Noisy-le-Grand, France)*, 52(1), pp. 29–41.

Lu, Y.C., Yeh, W.C. and Ohashi, P.S. (2008) "LPS/TLR4 signal transduction pathway," *Cytokine*, 42(2), pp. 145–151. doi:10.1016/j.cyto.2008.01.006.

Lund, E., Güttinger, S., Calado, A., Dahlberg, J.E. and Kutay, U. (2004) "Nuclear Export of MicroRNA Precursors," *Science*, 303(5654), pp. 95–98. doi:10.1126/science.1090599.

Lunney, Joan K., Fang, Y., Ladinig, A., Chen, N., Li, Y., Rowland, B. and Renukaradhya, G.J. (2016) "Porcine Reproductive and Respiratory Syndrome Virus (PRRSV): Pathogenesis and Interaction with the Immune System," *Annu. Rev. Anim. Biosci*, 4(1), pp. 129–154. doi:10.1146/annurev-animal-022114-111025.

Ma, J. and Cao, X. (2006) "Regulation of Stat3 nuclear import by importin α5 and importin α7 via two different functional sequence elements," *Cell. Signal*, 18(8), pp. 1117–1126. doi:10.1016/j.cellsig.2005.06.016.

Ma, Y.J., Hein, E., Munthe-Fog, L., Skjoedt, M.-O., Bayarri-Olmos, R., Romani, L. and Garred, P. (2015) "Soluble Collectin-12 (CL-12) Is a Pattern Recognition Molecule Initiating

Complement Activation via the Alternative Pathway," *J. Immunol*, 195(7), pp. 3365–3373. doi:10.4049/jimmunol.1500493

Macara, I.G. (2001) "Transport into and out of the Nucleus," *Microbiol. Mol. Biol. Rev*, 65(4), p. 570. doi:10.1128/mmbr.65.4.570-594.2001.

Mahon, C., Krogan, N.J., Craik, C.S. and Pick, E. (2014) "Cullin E3 ligases and their rewiring by viral factors.," *Biomolecules*, 4(4), pp. 897–930. doi:10.3390/biom4040897.

Malhotra, R., Haurum, J.S., Thiel, S. and Sim, R.B. (1994) "Binding of human collectins (SP-A and MBP) to influenza virus," *Biochem. J*, 304(2), pp. 455–461. doi:10.1042/bj3040455.

Malhotra, R. and Sim, R.B. (1995) "Collectins and viral infection," *Trends Microbiol*, 3(6), pp. 240–244. doi:10.1016/s0966-842x(00)88932-5.

Marini, B., Kertesz-Farkas, A., Ali, H., Lucic, B., Lisek, K., Manganaro, L., Pongor, S., Luzzati, R., Recchia, A., Mavilio, F., Giacca, M. and Lusic, M. (2015) "Nuclear architecture dictates HIV-1 integration site selection," *Nature*, 521(7551), pp. 227–231. doi:10.1038/nature14226.

Mayer, M.P. and Bukau, B. (2005) "Hsp70 chaperones: Cellular functions and molecular mechanism," *Cell. Mol. Life Sci*, 62(6), p. 670. doi:10.1007/s00018-004-4464-6.

McCarthy, M.K. and Weinberg, J.B. (2015) "The immunoproteasome and viral infection: a complex regulator of inflammation," *Front. Microbiol*, 6. doi:10.3389/fmicb.2015.00021.

McCloskey, A., Ibarra, A. and Hetzer, M.W. (2018) "Tpr regulates the total number of nuclear pore complexes per cell nucleus," *Genes Dev*, 32(19–20), pp. 1321–1331. doi:10.1101/gad.315523.118.

van der Meer, Y., van Tol, H., Krijnse Locker, J. and Snijder, E.J. (1998) "ORF1a-Encoded Replicase Subunits Are Involved in the Membrane Association of the Arterivirus Replication Complex," *J. Virol*, 72(8), pp. 6689–6698. doi:10.1128/jvi.72.8.6689-6698.1998.

Mendoza, H., Campbell, D.G., Burness, K., Hastie, J., Ronkina, N., Shim, J.-H., Arthur, J.S.C., Davis, R.J., Gaestel, M., Johnson, G.L., Ghosh, S. and Cohen, P. (2008) "Roles for TAB1 in regulating the IL-1-dependent phosphorylation of the TAB3 regulatory subunit and activity of the TAK1 complex," *Biochem. J*, 409(3), pp. 711–722. doi:10.1042/BJ20071149.

Meng, X.J., Paul, P.S., Halbur, P.G. and Lum, M.A. (1995) "Phylogenetic analyses of the putative M (ORF 6) and N (ORF 7) genes of porcine reproductive and respiratory syndrome virus (PRRSV): implication for the existence of two genotypes of PRRSV in the U.S.A. and Europe," *Arch. Virol*, 140(4), pp. 745–755. doi:10.1007/bf01309962.

Meng, X.W., Fraser, M.J., Feller, J.M. and Ziegler, J.B. (2000) 'Caspase-3-dependent and caspase-3-independent pathways leading to chromatin DNA fragmentation in HL-60 cells', *Apoptosis*, 5(1), pp. 61–67. Available at: https://doi.org/10.1023/A:1009689710184.

Mengeling, W.L., Lager, K.M. and Vorwald, A.C. (1998) "Clinical consequences of exposing pregnant gilts to strains of porcine reproductive and respiratory syndrome (PRRS) virus isolated from field cases of 'atypical' PRRS," *Am. J. Vet. Res,* 1998;59(12):1540-1544.

Meulenberg, J.J.M., de Meijer, E.J. and Moormann, R.J.M. (1993) "Subgenomic RNAs of Lelystad virus contain a conserved leader-body junction sequence," *J. Gen. Virol*, 74(8), pp. 1697–1701. doi:10.1099/0022-1317-74-8-1697.

Micheau, O. and Tschopp, J. (2003) 'Induction of TNF receptor I-mediated apoptosis via two sequential signaling complexes', *Cell*, 114(2), pp. 181–190. Available at: https://doi.org/10.1016/S0092-8674(03)00521-X.

Misinzo, G.M., Delputte, P.L. and Nauwynck, H.J. (2008) "Involvement of proteases in porcine reproductive and respiratory syndrome virus uncoating upon internalization in primary macrophages," *Vet. Res*, 39(6), p. 55. doi:10.1051/vetres:2008031.

Miskin, J.E., Abrams, C.C., Goatley, L.C. and Dixon, L.K. (1998) "A viral mechanism for inhibition of the cellular phosphatase calcineurin," *Science*, 281(5376), pp. 562–565. doi:10.1126/science.281.5376.562.

Misra, A. and Green, M.R. (2016) "From polyadenylation to splicing: Dual role for mRNA 3' end formation factors," *RNA Biol*, 13(3), p. 259. doi:10.1080/15476286.2015.1112490.

Mogensen, T.H. (2009) "Pathogen Recognition and Inflammatory Signaling in Innate Immune Defenses," *Clin. Microbiol. Rev*, 22(2), p. 240. doi:10.1128/cmr.00046-08.

Molenkamp, R., van Tol, H., Rozier, B.C.D., van der Meer, Y., Spaan, W.J.M. and Snijder, E.J. (2000) "The arterivirus replicase is the only viral protein required for genome replication and subgenomic mRNA transcription," *J. Gen. Virol*, 81(10), pp. 2491–2496. doi:10.1099/0022-1317-81-10-2491.

Montaner-Tarbes, S., del Portillo, H.A., Montoya, M. and Fraile, L. (2019) "Key gaps in the knowledge of the porcine respiratory reproductive syndrome virus (PRRSV)," *Front. Vet. Sci*, p. 38. doi:10.3389/fvets.2019.00038.

Montpetit, B., Thomsen, N.D., Helmke, K.J., Seeliger, M.A., Berger, J.M. and Weis, K. (2011) "A conserved mechanism of DEAD-box ATPase activation by nucleoporins and InsP6 in mRNA export," *Nature*, 472(7342), pp. 238–244. doi:10.1038/nature09862.

Morandell, D., Kaiser, A., Herold, S., Rostek, U., Lechner, S., Mitterberger, M.C., Jansen-Dürr, P., Eilers, M. and Zwerschke, W. (2012) "The human papillomavirus type 16 E7 oncoprotein targets Myc-interacting zinc-finger protein-1," *Virology*, 422(2), pp. 242–253. doi:10.1016/j.virol.2011.10.027.

Morgan, S.B., Frossard, J.P., Pallares, F.J., Gough, J., Stadejek, T., Graham, S.P., Steinbach, F., Drew, T.W. and Salguero, F.J. (2016) "Pathology and Virus Distribution in the Lung and Lymphoid Tissues of Pigs Experimentally Inoculated with Three Distinct Type 1 PRRS Virus Isolates of Varying Pathogenicity," *Transboundary Emerging Dis*, 63(3), pp. 285–295. doi:10.1111/tbed.12272.

Morgan, S.B., Graham, S.P., Salguero, F.J., Sánchez Cordón, P.J., Mokhtar, H., Rebel, J.M.J., Weesendorp, E., Bodman-Smith, K.B., Steinbach, F. and Frossard, J.P. (2013) "Increased pathogenicity of European porcine reproductive and respiratory syndrome virus is associated with enhanced adaptive responses and viral clearance," *Vet. Microbiol*, 163(1), pp. 13–22. doi:10.1016/j.vetmic.2012.11.024.

Mullan, R.H., Bresnihan, B., Golden-Mason, L., Markham, T., O'Hara, R., FitzGerald, O., Veale, D.J. and Fearon, U. (2006) 'Acute-phase serum amyloid A stimulation of angiogenesis, leukocyte recruitment, and matrix degradation in rheumatoid arthritis through an NF-κB–dependent signal transduction pathway', *Arthritis Rheum.,* 54(1), pp. 105–114. Available at: https://doi.org/10.1002/art.21518.

Münz, C. (2011) “Beclin-1 Targeting for Viral Immune Escape,” *Viruses 2011, Vol. 3, Pages 1166-1178*, 3(7), pp. 1166–1178. doi:10.3390/v3071166.

Murata, S., Takahama, Y., Kasahara, M. and Tanaka, K. (2018) “The immunoproteasome and thymoproteasome: functions, evolution and human disease,” *Nat. Immunol 2018 19:9*, 19(9), pp. 923–931. doi:10.1038/s41590-018-0186-z.

Murphy, R. and Wente, S.R. (1996) “An RNA-export mediator with an essential nuclear export signal,” *Nature 1996 383:6598*, 383(6598), pp. 357–360. doi:10.1038/383357a0.

Nan, H., Lan, J., Tian, M., Dong, S., Tian, J., Liu, L., Xu, X. and Chen, H. (2018) “The network of interactions among porcine reproductive and respiratory syndrome virus non-structural proteins,” *Front. Microbiol*, 9(MAY), pp. 1–9. doi:10.3389/fmicb.2018.00970.

Nan, Y., Wu, C., Gu, G., Sun, W., Zhang, Y.J. and Zhou, E.M. (2017) “Improved vaccine against PRRSV: Current Progress and future perspective,” *Front. Microbiol*. doi:10.3389/fmicb.2017.01635.

Nauwynck, H.J., Duan, X., Favoreel, H.W., Van Oostveldt, P. and Pensaert, M.B. (1999) “Entry of porcine reproductive and respiratory syndrome virus into porcine alveolar macrophages via receptor-mediated endocytosis,” *J. Gen. Virol*, 80(2), pp. 297–305. doi:10.1099/0022-1317-80-2-297.

Nedialkova, D.D., Gorbalenya, A.E. and Snijder, E.J. (2010) “Arterivirus Nsp1 modulates the accumulation of minus-strand templates to control the relative abundance of viral mRNAs,” *PLoS Pathog*, 6(2). doi:10.1371/journal.ppat.1000772.

Nedialkova, D.D., Ulferts, R., van den Born, E., Lauber, C., Gorbalenya, A.E., Ziebuhr, J. and Snijder, E.J. (2009) “Biochemical Characterization of Arterivirus Nonstructural Protein 11 Reveals the Nidovirus-Wide Conservation of a Replicative Endoribonuclease,” *J. Virol*, 83(11), pp. 5671–5682. doi:10.1128/jvi.00261-09.

Nemeroff, M.E., Barabino, S.M.L., Li, Y., Keller, W. and Krug, R.M. (1998) “Influenza Virus NS1 Protein Interacts with the Cellular 30 kDa Subunit of CPSF and Inhibits 3’ End Formation of Cellular Pre-mRNAs,” *Mol. Cell*, 1(7), pp. 991–1000. doi:10.1016/s1097-2765(00)80099-4.

Ng, A.C.-H., Baird, S.D. and Screaton, R.A. (2014) “Essential Role of TID1 in Maintaining Mitochondrial Membrane Potential Homogeneity and Mitochondrial DNA Integrity,” *Mol. Cell. Biol*, 34(8), p. 1427. doi:10.1128/mcb.01021-13.

Niemand, C., Nimmesgern, A., Haan, S., Fischer, P., Schaper, F., Rossaint, R., Heinrich, P.C. and Müller-Newen, G. (2003) “Activation of STAT3 by IL-6 and IL-10 in primary human macrophages is differentially modulated by suppressor of cytokine signaling 3,” *J. Immunol*, 170(6), pp. 3263–3272. doi:10.4049/jimmunol.170.6.3263.

Nikolaev, A.Y., Li, M., Puskas, N., Qin, J. and Gu, W. (2003) “Parc: a cytoplasmic anchor for p53.,” *Cell*, 112(1), pp. 29–40. doi:10.1016/s0092-8674(02)01255-2.

Nishi, K., Iwaihara, Y., Tsunoda, T., Doi, K., Sakata, T., Shirasawa, S. and Ishikura, S. (2017) “ROS-induced cleavage of NHLRC2 by caspase-8 leads to apoptotic cell death in the HCT116 human colon cancer cell line,” *Cell Death Dis, 2017 8:12*, 8(12), pp. 1–13. doi:10.1038/s41419-017-0006-7.

Niso-Santano, M., Criollo, A., Malik, S.A., Michaud, M., Morselli, E., Mariño, G., Lachkar, S., Galluzzi, L., Maiuri, M.C. and Kroemer, G. (2012) "Direct molecular interactions between Beclin 1 and the canonical NFκB activation pathway," *Autophagy,* doi:10.4161/auto.8.2.18845.

Noble, K.N., Tran, E.J., Alcázar-Román, A.R., Hodge, C.A., Cole, C.N. and Wente, S.R. (2011) "The Dbp5 cycle at the nuclear pore complex during mRNA export II: nucleotide cycling and mRNP remodeling by Dbp5 are controlled by Nup159 and Gle1," *Genes Dev*, 25(10), p. 1065. doi:10.1101/gad.2040611.

di Noia, J.M. and Neuberger, M.S. (2007) 'Molecular Mechanisms of Antibody Somatic Hypermutation', *Annu. Rev. Biochem.*, 76(1), pp. 1–22. Available at: https://doi.org/10.1146/annurev.biochem.76.061705.090740.

Oeckinghaus, A. and Ghosh, S. (2009) "The NF-kappaB family of transcription factors and its regulation.," *Cold Spring Harbor Perspect. Biol*. doi:10.1101/cshperspect.a000034.

Oh, H. and Ghosh, S. (2013) "NF-κB: roles and regulation in different CD4(+) T-cell subsets," *Immunol. Rev*, 252(1), pp. 41–51. doi:10.1111/imr.12033.

Ohtani, K., Suzuki, Y., Eda, S., Kawai, T., Kase, T., Keshi, H., Sakai, Y., Fukuoh, A., Sakamoto, T., Itabe, H., Suzutani, T., Ogasawara, M., Yoshida, I. and Wakamiya, N. (2001) "The membrane-type collectin CL-P1 is a scavenger receptor on vascular endothelial cells," *J. Biol. Chem*, 276(47), pp. 44222–44228. doi:10.1074/jbc.m103942200.

Okubo, S., Hara, F., Tsuchida, Y., Shimotakahara, S., Suzuki, S., Hatanaka, H., Yokoyama, S., Tanaka, H., Yasuda, H. and Shindo, H. (2004) "NMR Structure of the N-terminal Domain of SUMO Ligase PIAS1 and Its Interaction with Tumor Suppressor p53 and A/T-rich DNA Oligomers *," *J. Biol. Chem*, 279(30), pp. 31455–31461. doi:10.1074/jbc.m403561200.

Opriessnig, T., Giménez-Lirola, L.G. and Halbur, P.G. (2011) "Polymicrobial respiratory disease in pigs," *Anim. Health Res. Rev*, 12(02), pp. 133–148. doi:10.1017/s1466252311000120.

Ortolano, N.A., Romero-Morales, A.I., Rasmussen, M.L., Bodnya, C., Kline, L.A., Joshi, P., Connelly, J.P., Rose, K.L., Pruett-Miller, S.M. and Gama, V. (2021) "A proteomics approach for the identification of cullin-9 (CUL9) related signaling pathways in induced pluripotent stem cell models," *PLoS One*, 16(3), p. e0248000. doi:10.1371/journal.pone.0248000.

Pager, C.T., Craft, W.W., Patch, J. and Dutch, R.E. (2006) "A mature and fusogenic form of the Nipah virus fusion protein requires proteolytic processing by cathepsin L," *Virology*, 346(2), pp. 251–257. doi:10.1016/j.virol.2006.01.007.

Pager, C.T. and Dutch, R.E. (2005) "Cathepsin L Is Involved in Proteolytic Processing of the Hendra Virus Fusion Protein," *J. Virol*, 79(20), pp. 12714–12720. doi:10.1128/jvi.79.20.12714-12720.2005

Palazon, A., Goldrath, A.W., Nizet, V. and Johnson, R.S. (2014) "HIF transcription factors, inflammation, and immunity," *Immunity*, 41(4), pp. 518–528. doi:10.1016/j.immuni.2014.09.008.

Pang, Y., Li, M., Zhou, Y., Liu, W., Tao, R., Zhang, H., Xiao, S., & Fang, L. (2021) "The ubiquitin proteasome system is necessary for efficient proliferation of porcine reproductive and

respiratory syndrome virus," *Vet Microbiol,* 2021;253:108947. doi:10.1016/j.vetmic.2020.108947.

Patel, D., Nan, Y., Shen, M., Ritthipichai, K., Zhu, X. and Zhang, Y.-J. (2010) "Porcine Reproductive and Respiratory Syndrome Virus Inhibits Type I Interferon Signaling by Blocking STAT1/STAT2 Nuclear Translocation," *J. Virol*, 84(21), pp. 11045–11055. doi:10.1128/jvi.00655-10.

Pattingre, S., Tassa, A., Qu, X., Garuti, R., Xiao, H.L., Mizushima, N., Packer, M., Schneider, M.D. and Levine, B. (2005) "Bcl-2 antiapoptotic proteins inhibit Beclin 1-dependent autophagy," *Cell*, 122(6), pp. 927–939. doi:10.1016/j.cell.2005.07.002.

Paul, S. and Lal, G. (2017) 'The molecular mechanism of natural killer cells function and its importance in cancer immunotherapy', *Front. Immunol.*, 8(SEP), p. 1124. Available at: https://doi.org/10.3389/FIMMU.2017.01124/XML/NLM.

Paz, X. de (2015) "PRRS cost for the European swine industry," Available at: https://www.pig333.com/articles/prrs-cost-for-the-european-swine-industry_10069/

Pedersen, K.W., van der Meer, Y., Roos, N. and Snijder, E.J. (1999) "Open Reading Frame 1a-Encoded Subunits of the Arterivirus Replicase Induce Endoplasmic Reticulum-Derived Double-Membrane Vesicles Which Carry the Viral Replication Complex," *J. Virol*, 73(3), pp. 2016–2026. doi:10.1128/jvi.73.3.2016-2026.1999.

Peng, W., Shi, Y., Wang, B., Liu, B., Peng, Z., Zhang, J., Chen, L. and Zhang, H. (2016) "Upregulation of GLE1 and LCP2 Genes in H5N1 Influenza Virus Infected Patients," *Adv. Infect. Dis*, 06(03), pp. 138–144. doi:10.4236/aid.2016.63017.

Perng, Y.-C. and Lenschow, D.J. (2018) 'ISG15 in antiviral immunity and beyond', *Nat. Rev. Microbiol.*, 16(7), pp. 423–439. Available at: https://doi.org/10.1038/s41579-018-0020-5.

Peters, J.M., Franke, W.W. and Kleinschmidt, J.A. (1994) "Distinct 19 S and 20 S subcomplexes of the 26 S proteasome and their distribution in the nucleus and the cytoplasm.," *J. Biol. Chem*, 269(10), pp. 7709–18.

Pileri, E. and Mateu, E. (2016) "Review on the transmission porcine reproductive and respiratory syndrome virus between pigs and farms and impact on vaccination," *Vet. Res*. BioMed Central Ltd., pp. 1–13. doi:10.1186/s13567-016-0391-4.

Platanias, L.C. (2005) 'Mechanisms of type-I- and type-II-interferon-mediated signalling', *Nat. Rev. Immunol.*, 5(5), pp. 375–386. Available at: https://doi.org/10.1038/nri1604.

Posthuma, C.C., Nedialkova, D.D., Zevenhoven-Dobbe, J.C., Blokhuis, J.H., Gorbalenya, A.E. and Snijder, E.J. (2006) "Site-directed mutagenesis of the Nidovirus replicative endoribonuclease NendoU exerts pleiotropic effects on the arterivirus life cycle.," *J. Virol*, 80(4), pp. 1653–1661. doi:10.1128/jvi.80.4.1653-1661.2006.

Prather, R.S., Rowland, R.R.R., Ewen, C., Trible, B., Kerrigan, M., Bawa, B., Teson, J.M., Mao, J., Lee, K., Samuel, M.S., Whitworth, K.M., Murphy, C.N., Egen, T. and Green, J.A. (2013) "An Intact Sialoadhesin (Sn/SIGLEC1/CD169) Is Not Required for Attachment/Internalization of the Porcine Reproductive and Respiratory Syndrome Virus," *J. Virol*, 87(17), pp. 9538–9546. doi:10.1128/jvi.00177-13

Pugazhenthi, S., Zhang, Y., Bouchard, R. and Mahaffey, G. (2013) 'Induction of an Inflammatory Loop by Interleukin-1β and Tumor Necrosis Factor-α Involves NF-kB and STAT-1 in Differentiated Human Neuroprogenitor Cells', *PLoS One*, 8(7), p. 69585. Available at: https://doi.org/10.1371/JOURNAL.PONE.0069585.

Qi, P., Liu, K., Wei, J., Li, Y., Li, B., Shao, D., Wu, Z., Shi, Y., Tong, G., Qiu, Y. and Ma, Z. (2017) "Nonstructural Protein 4 of Porcine Reproductive and Respiratory Syndrome Virus Modulates Cell Surface Swine Leukocyte Antigen Class I Expression by Downregulating β2-Microglobulin Transcription," *J. Virol*, 91(5). doi:10.1128/jvi.01755-16.

Qiao, Y., Wang, P., Qi, J., Zhang, L. and Gao, C. (2012) "TLR-induced NF-κB activation regulates NLRP3 expression in murine macrophages," *FEBS Lett.*, 586(7), pp. 1022–1026. doi:10.1016/j.febslet.2012.02.045.

Qiu, X.-B., Shao, Y.-M., Miao, S. and Wang, L. (2006) "The diversity of the DnaJ/Hsp40 family, the crucial partners for Hsp70 chaperones," *Cell. Mol. Life Sci*, 63(22), pp. 2560–2570. doi:10.1007/s00018-006-6192-6.

Raaben, M., Posthuma, C.C., Verheije, M.H., te Lintelo, E.G., Kikkert, M., Drijfhout, J.W., Snijder, E.J., Rottier, P.J.M. and de Haan, C.A.M. (2010) "The Ubiquitin-Proteasome System Plays an Important Role during Various Stages of the Coronavirus Infection Cycle," *J. Virol*, 84(15), pp. 7869–7879. doi:10.1128/jvi.00485-10.

Ramanathan, A., Robb, G.B. and Chan, S.-H. (2016) "mRNA capping: biological functions and applications," *Nucleic Acids Res*, 44(16), pp. 7511–7526. doi:10.1093/nar/gkw551.

Raney, A., Kuo, L.S., Baugh, L.L., Foster, J.L. and Garcia, J.V. (2005) "Reconstitution and Molecular Analysis of an Active Human Immunodeficiency Virus Type 1 Nef/p21-Activated Kinase 2 Complex," *J. Virol*, 79(20), pp. 12732–12741. doi:10.1128/jvi.79.20.12732-12741.2005

Raphael, I., Nalawade, S., Eagar, T.N. and Forsthuber, T.G. (2015) 'T cell subsets and their signature cytokines in autoimmune and inflammatory diseases', *Cytokine*, 74(1), pp. 5–17. Available at: https://doi.org/10.1016/j.cyto.2014.09.011.

Rascón-Castelo, E., Burgara-Estrella, A., Mateu, E. and Hernández, J. (2015) "Immunological features of the non-structural proteins of porcine reproductive and respiratory syndrome virus," *Viruses*, pp. 873–886. doi:10.3390/v7030873.

Rayala, H.J., Kendirgi, F., Barry, D.M., Mjerus, P.W. and Wente, S.R. (2004) "The mRNA Export Factor Human Gle1 Interacts with the Nuclear Pore Complex Protein Nup155 *," *Mol. Cell. Proteomics*, 3(2), pp. 145–155. doi:10.1074/mcp.m300106-mcp200.

Reichelt, M., Wang, L., Sommer, M., Perrino, J., Nour, A.M., Sen, N., Baiker, A., Zerboni, L. and Arvin, A.M. (2011) "Entrapment of Viral Capsids in Nuclear PML Cages Is an Intrinsic Antiviral Host Defense against Varicella-Zoster Virus," *PLoS Pathog*, 7(2), p. e1001266. doi:10.1371/journal.ppat.1001266.

Renkema, G.H., Manninen, A. and Saksela, K. (2001) "Human Immunodeficiency Virus Type 1 Nef Selectively Associates with a Catalytically Active Subpopulation of p21-Activated Kinase 2 (PAK2) Independently of PAK2 Binding to Nck or β-PIX," *J. Virol*, 75(5), pp. 2154–2160. doi:10.1128/JVI.75.5.2154-2160.2001

Ricciotti, E. and Fitzgerald, G.A. (2011) 'Prostaglandins and Inflammation', *Arterioscler. Thromb. Vasc. Biol.*, 31(5), p. 986. Available at: https://doi.org/10.1161/ATVBAHA.110.207449.

Robzyk, K., Recht, J. and Osley, M.A. (2000) "Rad6-Dependent Ubiquitination of Histone H2B in Yeast," *Science*, 287(5452), pp. 501–504. doi:10.1126/science.287.5452.501.

Rossow, K.D. (1998) "Porcine Reproductive and Respiratory Syndrome," *Vet. Pathol*, 35(1), pp. 1–20. doi:10.1177/030098589803500101.

Roth, D.B. (2014) 'V(D)J Recombination: Mechanism, Errors, and Fidelity', *Microbiol. Spectrum.*, 2(6). Available at: https://doi.org/10.1128/MICROBIOLSPEC.MDNA3-0041-2014.

Rowland, R.R.R., Lawson, S., Rossow, K. and Benfield, D.A. (2003) "Lymphoid tissue tropism of porcine reproductive and respiratory syndrome virus replication during persistent infection of pigs originally exposed to virus in utero," *Vet. Microbiol*, 96(3), pp. 219–235. doi:10.1016/j.vetmic.2003.07.006.

Rowland, R.R.R. and Yoo, D. (2003) "Nucleolar-cytoplasmic shuttling of PRRSV nucleocapsid protein: a simple case of molecular mimicry or the complex regulation by nuclear import, nucleolar localization and nuclear export signal sequences," *Virus Res*, 95(1–2), pp. 23–33. doi:10.1016/s0168-1702(03)00161-8.

Ruedas-Torres, I., Rodríguez-Gómez, I.M., Sánchez-Carvajal, J.M., Larenas-Muñoz, F., Pallarés, F.J., Carrasco, L. and Gómez-Laguna, J. (2021) "The jigsaw of PRRSV virulence," *Vet. Microbiol.*, 260. Available at: https://doi.org/10.1016/J.VETMIC.2021.109168.

Sachdev, S., Bruhn, L., Sieber, H., Pichler, A., Melchior, F. and Grosschedl, R. (2001) "PIASy, a nuclear matrix-associated SUMO E3 ligase, represses LEF1 activity by sequestration into nuclear bodies," *Genes Dev.*, 15(23), pp. 3088–3103. doi:10.1101/gad.944801.

Sagripanti, J.L., Zandomeni, R.O. and Weinmann, R. (1986) "The cap structure of simian hemorrhagic fever virion RNA," *Virology*, 151(1), pp. 146–150. doi:10.1016/0042-6822(86)90113-3.

Samuel, C.E. (2001) "Antiviral Actions of Interferons," *Clin. Microbiol. Rev*, 14(4), pp. 778–809. doi:10.1128/cmr.14.4.778-809.2001.

Sánchez-Carvajal, J.M., Rodríguez-Gómez, I.M., Ruedas-Torres, I., Larenas-Muñoz, F., Díaz, I., Revilla, C., Mateu, E., Domínguez, J., Martín-Valls, G., Barranco, I., Pallarés, F.J., Carrasco, L. and Gómez-Laguna, J. (2020) "Activation of pro- and anti-inflammatory responses in lung tissue injury during the acute phase of PRRSV-1 infection with the virulent strain Lena," *Vet. Microbiol.*, 246, p. 108744. Available at: https://doi.org/10.1016/J.VETMIC.2020.108744.

Sarikas, A., Hartmann, T. and Pan, Z.Q. (2011) "The cullin protein family," *Genome Biol.*, 12(4), pp. 1–12. doi:10.1186/gb-2011-12-4-220

Sarkar, S., Pollack, B.P., Lin, K.T., Kotenko, S. v., Cook, J.R., Lewis, A. and Pestka, S. (2001) "hTid-1, a Human DnaJ Protein, Modulates the Interferon Signaling Pathway *," *J. Biol. Chem*, 276(52), pp. 49034–49042. doi:10.1074/jbc.m103683200.

Schluns, K.S. and Lefrançois, L. (2003) 'Cytokine control of memory T-cell development and survival', *Nat. Rev. Immunol.*, 3(4), pp. 269–279. Available at: https://doi.org/10.1038/nri1052.

Schmeisser, H., Bekisz, J. and Zoon, K.C. (2014) “New Function of Type I IFN: Induction of Autophagy,” *J Interferon Cytokine Res*, 34(2), pp. 71–78. doi:10.1089/JIR.2013.0128.

Schmidt, D. and Müller, S. (2002) “Members of the PIAS family act as SUMO ligases for c-Jun and p53 and repress p53 activity,” *PNAS*, 99(5), pp. 2872–2877. doi:10.1073/pnas.052559499.

Schneider, W.M., Chevillotte, M.D. and Rice, C.M. (2014) “Interferon-Stimulated Genes: A Complex Web of Host Defenses,” *Annu. Rev. Immunol*, 32, p. 513. doi:10.1146/annurev-immunol-032713-120231.

Schönemann, L., Kühn, U., Martin, G., Schäfer, P., Gruber, A.R., Keller, W., Zavolan, M. and Wahle, E. (2014) “Reconstitution of CPSF active in polyadenylation: recognition of the polyadenylation signal by WDR33,” *Genes Dev.*, 28(21), p. 2381. doi:10.1101/gad.250985.114.

Schornberg, K., Matsuyama, S., Kabsch, K., Delos, S., Bouton, A. and White, J. (2006) “Role of Endosomal Cathepsins in Entry Mediated by the Ebola Virus Glycoprotein,” *J. Virol*, 80(8), pp. 4174–4178. doi:10.1128/jvi.80.8.4174-4178.2006

Schroder, K., Hertzog, P.J., Ravasi, T. and Hume, D.A. (2004) ‘Interferon-γ: an overview of signals, mechanisms and functions’, *J. Leukocyte Biol.*, 75(2), pp. 163–189. Available at: https://doi.org/10.1189/JLB.0603252.

Schwartz, T.U. (2016) “The Structure Inventory of the Nuclear Pore Complex.,” *J. Mol. Biol*, 428(10 Pt A), pp. 1986–2000. doi:10.1016/j.jmb.2016.03.015.

Seder, R.A. and Ahmed, R. (2003) ‘Similarities and differences in CD4+ and CD8+ effector and memory T cell generation’, *Nat. Immunol.*, 4(9), pp. 835–842. Available at: https://doi.org/10.1038/ni969.

Seybert, A., van Dinten, L.C., Snijder, E.J. and Ziebuhr, J. (2000) “Biochemical Characterization of the Equine Arteritis Virus Helicase Suggests a Close Functional Relationship between Arterivirus and Coronavirus Helicases,” *J. Virol*, 74(20), pp. 9586–9593. doi:10.1128/jvi.74.20.9586-9593.2000.

Shanmukhappa, K., Kim, J.K. and Kapil, S. (2007) “Role of CD151, A tetraspanin, in porcine reproductive and respiratory syndrome virus infection,” V*irol.J*, 4. doi:10.1186/1743-422x-4-62.

Sharma, M. and Wente, S.R. (2020) “Nucleocytoplasmic shuttling of Gle1 impacts DDX1 at transcription termination sites,” *Mol. Biol. Cell*, 31(21), pp. 2398–2408. doi:10.1091/mbc.e20-03-0215.

Shi, C., Liu, Y., Ding, Y., Zhang, Y. and Zhang, J. (2015) “PRRSV receptors and their roles in virus infection,” *Arch. Microbiol,* 197(4), pp. 503–512. doi:10.1007/s00203-015-1088-1.

Shi, M., Lam, T.T.Y., Hon, C.C., Hui, R.K.H., Faaberg, K.S., Wennblom, T., Murtaugh, M.P., Stadejek, T. and Leung, F.C.C. (2010) “Molecular epidemiology of PRRSV: A phylogenetic perspective,” *Virus Res*, 2010;154(1-2), pp. 7–17. doi:10.1016/j.virusres.2010.08.014.

Shi, X., Wang, L., Li, X., Zhang, G., Guo, J., Zhao, D., Chai, S. and Deng, R. (2011) “Endoribonuclease activities of porcine reproductive and respiratory syndrome virus nsp11

was essential for nsp11 to inhibit IFN-β induction," *Mol. Immunol*, 48(12–13), pp. 1568–1572. doi:10.1016/j.molimm.2011.03.004.

Shi, X., Zhang, X., Chang, Y., Jiang, B., Deng, R., Wang, A. and Zhang, G. (2016) "Nonstructural protein 11 (nsp11) of porcine reproductive and respiratory syndrome virus (PRRSV) promotes PRRSV infection in MARC-145 cells," *BMC Vet. Res*, 12(1), p. 90. doi:10.1186/s12917-016-0717-5.

Shi, Y., Li, Y., Lei, Y., Ye, G., Shen, Z., Sun, L., Luo, R., Wang, D., Fu, Z.F., Xiao, S. and Peng, G. (2016) "A Dimerization-Dependent Mechanism Drives the Endoribonuclease Function of Porcine Reproductive and Respiratory Syndrome Virus nsp11.," *J. Virol*, 90(9), pp. 4579–92. doi:10.1128/jvi.03065-15.

Shih, S.C., Sloper-Mould, K.E. and Hicke, L. (2000) "Monoubiquitin carries a novel internalization signal that is appended to activated receptors," *EMBO J*, 19(2), p. 187. doi:10.1093/emboj/19.2.187.

Shinohara, H., Yasuda, T. and Kurosaki, T. (2016) "TAK1 adaptor proteins, TAB2 and TAB3, link the signalosome to B-cell receptor-induced IKK activation," *FEBS Lett.*, 590(18), pp. 3264–3269. doi:10.1002/1873-3468.12342.

Shuai, K. (2006) "Regulation of cytokine signaling pathways by PIAS proteins," *Cell Res 2006 16:2*, 16(2), pp. 196–202. doi:10.1038/sj.cr.7310027.

Shuai, K. and Liu, B. (2005) "Regulation of gene-activation pathways by PIAS proteins in the immune system," *Nat. Rev. Immunol*, 5(8), pp. 593–605. doi:10.1038/nri1667.

Siddell, S.G., Peter, ·, Walker, J., Lefkowitz, E.J., Arcady, ·, Mushegian, R., Michael, ·, Adams, J., Bas, ·, Dutilh, E., Alexander, ·, Gorbalenya, E., Harrach, B., Robert, ·, Harrison, L., Junglen, S., Nick, ·, Knowles, J., Andrew, ·, Kropinski, M., Krupovic, M., Kuhn, J.H., Nibert, M., Rubino, · Luisa, Sabanadzovic, · Sead, Sanfaçon, · Hélène, Simmonds, · Peter, Varsani, A., Francisco, ·, Zerbini, M., Davison, J., Walker, P.J., Adams, M.J., Dutilh, B.E., Gorbalenya, A.E., Harrison, R.L., Knowles, N.J., Kropinski, A.M., Rubino, L., Sabanadzovic, S. and Sanfaçon, H. (2019) "Additional changes to taxonomy ratified in a special vote by the International Committee on Taxonomy of Viruses (October 2018)," 164, pp. 943–946. doi:10.1007/s00705-018-04136-2.

Siegel, J.P. (1988) "Effects of interferon-gamma on the activation of human T lymphocytes," *Cell. Immunol*, 111(2), pp. 461–472. doi:10.1016/0008-8749(88)90109-8.

Sizova, D. v., Kolupaeva, V.G., Pestova, T. v., Shatsky, I.N. and Hellen, C.U.T. (1998) "Specific Interaction of Eukaryotic Translation Initiation Factor 3 with the 5′ Nontranslated Regions of Hepatitis C Virus and Classical Swine Fever Virus RNAs," *J. Virol*, 72(6), pp. 4775–4782. doi:10.1128/jvi.72.6.4775-4782.1998.

Snijder, E.J., Kikkert, M. and Fang, Y. (2013) "Arterivirus molecular biology and pathogenesis," *J. Gen. Virol*. pp. 2141–2163. doi:10.1099/vir.0.056341-0.

Snijder, E.J., Van Tol, H., Roos, N. and Pedersen, K.W. (2001) "Non-structural proteins 2 and 3 interact to modify host cell membranes during the formation of the arterivirus replication complex," *J. Gen. Virol*, 82(5), pp. 985–994. doi:DOI 10.1099/vir.0.17499-0.

Snijder, E.J., Wassenaar, A.L.M., Van Dinten, L.C., Spaan, W.J.M. and Gorbalenya, A.E. (1996) "The arterrvirus Nsp4 protease is the prototype of a novel group of chymotrypsin-like

enzymes, the 3C-like serine proteases," *J. Biol. Chem*, 271(9), pp. 4864–4871. doi:10.1074/jbc.271.9.4864.

Song, C., Du, Y., Kim, O., Liu, H.C. and Yoo, D. (2010) "Interaction of PRRSV Nsp1α and protein inhibitor of activated STAT1 (PIAS1) mediated sumolation of Nsp1α," PhD thesis, University of Illinois at Urbana-Champaign, Urbana, IL, USA. *Unpublished work*.

Song, C., Krell, P. and Yoo, D. (2010) "Nonstructural protein 1α subunit-based inhibition of NF-κB activation and suppression of interferon-β production by porcine reproductive and respiratory syndrome virus," *Virology*, 407(2), pp. 268–280. doi:10.1016/j.virol.2010.08.025.

Song, C., Lu, R., Bienzle, D., Liu, H.-C. and Yoo, D. (2009) "Interaction of the porcine reproductive and respiratory syndrome virus nucleocapsid protein with the inhibitor of MyoD family-a domain-containing protein," *Biol. Chem*, 390(3), pp. 215–23. doi:10.1515/bc.2009.028.

Song, J., Liu, Y., Gao, P., Hu, Y., Chai, Y., Zhou, S., Kong, C., Zhou, L., Ge, X., Guo, X., Han, J. and Yang, H. (2018) "Mapping the Nonstructural Protein Interaction Network of Porcine Reproductive and Respiratory Syndrome Virus," *J. Virol*, 92(24). doi:10.1128/jvi.01112-18.

Stadejek, T., Stankevicius, A., Murtaugh, M.P. and Oleksiewicz, M.B. (2013) "Molecular evolution of PRRSV in Europe: Current state of play," *Vet. Microbiol*, 165(1–2), pp. 21–28. doi:10.1016/j.vetmic.2013.02.029.

Stavnezer, J., Guikema, J.E.J. and Schrader, C.E. (2008) 'Mechanism and Regulation of Class Switch Recombination', *Annu. Rev. Immunol.*, 26(1), pp. 261–292. Available at: https://doi.org/10.1146/annurev.immunol.26.021607.090248.

Steiner, E., Holzmann, K., Pirker, C., Elbling, L., Micksche, M., Sutterlüty, H. and Berger, W. (2006) "The major vault protein is responsive to and interferes with interferon-γ-mediated STAT1 signals," *J. Cell Sci*, 119(3), pp. 459–469. doi:10.1242/JCS.02773.

Stewart, M. (2007) "Molecular mechanism of the nuclear protein import cycle," *Nat. Rev. Mol. Cell Biol, 2007 8:3*, 8(3), pp. 195–208. doi:10.1038/nrm2114.

Stout, B.A., Bates, M.E., Liu, L.Y., Farrington, N.N. and Bertics, P.J. (2004) "IL-5 and granulocyte-macrophage colony-stimulating factor activate STAT3 and STAT5 and promote Pim-1 and cyclin D3 protein expression in human eosinophils," *J. Immunol,* 173(10), pp. 6409–6417. doi:10.4049/jimmunol.173.10.6409.

Strabetaer, K. (2000) "Yra1p, a conserved nuclear RNA-binding protein, interacts directly with Mex67p and is required for mRNA export," *EMBO J*, 19(3), pp. 410–420. doi:10.1093/emboj/19.3.410.

Strambio-De-Castillia, C., Niepel, M. and Rout, M.P. (2010) "The nuclear pore complex: bridging nuclear transport and gene regulation," *Nat. Rev. Mol. Cell Biol*, 11(7), pp. 490–501. doi:10.1038/nrm2928.

Suárez, P., Díaz-Guerra, M., Prieto, C., Esteban, M., Castro, J.M., Nieto, A. and Ortín, J. (1996) "Open reading frame 5 of porcine reproductive and respiratory syndrome virus as a cause of virus-induced apoptosis.," *J. Virol*, 70(5), pp. 2876–82. doi:10.1128/JVI.70.5.2876-2882.1996.

Subramaniam, S., Kwon, B., Beura, L.K., Kuszynski, C.A., Pattnaik, A.K. and Osorio, F.A. (2010) "Porcine reproductive and respiratory syndrome virus non-structural protein 1 suppresses

tumor necrosis factor-alpha promoter activation by inhibiting NF-κB and Sp1," *Virology*, 406(2), pp. 270–279. doi:10.1016/j.virol.2010.07.016.

Sun, M.-X., Huang, L., Wang, R., Yu, Y.-L., Li, C., Li, P.-P., Hu, X.-C., Hao, H.-P., Ishag, H.A. and Mao, X. (2012) "Porcine reproductive and respiratory syndrome virus induces autophagy to promote virus replication," *Autophagy*, 8(10), pp. 1434–1447. doi:10.4161/auto.21159.

Sun, R., Guo, Y., Li, X., Li, R., Shi, J., Tan, Z., Zhang, Lilin, Zhang, Lei, Han, J. and Huang, J. (2022) "PRRSV Non-Structural Proteins Orchestrate Porcine E3 Ubiquitin Ligase RNF122 to Promote PRRSV Proliferation," *Viruses*, 14(2), p. 424. doi:10.3390/v14020424.

Sun, Y., Xue, F., Guo, Y., Ma, M., Hao, N., Zhang, X.C., Lou, Z., Li, X. and Rao, Z. (2009) "Crystal Structure of Porcine Reproductive and Respiratory Syndrome Virus Leader Protease Nsp1alpha," *J. Virol*, 83(21), pp. 10931–10940. doi:10.1128/jvi.02579-08.

Sun, Z., Chen, Z., Lawson, S.R. and Fang, Y. (2010) "The Cysteine Protease Domain of Porcine Reproductive and Respiratory Syndrome Virus Nonstructural Protein 2 Possesses Deubiquitinating and Interferon Antagonism Functions," *J. Virol*, 84(15), pp. 7832–7846. doi:10.1128/jvi.00217-10.

Suryadevara, N., Shiakolas, A.R., VanBlargan, L.A., Binshtein, E., Chen, R.E., Case, J.B., Kramer, K.J., Armstrong, E.C., Myers, L., Trivette, A., Gainza, C., Nargi, R.S., Selverian, C.N., Davidson, E., Doranz, B.J., Diaz, S.M., Handal, L.S., Carnahan, R.H., Diamond, M.S., Georgiev, I.S. and Crowe, J.E. (2022) 'An antibody targeting the N-terminal domain of SARS-CoV-2 disrupts the spike trimer', *J. Clin. Investig.*, 132(11). Available at: https://doi.org/10.1172/JCI159062.

Sutter, G., Ohlmann, M. and Erfle, V. (1995) "Non-replicating vaccinia vector efficiently expresses bacteriophage T7 RNA polymerase," *FEBS Lett.*, 371(1), pp. 9–12. doi:10.1016/0014-5793(95)00843-x.

Szabo, S.J., Kim, S.T., Costa, G.L., Zhang, X., Fathman, C.G. and Glimcher, L.H. (2000) 'A novel transcription factor, T-bet, directs Th1 lineage commitment', *Cell*, 100(6), pp. 655–669. Available at: https://doi.org/10.1016/S0092-8674(00)80702-3.

Takaesu, G., Kobayashi, T. and Yoshimura, A. (2012) "TGFβ-activated kinase 1 (TAK1)-binding proteins (TAB) 2 and 3 negatively regulate autophagy," *J. Biochem*, 151(2), pp. 157–166. doi:10.1093/jb/mvr123.

Takaoka, A., Hayakawa, S., Yanai, H., Stoiber, D., Negishi, H., Kikuchi, H., Sasaki, S., Imai, K., Shibue, T., Honda, K. and Taniguchi, T. (2003) "Integration of interferon-α/β signalling to p53 responses in tumour suppression and antiviral defence," *Nature,* 2003 424:6948, 424(6948), pp. 516–523. doi:10.1038/nature01850.

Takeda, K., Kaisho, T., Yoshida, N., Takeda, J., Kishimoto, T. and Akira, S. (2015) "Stat3 Activation Is Responsible for IL-6–Dependent T Cell Proliferation through Preventing Apoptosis: Generation and Characterization of T Cell–Specific Stat3-Deficient Mice," *J. Immunol*, 194(7), pp. 3526–3526. doi:10.4049/jimmunol.1500168.

Takeuchi, O. and Akira, S. (2010) 'Pattern Recognition Receptors and Inflammation', *Cell*, 140(6), pp. 805–820. Available at: https://doi.org/10.1016/J.CELL.2010.01.022.

Tan, J.-A., Hall, S.H., Hamil, K.G., Grossman, G., Petrusz, P. and French, F.S. (2002) “Protein Inhibitors of Activated STAT Resemble Scaffold Attachment Factors and Function as Interacting Nuclear Receptor Coregulators*,” *J. Biol. Chem*, 277(19), pp. 16993–17001. doi:10.1074/jbc.m109217200.

Tanaka, K. (2009) “The proteasome: Overview of structure and functions,” *Proc. Jpn. Acad. B: Phys. Biol. Sci*, 85(1), p. 12. doi:10.2183/pjab.85.12.

Tecle, T., White, M.R., Crouch, E.C. and Hartshorn, K.L. (2007) “Inhibition of influenza viral neuraminidase activity by collectins,” *Arch Virol*, 152, pp. 1731–1742. doi:10.1007/s00705-007-0983-4.

Thakar, K., Karaca, S., Port, S.A., Urlaub, H. and Kehlenbach, R.H. (2013) “Identification of CRM1-dependent Nuclear Export Cargos Using Quantitative Mass Spectrometry,” *Mol. Cell. Proteomics : MCP*, 12(3), pp. 664–678. doi:10.1074/mcp.m112.024877.

Theoharides, T.C., Alysandratos, K.D., Angelidou, A., Delivanis, D.A., Sismanopoulos, N., Zhang, B., Asadi, S., Vasiadi, M., Weng, Z., Miniati, A. and Kalogeromitros, D. (2012) ‘Mast cells and inflammation’, *Biochim Biophys Acta.*, 1822(1), pp. 21–33. Available at: https://doi.org/10.1016/J.BBADIS.2010.12.014.

Tian, D., Wei, Z., Zevenhoven-Dobbe, J.C., Liu, R., Tong, G., Snijder, E.J. and Yuan, S. (2012) “Arterivirus Minor Envelope Proteins Are a Major Determinant of Viral Tropism in Cell Culture,” *J. Virol.*, 86(7), p. 3701. Available at: https://doi.org/10.1128/JVI.06836-11.

Tian, H., McKnight, S.L. and Russell, D.W. (1997) “Endothelial PAS domain protein 1 (EPAS1), a transcription factor selectively expressed in endothelial cells,” *Genes Dev.*, 11(1), pp. 72–82. doi:10.1101/gad.11.1.72.

Tian, K., Yu, X., Zhao, T., Feng, Y., Cao, Z., Wang, C., Hu, Y., Chen, X., Hu, D., Tian, X., Liu, D., Zhang, S., Deng, X., Ding, Y., Yang, L., Zhang, Y., Xiao, H., Qiao, M., Wang, B., Hou, L., Wang, X., Yang, X., Kang, L., Sun, M., Jin, P., Wang, S., Kitamura, Y., Yan, J. and Gao, G.F. (2007) “Emergence of Fatal PRRSV Variants: Unparalleled Outbreaks of Atypical PRRS in China and Molecular Dissection of the Unique Hallmark,” *PLoS One*, 2(6):e526. doi:10.1371/journal.pone.0000526.

Tian, X., Lu, G., Gao, F., Peng, H., Feng, Y., Ma, G., Bartlam, M., Tian, K., Yan, J., Hilgenfeld, R. and Gao, G.F. (2009) “Structure and Cleavage Specificity of the Chymotrypsin-Like Serine Protease (3CLSP/nsp4) of Porcine Reproductive and Respiratory Syndrome Virus (PRRSV),” *J. Mol. Biol*, 392(4), pp. 977–993. doi:10.1016/j.jmb.2009.07.062.

Trinh, D.L.N., Elwi, A.N. and Kim, S.W. (2010) “Direct interaction between p53 and Tid1 proteins affects p53 mitochondrial localization and apoptosis,” *Oncotarget*, 1(6), p. 396. doi:10.18632/oncotarget.174.

Ulane, C.M., Rodriguez, J.J., Parisien, J.-P. and Horvath, C.M. (2003) “STAT3 Ubiquitylation and Degradation by Mumps Virus Suppress Cytokine and Oncogene Signaling,” *J. Virol*, 77(11), pp. 6385–6393. doi:10.1128/jvi.77.11.6385-6393.2003.

Ulferts, R. and Ziebuhr, J. (2011) “Nidovirus ribonucleases: Structures and functions in viral replication,” *RNA Biol*, 8(2). doi:10.4161/rna.8.2.15196.

Uribe-Querol, E. and Rosales, C. (2020) 'Phagocytosis: Our Current Understanding of a Universal Biological Process', *Front. Immunol.*, 11, p. 1066. Available at: https://doi.org/10.3389/FIMMU.2020.01066/XML/NLM.

Vanderheijden, N., Delputte, P.L., Favoreel, H.W., Vandekerckhove, J., van Damme, J., van Woensel, P.A. and Nauwynck, H.J. (2003) "Involvement of Sialoadhesin in Entry of Porcine Reproductive and Respiratory Syndrome Virus into Porcine Alveolar Macrophages," *J. Virol*, 77(15), pp. 8207–8215. doi:10.1128/jvi.77.15.8207-8215.2003.

vande Walle, L., Lamkanfi, M. and Vandenabeele, P. (2008) "The mitochondrial serine protease HtrA2/Omi: an overview," *Cell Death Differ, 2008 15:3*, 15(3), pp. 453–460. doi:10.1038/sj.cdd.4402291.

Walsh, D., Mathews, M.B. and Mohr, I. (2013) "Tinkering with translation: protein synthesis in virus-infected cells.," *Cold Spring Harbor Perspect. Biol*, 5(1), p. a012351. doi:10.1101/cshperspect.a012351.

Wang, A., Chen, Q., Wang, L., Madson, D., Harmon, K., Gauger, P., Zhang, J. and Li, G. (2019) "Recombination between Vaccine and Field Strains of Porcine Reproductive and Respiratory Syndrome Virus," *Emerg. Infect. Dis*, 25(12), pp. 2335–2337. doi:10.3201/eid2512.191111.

Wang, C., Shi, X., Zhang, X., Wang, A., Wang, L., Chen, J., Deng, R. and Zhang, G. (2015) "The Endoribonuclease Activity Essential for the Nonstructural Protein 11 of Porcine Reproductive and Respiratory Syndrome Virus to Inhibit NLRP3 Inflammasome-Mediated IL-1β Induction," *DNA Cell Biol*, 34(12), pp. 728–735. doi:10.1089/dna.2015.2929.

Wang, C., Zeng, N., Liu, S., Miao, Q., Zhou, L., Ge, X., Han, J., Guo, X. and Yang, H. (2017) "Interaction of porcine reproductive and respiratory syndrome virus proteins with SUMO-conjugating enzyme reveals the SUMOylation of nucleocapsid protein," *PLoS One*, 12(12), p. e0189191. doi:10.1371/journal.pone.0189191.

Wang, D., Fan, J., Fang, L., Luo, R., Ouyang, H., Ouyang, C., Zhang, H., Chen, H., Li, K. and Xiao, S. (2015) "The nonstructural protein 11 of porcine reproductive and respiratory syndrome virus inhibits NF-κB signaling by means of its deubiquitinating activity," *Mol. Immunol*, 68(2), pp. 357–366. doi:10.1016/j.molimm.2015.08.011.

Wang, F., Wendling, K.S., Soprano, K.J. and Soprano, D.R. (2014) "The SAP Motif and the C-terminal RS- and RD/E-rich Region Influences the Sub-Nuclear Localization of Acinus Isoforms," *J. Cell. Biochem*, 115(12), p. 2165. doi:10.1002/jcb.24893.

Wang, L., He, Q., Gao, Y., Guo, X., Ge, X., Zhou, L. and Yang, H. (2012) "Interaction of cellular poly(C)-binding protein 2 with nonstructural protein 1β is beneficial to Chinese highly pathogenic porcine reproductive and respiratory syndrome virus replication," *Virus Res*, 169(1), pp. 222–230. doi:10.1016/j.virusres.2012.08.002.

Wang, L., Li, R., Geng, R., Zhang, L., Chen, X., Qiao, S. and Zhang, G. (2022) "Heat Shock Protein Member 8 (HSPA8) Is Involved in Porcine Reproductive and Respiratory Syndrome Virus Attachment and Internalization," *Microbiol. Spectrum*, 10(1). doi:10.1128/spectrum.01860-21.

Wang, L., Zhou, L., Zhang, H., Li, Y., Ge, X., Guo, X., Yu, K. and Yang, H. (2014) "Interactome profile of the host cellular proteins and the nonstructural protein 2 of porcine reproductive

and respiratory syndrome virus," *PLoS One*, 9(6), p. e99176. doi:10.1371/journal.pone.0099176.

Wang, N., Liang, H. and Zen, K. (2014) "Molecular mechanisms that influence the macrophage M1-M2 polarization balance," *Front. Immunol*, 5(NOV), p. 614. doi:10.3389/FIMMU.2014.00614.

Wang, R., Nan, Y., Yu, Y. and Zhang, Y.-J. (2013) "Porcine Reproductive and Respiratory Syndrome Virus Nsp1β Inhibits Interferon-Activated JAK/STAT Signal Transduction by Inducing Karyopherin- 1 Degradation," *J. Virol*, 87(9), pp. 5219–5228. doi:10.1128/jvi.02643-12.

Wang, T., Fang, L., Zhao, F., Wang, D. and Xiao, S. (2017) "Exosomes mediate intercellular transmission of porcine reproductive and respiratory syndrome virus (PRRSV)," *J. Virol*, p. JVI.01734-17. doi:10.1128/jvi.01734-17.

Wang, T.Y., Fang, Q.Q., Cong, F., Liu, Y.G., Wang, H.M., Zhang, H.L., Tian, Z.J., Tang, Y.D. and Cai, X.H. (2019) "The Nsp12-coding region of type 2 PRRSV is required for viral subgenomic mRNA synthesis," *Emerg. Microbes Infect*, 8(1), pp. 1501–1510. doi:10.1080/22221751.2019.1679010.

Waring, P. and Müllbacher, A. (1999) 'Cell death induced by the Fas/Fas ligand pathway and its role in pathology', *Immunol. Cell Biol.*, 77(4), pp. 312–317. Available at: https://doi.org/10.1046/J.1440-1711.1999.00837.X.

Wassenaar, A.L., Spaan, W.J., Gorbalenya, A.E. and Snijder, E.J. (1997) "Alternative proteolytic processing of the arterivirus replicase ORF1a polyprotein: evidence that NSP2 acts as a cofactor for the NSP4 serine protease.," *J. Virol*, 71(12), pp. 9313–22. doi:10.1128/jvi.71.12.9313-9322.1997.

Wei, X., Li, R., Qiao, S., Chen, X., Xing, G. and Zhang, G. (2020) "Porcine Reproductive and Respiratory Syndrome Virus Utilizes Viral Apoptotic Mimicry as an Alternative Pathway To Infect Host Cells," *J. Virol*, 94(17). doi:10.1128/jvi.00709-20.

Wenhui, L., Zhongyan, W., Guanqun, Z., Zhili, L., JingYun, M., Qingmei, X., Baoli, S. and Yingzuo, B. (2012) "Complete Genome Sequence of a Novel Variant Porcine Reproductive and Respiratory Syndrome Virus (PRRSV) Strain: Evidence for Recombination between Vaccine and Wild-Type PRRSV Strains," *J. Virol*, 86(17), pp. 9543–9543. doi:10.1128/jvi.01341-12.

Wensvoort, G., Terpstra, C., Pol, J.M., ter Laak, E.A., Bloemraad, M., de Kluyver, E.P., Kragten, C., van Buiten, L., den Besten, A. and Wagenaar, F. (1991) "Mystery swine disease in The Netherlands: the isolation of Lelystad virus.," *Vet Q*, 13(3), pp. 121–130. doi:10.1080/01652176.1991.9694296.

Wiggins, K.A., Parry, A.J., Cassidy, L.D., Humphry, M., Webster, S.J., Goodall, J.C., Narita, M. and Clarke, M.C.H. (2019) 'IL-1α cleavage by inflammatory caspases of the noncanonical inflammasome controls the senescence-associated secretory phenotype', *Aging cell*, 18(3). Available at: https://doi.org/10.1111/ACEL.12946.

Williams, T.J. (1983) 'Vascular permeability changes induced by complement-derived peptides', *Agents Actions.*, 13(5–6), pp. 451–455. Available at: https://doi.org/10.1007/BF02176415.

Wimuttisuk, W., West, M., Davidge, B., Yu, K., Salomon, A. and Singer, J.D. (2014) "Novel Cul3 binding proteins function to remodel E3 ligase complexes," *BMC Cell Biol*, 15(1), p. 28. doi:10.1186/1471-2121-15-28.

Wirawan, E., vande Walle, L., Kersse, K., Cornelis, S., Claerhout, S., Vanoverberghe, I., Roelandt, R., de Rycke, R., Verspurten, J., Declercq, W., Agostinis, P., vanden Berghe, T., Lippens, S. and Vandenabeele, P. (2010) "Caspase-mediated cleavage of Beclin-1 inactivates Beclin-1-induced autophagy and enhances apoptosis by promoting the release of proapoptotic factors from mitochondria," *Cell Death Dis, 2010 1:1*, 1(1), pp. e18–e18. doi:10.1038/cddis.2009.16.

Witt, E., Zantopf, D., Schmidt, M., Kraft, R., Kloetzel, P.-M. and Krüger, E. (2000) "Characterisation of the newly identified human Ump1 homologue POMP and analysis of LMP7(β5i) incorporation into 20 S proteasomes 1," *J. Mol. Biol*, 301(1), pp. 1–9. doi:10.1006/jmbi.2000.3959.

Wong, R.W., Mamede, J.I. and Hope, T.J. (2015) "Impact of Nucleoporin-Mediated Chromatin Localization and Nuclear Architecture on HIV Integration Site Selection," *J. Virol*, 89, pp. 9702–9705. doi:10.1128/JVI.01669-15.

Wozniak, R.W. and Blobel, G. (1992) "The single transmembrane segment of gp210 is sufficient for sorting to the pore membrane domain of the nuclear envelope," *J. Cell Biol*, 119(6), p. 1441. doi:10.1083/JCB.119.6.1441.

Wu, D. and Yotnda, P. (2011) "Induction and testing of hypoxia in cell culture.," *J. Vis. Exp*, 2011;(54):2899. doi:10.3791/2899.

Wu, X., Fang, J., Huang, Q., Chen, X., Guo, Z., Tian, L., Zhou, E., Chen, J., Mu, Y. and Du, T. (2021) "Major Vault Protein Inhibits Porcine Reproductive and Respiratory Syndrome Virus Infection in CRL2843CD163 Cell Lines and Primary Porcine Alveolar Macrophages," *Viruses, 2021, Vol. 13, Page 2267*, 13(11), p. 2267. doi:10.3390/V13112267.

Wysocki, M., Chen, H., Steibel, J.P., Kuhar, D., Petry, D., Bates, J., Johnson, R., Ernst, C.W. and Lunney, J.K. (2012) "Identifying putative candidate genes and pathways involved in immune responses to porcine reproductive and respiratory syndrome virus (PRRSV) infection," *Anim. Genet*, 43(3), pp. 328–332. doi:10.1111/j.1365-2052.2011.02251.x.

Xiahou, Z., Wang, X., Shen, J., Zhu, X., Xu, F., Hu, R., Guo, D., Li, H., Tian, Y., Liu, Y. and Liang, H. (2017) "NMI and IFP35 serve as proinflammatory DAMPs during cellular infection and injury," *Nat. Commun*, 8(1). doi:10.1038/S41467-017-00930-9.

Xie, J., Christiaens, I., Yang, B., van Breedam, W., Cui, T. and Nauwynck, H.J. (2017) "Molecular cloning of porcine Siglec-3, Siglec-5 and Siglec-10, and identification of Siglec-10 as an alternative receptor for porcine reproductive and respiratory syndrome virus (PRRSV),"*J. Gen. Virol*, 98(8), p. 2030. doi:10.1099/jgv.0.000859.

Xie, J., Christiaens, I., Yang, B., Trus, I., Devriendt, B., Cui, T., Wei, R. and Nauwynck, H.J. (2018) "Preferential use of Siglec-1 or Siglec-10 by type 1 and type 2 PRRSV strains to infect PK15S1-CD163 and PK15S10-CD163 cells," *Vet. Res*, 49(1), pp. 1–13. doi:10.1186/s13567-018-0569-z

Xu, H., Liu, Z., Zheng, S., Han, G. and He, F. (2020) 'CD163 Antibodies Inhibit PRRSV Infection via Receptor Blocking and Transcription Suppression', *Vaccines*, 8(4), pp. 1–16. Available at: https://doi.org/10.3390/VACCINES8040592.

Xu, L., Zhou, L., Sun, W., Zhang, P., Ge, X., Guo, X., Han, J. and Yang, H. (2018) "Nonstructural protein 9 residues 586 and 592 are critical sites in determining the replication efficiency and fatal virulence of the Chinese highly pathogenic porcine reproductive and respiratory syndrome virus," *Virology*, 517, pp. 135–147. Available at: https://doi.org/10.1016/J.VIROL.2018.01.018.

Xu, P.C., Lin, S., Yang, X.W., Gu, D.M., Yan, T.K., Wei, L. and Wang, B.L. (2015) 'C-reactive protein enhances activation of coagulation system and inflammatory response through dissociating into monomeric form in antineutrophil cytoplasmic antibody-associated vasculitis', *BMC Immunol.*, 16(1), pp. 1–12. Available at: https://doi.org/10.1186/S12865-015-0077-0.

Xue, F., Sun, Y., Yan, L., Zhao, C., Chen, J., Bartlam, M., Li, X., Lou, Z. and Rao, Z. (2010) "The crystal structure of porcine reproductive and respiratory syndrome virus nonstructural protein Nsp1beta reveals a novel metal-dependent nuclease.," *J. Virol*, 84(13), pp. 6461–71. doi:10.1128/jvi.00301-10.

Yang, L., He, J., Wang, R., Zhang, X., Lin, S., Ma, Z. and Zhang, Y. (2019) "Nonstructural Protein 11 of Porcine Reproductive and Respiratory Syndrome Virus Induces STAT2 Degradation To Inhibit Interferon Signaling," *J. Virol*, 93(22). doi:10.1128/jvi.01352-19.

Yang, L., Wang, R., Ma, Z., Wang, Y. and Zhang, Y. (2015) "Inducing Autophagic Cell Death by Nsp5 of Porcine Reproductive and Respiratory Syndrome Virus," *Austin Virol Retrovirol*, 2(2), p. 1014. doi.org/10.13016/m23775v79.

Yang, L., Wang, R., Ma, Z., Xiao, Y., Nan, Y., Wang, Y., Lin, S. and Zhang, Y.-J. (2017) "Porcine Reproductive and Respiratory Syndrome Virus Antagonizes JAK/STAT3 Signaling via nsp5, Which Induces STAT3 Degradation," *J. Virol*, 91(3), pp. 2087–2103. doi:10.1128/jvi.02087-16.

Yang, L., Wang, R., Yang, S., Ma, Z., Lin, S., Nan, Y., Li, Q., Tang, Q. and Zhang, Y.-J. (2018) "Karyopherin Alpha 6 Is Required for Replication of Porcine Reproductive and Respiratory Syndrome Virus and Zika Virus," *J. Virol*, 92(9). doi:10.1128/jvi.00072-18.

Yang, M., Hay, J. and Ruyechan, W.T. (2008) "Varicella-Zoster Virus IE62 Protein Utilizes the Human Mediator Complex in Promoter Activation," *J. Virol*, 82(24), pp. 12154–12163. doi:10.1128/jvi.01693-08.

Yang, S., Oh, T., Cho, H. and Chae, C. (2020) "A comparison of commercial modified-live PRRSV-1 and PRRSV-2 vaccines against a dual heterologous PRRSV-1 and PRRSV-2 challenge in late term pregnancy gilts," *Comp. Immunol. Microbiol. Infect. Dis.*, 69, p. 101423. Available at: https://doi.org/10.1016/J.CIMID.2020.101423.

Yang, X.O., Panopoulos, A.D., Nurieva, R., Seon, H.C., Wang, D., Watowich, S.S. and Dong, C. (2007) "STAT3 Regulates Cytokine-mediated Generation of Inflammatory Helper T Cells *," *J. Biol. Chem*, 282(13), pp. 9358–9363. doi:10.1074/jbc.c600321200.

Ye, Q. and Worman, H.J. (1995) "Protein-protein interactions between human nuclear lamins expressed in yeast," *Exp. Cell. Res*, 219(1), pp. 292–298. doi:10.1006/excr.1995.1230.

Yin, S., Huo, Y., Dong, Y., Fan, L., Yang, H., Wang, L., Ning, Y. and Hu, H. (2012) "Activation of c-Jun NH(2)-terminal kinase is required for porcine reproductive and respiratory syndrome virus-induced apoptosis but not for virus replication," *Virus Res*, 166(1–2), pp. 103–108. doi:10.1016/j.virusres.2012.03.010.

Yoo, D., Song, C., Sun, Y., Du, Y., Kim, O. and Liu, H.C. (2010) "Modulation of host cell responses and evasion strategies for porcine reproductive and respiratory syndrome virus," *Virus Res*, pp. 48–60. doi:10.1016/j.virusres.2010.07.019.

Yoshida, T., Hanada, T., Tokuhisa, T., Kosai, K.I., Sata, M., Kohara, M. and Yoshimura, A. (2002) "Activation of STAT3 by the Hepatitis C Virus Core Protein Leads to Cellular Transformation," *J. Exp. Med*, 196(5), pp. 641–653. doi:10.1084/jem.20012127.

Yu, Y., Wang, M., Zhang, X., Li, S., Lu, Q., Zeng, H., Hou, H., Li, Hao, Zhang, M., Jiang, F., Wu, J., Ding, R., Zhou, Z., Liu, M., Si, W., Zhu, T., Li, Hangwen, Ma, J., Gu, Y., She, G., Li, X., Zhang, Y., Peng, K., Huang, W., Liu, W. and Wang, Y. (2021) 'Antibody-dependent cellular cytotoxicity response to SARS-CoV-2 in COVID-19 patients', *Signal Transduction Targeted Ther.*, 6(1), pp. 1–10. Available at: https://doi.org/10.1038/s41392-021-00759-1.

Yuan, S., Zhang, N., Xu, L., Zhou, L., Ge, X., Guo, X. and Yang, H. (2016) "Induction of apoptosis by the nonstructural protein 4 and 10 of porcine reproductive and respiratory syndrome virus," *PLoS One*, 11(6). doi:10.1371/journal.pone.0156518.

Yuh, M.C. and Blobel, G. (2001) "Karyopherins and nuclear import," *Curr. Opin. Struct. Biol*, 11(6), pp. 703–715. doi:10.1016/s0959-440x(01)00264-0.

Yuseff, M.I., Pierobon, P., Reversat, A. and Lennon-Duménil, A.M. (2013) 'How B cells capture, process and present antigens: a crucial role for cell polarity', *Nat. Rev. Immunol.*, 13(7), pp. 475–486. Available at: https://doi.org/10.1038/nri3469.

Zabel, F., Mohanan, D., Bessa, J., Link, A., Fettelschoss, A., Saudan, P., Kündig, T.M. and Bachmann, M.F. (2014) 'Viral particles drive rapid differentiation of memory B cells into secondary plasma cells producing increased levels of antibodies', *J Immunol. (Baltimore, Md. : 1950)*, 192(12), pp. 5499–5508. Available at: https://doi.org/10.4049/JIMMUNOL.1400065.

Zárate, S., Cuadras, M. a, Espinosa, R., Romero, P., Juárez, K.O., Camacho-Nuez, M., Arias, C.F. and López, S. (2003) "Interaction of rotaviruses with Hsc70 during cell entry is mediated by VP5.," *J. Virol*, 77(13), pp. 7254–7260. doi:10.1128/JVI.77.13.7254-7260.2003.

Zhang, H., Fang, L., Zhu, X., Wang, D. and Xiao, S. (2018) "Global analysis of ubiquitome in PRRSV-infected pulmonary alveolar macrophages," *J. Proteomics*, 184, pp. 16–24. doi:10.1016/j.jprot.2018.06.010.

Zhang, H., Guo, X., Ge, X., Chen, Y., Sun, Q. and Yang, H. (2009) "Changes in the Cellular Proteins of Pulmonary Alveolar Macrophage Infected with Porcine Reproductive and Respiratory Syndrome Virus by Proteomics Analysis," *J. Proteome Res*, 8(6), pp. 3091–3097. doi:10.1021/pr900002f.

Zhang, K., Lv, D.W. and Li, R. (2017) "B Cell Receptor Activation and Chemical Induction Trigger Caspase-Mediated Cleavage of PIAS1 to Facilitate Epstein-Barr Virus Reactivation," *Cell Rep*, 21(12), pp. 3445–3457. doi:10.1016/j.celrep.2017.11.071.

Zhang, W., Chen, K., Guo, Y., Chen, Y. and Liu, X. (2019) "Involvement of PRRSV NSP3 and NSP5 in the autophagy process," *Virol. J*, 16(1), p. 13. doi:10.1186/s12985-019-1116-x.

Zhang, W., Chen, K., Zhang, X., Guo, C., Chen, Y. and Liu, X. (2018) “An integrated analysis of membrane remodeling during porcine reproductive and respiratory syndrome virus replication and assembly,” *PLoS One*, 13(7). doi:10.1371/journal.pone.0200919.

Zhang, W., Yang, F., Zhu, Z., Yang, Y., Wang, Z., Cao, W., Dang, W., Li, L., Mao, R., Liu, Y., Tian, H., Zhang, K., Liu, X., Ma, J. and Zheng, H. (2019) “Cellular DNAJA3, a Novel VP1-Interacting Protein, Inhibits Foot-and-Mouth Disease Virus Replication by Inducing Lysosomal Degradation of VP1 and Attenuating Its Antagonistic Role in the Beta Interferon Signaling Pathway,” *J. Virol*, 93(13). doi:10.1128/jvi.00588-19.

Zhang, Y., Li, L.F., Munir, M. and Qiu, H.J. (2018) “RING-domain E3 ligase-mediated host-virus interactions: Orchestrating immune responses by the host and antagonizing immune defense by viruses,” *Front. Immunol*, 2018;9:1083. doi:10.3389/fimmu.2018.01083.

Zhao, C.L., Mahboobi, S.H., Moussavi-Baygi, R. and Mofrad, M.R.K. (2014) “The Interaction of CRM1 and the Nuclear Pore Protein Tpr,” *PLoS One*, 9(4), p. 93709. doi:10.1371/journal.pone.0093709.

Zhao, J., He, S., Minassian, A., Li, J. and Feng, P. (2015) “Recent advances on viral manipulation of NF-κB signaling pathway.,” *Curr. Opin. Virol*, 15, pp. 103–11. doi:10.1016/j.coviro.2015.08.013.

Zhao, S., Ge, X., Wang, X., Liu, A., Guo, X., Zhou, L., Yu, K. and Yang, H. (2015) “The DEAD-box RNA helicase 5 positively regulates the replication of porcine reproductive and respiratory syndrome virus by interacting with viral Nsp9 in vitro,” *Virus Res*, 195, pp. 217–224. doi:10.1016/j.virusres.2014.10.021.

Zheng, X. xian, Li, R., Qiao, S., Chen, X. xin, Zhang, L., Lu, Q., Xing, G., Zhou, E. min and Zhang, G. (2021) “Vimentin rearrangement by phosphorylation is beneficial for porcine reproductive and respiratory syndrome virus replication in vitro,” *Vet. Microbiol*, 259, p. 109133. doi:10.1016/j.vetmic.2021.109133.

Zhou, A., Li, S., Khan, F.A. and Zhang, S. (2016) “Autophagy postpones apoptotic cell death in PRRSV infection through Bad-Beclin1 interaction,” *Virulence*, 7(2), pp. 98–109. doi:10.1080/21505594.2015.1131381.

Zhou, F. (2009) “Molecular Mechanisms of IFN-γ to Up-Regulate MHC Class I Antigen Processing and Presentation,” *Int Rev Immunol*, 28(3–4), pp. 239–260. doi:10.1080/08830180902978120.

Zhou, L., Zhang, J., Zeng, J., Yin, S., Li, Y., Zheng, L., Guo, X., Ge, X. and Yang, H. (2009) “The 30-Amino-Acid Deletion in the Nsp2 of Highly Pathogenic Porcine Reproductive and Respiratory Syndrome Virus Emerging in China Is Not Related to Its Virulence,” *J. Virol*, 83(10), pp. 5156–5167. doi:10.1128/jvi.02678-08.

Zhou, X., Liao, J., Meyerdierks, A., Feng, L., Naumovski, L., Böttger, E.C. and Omary, M.B. (2000) “Interferon-α Induces Nmi-IFP35 Heterodimeric Complex Formation That Is Affected by the Phosphorylation of IFP35,” *J. Biol. Chem*, 275(28), pp. 21364–21371. doi:10.1074/jbc.m003177200.

Zhou, Y., Fang, L., Wang, D., Cai, K., Chen, H. and Xiao, S. (2017) “Porcine Reproductive and Respiratory Syndrome Virus Infection Induces Stress Granule Formation Depending on

Protein Kinase R-like Endoplasmic Reticulum Kinase (PERK) in MARC-145 Cells," *Front. Cell. Infect. Microbiol*, 7(APR). doi:10.3389/fcimb.2017.00111.

Zhou, Y., Zheng, H.H., Gao, F., Tian, D. Bin and Yuan, S.S. (2011) "Mutational analysis of the SDD sequence motif of a PRRSV RNA-dependent RNA polymerase," *Sci. China Life Sci*, 54(9), pp. 870–879. doi:10.1007/s11427-011-4216-4.

Zhu, Z., Zhang, H., Zhang, X., He, S., Dong, W., Wang, X., Chen, Y., Liu, X. and Guo, C. (2020) "Lipopolysaccharide Downregulates CD163 Expression to Inhibit PRRSV Infection via TLR4-NF-κB Pathway," *Front. Microbiol*, 11, p. 501. doi:10.3389/fmicb.2020.00501.

Zimmerman, J.J., Karriker, L.A., Ramirez, A., Schwartz, K.J. and Stevenson, G.W. (2012) *Diseases of Swine, 10th Edition*.

Zu, S., Xue, Q., He, Z., Shi, C., Wu, W., Zhang, J., Li, W., Huang, J., Jiao, P. and Liao, M. (2020) "Duck PIAS2 negatively regulates RIG-I mediated IFN-β production by interacting with IRF7," *Dev. Comp. Immunol*, 108, p. 103664. doi:10.1016/j.dci.2020.103664.

Zuckermann, F.A., Garcia, E.A., Luque, I.D., Christopher-Hennings, J., Doster, A., Brito, M. and Osorio, F. (2007) "Assessment of the efficacy of commercial porcine reproductive and respiratory syndrome virus (PRRSV) vaccines based on measurement of serologic response, frequency of gamma-IFN-producing cells and virological parameters of protection upon challenge," *Vet. Microbiol*, 123(1–3), pp. 69–85. doi:10.1016/j.vetmic.2007.02.009.

Chapter 9: Appendices

9.1 PCR of inserts of prey plasmids from PRRSV-1 NSP1β colonies

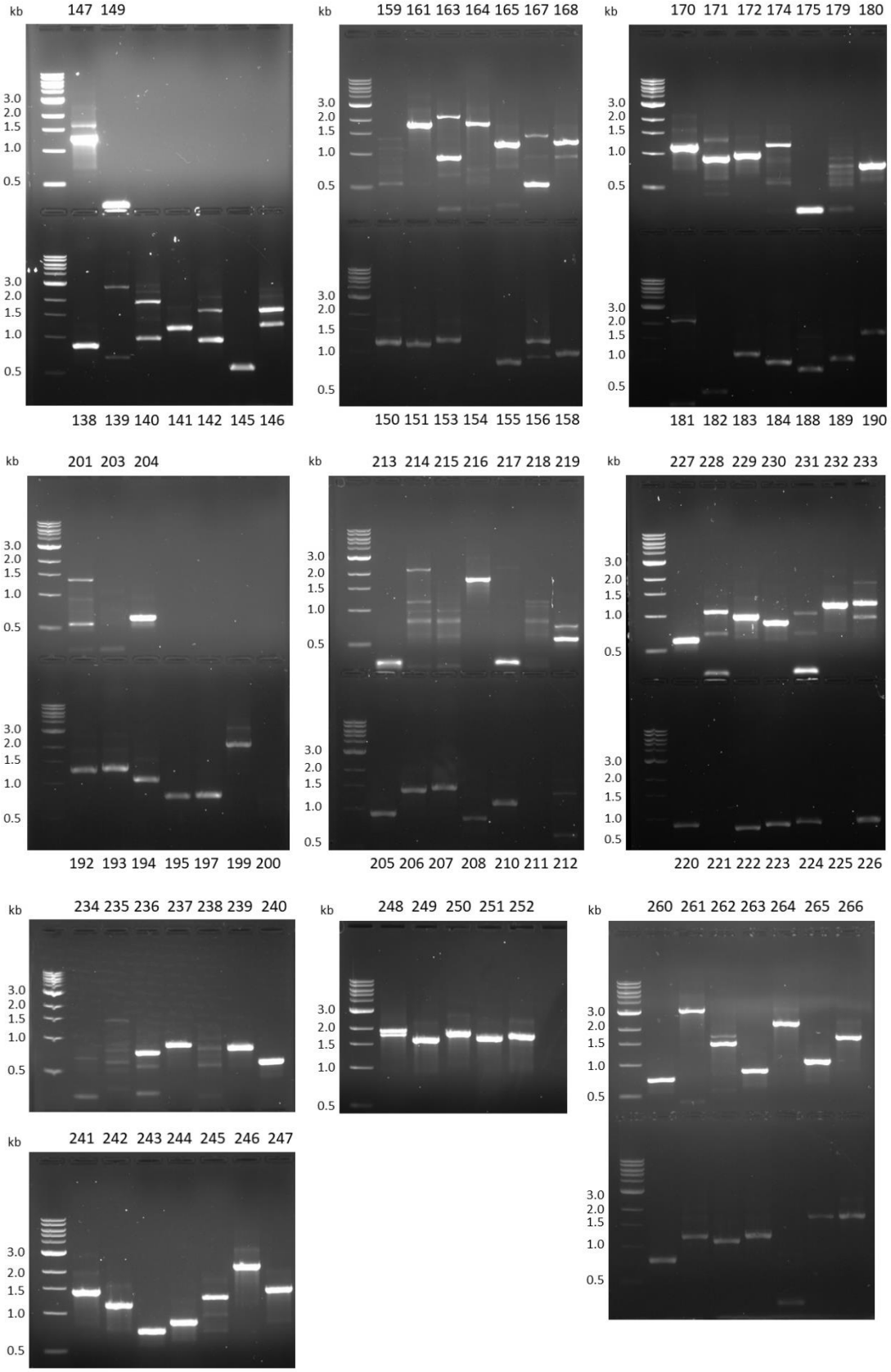

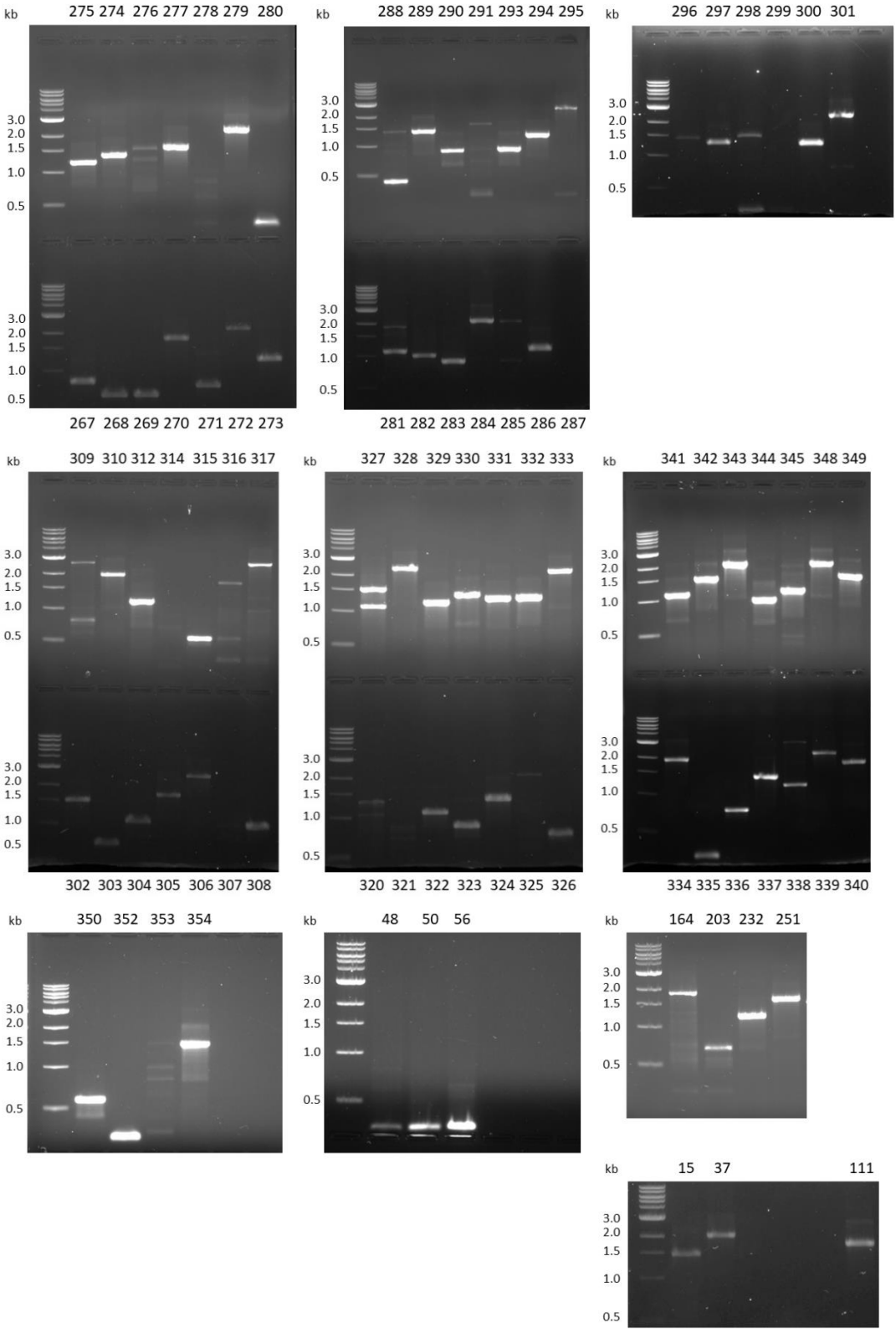

Figure 9.1: PCR of inserts of prey plasmids from remaining PRRSV-1 NSP1β colonies. PCR was used to amplify the cDNA inserts within 308 extracted plasmids from the NSP1β screen. The PCR products were analysed by agarose gel electrophoresis. The lane number indicates the colony number. Selected samples were re-run if they had run off the gel/into the next gel. Extension of **Figure 3.8.**

9.2 Putative interacting proteins identified in the NSP1α yeast-2-hybrid screen

Table 9.1: Detailed functions of putative interacting proteins identified in the NSP1α yeast-2-hybrid screen

Clone #	Protein and NCBI Sequence ID	Region N or AA	Function	Ubiquitin motifs: KXXP RXXXXLXK KQ	E value
			Ubiquitin related		
29 32	**Ubiquitin B** AB084843.1	23-96 23-96	Ubiquitination affects proteins in many ways: it can mark them for degradation via the proteasome, alter their cellular location, affect their activity, and promote or prevent protein interactions. PRRSV has been shown to alter the ubiquitome of the cell through selected motifs in target proteins (H. Zhang *et al.*, 2018).	KQ KQ	3e-46 4e-46
47	**E3 ubiquitin-protein ligase MARCH7 isoform X8** XP_020930440.1	313-444	E3 ubiquitin-protein ligase which may specifically enhance the E2 activity of HIP2. E3 ubiquitin ligases accept ubiquitin from an E2 ubiquitin-conjugating enzyme in the form of a thioester and then directly transfer the ubiquitin to targeted substrates. MARCH7 is a member of the MARCH family of membrane bound E3 ubiquitin ligases, MARCH proteins add ubiquitin to target lysines in substrate proteins, thereby signalling their vesicular transport between membrane compartments. E3 ubiquitin ligases are targeted by viruses to facilitate viral replication, such as Ebola virus protein VP35 hijacking TRIM6 to enhance viral polymerase activity (Y. Zhang *et al.*, 2018).	KNVP RDPERLQK	1e-88
42	**anaphase-promoting**	1-149	Anaphase-promoting complex (also called the cyclosome or APC/C) is an E3 ubiquitin ligase	KTPP, KQ	1e-08

	complex subunit 10 NP_001171398.1		that marks target cell cycle proteins for degradation by the 26S proteasome. The APC/C is a large complex of 11–13 subunit proteins, including a cullin (Apc2) and RING (Apc11) subunit much like SCF. Targeted by viruses to manipulate cell cycle progression (Fehr and Yu, 2013).		
			MHC related		
10 93 94 128	**beta-2-microglobulin precursor** NP_999143.1	 25-118 25-118 25-118	β2 microglobulin also known as B2M is a component of MHC class I molecules, which are present on all nucleated cells (excludes red blood cells).	 - - -	 3e-66 2e-66 5e-65
100 108	**zinc finger protein ZXDC** NP_001231151.1	575-821 703-842	Zinc finger, X-linked, duplicated family member C (ZXDC) is a human CIITA-binding protein involved in the activation of major histocompatibility complex (MHC) class I and II. For binding to occur, ZXDC must form an oligomeric complex with another copy of itself or with ZXDA; ZXDC is activated by sumolyation.	KQ KQ	3e-162 5e-84
			Heat shock proteins		
35 76	**heat shock cognate 71 kDa protein** NP_001230836.1	400-485 332-498	Molecular chaperone implicated in a wide variety of cellular processes, including protection of the proteome from stress, folding and transport of newly synthesised polypeptides, activation of proteolysis of misfolded proteins and the formation and dissociation of protein complexes. Key role in the protein quality control system, ensuring correct protein folding, the re-folding of misfolded proteins and controlling the targeting of proteins for subsequent degradation. Binds to PRRSV GP4 to facilitate attachment and internalisation (Wang *et al.*, 2022).	3 KQ KQ	2e-116 3e-112

			Targeted by Rotaviruses for entry (Guerrero *et al.*, 2002) and involved in the regulation of the antiviral response (Article *et al.*, 2013) Inhibiting HSP70 reduces PRRSV replication (Gao *et al.*, 2014); PRRSV has also been shown previously to alter expression levels of other heat shock proteins (Zhang *et al.*, 2009). PRRSV has recently been shown to interact with and use HSC70 for virus internalisation and attachment (Wang *et al.*, 2022).		
84	**DNAJ homolog subfamily A member 3, mitochondrial isoform X2** XP_003354674.1	175-453	Chaperone DNAJ, also known as Hsp40 (heat shock protein 40 kDa), is a molecular chaperone protein. Molecular chaperones function to protect proteins from irreversible aggregation during synthesis and in times of cellular stress. HSP40 is used by other viruses e.g. to enhance HIV viral gene expression (Kumar and Mitra, 2005) and assists IAV replication (Batra *et al.*, 2016). PRRSV has also been shown previously to alter expression levels of heat shock proteins (Zhang *et al.*, 2009).	KGIP KQ	4e-174
			Secretion and Endocytic pathways/compartments		
30 142	**VPS29** XM_003483426.4 **vacuolar protein sorting-associated protein 29 isoform X2** XP_003483474.1	590-872 104-182 *In frame ?*	VPS29 is a vacuolar protein sorting (VPS) protein that, when functionally impaired, disrupts the efficient delivery of vacuolar hydrolases. Vps29, is a component of a large multimeric complex, termed the retromer complex, which is involved in retrograde transport of proteins from endosomes to the trans-Golgi network. Vps29 may be involved in the formation of the inner shell of the retromer coat	 KKCP, KCPP, KTPP	2e-128 0

			for retrograde vesicles leaving the prevacuolar compartment.		
91	**vesicle-trafficking protein SEC22a isoform X4** XP_020925910.1	233-255	This protein has similarity to rat SEC22 and may act in the early stages of the secretory pathway.		2e-06
102	**oxysterol binding protein like 9 (OSBPL9), transcript variant X11** XM_021096665.1	2403-2519	Oxysterol-binding proteins (OSBP) are a group of intracellular lipid receptors. Most members contain an N-terminal pleckstrin homology domain and a highly conserved C-terminal OSBP-like sterol-binding domain. It functions as a cholesterol transfer protein that regulates Golgi structure and function.	-	1e-52
137	**phosphatidylinositol 4-phosphate 3-kinase C2 domain-containing subunit alpha** XP_020938934.1	400-501	Generates phosphatidylinositol 3-phosphate (PtdIns3P) and phosphatidylinositol 3,4-bisphosphate (PtdIns(3,4)P2) that act as second messengers. Has a role in several intracellular trafficking events. Functions in insulin signalling and secretion.	-	2e-67
			IFN related		
6	**interferon induced protein 35 mRNA** XM_003358024.3		IFI35 has been shown to interact with NMI and BATF. NMI association with IFP35 prevents proteasome mediated degradation of IFP35 (Chen *et al.*, 2000)		4e-136
53	**interferon-induced 35 kDa protein (IFP35)** XP_003358072.1	27-275	IFP35 inhibited activation of the RNA sensor, the retinoic acid-inducible gene I (RIG-I), leading to inhibition of IFN production. Negative regulator of RIG-I-mediated antiviral signalling - required for VSV infection and negatively regulates antiviral signalling of RIG-I in HEK293 cells infected with Sendai virus (Das *et al.*, 2014)		

19	**E3 Sumo ligase PIAS1** XP_003121797	383-595	PIAS1 regulates STAT1 activity and inhibits STAT1 mediated gene expression (B Liu *et al.*, 1998); critical for IFNγ and IFNβ mediated immune response (Liu *et al.*, 2004). Functions as a either a SUMO ligase or regulator of the SUMO ligase in the sumoylation of p53 (Kahyo, Nishida and Yasuda, 2001). Targeted by multiple viruses: involved in Epstein-Barr virus reactivation (Zhang, Lv and Li, 2017), and involved in the antiviral response against herpes-simple virus 1 (HSV-1) and therefore targeted by HSV-1 protein ICP0 (Brown *et al.*, 2016). Also known to interact with PRRSV N protein to mediate NF-κB activation during infection (H. Ke, Lee, et al., 2019). PRRSV NSP1α reportedly interacts with PIAS1 (Song *et al.*, 2010) Unpublished.		
62	**Zinc finger MIZ domain-containing protein 1 (ZMIZ1)** XP_013838828.2	580-832	This gene encodes a member of the PIAS (protein inhibitor of activated STAT) family of proteins. Regulates the activity of various transcription factors, including the androgen receptor, Smad3/4, and p53. The encoded protein may also play a role in sumoylation. A translocation between this locus on chromosome 10 and the protein tyrosine kinase ABL1 locus on chromosome 9 has been associated with acute lymphoblastic leukaemia. Human papilloma virus 16 E7 protein complexes with ZMIZ1 to overcome cell cycle arrest (Morandell *et al.*, 2012).		1e-179
86	**E3 SUMO-protein**	352-542	PIAS2 is a protein inhibitor of activated STAT family, which		9e-130

	ligase PIAS2 isoform 7 XP_020948317.1		function as SUMO E3 ligases and play important roles in many cellular processes by mediating the sumoylation of target proteins. PIAS2 enhances the sumoylation of specific target proteins including the p53 tumour suppressor protein, c-Jun, and the androgen receptor. Protein inhibitor of activated STAT2 has been shown to interact with: Androgen receptor, DNMT3A, PARK7 and UBE2I. Avian PIAS2 interacts with IRF7 to RIG-1 induced IFNβ production (Zu *et al.*, 2020). Also shown to modulate virus protein degradation to restrict hepatitis C virus replication (Guo *et al.*, 2017).		
			DNA binding/modifying		
36	**histone-binding protein RBBP4** XP_013854580.1	1-145	Ubiquitously expressed nuclear protein, belongs to a highly conserved subfamily of WD-repeat proteins. It is present in protein complexes involved in histone acetylation and chromatin asse mbly. It is part of the Mi-2/NuRD complex that has been implicated in chromatin re-modelling and transcriptional repression associated with histone deacetylation. Also, part of corepressor complexes, which is an integral component of transcriptional silencing. Seems to be involved in transcriptional repression of E2F-responsive genes. RBBP4 has been shown to interact with: BRCA1, CREBBP, GATAD2B, HDAC1, HDAC2, HDAC3, MTA2, RB, SAP30, and SIN3A.	KNTP	1e-92
55	**GA-binding protein**	45-254	One of three GA-binding protein transcription factor subunits		2e-150

	alpha chain isoform X1 XP_020927099.1		which functions as a DNA-binding subunit. GABPA has been shown to interact with host cell factor C1, Sp1 transcription factor and Sp3 transcription factor.		
64	**TATA box-binding protein-associated factor RNA polymerase I subunit B isoform X3** XP_020943519.1	7-175 *In frame ?*	Initiation of transcription by RNA polymerase I requires the formation of a complex composed of the TATA-binding protein (TBP) and three TBP-associated factors (TAFs) specific for RNA polymerase I. This complex, known as SL1, binds to the core promoter of ribosomal RNA genes to position the polymerase properly and acts as a channel for regulatory signals. This gene encodes one of the SL1-specific TAFs. TAF1B has been shown to interact with RRN3.	KQ	2e-122
75	**proliferating cell nuclear antigen** NP_001278854.1	149-261	Proliferating cell nuclear antigen (PCNA) is a DNA clamp that acts as a processivity factor for DNA polymerase δ in eukaryotic cells and is essential for replication. PCNA is a homotrimer and achieves its processivity by encircling the DNA, where it acts as a scaffold to recruit proteins involved in DNA replication, DNA repair, chromatin remodelling and epigenetics. Interacts with many proteins via the two known PCNA-interacting motifs PCNA-interacting peptide (PIP) box and AlkB homologue 2 PCNA interacting motif (APIM).	2 KQ KATP	7e-77
			Apoptosis		
101	**NHL repeat-containing protein 2** NP_001230490.1	626-725	The function of NHLRC2 is not yet fully understood. Using bioinformatic analysis, a "YVAD" motif was found to be conserved in eukaryotes, bacteria, and archaea. "YVAD" shows up three times alone in the human NHLRC2 protein. This motif is potential involved in inhibiting caspases 1, 2, 3, 4 & 5,	-	2e-63

			thus possibly having anti-apoptotic properties. It is an essential protein with 3 domains, mutations in which are associated with disease (Biterova *et al.*, 2018). Interacts with and is cleaved by caspase 8 resulting in apoptosis in colon cancer cell lines (Nishi *et al.*, 2017).		
			Complement		
110	**complement C3 precursor** NP_999174.1	22-313	C3 activation is required for both classical and alternative complement activation pathways.	-	3e-173
			Ribosomal		
120	**40S ribosomal protein S20** AAS55928.1	33-105	40S ribosomal protein S20 is a component of the 40S subunit and is located in the cytoplasm. Ribosomes, the organelles that catalyse protein synthesis, consist of a small 40S subunit and a large 60S subunit. Together these subunits are composed of 4 RNA species and approximately 80 structurally distinct proteins.	KQ	7e-49
			Receptors/Cell surface molecules/Plasma membrane		
1	**cadherin-23 isoform X3** XP_020928318.1		Cadherins are calcium dependent cell-cell adhesion glycoproteins. A large, single-pass transmembrane protein composed of an extracellular domain containing 27 repeats that show significant homology to the cadherin ectodomain.		
1154	**integrin beta-2 precursor** ABU86738.1	361-667	Integrin beta-2 (CD18) is a protein that plays significant roles in cellular adhesion and cell surface signalling. It is the beta subunit of four different structures: LFA-1 (paired with CD11a) Macrophage-1 antigen (paired with CD11b) Integrin alphaXbeta2 (paired with CD11c)	54 -	0

			Integrin alphaDbeta2 (paired with CD11d).		
25	**Macrosialin-like** XP_013847091.1		Macrosialin, also known as CD68 (Cluster of Differentiation 68) is a protein highly expressed by cells in the monocyte lineage, by circulating macrophages, and by tissue macrophages. CD68 is a transmembrane glycoprotein, heavily glycosylated in its extracellular domain, with a molecular weight of 110 kDa (human form). Could play a role in phagocytic activities of tissue macrophages, both in intracellular lysosomal metabolism and extracellular cell-cell and cell-pathogen interactions. Binds to tissue- and organ-specific lectins or selectins, allowing homing of macrophage subsets to particular sites.		
95	**sialoadhesin precursor** NP_999511.1	442-649	Sialoadhesin is a cell adhesion molecule found on the surface of macrophages. It is found in especially high amounts on macrophages of the spleen, liver, lymph node, bone marrow, colon, and lungs. It is an I-type lectin, as it contains 17 immunoglobulin (Ig) domains (one variable domain and 16 constant domains), and thus also belongs to the immunoglobulin superfamily (IgSF). Sialoadhesin binds to sialic acids. Sialoadhesin predominantly binds neutrophils, but can also bind monocytes, natural killer cells, B cells and a subset of cytotoxic T cells by interacting with sialic acid molecules in the ligands on their surfaces. Sialoadhesin, in combination with other proteins, is the entry receptor for PRRSV (van Gorp *et al.*, 2008; Shi *et al.*, 2015).	-	2e-128
106	**stabilin-1 isoform X2**	176-480	Large, transmembrane receptor protein which may function in	-	8e-167

	XP_020924550.1		angiogenesis, lymphocyte homing, cell adhesion, or receptor scavenging. Contains 7 fasciclin, 16 epidermal growth factor (EGF)-like, and 2 laminin-type EGF-like domains as well as a C-type lectin-like hyaluronan-binding Link module. Shown to endocytose ligands such as low-density lipoprotein, Gram-positive and Gram-negative bacteria, and advanced glycosylation end products. Possible role as a scavenger receptor, as the protein rapidly cycles between the plasma membrane and early endosomes. Also known to interact with the protein chitinase domain-containing protein.		
117	**CB1 cannabinoid receptor-interacting protein 1** XP_003481247.1	1-115	Suppresses cannabinoid receptor CNR1-mediated tonic inhibition of voltage-gated calcium channels.	KIKP	1e-71
131	**integrin beta-1 isoform X1** XP_020919724.1	351-497	Integrin beta-1 (ITGB1), also known as CD29, is a cell surface receptor that in humans is encoded by the ITGB1 gene. Associates with integrins alpha 1 and 2 to form integrin complexes which function as collagen receptors. Also forms dimers with integrin alpha 3 to form integrin receptors for netrin 1 and reelin.	KIKP	1e-83

18 103*	**Na/K transporting ATPase subunit beta** NP001001542.1 **Na+/K+ transporting ATPase beta 1 polypeptide** AAX55911.1	228-303	Na+/K+-ATPase is an integral membrane protein responsible for establishing and maintaining the electrochemical gradients of Na and K ions across the plasma membrane. These gradients are essential for osmoregulation, for sodium-coupled transport of a variety of organic and inorganic molecules, and for electrical excitability of nerve and muscle. This enzyme is composed of two subunits, a large catalytic subunit (alpha) and a smaller glycoprotein subunit (beta). The beta subunit regulates, through assembly of alpha/beta heterodimers, the number of sodium pumps transported to the plasma membrane.	KQ	2e-39
56	**sodium/potassium-transporting ATPase subunit beta-3 isoform X1** XP_013837554.1	150-279	Na+/K+ -ATPase is an integral membrane protein responsible for establishing and maintaining the electrochemical gradients of Na and K ions across the plasma membrane. These gradients are essential for osmoregulation, for sodium-coupled transport of a variety of organic and inorganic molecules, and for electrical excitability of nerve and muscle. This enzyme is composed of two subunits, a large catalytic subunit (alpha) and a smaller glycoprotein subunit (beta). The beta subunit regulates, through assembly of alpha/beta heterodimers, the number of sodium pumps transported to the plasma membrane.		2e-91
			Extracellular Matrix		
15 43 60 68	**fibronectin** XP_003133690.2	1160-1334 991-1188	Fibronectin is a high-molecular weight (~440 kDa) glycoprotein of the extracellular matrix that binds to membrane-spanning receptor proteins called integrins. Fibronectin binds extracellular matrix components such as collagen, fibrin, and heparan sulfate proteoglycans (e.g. syndecans).	43 - KQ, KLAP 60 -KKVP KSSP KPLT, RTCSLWK, KQ 68 –	2e-102 3e-16 2e-94

111	AAV88080.1	1615-1766 32-305		111 - KTGP	2e-156
79	**EMILIN-2 isoform X1** XP_020951794.1	946-1070	Elastin microfibril interfacer 1 (EMILIN-1) is a protein member of the EMILIN family of extracellular matrix glycoproteins.		6e-81
			Structural		
45 78 132 135 113 135 141	**filamin-A isoform X10** XP_020936395.1 **filamin-A isoform X11** XP_020936398.1 **filamin A (FLNA), transcript variant X9** XM_021080731.1 **filamin-A isoform X11** XP_020936390.1	1769-1896 743-1074 1685-1912 1024-1324 5107-5596 3619-4549 1024-1305	Actin-binding protein, or filamin, is a 280-kD protein that crosslinks actin filaments into orthogonal networks in cortical cytoplasm and participates in the anchoring of membrane proteins for the actin cytoskeleton. Remodelling of the cytoskeleton is central to the modulation of cell shape and migration.	RTAKSLGK KVLP 132 - 135 - 113 – 135 - 141 -	6e-26 7e-159 1e-68 4e-134 3e-80 0 1e-172
48	**actin gamma 1 (ACTG1)** XM_003357928.4	196-781 *In frame ?*	Gamma-actin is widely expressed in cellular cytoskeletons of many tissues; in adult striated muscle cells, gamma-actin is localised to Z-discs and costamere structures,	-	0

73	**actin, cytoplasmic 2** XP_003357976.1	1-210 *In frame ?*	which are responsible for force transduction and transmission in muscle cells.	RGILTLK	2e-155
58	**drebrin like (DBNL), transcript variant X2** XM_005673326.2	1546-1832	Drebrin-like has been shown to interact with Cyclin-dependent kinase 4, MAP4K1 and ZAP-70. Adapter protein that binds F-actin and DNM1, and thereby plays a role in receptor-mediated endocytosis. Plays a role in the reorganization of the actin cytoskeleton, formation of cell projections, such as neurites, in neuron morphogenesis and synapse formation via its interaction with WASL and COBL. May act as a common effector of antigen receptor-signalling pathways in leukocytes. Key component of the immunological synapse that regulates T-cell activation by bridging TCRs and the actin cytoskeleton to gene activation and endocytic processes.	/	2e-116
			Cell division		
2	**serologically defined colon cancer antigen 8 (SDCCAG8), transcript variant X14** XM_021064185.1		Associated with the centrosome. Plays a role in the establishment of cell polarity and epithelial lumen formation. Interacts with and mediates RABEP2 centrosomal localization which is critical for ciliogenesis.		
			Signalling		
3	**thioredoxin like 1 (TXNL1), transcript variant X2** XR_002337500.1				
34	**TYRO protein tyrosine kinase binding**	303-562	Adapter protein which non-covalently associates with activating receptors found on the surface of a variety of immune cells to mediate		2e-129

	protein (TYROBP), transcript variant X1 XM_005664506.3		signalling and cell activation following ligand binding by the receptors. TYROBP is tyrosine-phosphorylated in the ITAM domain following ligand binding by the associated receptors which leads to activation of additional tyrosine kinases and subsequent cell activation. Previously found to be downregulated during PRRSV infection (Wysocki *et al.*, 2012).		
102*	**p21 (RAC1) activated kinase 2 (PAK2), transcript variant X4** XM_021070138.1	4161-4601	PAK2 is one of three members of Group I PAK family of serine/threonine kinases. The PAKs are evolutionary conserved. PAK2 and its cleaved fragment localise in both the cytoplasmic and nuclear compartments. PAK2 signalling modulates apoptosis, endothelial lumen formation, viral pathogenesis, and cancer including, breast, hepatocarcinoma, and gastric and cancer, at-large. PAK2 interacts with and is activated by human immunodeficiency virus-1 Nef protein (Renkema, Manninen and Saksela, 2001; Raney *et al.*, 2005)		0
			RNA binding/modifying		
33	**RNA-binding protein 39 isoform X7** XP_020933927.1	201-373	Transcriptional coactivator for steroid nuclear receptors ESR1/ER-alpha and ESR2/ER-beta, and JUN/AP-1. May be involved in pre-mRNA splicing process.	R K I - S L	1e-109

44 63 82 119	**small nuclear ribonucleo protein G** XP_003125100.1	1-76 *In frame ?* 1-76 1-76 1-76 *In frame ?*	snRNPs, or small nuclear ribonucleoproteins, are RNA-protein complexes that combine with unmodified pre-mRNA and various other proteins to form a spliceosome, a large RNA-protein molecular complex upon which splicing of pre-mRNA occurs. The action of snRNPs is essential to the removal of introns from pre-mRNA, a critical aspect of post-transcriptional modification of RNA, occurring only in the nucleus of eukaryotic cells. Additionally, U7 snRNP is responsible for processing the 3' stem-loop of histone pre-mRNA.	44 - KAHP 63 - KAHP 82 - KAHP 119 - KAHP	5e-49 3e-49 5e-50 9e-51
52	**heterogeneous nuclear ribonucleo protein H isoform X4** XP_005654996.1	294-472	Component of the heterogeneous nuclear ribonucleoprotein (hnRNP) complexes which provide the substrate for the processing events that pre-mRNAs undergo before becoming functional, translatable mRNAs in the cytoplasm. Mediates pre-mRNA alternative splicing regulation.	2 KQ	2e-118
77	**valine-tRNA ligase** NP_001182307.1	77-338	Enzyme that catalyses the chemical reaction ATP + L-valine + tRNA Val AMP + diphosphate + L-valyl-tRNA Val The 3 substrates of this enzyme are ATP, L-valine, and tRNA (Val), whereas its products are AMP, diphosphate, and L-valyl-tRNA(Val). This enzyme belongs to the family of ligases, to be specific those forming carbon-oxygen bonds in aminoacyl-tRNA and related compounds. This enzyme participates in valine, leucine, and isoleucine biosynthesis and aminoacyl-tRNA biosynthesis.	KQ	5e-127
99	**RNA-binding protein 39 isoform X7** XP_020933927.1	116-364	RNA binding protein and possible splicing factor. Found in the nucleus, where it co-localises with core spliceosomal proteins. Studies of a mouse protein with high sequence	-	5e-105

			similarity to this protein suggest that this protein may act as a transcriptional coactivator for JUN/AP-1 and oestrogen receptors. RBM39 has been shown to interact with oestrogen receptor alpha, oestrogen receptor beta and C-jun.		
109	**serine and arginine rich splicing factor 2 (SRSF2), transcript variant X7, misc_RNA** XR_002336827.1	649-732	Necessary for the splicing of pre-mRNA. It is required for formation of the earliest ATP-dependent splicing complex and interacts with spliceosomal components bound to both the 5'- and 3'-splice sites during spliceosome assembly. It also is required for ATP-dependent interactions of both U1 and U2 snRNPs with pre-mRNA.	-	2e-34
144	**protein virilizer homolog isoform X1** XP_020944755.1	50-173	Protein virilizer may be involved in mRNA splicing regulation. Most of the studies on virilizer were carried out in fruit fly. In Drosophila, protein virilizer is required for male and female viability, sex determination and dosage compensation. It is involved in the female-specific splicing of Sxl transcripts. It is required for proper inclusion of regulated exons in Ubx transcripts.	KRNP	2e-81
			GTP related		
20 71	**rho GDP-dissociation inhibitor 2** XP_ 008069400 NP_001231169.1	1-143	RHO protein GDP dissociation inhibitor of Rho proteins (rho GDI) regulates GDP/GTP exchange. Plays an important role in the activation of the oxygen superoxide-generating NADPH oxidase of phagocytes.	KPPP	3e-82
81	**putative GTP-binding protein 6** XP_020937869.1	308-476 *In frame ?*	Function unknown.		1e-102

146	**A-kinase anchor protein 13 isoform X2** XP_020955571.1	122-347	The A-kinase anchor proteins (AKAPs) are a group of structurally diverse proteins that have the common function of binding to the regulatory subunit of protein kinase A (PKA) and confining the holoenzyme to discrete locations within the cell.	KQ	1e-153
			Transcriptional regulation		
90	**forkhead-associated domain-containing protein 1** XP_020953256.1	128-306	The forkhead-associated domain (FHA domain) is a phosphopeptide recognition domain found in many regulatory proteins. It displays specificity for phosphothreonine-containing epitopes but also recognises phosphotyrosine with relatively high affinity. The domain is present in a diverse range of proteins, including kinases, phosphatases, kinesins, transcription factors, RNA-binding proteins and metabolic enzymes which are involved in many different cellular processes (DNA repair, signal transduction, vesicular transport and protein degradation). It is predicted to have a function related to DNA transcription. It localises to the nucleus and has a nuclear localisation signal.	KLLP	5e-128
			Galectin		
31 98 107 118 123	**Galectin 3** NP_001090970.1	29-234 5-62 *In frame ?* 1-241 34-260 34-259	Galectin-3 is a member of the lectin family, of which 14 mammalian galectins have been identified. Galectin-3 is approximately 30 kDa and contains a carbohydrate-recognition-binding domain (CRD) of about 130 amino acids that enables the specific binding of β-galactosides. Galectin-3 is also a member of the beta-galactoside-binding protein family that plays an important role in cell-cell adhesion, cell-matrix interactions, macrophage	KGGP KGGP KPNP 118 - 123 – KIYP, KKRP	2e-141 2e-25 3e-134 6e-162 5e-129

			activation, angiogenesis, metastasis, apoptosis. It is expressed in the nucleus, cytoplasm, mitochondrion, cell surface, and extracellular space.		
			NADPH Oxidase		
38	**neutrophil cytosol factor 2 isoform X1** XP_005667867.2	390-571	Neutrophil cytosolic factor 2, is the 67-kilodalton cytosolic subunit of the multi-protein complex known as NADPH oxidase found in neutrophils. This oxidase produces a burst of superoxide which is delivered to the lumen of the neutrophil phagosome.		8e-128
			DNA/RNA processing		
59	**protein archease** XP_005665243.2	1-141	Archease genes are generally located adjacent to genes encoding proteins involved in DNA or RNA processing and therefore been predicted to be modulators or chaperones involved in DNA or RNA metabolism. Many of the roles of archeases remain to be established experimentally.	KYPP KSFP – not in matching sequence	2e-100
96	**isoform X1** XP_005665243.2	1-159		KYPP	6e-117
			Protein processing		
124	**cytosol aminopeptidase isoform X2** XP_003356918.4	15-278	Presumably involved in the processing and regular turnover of intracellular proteins. Catalyses the removal of unsubstituted N-terminal amino acids from various peptides. Amino acid amides and methyl esters are also readily hydrolysed, but rates on arylamides are exceedingly low. Release of N-terminal proline from a peptide.	R-RPPDLLK 3 KQ	7e-116
			Mitochondria		
67	**voltage-dependent anion-selective channel protein 2 isoform X1** NP_999534.1	185-294	Voltage-dependent anion channels are a class of porin ion channel located on the outer mitochondrial membrane; it is disputed whether this channel is expressed in the cell surface membrane. This major protein of the outer mitochondrial membrane of eukaryotes forms a voltage-	KQ – not in matching sequence	1e-72

			dependent anion-selective channel (VDAC) that behaves as a general diffusion pore for small hydrophilic molecules. VDAC facilitates the exchange of ions and molecules between mitochondria and cytosol and is regulated by the interactions with other proteins and small molecules.		
24 74 103	**cytochrome c oxidase subunit II** YP-220722.1 ABP63291.1	130-229 77-229	Subunit 2 (COII) transfers the electrons from cytochrome c to the catalytic subunit 1. It contains two adjacent transmembrane regions in its N-terminus and the major part of the protein is exposed to the periplasmic or to the mitochondrial intermembrane space, respectively. COII provides the substrate-binding site and contains a copper centre called Cu(A), probably the primary acceptor in cytochrome c oxidase.	- KNPP	2e-63 2e-65
			Protease/protease related		
4 49 50 70	**cathepsin D protein** AY792822.1 **cathepsin D protein, partial** AAV90625.1	143-584 143-584 *In frame ?* 81-395 *In frame ?*	Cathepsin D is a lysosomal aspartyl protease composed of a protein dimer of disulphide-linked heavy and light chains, both produced from a single protein precursor. Cathepsin D is an aspartic endo-protease that is ubiquitously distributed in lysosomes. Its main function is to degrade proteins and activate precursors of bioactive proteins in pre-lysosomal compartments. Various cathepsins are utilised by viruses during replication: both Nipah virus and Hendra virus require Cathepsin L to process their proteins (Pager and Dutch, 2005; Pager *et al.*, 2006) and Ebola virus glycoprotein 1 requires cleavage by Cathepsin B and L for entry (Schornberg *et al.*, 2006).	49 - 50 – KQ 70 - KSSP KQ	0 2e-103 2e-158
57	**inter-alpha-**	1878-2246	Inter-alpha-trypsin inhibitors (IαI) are plasma proteins		2e-149

	trypsin inhibitor heavy chain 3 (ITIH3) transcript variant X7 XM_021068271.1		consisting of three of four heavy chains selected from the group ITIH1, ITIH2, ITIH3, ITIH4 and one light chain selected from the group AMBP or SPINT2. They function as protease inhibitors. IαI form complexes with hyaluronan (HA), generating a serum-derived hyaluronan-associated protein (SHAP)-HA complex.		
			Enzymes		
66	**ribulose-phosphate 3-epimerase isoform X3** XP_003133677.1	22-228	Phosphopentose epimerase (also known as ribulose-phosphate 3-epimerase and ribulose 5-phosphate 3-epimerase) is a metalloprotein that catalyses the interconversion between D-ribulose 5-phosphate and D-xylulose 5-phosphate. This reversible conversion is required for nonoxidative phase of the pentose phosphate pathway.	KQ	2e-153
87	**N(alpha)-acetyltransferase 25, NatB auxiliary subunit (NAA25)** XM_021074209.1	3656-3936	NatA acetyltransferase is an enzyme that catalyses the addition of acetyl groups to various proteins emerging from the ribosome. Upon translation, the NatA binds to the ribosome and then "stretches" to the front end of the forming, or nascent, polypeptide, where it adds this acetyl group. This acetyl group is added to the front end, or N-terminus of the new protein. Forty percent of all proteins in the yeast proteome are thought to be N-terminally acetylated, with a corresponding figure of 90% in mammalian proteins. To be specific, NatA is the main N-alpha-terminal acetyltransferase in the yeast cytosol, responsible for the acetylation of proteins at locations in which L-serine, L-alanine, L-threonine, or glycine are present.		2e-140

			NatA Acetyltransferase is not a single protein but a complex of three subunits.		
88	**nicotinate phosphoribosyltransferase isoform X2** XP_020946125.1	172-459	Nicotinate phosphoribosyltransferase is an enzyme that catalyses the chemical reaction nicotinate + 5-phospho-alpha-D-ribose 1-diphosphate + ATP + H2O = nicotinate D-ribonucleotide + diphosphate + ADP + phosphate. Thus, the four substrates of this enzyme are nicotinate, 5-phospho-alpha-D-ribose 1-diphosphate, ATP, and H2O, whereas its four products are nicotinate D-ribonucleotide, diphosphate, ADP, and phosphate. This enzyme participates in nicotinate and nicotinamide metabolism.		4e-160
115	**UMP-CMP kinase** Q29561.1	15-195	Uridine monophosphate (UMP)/cytidine monophosphate (CMP) kinase catalyses the phosphoryl transfer from ATP to UMP, CMP, and deoxy-CMP (dCMP), resulting in the formation of ADP and the corresponding nucleoside diphosphate. These nucleoside diphosphates are required for cellular nucleic acid synthesis.	KIVP	4e-131

Information on protein function and known interactions with PRRSV or other viruses was recorded directly from a combination of https://www.uniprot.org/, https://en.wikipedia.org/wiki/Main_Page, https://www.ncbi.nlm.nih.gov/ and selected referenced papers. Nucleotides in red or amino acid region in black; note 5e-120 = $5x10^{-120}$. Proteins selected to take forward for further investigation were highlighted in green. Key: # – number; K – lysine; X – any amino acid; R – arginine; P – proline, Q – glutamine; L – Leucine; residues highlighted in blue are ubiquitinated.

9.3 Putative interacting proteins identified in the NSP1β yeast-2-hybrid screen

Table 9.2: Detailed functions of putative interacting proteins identified in the NSP1β yeast-2-hybrid screen

Clone #	Protein and NCBI Sequence ID	Region N or AA	Function	Ubiquitin motifs: KXXP RXXXXLXK KQ	E value
			IFN related		
78	**signal transducer and activator of transcription 3** NP_001038045.1	1-165	STAT3 is a member of the STAT protein family. In response to cytokines and growth factors, STAT3 is phosphorylated by receptor-associated Janus kinases (JAK), form homo- or heterodimers, and translocate to the cell nucleus where they act as transcription activators. Specifically, STAT3 becomes activated after phosphorylation of tyrosine 705 in response to such ligands as interferons, epidermal growth factor (EGF), Interleukin (IL-)5 and IL-6. Additionally, activation of STAT3 may occur via phosphorylation of serine 727 by Mitogen-activated protein kinases (MAPK) and through c-src non-receptor tyrosine kinase. Hepatitis C virus core protein interacts with STAT3 and activates it via phosphorylation, resulting in cell proliferation (Yoshida *et al.*, 2002). Conversely, STAT3 is ubiquitinated and targeted for degradation by mumps virus (Ulane *et al.*, 2003). PRRSV NPS5 has been shown to induce STAT3 degradation to inhibit JAK/STAT3 signalling (Yang *et al.*, 2017) and PRRSV NSP1β blocks STAT1 and STAT2 nuclear translocation (Patel *et al.*, 2010).	KPVP KPTP	9e-37

			NF-κB		
51	**TGF-beta-activated kinase 1 and MAP3K7-binding protein 3** XP_020936488.1	414-701	Adapter linking MAP3K7/TAK1 and TRAF6 or TRAF2. Mediator of MAP3K7 activation, respectively in the IL1 and TNF signalling pathways. Plays a role in activation of NF-κB and AP1 transcription factor. Binds to TAK1 and regulates its activity (Cheung, Nebreda and Cohen, 2004). TAB3 binding to TAK1 leads to TAK1 activation of subsequent of the NF-κB pathway (Ishitani *et al.*, 2003). Additionally, TAB3 binds to Beclin-1 and negatively regulates autophagy (Criollo *et al.*, 2011) . PRRSV has been shown to inhibit the NF-κB pathway using NSP1α (Song, Krell and Yoo, 2010; Jing *et al.*, 2016), and induce autophagy using NSP3, NSP5 and NSP9 (Sun *et al.*, 2012; Zhang, Chen, *et al.*, 2019)	KGSP	6e-61
			GTP related		
63	**Rho GDP dissociation inhibitor alpha (ARHGDIA), transcript variant X3** XM_021066139.1	1543-2039	Controls Rho proteins homeostasis. Regulates the GDP/GTP exchange reaction of the Rho proteins by inhibiting the dissociation of GDP from them, and the subsequent binding of GTP to them.		0
105	**putative GTP-binding protein 6 (LOC110257936)** XM_021080945.1	4558-4977			4e-104
229	**DENN domain-containing protein**	1-142	Guanine nucleotide exchange factor (GEF) activating RAB10. Promotes the exchange of GDP to GTP, converting inactive GDP-	KRRP KPSP	3e-30

	4C isoform X1 XP_020918843.1		bound RAB10 into its active GTP-bound form. Thereby, stimulates SLC2A4/GLUT4 glucose transporter-enriched vesicles delivery to the plasma membrane in response to insulin.		
			Complement		
268	**Sus scrofa complement C3 (C3), transcript variant X1, mRNA** XM_021080819.1	4257-4535	C3 plays a central role in the activation of complement system. Its activation is required for both classical and alternative complement activation pathways.		3e-144
			Autophagy		
328	**beclin-1 isoform X1** XP_013836386.1	5-448	Beclin-1 interacts with either anti-apoptotic protein Bcl-2 (Liang *et al.*, 1998) or PI3k class III, playing a critical role in the regulation of both autophagy and apoptosis (Kang *et al.*, 2011) Beclin-1 has been shown to interact with: Bcl-2, BCL2L2, GOPC and MAP1LC3A. TAB3 binds to beclin-1 and negatively regulates autophagy (Criollo *et al.*, 2011; Takaesu, Kobayashi and Yoshimura, 2012). Beclin-1 is targeted by multiple viruses to inhibit macroautophagy (Münz, 2011). PRRSV interferes with both apoptosis and autophagy during infection (Li *et al.*, 2016)		1e-85
			Heat shock proteins		
290	**10 kDa heat shock protein, mitochondrial**	1-102	Heat shock 10 kDa protein 1 (Hsp10) also known as chaperonin 10 (cpn10) or early-pregnancy factor (EPF) is a protein that in humans is encoded by the HSPE1 gene. Selected HSPs, also known as	KLPP	7e-65

	NP_999472.1		chaperones, play crucial roles in folding/unfolding of proteins, assembly of multiprotein complexes, transport/sorting of proteins into correct subcellular compartments, cell-cycle control and signalling, and protection of cells against stress/apoptosis (Li and Srivastava, 2003). Heat shock proteins are targeted by viruses: rotavirus VP5 protein binds heat shock cognate protein 70 during cell entry (Zárate *et al.*, 2003) .		
350	**DNAJ homolog subfamily C member 10** XP_020931971.1	422-515 *In frame ?*	Endoplasmic reticulum disulphide reductase involved both in the correct folding of proteins and degradation of misfolded proteins. Required for efficient folding of proteins in the endoplasmic reticulum by catalysing the removal of non-native disulphide bonds formed during the folding of proteins, such as LDLR. Also involved in endoplasmic reticulum-associated degradation (ERAD) by reducing incorrect disulphide bonds in misfolded glycoproteins recognised by EDEM1. Interaction with HSPA5 is required its activity, not for the disulphide reductase activity, but to facilitate the release of DNAJC10 from its substrate. Promotes apoptotic signalling pathway in response to endoplasmic reticulum stress.		4e-58
			Transcriptional regulation		
323	**MyoD family inhibitor domain-containing protein isoform X2** XP_020934777.1	110-242	Also known as I-mfa domain-containing protein. Acts as a transcriptional activator or repressor. Inhibits the transcriptional activation of Zic family proteins ZIC1, ZIC2 and ZIC3. Retains nuclear Zic proteins ZIC1, ZIC2 and ZIC3 in the cytoplasm. Modulates the expression from both cellular		1e-61

			and viral promoters. Binds to the axin complex, resulting in an increase in the level of free beta-catenin. Affects axin regulation of the WNT and JNK signalling pathways. Down-regulates Tat-dependent transcription of the HIV-1 LTR by interacting with HIV-1 Tat and Rev and impairing their nuclear import, probably by rendering the NLS domains inaccessible to importin-beta (Gautier *et al.*, 2005). PRRSV N protein binds to MyoD family inhibitor domain-containing protein (Song *et al.*, 2009).		
			Cell division		
37	**transmembrane protein 250 (TMEM250), transcript variant X2** XM_021081256.1	903-1469	May play a role in cell proliferation by promoting progression into S phase. Promotes human herpesvirus 1 (HHV-1) proliferation.		4e-180
204	**cAMP regulated phosphoprotein 19 (ARPP19), transcript variant X3** XM_021082942.1	4650-4963	Protein phosphatase inhibitor that specifically inhibits protein phosphatase 2A (PP2A) during mitosis. When phosphorylated at Ser-62 during mitosis, specifically interacts with PPP2R2D (PR55-delta) and inhibits its activity, leading to inactivation of PP2A, an essential condition to keep cyclin-B1-CDK1 activity high during M phase. May indirectly enhance GAP-43 expression		9e-164
216	**centromere-associated protein**	2223-2456	Centromere-associated protein E is a kinesin-like motor protein that accumulates in the G2 phase of the cell cycle. Unlike		7e-134

	E isoform X5 XP_020956377.1		other centromere-associated proteins, it is not present during interphase and first appears at the centromere region of chromosomes during prometaphase. CENPE is proposed to be one of the motors responsible for mammalian chromosome movement and/or spindle elongation		
240	**metalloproteinase inhibitor 2 isoform X3** XP_013845300.1	89-183 *In frame ?*	Thought to be a metastasis suppressor. The proteins encoded by this gene family are natural inhibitors of the matrix metalloproteinases (MMP), a group of peptidases involved in degradation of the extracellular matrix. In addition to an inhibitory role against metalloproteinases, it has a unique role among TIMP family members in its ability to directly suppress the proliferation of endothelial cells. As a result, the encoded protein may be critical to the maintenance of tissue homeostasis by suppressing the proliferation of quiescent tissues in response to angiogenic factors, and by inhibiting protease activity in tissues undergoing remodelling of the extracellular matrix. TIMP2 functions as both an MMP inhibitor and an activator.	KQ	5e-53
255	**centrosomal protein of 57 kDa isoform X2** XP_020918349.1	153-356	Centrosomal protein which may be required for microtubule attachment to centrosomes. May act by forming ring-like structures around microtubules. Mediates nuclear translocation and mitogenic activity of the internalised growth factor FGF2, but that of FGF1.	KSRP	2e-94
			MHC related		
36 345	**MHC class II antigen, partial**	9-98 175-249	MHC class II molecules are a class of major histocompatibility complex (MHC) molecules normally found only on antigen-presenting cells such as dendritic	36 - 345 - KEIP	2e-57 7e-34

	AEX59168.1 AAP37552.1		cells, mononuclear phagocytes, some endothelial cells, thymic epithelial cells, and B cells. These cells are important in initiating immune responses. The antigens presented by class II peptides are derived from extracellular proteins (not cytosolic as in MHC class I). Porcine MHC, known as SLA molecules. SLA-1 targeted for proteasomal degradation by NSP1α (Du *et al.*, 2016).		
348	**minor histocompatibility protein HA-1 isoform X3** XP_003354009.1	1-244	Minor histocompatibility antigen (also known as MiHA) are receptors on the cellular surface. Minor histocompatibility antigens (MiHAs) are diverse, short segments of proteins and are referred to as peptides. These peptides are normally around 9-12 amino acids in length and are bound to both the major histocompatibility complex (MHC) class I and class II proteins.	KQ RKKRELMK RFAEALEK	7e-101
			RNA binding/modifying		
77	**methylosome subunit pICln** XP_003482618.1	43-218	Chaperone that regulates the assembly of spliceosomal U1, U2, U4 and U5 small nuclear ribonucleoproteins, the building blocks of the spliceosome. Thereby, plays an important role in the splicing of cellular pre-mRNAs.		5e-60
104	**pre-mRNA cleavage complex 2 protein Pcf11 isoform X1** XP_013834646.1	1163-1260	The CFIIm complex is responsible for transcription termination and triggering the disassembly of the elongation complex. It is composed of only two proteins: PCF11 & CLP1.		2e-60
126	**small nuclear**	1-85	Core component of the spliceosomal U1, U2, U4 and U5		4e-55

	ribonucleoprotein F NP_001177142.1		small nuclear ribonucleoproteins (snRNPs), the building blocks of the spliceosome. Thereby, plays an important role in the splicing of cellular pre-mRNAs. Small nuclear ribonucleoprotein polypeptide F has been shown to interact with DDX20, small nuclear ribonucleoprotein D2 and small nuclear ribonucleoprotein polypeptide E		
132	**cleavage and polyadenylation specificity factor subunit 4 isoform X1** XP_020941778.1	2-213	Component of the cleavage and polyadenylation specificity factor (CPSF) complex that play a key role in pre-mRNA 3'-end formation, recognizing the AAUAAA signal sequence and interacting with poly(A) polymerase and other factors to bring about cleavage and poly(A) addition. CPSF4 binds RNA polymers with a preference for poly(U). Influenza A NS1 protein selectively inhibits the nuclear export of cellular, and not viral, mRNAs through binding CPSF (Nemeroff *et al.*, 1998). Additionally, Influenza A NS1 uses CPSF4 to modulate splicing of the p53 gene (Dubois *et al.*, 2019).	KQ	3e-77
190	**poly(rC)-binding protein 1** XP_003125105.1	122-281	It along with PCBP-2 and hnRNPK corresponds to the major cellular poly(rC)-binding protein. It contains three K-homologous (KH) domains which may be involved in RNA binding. Also suggested to play a part in formation of a sequence-specific alpha-globin mRNP complex which is associated with alpha-globin mRNA stability PRRSV NSP1β interacts with PCBP1 and 2 to regulate RNA synthesis (Beura *et al.*, 2011).	KQ	2e-115
243	**clustered mitochondria**	435-571	mRNA-binding protein involved in proper cytoplasmic distribution of mitochondria.		2e-66

	protein homolog isoform X5 XP_02092 3287.1		Specifically binds mRNAs of nuclear-encoded mitochondrial proteins in the cytoplasm and regulates transport or translation of these transcripts close to mitochondria, playing a role in mitochondrial biogenesis.		
244	**RNA-binding protein 39 isoform X7** XP_02093 3927.1	195-310	Transcriptional coactivator for steroid nuclear receptors ESR1/ER-alpha and ESR2/ER-beta, and JUN/AP-1 (By similarity). May be involved in pre-mRNA splicing process.		2e-64
250	**RNA-binding protein 12** XP_00348 3994.1	395-623	Protein that contains several RNA-binding motifs, potential transmembrane domains, and proline-rich regions. Alternative splicing in the 5' UTR results in two transcript variants. Both variants encode the same protein.	KQ KGLP	2e-102
282	**ATP-dependent RNA helicase DDX18** XP_00565 4221.2	4-216 *In frame ?*	DEAD box proteins, characterised by the conserved motif Asp-Glu-Ala-Asp (DEAD), are putative RNA helicases. They are implicated in several cellular processes involving alteration of RNA secondary structure such as translation initiation, nuclear and mitochondrial splicing, and ribosome and spliceosome assembly. This gene encodes a DEAD box protein, and it is activated by Myc protein. PRRSV NSP2 and NSP10 interact with DDX18, which relocate it from the nucleus to cytoplasm, to enhance PRRSV replication (Jin *et al.*, 2017).		9e-120
286	**RNA-binding protein 45 isoform X5** XP_02093 0624.1	1-220 *In frame ?*	RNA-binding protein with binding specificity for poly(C). May play an important role in neural development		1e-111

295	**heterogeneous nuclear ribonucleoprotein K** NP_001254774.1	89-279	The hnRNPs are RNA binding proteins and they complex with heterogeneous nuclear RNA. These proteins are associated with pre-mRNAs in the nucleus and appear to influence pre-mRNA processing and other aspects of mRNA metabolism and transport. While all the hnRNPs are present in the nucleus, some seem to shuttle between the nucleus and the cytoplasm. The hnRNP proteins have distinct nucleic acid binding properties. Located in the nucleoplasm and has three repeats of KH domains that binds to RNAs. It is distinct among other hnRNP proteins in its binding preference; it binds tenaciously to poly(C). Also thought to have a role during cell cycle progression.	KIIP	4e-109
300	**heterogeneous nuclear ribonucleoprotein H isoform X4** XP_005654996.1	50-86 113-189 291-436	The hnRNPs are RNA binding proteins and they complex with heterogeneous nuclear RNA. These proteins are associated with pre-mRNAs in the nucleus and appear to influence pre-mRNA processing and other aspects of mRNA metabolism and transport. While all of the hnRNPs are present in the nucleus, some seem to shuttle between the nucleus and the cytoplasm. The hnRNP proteins have distinct nucleic acid binding properties. The protein encoded by this gene has three repeats of quasi-RRM domains that bind to RNAs.		0.0032 e-06 3e-74
			Ribosomal		
67	**Sus scrofa ribosomal protein L28 (RPL28), transcript variant X6,**	52-600	Ribosomes, the organelles that catalyse protein synthesis, consist of a small 40S subunit and a large 60S subunit. Together these subunits are composed of 4 RNA species and approximately 80 structurally distinct proteins. This a ribosomal protein that is a		2e-11

	XM_021095014.1		component of the 60S subunit and belongs to the L28E family of ribosomal proteins.		
88	**60S ribosomal protein L27** NP_001090948.1	1-136 *Not in frame*	Ribosomes, the organelles that catalyse protein synthesis, consist of a small 40S subunit and a large 60S subunit. Together these subunits are composed of 4 RNA species and approximately 80 structurally distinct proteins. This is a ribosomal protein that is a component of the 60S subunit and belongs to the L27E family of ribosomal proteins. It is located in the cytoplasm.	88 - KKRP	2e-93
101	**40S ribosomal protein S20** AAS55928.1	18-105	A ribosomal protein that is a component of the 40S subunit and belongs to the S10P family of ribosomal proteins. It is located in the cytoplasm.	KQ KKGP	1e-58
130 208 257	**40S ribosomal protein SA** NP_001032223.1	129-277 153-275 168-283	Required for the assembly and/or stability of the 40S ribosomal subunit. Required for the processing of the 20S rRNA-precursor to mature 18S rRNA in a late step of the maturation of 40S ribosomal subunits. Also functions as a cell surface receptor for laminin. Plays a role in cell adhesion to the basement membrane and in the consequent activation of signalling transduction pathways. May play a role in cell fate determination and tissue morphogenesis. Acts as a PPP1R16B-dependent substrate of PPP1CA.	130 - KQ 208 - KFFP	5e-87 2e-82 6e-67
155	**40S ribosomal protein S18** NP_999105.1	1-152	A ribosomal protein that is a component of the 40S subunit and belongs to the S13P family of ribosomal proteins. It is located in the cytoplasm. The gene product of the E. coli ortholog (ribosomal protein S13) is involved in the binding of fMet-tRNA, and thus, in the initiation of translation.		7e-108

329	**fragile X mental retardation syndrome-related protein 1 isoform X8** XP_003358742.1	131-347	An RNA binding protein that interacts with the functionally similar proteins FMR1 and FXR2. These proteins shuttle between the nucleus and cytoplasm and associate with polyribosomes, predominantly with the 60S ribosomal subunit. Three transcript variants encoding different isoforms have been found for this gene. FXR1 has been shown to interact with FXR2, FMR1 and CYFIP2.		3e-124
			Galectin		
19	**galectin 3 (LGALS3), transcript variant X1** XM_005659974.3	8-420	Galectin-3 is approximately 30 kDa and, like all galectins, contains a carbohydrate-recognition-binding domain (CRD) of about 130 amino acids that enable the specific binding of β-galactosides. Galectin-3 is also a member of the beta-galactoside-binding protein family that plays an important role in cell-cell adhesion, cell-matrix interactions, macrophage activation, angiogenesis, metastasis, apoptosis. Galectin-3 is expressed in the nucleus, cytoplasm, mitochondrion, cell surface, and extracellular space	19 -	8e-143
20	**galectin-3** NP_001090970.1	1-187		20 - KLSP, KPNP	2e-86
21		1-229		21 - KPNP	1e-53
156		1-82		156 - KIFP, KRLP, RYPWGLSK	9e-31
205		1-203		205 - KPNP	1e-74
267		1-181			4e-80
304		1-200			7e-99
			Apoptosis		
90	**serine protease HTRA2, mitochondrial** XP_020942985.1	204-443	Serine protease HTRA2, mitochondrial is involved in caspase-dependent apoptosis and in Parkinson's disease. When HtrA2/Omi is released in the cytosol, it activates apoptosis using both caspase-dependent and independent pathways (vande Walle,	-	1e-99

			Lamkanfi and Vandenabeele, 2008). PRRSV has been shown to inhibit apoptosis (Kang *et al.*, 2011).		
234	**NHL repeat-containing protein 2** NP_001230490.1	637-725	The function of NHLRC2 is not yet fully understood. Using bioinformatic analysis, a "YVAD" motif was found to be conserved in eukaryotes, bacteria, and archaea. "YVAD" shows up three times alone in the human NHLRC2 protein. This motif is potential involved in inhibiting caspases 1, 2, 3, 4 & 5, thus possibly having anti-apoptotic properties. PRRSV has been shown to inhibit apoptosis (Kang *et al.*, 2011).	-	8e-39
			Nuclear proteins		
112	**nucleoporin GLE1** XP_003122270.2	1-202	RNA export mediator (GLE1) (Murphy and Wente, 1996). Is 75 kDa polypeptide with high sequence and structure homology to yeast Gle1p, which is nuclear protein with a leucine-rich nuclear export sequence essential for poly(A)+RNA export. Inhibition of human GLE1L by microinjection of antibodies against GLE1L in HeLa cells resulted in inhibition of poly(A)+RNA export. Immunofluorescence studies show that GLE1L is localised at the nuclear pore complexes. This localization suggests that GLE1L may act at a terminal step in the export of mature RNA messages to the cytoplasm. GLE1L has been shown to interact with NUP155 (Rayala *et al.*, 2004). PRRSV NSP1β inhibits nuclear export of host mRNAs (Han *et al.*, 2017) and has been shown to interact with nucleoporin 62 to disintegrate the nuclear pore complex (H. Ke, Han, *et al.*, 2019)		3e-142

164	**peroxisome proliferator-activated receptor-gamma 2** CAA07225.1	1-86	Peroxisome proliferator-activated receptor gamma (PPAR-γ or PPARG), also known as the glitazone receptor, or NR1C3 (nuclear receptor subfamily 1, group C, member 3) is a type II nuclear receptor. PPARG regulates fatty acid storage and glucose metabolism.		1e-32
227	**nucleoprotein TPR isoform X2** XP_013833352.2	458-554	Component of the nuclear pore complex (NPC), a complex required for the trafficking across the nuclear envelope. TPR is involved in mRNA export (Frosst *et al.*, 2002) and regulates mRNA export via the NXF1:NXT1 pathway (Coyle *et al.*, 2011), helping to prevent export of incorrectly spliced mRNAs. Functions as a scaffolding element in the nuclear phase of the NPC essential for normal nucleocytoplasmic transport of proteins and mRNAs, plays a role in the establishment of nuclear-peripheral chromatin compartmentalization in interphase, and in the mitotic spindle checkpoint signalling during mitosis. Involved in the quality control and retention of unspliced mRNAs in the nucleus; in association with NUP153, regulates the nuclear export of unspliced mRNA species bearing constitutive transport element (CTE) in an NXF1- and KHDRBS1-independent manner. Negatively regulates both the association of CTE-containing mRNA with large polyribosomes and translation initiation. PRRSV NSP1β inhibits nuclear export of host mRNAs (Han *et al.*, 2017) and has been shown to interact with nucleoporin 62 to	-	2e-54

			disintegrate the nuclear pore complex (H. Ke, Han, *et al.*, 2019)		
260	**nuclear pore membrane glycoprotein 210** XP_020925047.1	655-721	Nucleoporin essential for nuclear pore assembly and fusion, nuclear pore spacing, as well as structural integrity. Nuclear pore glycoprotein-210 (gp210) is an essential trafficking regulator in the eukaryotic nuclear pore complex. Gp-210 anchors the pore complex to the nuclear membrane. and protein tagging reveals its primarily located on the luminal side of double layer membrane at the pore. A single polypeptide motif of gp210 is responsible for sorting to nuclear membrane and indicate the carboxyl tail of the protein is oriented toward the cytoplasmic side of the membrane. PRRSV NSP1β inhibits nuclear export of host mRNAs (Han *et al.*, 2017) and has been shown to interact with nucleoporin 62 to disintegrate the nuclear pore complex (H. Ke, Han, *et al.*, 2019)		2e-38
			Signalling		
66	**p21 (RAC1) activated kinase 1 (PAK1), transcript variant X9, mRNA** XM_021062561.1	557-869	Protein kinase involved in intracellular signalling pathways downstream of integrins and receptor-type kinases that plays an important role in cytoskeleton dynamics, in cell adhesion, migration, proliferation, apoptosis, mitosis, and in vesicle-mediated transport processes. Can directly phosphorylate BAD and protects cells against apoptosis. Activated by interaction with CDC42 and RAC1. Functions as GTPase effector that links the Rho-related GTPases CDC42 and RAC1 to the JNK MAP kinase pathway. Phosphorylates and activates MAP2K1, and thereby mediates activation of downstream MAP kinases.		1e-147

			PRRSV induces macropinocytosis via the Rac1/Cdc42-Pak1 pathway using molecular mimicry as an alternative pathway of infection (Wei *et al.*, 2020).		
99	**A-kinase anchor protein 13 (AKAP13) isoform X2** XP_020955571.1	122-356	Scaffold protein that plays an important role in assembling signalling complexes downstream of several types of G protein-coupled receptors. Activates RHOA in response to signalling via G protein-coupled receptors via its function as Rho guanine nucleotide exchange factor.	KQ	4e-153
119	**myoferlin isoform X4** XP_020929514.1	83-315	Calcium/phospholipid-binding protein that plays a role in the plasmalemma repair mechanism of endothelial cells that permits rapid resealing of membranes disrupted by mechanical stress. Involved in endocytic recycling. Implicated in VEGF signal transduction by regulating the levels of the receptor KDR also known as FER1L3, MOF.		3e-76
133	**dedicator of cytokinesis protein 10 isoform X33** XP_020930475.1	601-714	Dock10 (Dedicator of cytokinesis), also known as Zizimin3, is a large (~240 kDa) protein involved in intracellular signalling networks. It is a member of the DOCK-D subfamily of the DOCK family of guanine nucleotide exchange factors, which function as activators of small G proteins. It contains a DHR2 domain that is involved in G protein binding and a DHR1 domain, which, in some DOCK family proteins, interacts with membrane phospholipids. Like other DOCK-D subfamily proteins Dock10 contains an N-terminal PH domain, which, in Dock9/Zizimin1, mediates recruitment to the plasma membrane	KQ	1e-70

			Involved in lymphocyte signalling.		
192	**Protein AF-17** XP_02092 2727.1	616-821	Involved in T cell signalling likely to be involved in the beta-catenin-T-cell factor/lymphoid enhancer factor signalling pathway and to function as a growth-promoting, oncogenic protein.	KQ	3e-109
199	**1-phosphatidylinositol 4,5-bisphosphate phosphodiesterase delta-1** NP_0012 30518.1	34-116	The production of the second messenger molecules diacylglycerol (DAG) and inositol 1,4,5-trisphosphate (IP3) is mediated by activated phosphatidylinositol-specific phospholipase C enzymes. Essential for trophoblast and placental development.		6e-115
			PRRs		
69	**collectin-12 isoform X2** XP_02095 1815.1	533-737	Collectins (collagen-containing C-type lectins) are a part of the innate immune system. They form a family of collagenous Ca2+-dependent defence lectins, which are found in animals. Collectins are soluble pattern recognition receptors (PRRs). Their function is to bind to oligosaccharide structure or lipids that are on the surface of microorganisms. Activates the alternative pathway of complement (Ma *et al.*, 2015) .	KQ KGPP	8e-148
103 159	**toll-like receptor 4** ACL97681 .1	24-100 24-100	TLR4 is a transmembrane protein, member of the toll-like receptor family, which belongs to the pattern recognition receptor (PRR) family. Its activation leads to an intracellular signalling pathway NF-κB and inflammatory cytokine production which is responsible for activating the innate immune system. Its ligands also include several viral proteins, polysaccharide, and a variety of endogenous proteins such as low-density lipoprotein, beta-defensins, and heat shock	103 - 159 -	2e-50 2e-47

			protein, Involved in the innate immune response to respiratory syncytial virus F protein (Kurt-Jones *et al.*, 2000). Use of LPS to activate the TLR4-NF-κB pathway leads to downregulation of CD163 and inhibition of PRRSV infection (Zhu *et al.*, 2020).		
			Translation		
127	**eukaryotic translation initiation factor 3 subunit K isoform X2** XP_003127167.2	36-133 *Not in frame ?*	Eukaryotic initiation factor 3 (eIF3) is a multiprotein complex that functions during the initiation phase of eukaryotic translation. it is essential for most forms of cap-dependent and cap-independent translation initiation. In humans, eIF3 consists of 13 nonidentical subunits (eIF3a-m) with a combined molecular weight of ~800 kDa, making it the largest translation initiation factor. eIF3 plays an essential role in translation by binding directly to the 40S ribosomal subunit and promoting formation of the 43S preinitiation complex. Components of eIF3 are utilised by viruses to enhance viral replication and translation: classical swine fever NS5A protein binds to eIF-3 subunit E (X. Liu *et al.*, 2018) and both classical swine fever virus and hepatitis C virus RNA use 5' IRESs to bind eIF3 (Sizova *et al.*, 1998).		2e-38
			Intracellular transport		
141 184 320	**major vault protein** XP_020942083.1	1-179 1-157 589-706	Vaults are multi-subunit structures that may be involved in nucleo-cytoplasmic transport. Known to block nuclear export of mRNAs. Induces type I interferon production to inhibit PRRSV infection (Wu *et al.*, 2021).	141 - KQ 184 - KWWP 320 -	2e-117 7e-90 5e-39
			Antibodies		

54 83 124 135 136 161 340	**IgG heavy chain precursor** BAM75557.1 BAM75568.1 BAM75543.1 BAM75562.1 BAM75552.1 BAM75568.1	130-459 14-240 19-342 20-241 103-333 20-311 14-275	The immunoglobulin heavy chain (IgH) is the large polypeptide subunit of an antibody (immunoglobulin). All heavy chains contain a series of immunoglobulin domains, usually with one variable domain (VH) that is important for binding antigen and several constant domains (CH1, CH2, etc.). Production of a viable heavy chain is a key step in B cell maturation.	54 – KTAP 83 - 124 - KTAP 135 - KTAP, KLLP 136 - KTAP, KTKP 161 - KQ, KTAP	6e-155 2e-103 1e-142 2e-93 2e-110 6e-141 2e-80
			DNA binding/modifying		
43	**mortality factor 4-like protein 2** XP_003135315.1	75-237	Component of the NuA4 histone acetyltransferase complex which is involved in transcriptional activation of select genes principally by acetylation of nucleosomal histone H4 and H2A. This modification may both alter nucleosome - DNA interactions and promote interaction of the modified histones with other proteins which positively regulate transcription.	2 KQ	3e-118
55 158	**E3 SUMO-protein ligase EGR2** NP_001090957.1	49-278 159-383	Sequence-specific DNA-binding transcription factor. Binds to two specific DNA sites located in the promoter region of HOXA4. E3 SUMO-protein ligase helping SUMO1 conjugation to its coregulators NAB1 and NAB2, whose sumoylation down-	55 - KLYP 158 - KPFP	9e-93 3e-160

			regulates EGR2 own transcriptional activity.		
81	**DNA polymerase epsilon subunit 2 isoform X1** XP_003480516.1	229-483	DNA polymerase epsilon is a member of the DNA polymerase family of enzymes found in eukaryotes. It is composed of the following four subunits: POLE (central catalytic unit), POLE2 (subunit 2), POLE3 (subunit 3), and POLE4 (subunit 4). Recent evidence suggests that it plays a major role in leading strand DNA synthesis and nucleotide and base excision repair. POLE2 has been shown to interact with SAP18 (part of HDAC)	KQ	0
89	**ATP-dependent DNA helicase Q1** NP_001240636.1	1-118	Member of the RecQ DNA helicase family. DNA helicases are enzymes involved in various types of DNA repair, including mismatch repair, nucleotide excision repair and direct repair. The biological function of this helicase has not yet been determined. RECQL has been shown to interact with KPNA4 and Karyopherin alpha 2	KQ KFRP	9e-66
97	**activator of transcription and developmental regulator AUTS2 (AUTS2)** NM_001246269.1	1755-2024	Chromatin binding. Component of a Polycomb group (PcG) multiprotein PRC1-like complex, a complex class required to maintain the transcriptionally repressive state of many genes, including Hox genes, throughout development. PcG PRC1 complex acts via chromatin remodelling and modification of histones; it mediates mono-ubiquitination of histone H2A 'Lys-119', rendering chromatin heritably changed in its expressibility. Complex mediates transcriptional activation. Promotes reorganization of the actin cytoskeleton, lamellipodia formation and neurite		2e-136

			elongation via its interaction with RAC guanine nucleotide exchange factors, which then leads to the activation of RAC1.		
108	**msx2-interacting protein** XP_020951052.1	2759-3015	Hormone inducible transcriptional repressor. Repression of transcription by this gene product can occur through interactions with other repressors, by the recruitment of proteins involved in histone deacetylation, or through sequestration of transcriptional activators. The product of this gene contains a carboxy-terminal domain that permits binding to other corepressor proteins. This domain also permits interaction with members of the NuRD complex, a nucleosome remodelling protein complex that contains deacetylase activity.	KQ KPEP KLPP	1e-124
171	**mediator of RNA polymerase II transcription subunit 4** XP_013834181.1	1-104	Component of the Mediator complex, a coactivator involved in the regulated transcription of nearly all RNA polymerase II-dependent genes. Mediator functions as a bridge to convey information from gene-specific regulatory proteins to the basal RNA polymerase II transcription machinery. Mediator is recruited to promoters by direct interactions with regulatory proteins and serves as a scaffold for the assembly of a functional preinitiation complex with RNA polymerase II and the general transcription factors. Varicella zoster virus IE62 interacts with and requires the mediator complex for activation (Yang, Hay and Ruyechan, 2008).	KERP	4e-42
305 317	**endothelial PAS domain-containing protein 1**	104-558 207-422	Also known as HIF2α. It is a type of hypoxia-inducible factor, a group of transcription factors involved in body response to oxygen level. The	317 -	4e-117 5e-92

	NP_0010 90889.1		gene is active under low oxygen condition called hypoxia. HIFs regulate expression of genes involved in cell proliferation, angiogenesis, apoptosis, and metabolism (Koh and Powis, 2012).		
342	**AT-rich interactive domain-containing protein 1A isoform X2** XP_02095 1290.1	2031-2119	ARID1A is a member of the SWI/SNF family, whose members have helicase and ATPase activities and are thought to regulate transcription of certain genes by altering the chromatin structure around those genes. The encoded protein is part of the large ATP-dependent chromatin remodelling complex SNF/SWI, which is required for transcriptional activation of genes normally repressed by chromatin		4e-55
			Secretion/Endocytic Pathways		
39	**glycosylated lysosomal membrane protein isoform X2** XP_00566 3352.1	191-320 *Not in frame*	Lysosome-associated membrane glycoproteins (lamp) are integral membrane proteins, specific to lysosomes, and whose exact biological function is not yet clear.	KQ	2e-87
138 230	**prolow-density lipoprotein receptor-related protein 1** XP_02094 7485.1	1157-1332 1157-1288	Endocytic receptor involved in endocytosis and in phagocytosis of apoptotic cells. Required for early embryonic development. Involved in cellular lipid homeostasis. Involved in the plasma clearance of chylomicron remnants and activated LRPAP1 (alpha 2-macroglobulin), as well as the local metabolism of complexes between plasminogen activators and their endogenous inhibitors. May modulate cellular events, such as APP metabolism, kinase-dependent intracellular signalling, neuronal calcium	138 - 230 -	3e-110 2e-57

			signalling as well as neurotransmission		
197	**protein transport protein Sec31A isoform X26** XP_020957515.1	626-796	SEC31 protein is known to be a component of the COPII protein complex which is responsible for vesicle budding from endoplasmic reticulum (ER). This protein was found to co-localise with SEC13, one of the other components of COPII, in the subcellular structures corresponding to the vesicle transport function. An immunodepletion experiment confirmed that this protein is required for ER-Golgi transport.	KGRP	4e-111
308	**leucine-zipper-like transcriptional regulator 1** XP_003133045.2	826-985	Member of the BTB-kelch superfamily. Initially described as a putative transcriptional regulator based on weak homology to members of the basic leucine zipper-like family, the encoded protein subsequently has been shown to localise exclusively to the Golgi network where it may help stabilise the Golgi complex		2e-106
Protease/protease related					
96	**cathepsin B precursor** NP_001090927.1	44-327	Cathepsin B belongs to a family of lysosomal cysteine proteases and plays an important role in intracellular proteolysis. Thiol protease which is believed to participate in intracellular degradation and turnover of proteins. Various cathepsins are utilised by viruses during replication: both Nipah virus and Hendra virus require Cathepsin L to process their proteins (Pager and Dutch, 2005; Pager *et al.*, 2006) and Ebola virus glycoprotein 1 requires cleavage by Cathepsin B and L for entry (Schornberg *et al.*, 2006).	-	0
172	**cathepsin D protein** AAV90625.1	451-1264	Lysosomal aspartyl protease composed of a protein dimer of disulphide-linked heavy and light chains, both produced from	172 -	9e-142

222	AAY42145.2	263-346	a single protein precursor. Cathepsin D is an aspartic endo-protease that is ubiquitously distributed in lysosomes. The main function of cathepsin D is to degrade proteins and activate precursors of bioactive proteins in pre-lysosomal compartments Various cathepsins are utilised by viruses during replication: both Nipah virus and Hendra virus require Cathepsin L to process their proteins (Pager and Dutch, 2005; Pager *et al.*, 2006) and Ebola virus glycoprotein 1 requires cleavage by Cathepsin B and L for entry (Schornberg *et al.*, 2006).	222 -	2e-27
330	**cathepsin H transcript variant 3** ACB70169.1	19-235	Lysosomal cysteine proteinase important in the overall degradation of lysosomal proteins. Various cathepsins are utilised by viruses during replication: both Nipah virus and Hendra virus require Cathepsin L to process their proteins (Pager and Dutch, 2005; Pager *et al.*, 2006) and Ebola virus glycoprotein 1 requires cleavage by Cathepsin B and L for entry (Schornberg *et al.*, 2006).	KFQP	6e-139
			Ubiquitin related		
195	**cullin-9 isoform X4** XP_001929303.2	296-458	Cullins are a family of hydrophobic proteins providing a scaffold for ubiquitin ligases (E3). All eukaryotes appear to have cullins. They combine with RING proteins to form Cullin-RING ubiquitin ligases (CRLs) that are highly diverse and play a role in myriad cellular processes. Cullin 9 – also known as PARC, known to interact with p53. Cytoplasmic anchor protein in p53-associated protein complex. Regulates the subcellular localization of p53 and subsequent function. Seems to	KGGP	3e-105

			be part of an atypical cullin-RING- based E3 ubiquitin-protein ligase complex. In vitro, complexes of CUL9/PARC with either CUL7 or TP53 contain E3 ubiquitin-protein ligase activity. PRRSV alters the ubiquitome of the cell (H. Zhang *et al.*, 2018).		
259	**kelch-like protein 20** XP_005656773.1	1-193	Substrate-specific adapter of a BCR (BTB-CUL3-RBX1) E3 ubiquitin-protein ligase complex involved in interferon response and anterograde Golgi to endosome transport. The BCR(KLHL20) E3 ubiquitin ligase complex mediates the ubiquitination of DAPK1, leading to its degradation by the proteasome, thereby acting as a negative regulator of apoptosis. The BCR(KLHL20) E3 ubiquitin ligase complex also specifically mediates 'Lys-33'-linked ubiquitination. Involved in anterograde Golgi to endosome transport by mediating 'Lys-33'-linked ubiquitination of CORO7, promoting interaction between CORO7 and EPS15, thereby facilitating actin polymerization and post-Golgi trafficking PRRSV alters the ubiquitome of the cell (H. Zhang *et al.*, 2018).		1e-121
			Mitochondria		
15 289	**fumarate hydratase, mitochondrial isoform X3** XP_020919702.1 **fumarate hydratase, mitochon**	68-335 138-189	Fumarase (or fumarate hydratase) is an enzyme that catalyses the reversible hydration/dehydration of fumarate to malate. Fumarase comes in two forms: mitochondrial and cytosolic. The mitochondrial isoenzyme is involved in the Krebs Cycle (also known as the Tricarboxylic Acid Cycle [TCA] or the Citric Acid Cycle)		2e-120 2e-05

	drial isoform X2 XP_02091 9701.1				
31	**NADH dehydrog enase [ubiquino ne] 1 beta subcompl ex subunit 9** XP_01385 1951.1	4-165	Accessory subunit of the mitochondrial membrane respiratory chain NADH dehydrogenase (Complex I), that is believed to be not involved in catalysis. Complex I functions in the transfer of electrons from NADH to the respiratory chain. The immediate electron acceptor for the enzyme is believed to be ubiquinone	KQ	1e-104
32	**methyltra nsferase-like protein 17, mitochon drial** NP_0012 31255.1	342-461	May be a component of the mitochondrial small ribosomal subunit	KQ	3e-83
110	**iron-sulphur cluster assembly 2 homolog, mitochon drial** XP_00348 2336.1	5-154	Involved in the maturation of mitochondrial 4Fe-4S proteins functioning late in the iron-sulphur cluster assembly pathway. May be involved in the binding of an intermediate of Fe/S cluster assembly	-	8e-104
118	**histidine triad nucleotid e-binding protein 2, mitochon drial isoform 1 precursor** NP_0012 31254.1	5-77	Hydrolase probably involved in steroid biosynthesis. May play a role in apoptosis. Has adenosine phosphoramidase activity.	-	1e-42
297	**enoyl-CoA**	1-228	Enoyl-CoA hydratase is an enzyme that hydrates the		1e-66

	hydratase, mitochondrial NP_001177104.1		double bond between the second and third carbons on acyl-CoA. This enzyme, also known as crotonase, is essential to metabolizing fatty acids to produce both acetyl CoA and energy.		
310	**citrate synthase, mitochondrial isoform X1** XP_020946802.1	3-262	The enzyme citrate synthase E.C. 2.3.3.1 exists in nearly all living cells and stands as a pace-making enzyme in the first step of the citric acid cycle (or Krebs cycle). Citrate synthase is localised within eukaryotic cells in the mitochondrial matrix but is encoded by nuclear DNA rather than mitochondrial. It is synthesised using cytoplasmic ribosomes, then transported into the mitochondrial matrix.		4e-44
			Cell migration/movement		
8	**absent in melanoma 1 protein isoform X3** XP_003121377.4	649-964	AIM1 is an actin-binding protein that suppresses cell migration and micrometastatic dissemination.	KKKP KLRP KDQP	3e-140
179	**neuroblast differentiation-associated protein AHNAK** XP_013849669.2	4475-4619	Neuroblast differentiation-associated protein AHNAK, also known as desmoyokin, has shown to be essential for pseudopod protrusion and cell migration. AHNAK has been shown to interact with S100B.	179 -	5e-83
237	**macrophage migration inhibitory factor** NP_001070681.1	1-67	Macrophage migration inhibitory factor (MIF or MMIF), also known as glycosylation-inhibiting factor (GIF), L-dopachrome isomerase, is an important regulator of innate immunity. Bacterial antigens stimulate white blood cells to release MIF into the blood stream. The circulating MIF binds to CD74 on other immune cells to trigger an	KRKP	N 0 P 1e-41

			acute immune response. Hence, MIF is classified as an inflammatory cytokine. Furthermore, glucocorticoids also stimulate white blood cells to release MIF and hence MIF partially counteracts the inhibitory effects that glucocorticoids have on the immune system. Macrophage migration inhibitory factor has been reported to interact with: BNIPL, CD74, COPS5, CXCR4, and RPS19. Porcine alveolar macrophages are the target cell of PRRSV (Albina, Carrat and Charley, 1998; Morgan *et al.*, 2016).		
239	**P-selectin glycoprotein ligand 1 propeptide precursor** CAO91826.1	96-161 *In frame ?*	A SLe(x)-type proteoglycan, which through high affinity, calcium-dependent interactions with E-, P- and L-selectins, mediates rapid rolling of leukocytes over vascular surfaces during the initial steps in inflammation. Critical for the initial leukocyte capture.	-	4e-35
			Proteasome		
16 82 117 254 256	**proteasome subunit beta type-4** NP_001231384.1	1-264 1-248 1-258 1-81 1-226	Proteasome subunit beta type-4 also known as 20S proteasome subunit beta-7 is one of the 17 essential subunits (alpha subunits 1-7, constitutive beta subunits 1-7, and inducible subunits including beta1i, beta2i, beta5i) that contributes to the complete assembly of 20S proteasome complex. In particular, proteasome subunit beta type-2, along with other beta subunits, assemble into two heptameric rings and subsequently a proteolytic chamber for substrate degradation. Inhibiting proteasomal system inhibits PRRSV replication (Pang *et al.*, 2021). PRRSV targets	16 – 2 KQ, KMNP 82 – 2 KQ, KMNP 117 - KQ, KMNP 254 - 256 - KQ, KMNP	2e-172 1e-154 2e-108 2e-46 6e-119

			multiple proteins for proteasomal degradation: NSP1α targets SLA-1, NSP5 targets STAT3 and E protein targets cholesterol 25-hydroxylase (Du *et al.*, 2016; Yang *et al.*, 2017; W. Ke *et al.*, 2019).		
123	**proteasome subunit alpha type-1** XP_003123013.1	74-263	Proteasome subunit alpha type-1 is one of the 17 essential subunits (alpha subunits 1-7, constitutive beta subunits 1-7, and inducible subunits including beta1i, beta2i, and beta5i) that contributes to the complete assembly of 20S proteasome complex. PRRSV upregulates expression of PSMA1 in infected cells (Zhang *et al.*, 2009). Inhibiting proteasomal system inhibits PRRSV replication (Pang *et al.*, 2021). PRRSV targets multiple proteins for proteasomal degradation: NSP1α targets SLA-1, NSP5 targets STAT3 and E protein targets cholesterol 25-hydroxylase (Du *et al.*, 2016; Yang *et al.*, 2017; W. Ke *et al.*, 2019).	KAQP	2e-140
194	**proteasome (prosome, macropain) subunit, beta type, 8 (large multifunctional protease 7)** CAN13318.1	37-208	Proteasome subunit beta type-8, also as known as 20S proteasome subunit beta-5i, is one of the 17 essential subunits (alpha subunits 1-7, constitutive beta subunits 1-7, and inducible subunits including beta1i, beta2i, beta5i) that contributes to the complete assembly of 20S proteasome complex. The constitutive subunit beta1, beta2, and beta 5 (systematic nomenclature) can be replaced by their inducible counterparts beta1i, 2i, and 5i when cells are under the treatment of interferon-γ. The resulting proteasome complex becomes	KKGP	2e-124

			the so-called immunoproteasome. An essential function of the modified proteasome complex, the immunoproteasome, is the processing of numerous MHC class-I restricted T cell epitopes. Inhibiting proteasomal system inhibits PRRSV replication (Pang *et al.*, 2021). PRRSV targets multiple proteins for proteasomal degradation: NSP1α targets SLA-1 , NSP5 targets STAT3 and E protein targets cholesterol 25-hydroxylase (Du *et al.*, 2016; Yang *et al.*, 2017; W. Ke *et al.*, 2019). Highly pathogenic PRRSV also inhibits IFN-γ induced immunoproteasome expression through targeting specific subunits (Q. Liu *et al.*, 2020).		
263	**proteasome maturation protein (POMP), ncRNA** XR_002336632.1	75-615	Molecular chaperone essential for the assembly of standard proteasomes and immunoproteasomes. Degraded after completion of proteasome maturation. Mediates the association of 20S pre-proteasome with the endoplasmic reticulum. Inhibiting proteasomal system inhibits PRRSV replication (Pang *et al.*, 2021). PRRSV targets multiple proteins for proteasomal degradation: NSP1α targets SLA-1 , NSP5 targets STAT3 and E protein targets cholesterol 25-hydroxylase (Du *et al.*, 2016; Yang *et al.*, 2017; W. Ke *et al.*, 2019). Highly pathogenic PRRSV also inhibits IFN-γ induced immunoproteasome expression through targeting specific subunits (Q. Liu *et al.*, 2020).		0
			Receptors/cell surface molecules		

10	**C5a anaphylatoxin receptor 1** NP_001231144.1	219-347 *Not in frame*	The C5a receptor also known as complement component 5a receptor 1 (C5AR1) or CD88 (Cluster of Differentiation 88) is a G protein-coupled receptor for C5a. It functions as a complement receptor. C5a receptor modulates inflammatory responses, obesity, development, and cancers.	KTLP	4e-82
22	**IGF-like family receptor 1** XP_020952886.1	79-122	The insulin-like growth factor 1 (IGF-1) receptor is a protein found on the surface of human cells. It is a transmembrane receptor that is activated by a hormone called insulin-like growth factor 1 (IGF-1) and by a related hormone called IGF-2.	KKIP	1e-18
25	**integrin beta-2 precursor** ABU86738.1	364-650	CD18 (Integrin beta chain-2) Upon binding with one of a number of alpha chains, CD18 is capable of forming multiple heterodimers, which play significant roles in cellular adhesion and cell surface signalling, as well as important roles in immune responses. CD18 also exists in soluble, ligand binding forms. Integrins are entry receptors for multiple virus: αvβ1 for FMDV (Jackson *et al.*, 2002) and αvβ3 for west Nile virus (Chu and Ng, 2004).	KITP	3e-164
64 106 122 303	**macrosialin isoform X1** XP_013834029.1	49-186 *In frame ?* 49-194 *In frame ?* 462-569 49-186	CD68 (Cluster of Differentiation 68) is a protein highly expressed by cells in the monocyte lineage (e.g., monocytic phagocytes, osteoclasts), by circulating macrophages, and by tissue macrophages (e.g., Kupffer cells, microglia).	64 - 106 - 122 – 303 -	2e-66 2e-79 7e-41 3e-73

		Not in frame			
109	**V-set and immunoglobulin domain-containing protein 4 isoform X3** XP_013841676.1	45-143	Phagocytic receptor, strong negative regulator of T-cell proliferation and IL2 production. Potent inhibitor of the alternative complement pathway convertases.	-	7e-67
150 165 226 322	**Scavenger receptor cysteine-rich type 1 protein M130 isoform X1** XP_020946779.1 **CD163** ADM07458.1	97-370 74-258 111-245 95-246	Also known as CD163. Acute phase-regulated receptor involved in clearance and endocytosis of haemoglobin/haptoglobin complexes by macrophages and may thereby protect tissues from free haemoglobin-mediated oxidative damage. 1100 amino acid protein, type 1 membrane protein exclusively expressed by cells of the monocyte/macrophage cell lineage. The cytoplasmic tail of human CD163 exists as a short tail and 2 long tail variants. Short tail variant has a higher capacity for ligand endocytosis. Long tail variants are most abundant in the Golgi region/endosomes and may have an unknown function. CD163 may be a hypoxia-responsive gene. Activation of cell surface Toll-like receptors causes shedding of the haemoglobin scavenger receptor CD163. CD163 is a PRRSV entry receptor (van Gorp *et al.*, 2008, 2010)	150 - 2 KQ 165 - KQ 226 -	0 6e-127 4e-68 3e-101
251 306	**stabilin-1 isoform X7** XP_020924555.1	361-489 1480-1742	Large, transmembrane receptor protein which may function in angiogenesis, lymphocyte homing, cell adhesion, or receptor scavenging.		3e-70 6e-110
			Structural		

24	**F-actin-capping protein subunit alpha-2** Q29221.3	178-286	F-actin capping protein is a protein which binds in a calcium-independent manner to the fast-growing ends of actin filaments (barbed end), thereby blocking the exchange of subunits at these ends. Unlike gelsolin and severin this protein does not sever actin filaments.		2e-70
27 45 65 74 180 224 246 258 261 264 270 272 284 333	**Vimentin, partial** ABA3952 7.1 **Vimentin isoform X2** XP_00566 8164.1	131-274 1-250 1-198 126-393 1-261 1-124 1-216 *In frame ?* 1-81 1-62 82-222 1-225 1-176 1-159	Vimentin is a type III intermediate filament (IF) protein that is expressed in mesenchymal cells. IF, along with tubulin-based microtubules and actin-based microfilaments, comprises the cytoskeleton. All IF proteins are expressed in a highly developmentally regulated fashion; vimentin is the major cytoskeletal component of mesenchymal cells. PRRSV uses vimentin for entry and induces vimentin rearrangement post-entry (Shi *et al.*, 2015; Zheng *et al.*, 2021).	27 – KQ 45 – KWNP, KRLP 65 - KNTP 74 - KQ 180 - 224 - 246 - KSAP, KEEP	1e-88 6e-139 6e-63 2e-144 2e-140 9e-82 2e-101 1e-30 2e-32 5e-14 2e-57 7e-72 1e-63 4e-77

343 354 279	 XP_00566 8163.1	1-222 1-233 213- 415 1-40		343 - KNTP, RTSCCLRK 354 – 279 -	1e-86 4e-68 3e-16
80 115 236 220 344	**ferritin heavy chain isoform X1** XP_00566 0860.1 **ferritin heavy chain 1 (FTH1), transcript variant X1** XM_0056 60803.3	1-181 *In frame ?* 1-156 118- 556 1-84 108- 405	The heavy subunit of ferritin, the major intracellular iron storage protein in prokaryotes and eukaryotes. It is composed of 24 subunits of the heavy and light ferritin chains. Variation in ferritin subunit composition may affect the rates of iron uptake and release in different tissues. A major function of ferritin is the storage of iron in a soluble and nontoxic state.	80 – KQ, KNDP 115 - 236 – 220 –	7e-111 1e-79 4e-167 5e-55 1e-79
91	**WD repeat-containing protein 1** XP_02095 6671.1	285- 588	Protein containing 9 WD repeats. WD repeats are approximately 30- to 40-amino acid domains containing several conserved residues, mostly including a Trp-asp at the C-terminal end. WD domains are involved in protein-protein interactions. The encoded protein may help induce the disassembly of actin filaments.	KIVP	3e-166
193 252	**actin, cytoplasmic 2** XP_00335 7976.1	36-322 *In frame ?*	Actins are highly conserved proteins that are involved in various types of cell motility and are ubiquitously expressed in all eukaryotic cells. In vertebrates 3 main groups of actin isoforms,	193 - 252 -	6e-176 4e-42

274 337	**beta actin** ABF19863.1 **beta actin** AAA17872.1	52-532 *In frame ?* 23-161 *In frame ?* 14-229 *In frame ?*	alpha, beta, and gamma have been identified. The alpha actins are found in muscle tissues and are a major constituent of the contractile apparatus. The beta and gamma actins coexist in most cell types as components of the cytoskeleton and as mediators of internal cell motility.		2e-115 2e-115
241 312	**macrophage-capping protein** XP_003124996.1 **capping actin protein, gelsolin like (CAPG), transcript variant X6** XM_003124949.4	27-191 813-1511	Macrophage-capping protein (CAPG) also known as actin regulatory protein CAP-G This gene encodes a member of the gelsolin/villin family of actin-regulatory proteins. The encoded protein reversibly blocks the barbed ends of F-actin filaments in a Ca2+ and phosphoinositide-regulated manner, but does not sever preformed actin filaments. By capping the barbed ends of actin filaments, the encoded protein contributes to the control of actin-based motility in non-muscle cells.	241 - KLKP, KCQP	8e-82 0
245	**PDZ and LIM domain protein 7 isoform X2** XP_020940036.1	109-367	LIM domains are proposed to function in protein–protein recognition in a variety of contexts including gene transcription and development and in cytoskeletal interaction. The LIM domains of this protein bind to protein kinases, whereas	KQ RAAHLLCK	3e-83

			the PDZ domain binds to actin filaments. The gene product is involved in the assembly of an actin filament-associated complex essential for transmission of ret/ptc2 mitogenic signalling. The biological function is likely to be that of an adapter, with the PDZ domain localizing the LIM-binding proteins to actin filaments of both skeletal muscle and non-muscle tissues.		
253	**Sus scrofa thymosin beta 4 X-linked (TMSB4X), mRNA** NM_001141991.2	52-532	This gene encodes an actin sequestering protein which plays a role in regulation of actin polymerization. The protein is also involved in cell proliferation, migration, and differentiation.		0
324	**laminin subunit beta-1** XP_003130317.3	652-875	Laminins, a family of extracellular matrix glycoproteins, are the major non collagenous constituent of basement membranes. They have been implicated in a wide variety of biological processes including cell adhesion, differentiation, migration, signalling, neurite outgrowth and metastasis. Laminins are composed of 3 non identical chains: laminin alpha, beta and gamma and they form a cruciform structure consisting of 3 short arms, each formed by a different chain, and a long arm composed of all 3 chains		3e-76
			Extracellular matrix		
23 183 206 223	**fibronectin** XP_003133690.2 **fibronectin**	2152-2376 2121-2358 85-329 96-175	Fibronectin is a high-molecular weight (~440 kDa) glycoprotein of the extracellular matrix that binds to membrane-spanning receptor proteins called integrins. Like integrins, fibronectin binds extracellular matrix components such as collagen, fibrin, and heparan sulphate proteoglycans (e.g. syndecans).	23 - KSEP 183 - KSEP 206 - KPEP 223 - KQ	1e-142 3e-132 5e-70 2e-121

247 334	AAV65602.1 **fibronectin** AAV88080.1	188-360 19-187 229-453		247 - KPEP	2e-83 1e-72
33	**extracellular matrix protein 1 isoform X5** XP_020945568.1	126-280	Extracellular protein containing motifs with a cysteine pattern characteristic of the cysteine pattern of the ligand-binding "double-loop" domains of the albumin protein family. This gene maps outside the epidermal differentiation complex (EDC), a cluster of three gene families involved in epidermal differentiation.		1e-78
283	**granulins precursor** NP_001038043.1		Each granulin protein is cleaved from the pre-cursor progranulin, a 593 amino acid long and 68.5 kDa protein. While the function of progranulin and granulin have yet to be determined, both forms of the protein have been implicated in development, inflammation, cell proliferation and protein homeostasis.		5e-60
			Enzymes		
40	**N(alpha)-acetyltransferase 40, NatD catalytic subunit (NAA40), transcript variant X2,** XM_013994174.2	2604-3479	N-alpha-acetyltransferase that specifically mediates the acetylation of the N-terminal residues of histones H4 and H2A. It has a very specific selectivity for histones H4 and H2A N-terminus and specifically recognises the 'Ser-Gly-Arg-Gly sequence'. Acts as a negative regulator of apoptosis.		0
61	**lon protease homolog 2, peroxisomal** XP_005664508.3	520-726	ATP-dependent serine protease that mediates the selective degradation of misfolded and unassembled polypeptides in the peroxisomal matrix. Necessary for type 2 peroxisome targeting signal (PTS2)-containing protein processing and facilitates peroxisome	KQ	7e-85

			matrix protein import. May indirectly regulate peroxisomal fatty acid beta-oxidation through degradation of the self-processed forms of TYSND1.		
71	**SH3 domain-binding glutamic acid-rich-like protein isoform X2** XP_020936361.1	1-85	SH3BGRL3 protein shows a significant similarity to glutaredoxin 1 of E. coli, and all the three proteins are predicted to belong to thioredoxin-like protein family. Glutaredoxins are ubiquitous oxidoreductases, which catalyse the reduction of many intra-cellular protein disulphides and play an important role in many redox pathways. However, the SH3BGRL3 protein lacks the enzymatic function of glutaredoxins and may have a role as a regulator of redox activity.	4 KQ	5e-49
75 76	**L-xylulose reductase** XP_020922060.1	113-244 *In frame ?* 134-199 *In frame ?*	DCSR catalyses the reduction of several L-xylylose as well as several pentoses, tetroses, trioses, alpha-dicarbonyl compounds. The enzyme is involved in carbohydrate metabolism, glucose metabolism, the uronate cycle and may play a role in the water absorption and cellular osmoregulation in the proximal renal tubules by producing xylitol.	75 – KASP, RPATGLLK 76 - KAPP, KRTP, KKRP	1e-85 4e-13
107	**acyl-coenzyme A thioesterase 1-like** XP_020955153.1	306-464	Part of a family of Acyl-CoA thioesterases, which catalyse the hydrolysis of various Coenzyme A esters of various molecules to the free acid plus CoA.	KEKP	2e-111
131	**sodium/potassium-transporting ATPase subunit alpha-1 isoform X1**	805-946	Belongs to the family of P-type cation transport ATPases, and to the subfamily of Na+/K+-ATPases. Na+/K+-ATPase is an integral membrane protein responsible for establishing and maintaining the electrochemical gradients of Na and K ions across the plasma membrane. These	KRQP	3e-95

	XP_020944376.1		gradients are essential for osmoregulation, for sodium-coupled transport of a variety of organic and inorganic molecules, and for electrical excitability of nerve and muscle. This enzyme is composed of two subunits, a large catalytic subunit (alpha) and a smaller glycoprotein subunit (beta).		
145	**adenylate kinase isoenzyme 6 isoform X2** XP_003134069.1	41-138	Broad-specificity nucleoside monophosphate (NMP) kinase that catalyses the reversible transfer of the terminal phosphate group between nucleoside triphosphates and monophosphates. Has also ATPase activity (By similarity). Involved in 18S rRNA maturation. Required for cleavage of the 20S pre-rRNA at site D in the cytoplasm. Involved in oxidative stress response. Required for POS9-dependent target gene transcription upon oxidative stress.	145 -	3e-51
153	**aflatoxin B1 aldehyde reductase member 2** NP_001230751.1	151-369	Aldo-keto reductases, such as AKR7A2, are involved in the detoxification of aldehydes and ketones	KQ	1e-161
207	**pyruvate kinase PKM isoform X8** XP_001929104.1	401-525	Glycolytic enzyme that catalyses the transfer of a phosphoryl group from phosphoenolpyruvate (PEP) to ADP, generating ATP. Stimulates POU5F1-mediated transcriptional activation. Plays a general role in caspase independent cell death of tumour cells.		5e-16
210	**dual oxidase 2 precursor** NP_999164.2	65-252	Generates hydrogen peroxide which is required for the activity of thyroid peroxidase/TPO and lactoperoxidase/LPO. Plays a role in thyroid hormones synthesis and lactoperoxidase-mediated antimicrobial defence	RFGSNLMK	2e-62

			at the surface of mucosa. May have its own peroxidase activity through its N-terminal peroxidase-like domain.		
265	**branched chain keto acid dehydrogenase E1, alpha polypeptide (BCKDHA)** NM_001123083.1	30-739			0
293	**glutathione peroxidase 1** AID58016.1	77-206	Glutathione peroxidase 1, also known as GPx1, is a member of the glutathione peroxidase family. Glutathione peroxidase functions in the detoxification of hydrogen peroxide, and is one of the most important antioxidant enzymes in humans		5e-94
302	**uridine-cytidine kinase-like 1 isoform X5** XP_020933287.1	29-100	May contribute to UTP accumulation needed for blast transformation and proliferation. Pathway: UMP biosynthesis via salvage pathway. This protein is involved in step 1 of the sub-pathway that synthesises UMP from uridine.		9e-38
331	**glutamate-ammonia ligase** BAI47709.1	71-236	Belongs to the glutamine synthetase family and catalyses the synthesis of glutamine from glutamate and ammonia in an ATP-dependent reaction. This protein plays a role in ammonia and glutamate detoxification, acid-base homeostasis, cell signalling, and cell proliferation.		4e-74
332	**serine/threonine-protein phosphatase 2A catalytic subunit**	134-309	PP2A is the major phosphatase for microtubule-associated proteins (MAPs). PP2A can modulate the activity of phosphorylase B kinase casein kinase 2, mitogen-stimulated S6 kinase, and MAP-2 kinase. Cooperates with SGO2 to		2e-129

	alpha isoform NP_999531.1		protect centromeric cohesin from separase-mediated cleavage in oocytes specifically during meiosis. Activates RAF1 by dephosphorylating it at 'Ser-259. Can dephosphorylate SV40 large T antigen and p53/TP53.		
4 59 249 266	**L-lactate dehydrogenase B chain isoform X1** XP_013843801.1 **L-lactate dehydrogenase B chain** NP_001106758.1	16-306 13-297 12-231 18-40	Lactate dehydrogenase (LDH or LD) is an enzyme found in nearly all living cells (animals, plants, and prokaryotes). LDH catalyses the conversion of lactate to pyruvic acid and back, as it converts NAD+ to NADH and back. A dehydrogenase is an enzyme that transfers a hydride from one molecule to another.	KYSP KYSP	2e-176 0 3e-104 2e-05
			Miscellaneous		
7	**uncharacterised protein C20orf96 homolog isoform X2** XP_013838676.1	28-187		KEGP	5e-61
181	**Sus scrofa mesoderm development candidate 2 (MESDC2)** XM_001928863.5	646-1488	LRP chaperone MESD (also known as mesoderm development candidate 2) represents a set of highly conserved proteins found from nematodes to humans. It is a chaperone that specifically assists with the folding of beta-propeller/EGF modules within the family of low-density lipoprotein receptors (LDLRs). It also acts as a modulator of the Wnt pathway, since some LDLRs are coreceptors for the canonical Wnt pathway and is essential for specification of		0

			embryonic polarity and mesoderm induction		
182	**myotubularin related protein 14 (MTMR14), transcript variant X3,** XR_002337651.1	1941-2112	Expression of Mtmr14 increased with myotubule formation and differentiation. MTMR14 is a phosphatidylinositol-3-phosphatase that dephosphorylates the same substrates as myotubularin, PtdIns(3)P and PtdIns(3,5)P2	/	1e-84
269	**annexin A5** XP_003129266.2	69-181	The function of the protein is unknown; however, annexin A5 has been proposed to play a role in the inhibition of blood coagulation by competing for phosphatidylserine binding sites with prothrombin and also to inhibit the activity of phospholipase A1. These properties have been found by in vitro experiments. Annexin A5 has been shown to interact with Kinase insert domain receptor and Integrin, beta 5.		3e-75
301	**neutrophil cytosol factor 2 isoform X1** XP_005667867.2	232-335	Neutrophil cytosolic factor 2, the 67-kilodalton cytosolic subunit of the multi-protein NADPH oxidase complex found in neutrophils. This oxidase produces a burst of superoxide which is delivered to the lumen of the neutrophil phagosome.	-	0.001

Information on protein function and known interactions with PRRSV or other viruses was recorded directly from a combination of https://www.uniprot.org/, https://en.wikipedia.org/wiki/Main_Page, https://www.ncbi.nlm.nih.gov/ and selected referenced papers. Nucleotides in red or amino acid region in black; note 5e-120 = $5x10^{-120}$. Proteins selected to take forward for further investigation were highlighted in green. Key: # – number; K – lysine; X – any amino acid; R – arginine; P – proline, Q – glutamine; L – Leucine; residues highlighted in blue are ubiquitinated.

9.4 Vector plasmids used in the project

Vector plasmids used throughout the project, their uses, the antibiotic resistance gene they carry for selection and amplification and the plasmid map figure reference are listed in **Table 9.3**. **Figures 9.2**, **9.3**, **9.4**, **9.5** and **9.6** show the respective plasmid maps.

Table 9.3: Vector plasmids used in the project and their antibiotic resistance genes

Plasmid	Use	Antibiotic	Plasmid Map
pACT2	y-2-h	Amp	**Figure 9.2**
pGBKT7	y-2-h	Kan	**Figure 9.3**
pcDNA 3.1+	IF	Amp	**Figure 9.4**
pEF	IF	Amp	**Figure 9.5**
pGADT7	y-2-h	Amp	**Figure 9.6**

Key: y-2-h – yeast-2-hybrid; IF – confocal immunofluorescence microscopy; Amp – ampicillin; Kan – kanamycin.

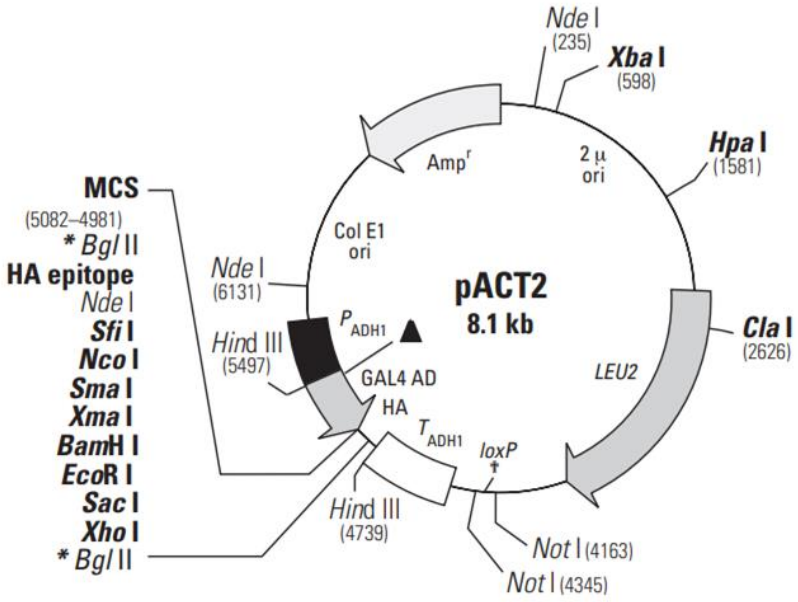

Figure 9.2: pACT2 plasmid map. pACT2 generates a fusion of the GAL4AD (amino acids 768–881), an HA epitope tag, and a protein of interest (or protein encoded by a cDNA in a fusion library) cloned into the multiple cloning site (MCS) in the correct orientation and reading frame. pACT2, which is derived from pACT (1), contains a unique *Eco*RI site in the MCS. The hybrid protein is expressed at high levels in yeast host cells from the constitutive ADH1 promoter (P); transcription is terminated at the ADH1 transcription termination signal (T). The protein is targeted to the yeast nucleus by the nuclear localization sequence from SV40 T-antigen which has been cloned into the 5' end of the GAL4 AD sequence. pACT2 is a shuttle vector that replicates autonomously in both *E. coli* and *S. cerevisiae* and carries the *bla* gene, which confers ampicillin resistance in *E. coli*. pACT2 also contains the *LEU2* nutritional gene that allows yeast auxotrophs to grow on limiting synthetic media. Transformants with AD/library plasmids can be selected by complementation by the *LEU2* gene by using an *E. coli* strain that carries a *leuB* mutation (e.g., HB101). *Plasmid map and description obtained from ClonTech, Takara Bio.*

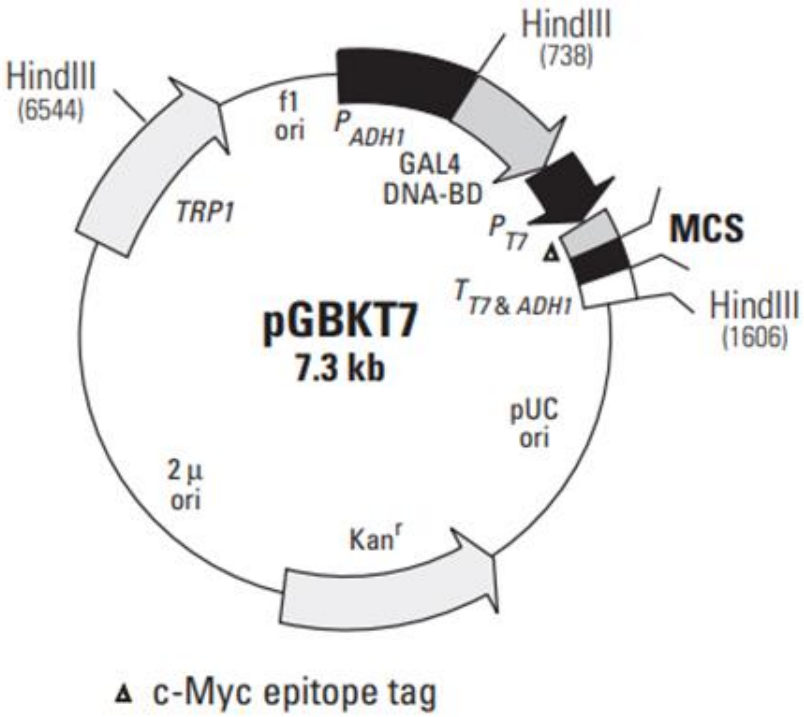

Figure 9.3: pGBKT7 plasmid map. The pGBKT7 vector expresses proteins fused to amino acids 1–147 of the GAL4 DNA binding domain (DNA-BD). In yeast, fusion proteins are expressed at high levels from the constitutive ADH1 promoter (P_{ADH1}); transcription is terminated by the T7 and ADH1 transcription termination signals (T_{T7} & $_{ADH1}$). pGBKT7 also contains the T7 promoter, a c-Myc epitope tag, and a multiple cloning site (MCS). pGBKT7 replicates autonomously in both E. coli and S. cerevisiae from the pUC and 2 µ ori, respectively. The vector carries the Kan^r for selection in E. coli and the TRP1 nutritional marker for selection in yeast. Yeast strains containing pGBKT7 exhibit a higher transformation efficiency than strains carrying other DNA-BD domain vectors. *Plasmid map and description obtained from ClonTech, Takara Bio.*

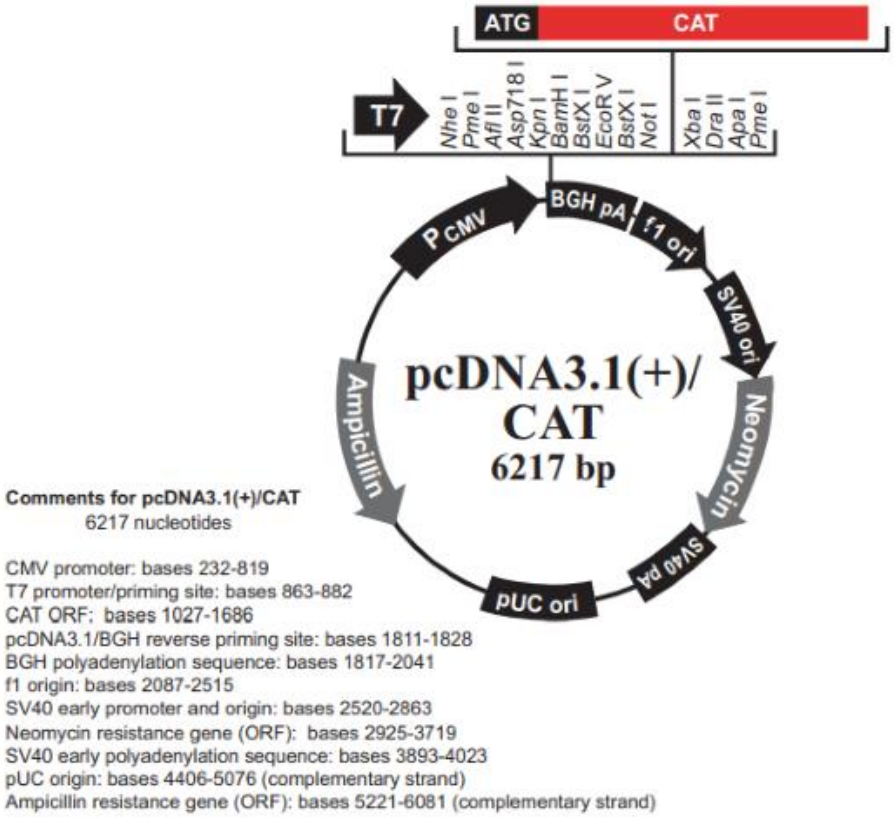

Figure 9.4: pcDNA 3.1+ plasmid map. pcDNA™3.1/CAT is a 6217 bp control vector containing the gene for CAT. It was constructed by digesting pcDNA™3.1(+) with *Xho*I and *Xba*I and treating with Klenow. An 800 bp *Hin*d III fragment containing the CAT gene was treated with Klenow and then ligated into pcDNA™3.1(+). *Plasmid map and description obtained from Invitrogen, Thermo Fisher Scientific.*

1 – 15	Filled-in *Eco*RI to *Sma*I half-site from pUC12 polylinker.
16 – 95	Residual SV40 fragment derived from origin but having NO origin, promoter, or enhancer activity.
96 – 1291	Enhancer and promoter region from EF1α gene (accession number J04617). This includes 203bp 5' flanking sequence, 33bp untranslated Exon 1, 943 bp intron 1 and 10bp exon 2.
1292 – 1349	5'UTR from human β-globin gene. Ends in *Nco*I site, which includes the AUG initiation codon.
1350 – 1394	Polylinker: *NcoI* *BamHI* *EcoRI* *XhoI* *ClaI* *SpeI* *XbaI* ..CCATGGCCGGATCCGAATTCCTCGAGATCGATTAGACTAGTCTAGAAATTC... *** *** *** - All polylinker sites save *Xho*I are unique. - Stop codons in all three frames.
1395 – 2169	3'UTR and poly(A) site from human β-globin gene. Includes about 200bp exon 3, all of 3'UTR, poly(A) site and some 3' flanking sequence.
2170 – 4809	pUC12 backbone.

Figure 9.5: pEF plasmid map. pEFplink2 (4809bp).

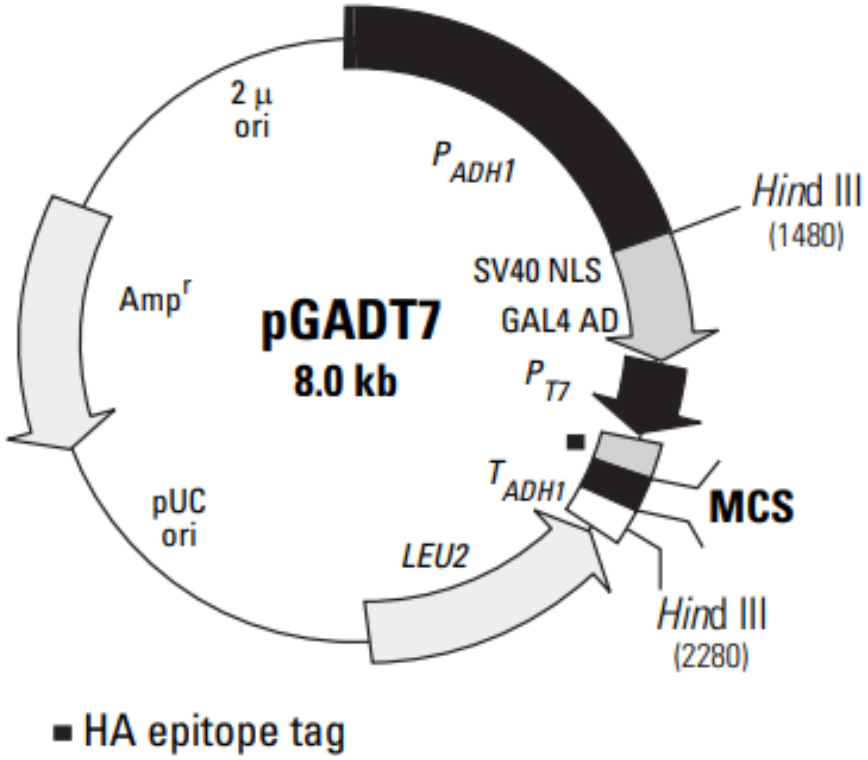

Figure 9.6: pGADT7 plasmid map. The pGADT7 AD vector expresses proteins fused to amino acids 768–881 of the GAL4 activation domain (AD). In yeast, fusion proteins are expressed at high levels from the constitutive ADH1 promoter (P_{ADH1}); transcription is terminated at the ADH1 transcription termination signal (T_{ADH1}).The fusion protein is targeted to the yeast nucleus by the SV40 nuclear localization sequences that have been added to the activation domain sequence (1). pGADT7 also contains the T7 promoter, an HA epitope tag, and a multiple cloning site (MCS). pGADT7 replicates autonomously in both E. coli and S. cerevisiae from the pUC and 2 µ ori, respectively. The vector carries Amp^r for selection in E. coli and the LEU2 nutritional marker for selection in yeast. *Plasmid map and description obtained from ClonTech, Takara Bio.*